UNIVERSIDADE FEDERAL DO RIO GRANDE DO SUL-UFRGS
PROGRAMA DE POS-GRADUACAO EM CIENCIAS BIOLOGICAS: BIOQUIMICA

Mucopolissacaridoses: mecanismos patogênicos e abordagens terapêuticas baseadas em terapia gênica e reposição enzimática

Guilherme Baldo

Orientador: Prof. Dr. Roberto Giugliani
Co-orientadora: Profa. Dra. Ursula Matte

Tese apresentada ao PPG em Ciências Biológicas: Bioquímica como requisito parcial para obtenção do titulo de Doutor em Bioquímica

Porto Alegre, maio de 2012

Agradecimentos

Professor Roberto Giugliani, pelas oportunidades oferecidas, pela confiança depositada, pela atenção, ensinamentos, e pelo exemplo de lutas e conquistas.

Profa Ursula Matte, pela confiança depositada neste trabalho, pela orientação e por contribuir para o meu crescimento intelectual, profissional e pessoal.

Dra Kathy Ponder, por me aceitar como seu aluno de doutorado sanduíche, pelos ensinamentos e oportunidades.

Amigos do Centro de Terapia Gênica, pelo companheirismo, amizade e ajuda. Em especial, a Dra Fabiana Mayer, que juntamente com a Talita de Carvalho, Barbara Martinelli e Anna Dilda continuaram os experimentos durante o meu periodo nos EUA.

Colegas e amigos em Saint Louis, em especial Suzan Wu e Andrew, Paul Bigg, Yuli Liu, Bruce Linders and Roger Lilyea, pelo apoio durante o doutorado sanduíche.

Amigos do Serviço de Genética Médica (professores e demais pesquisadores pelas discussões), especialmente a equipe da Dra Maira Burin no laboratório de erros inatos do metabolismo, pela disponibilidade e auxilio com os testes bioquímicos.

Amigos e colegas da QuatroG, em especial ao profesor Diógenes Santos e ao Dr. Daniel Lorenzini, pela oportunidae e ensinamentos no estudo proteomicos.

Angela Tavares, pela amizade, ensinamentos e ajuda nas ecocardiografias.

Hospital de Clinicas de Porto Alegre, especialmente amigos do Centro de Pesquisa Experimental, incluindo aqui toda a equipe da experimentação animal do HCPA (em Especial a Fabíola Meyer e Marta Cioatto), laboratório de doenças auto-imunes e infecciosas (em especial a Dra Patrícia de Oliveira), e o serviço de patolgoia experimental (Dra Luise Meurer e Flavia Giusti), que tiveram participação crucial durante o desenvolvimento do trabalho.

UFRGS e PPG Bioquímica, em especial a Cleia, que sempre se mostrou muito competente e rapida pra resolver situações nestes 4 anos de doutorado.

CNPq, pelas bolsas de doutorado no Brasil e durante o período sanduíche.

A todos meus pais (o oficial, Sr Celso Roque baldo) e mães (a oficial: Sra. Maria Claudete Vicari baldo) espalhados por ai (Adair Dai Pra, Clarice Dai Pra, Dona Gloria Mãe da Fer Pereira...), e tambem irmaos (Oficial: Vinicius Baldo) e extra-oficiais (Giovana Juliana e Tiago Dai Pra, Fernanda Pereira), e demais membros da família.

Meus amigos, que são muitos para ser mencionados aqui, mas podem ser conferidos na minha pagina do facebook!

INDICE

PARTE I

RESUMO

O presente trabalho teve como objetivo estudar a patogênese das mucopolissacaridoses (MPS), em especial em órgãos de difícil correção pelas terapias atualmente disponíveis, bem como desenvolver novos tratamentos para estas doenças. Nossos estudos em camundongos MPS I e VII evidenciaram um aumento na atividade de proteases, incluindo catepsinas e metaloproteases, que podem contribuir para a patogênese da doença na aorta, articulações e cérebro. Ainda nestes órgãos, foi observada a ativação de vias inflamatórias, como o sitema complemento e a via dos receptores *toll like,* bem como um processo neuroinflamatório, e também podem ter papel fundamental no aparecimento das anormalidades. Dois protocolos de terapia gênica foram testados e, enquanto a microencapsulação celular atingiu apenas uma correção transitória *in vivo* (possivelmente por uma formação de fibrose pericapsular), o uso de um vetor retroviral levou a níveis séricos de alfa-L-iduronidase (IDUA) superiores aos níveis normais, com correção da doença no sistema nervoso central. Por fim, o uso da terapia de reposição enzimática desde o nascimento demonstrou uma melhora nas vísceras, especialmente aorta e válvulas cardíacas, e uma redução na formação de anticorpos contra a enzima. De forma surpreendente, a enzima foi detectada no cérebro dos animais, sugerindo que a mesma atravessa a barreira-hemato-encefálica. Nossos dados em conjunto sugerem a participação de vias inflamatórias e proteases na patogênese das MPS, e enquanto o tratamento com as microcapsulas ainda apresenta limitações, a terapia gênica com o retrovírus e a terapia de reposição enzimática desde o nascimento se mostram como alternativas viáveis e promissoras.

ABSTRACT

In this work we aimed to study the pathogenesis of mucopolysaccharidosis (MPS), especially organs that have been described as difficult-to-reach by current therapies. We also aimed to evaluate new therapies for these diseases. Our studies focused on MPS I and VII mice showed an increase in the activity of proteases, including cathepsins and metallopeptidases, that can contribute to the disease pathogenesis in the aorta, joints and brain. In the same organs, we observed activation of inflammatory pathways, including the complement system, the toll-like recetor pathway and a neuroinflammatory process, who can also contribute to the abnormalities observed. Two gene terapy protocols were tested and, while the cell encapsulation only achieved transient correction *in vivo* (possibly due to a pericapsular fibrosis), the use of a retroviral gene vector reached supernormal serum IDUA levels and correction of brain abnormalities. Finally the use of enzyme replacement therapy from birth showed improvements in visceral organs, specially the aorta and heart valves, and a reduction in the levels of serum anti-IDUA antibodies. Surprisingly, the enzyme could be detected in the brain, suggesting that a fraction crosses the blood-brain-barier. Our data altogether suggest the participation of inflammatory pathways and proteases in the pathogenesis of MPS, and although the treatment with microcapsules still presents limitations, retroviral gene therapy and enzyme replacement therapy started from birth are promising treatment alternatives.

LISTA DE ABREVIATURAS

AAV- vetor adeno-associado
BMP-4 - proteína morfogénetica do osso tipo 4
BHE - barreira hemato-encefálica
BHK - *baby hamster kidney*
Cts - catepsina
DL - doenças lisossômicas
FGF-2 - fator de crescimento de fibroblastsos tipo 2
GAG - glicosaminoglicanos
GAP-43 - proteína associada ao crescimento 43
GFAP - *glial fibrillary acidic protein*
GUSB - beta-glucuronidase
HPLC - cromatografia liquida de alto desempenho
IDUA - alfa-L-iduronidase
JAK - janus cinase
LAMP - proteína associada à membrana lisossômica
LTR - *long term repeat*
M6P - manose-6-fosfato
MAC - complexo de ataque a membrana
MAPK - cinase ativadora de mitose
MASP - serina protease associada à manana
MHC - *major histocompatibility complex*
MLB - lectina ligadora de manose
MMP - metaloproteinase de matriz
MPS - mucopolissacaridose
PSD-95 - *post sinaptic density 95*
RE - retículo endoplasmático
SIN - auto-inativante
STAT - transdutores de sinal e ativadores de transcrição
TCTH - transplante de células-tronco hematopoiéticas
TFEB - fator de transcrição EB
TNF - fator de necrose tumoral
TLR - receptor *toll-like*
TER - terapia de reposição enzimática

INTRODUÇÃO

Doenças lisossômicas

O lisossomo e as enzimas lisossômicas

Os lisossomos são organelas acídicas, encontradas em todas as células de mamíferos, exceto em hemácias. São estruturas compostas por uma membrana celular formada por uma bicamada fosfolipídica, contendo no seu interior uma série de hidrolases, responsáveis pela degradação de biomoléculas (Saftig, 2006).

A biogênese dos lisossomos acontece por diferentes mecanismos, sendo os principais a partir da fusão de autofagosomas com endossomas ou pela acidificação de endossomas no citosol, mediado por bombas de prótons (H^+/ATPases) ancoradas à membrana (Saftig and Klumperman, 2009).

São diversas as funções do lisossomo na célula. Pode-se citar como sua principal e mais conhecida função a degradação de compostos (aminoácidos, açúcares, ácidos nucléicos e lipídios) no seu interior. No entanto, o lisossomo também é responsável por processos como homeostase do colesterol (Otomo et al, 2011), autofagia (Settembre et al, 2008) defesa contra patógenos (Nayak et al, 2006), remodelamento ósseo (Saftig et al, 2006), sinalização e morte celular (Repnik et al, 2012).

O proteoma do lisossomo é composto por mais de 50 hidrolases, com distintas funções. Ainda, a membrana apresenta algumas proteínas características, como as proteínas associadas à membrana lisossômica tipos I e II (LAMP I e LAMP II) (Schroder et al, 2010). As enzimas lisossômicas são levadas até os endossomas principalmente por meio de dois receptores de manose-6-fosfato (M6P) localizados na membrana celular (no caso de enzimas recicladas) e no complexo de golgi (no caso de enzimas recém-sintetizadas). No pH ácido do lisossomo o receptor se desliga das enzimas (sendo que no lisossomo maduro estes receptores estão ausentes), que se tornam ativas nesse meio (Saftig and Klumperman, 2009). A deficiência de alguma proteína lisossômica geralmente está associada a uma condição patológica. Este grupo de doenças é conhecido como doenças lisossômicas (DL).

Doenças lisossômicas

As DL são um grupo de aproximadamente 50 doenças, causadas por mutações em enzimas lisossômicas ou em proteínas responsáveis pela biogênese e maturação dos lisossomos (Meikle et al, 2004). Com poucas exceções (como a MPS II, que tem uma herança ligada ao cromossomo X), são doenças herdadas de forma recessiva.

Essas doenças são caracterizadas por acúmulo de substratos não-degradados dentro e fora do lisossomo. O tipo de substrato acumulado é utilizado para caracterizar os grandes grupos de DL, que incluem as mucopolissacaridoses (MPS, caracterizada por acúmulo de glicosaminoglicanos), lipidoses (lipídios), glicogenoses (glicogênio) e oligossacaridoses (de pequenos açúcares). Uma vez que as enzimas lisossômicas são expressas de forma constitutiva, suas deficiências geralmente levam a complicações multisistêmicas que variam de doença para doença. Além disso, o crescente e ininterrupto acúmulo de substrato faz com que estas doenças tenham um curso progressivo e muitas delas levam à morte do paciente nos primeiros anos de vida, como no caso das mucopolissacaridoses (Neufeld and Muenzer, 2001).

Mais detalhes sobre as DL podem ser encontrados no capitulo de livro *"Non Viral Gene Transfer Approaches for Lysosomal Storage Disorders"* contido na presente tese (Matte et al, 2011).

Mucopolissacaridoses

As mucopolissacaridoses: características gerais

As MPS são um conjunto de 11 doenças, caracterizadas por mutações em genes que codificam enzimas envolvidas na degradação dos glicosaminoglicanos (GAG, antigamente chamados mucopolissacarídeos) sulfato de dermatan, sulfato de heparan, sulfato de condroitin, sulfato de queratan e acido hialurônico. Estes podem ter sua degradação interrompida de forma isolada ou combinada, dependendo da enzima deficiente (Neufeld and Muenzer, 2001). A tabela 1 relaciona as MPS descritas até o momento, o gene mutado em cada uma delas, bem como sua prevalência, o(s) substrato(s) acumulado(s) e os principais órgãos afetados.

Tabela 1: As mucopolissacaridoses: características gerais.

Tipo	Nome da síndrome	Gene mutado	Prevalência*	Substrato Acumulado	Principais manifestações
MPS I	Hurler / Scheie	*IDUA*	1:75.000-1:88.000	HS, DS	Multisistêmica, SNC
MPS II	Hunter	*IDS*	1:92.000-1:149.000	HS, DS	Multisistêmica, SNC
MPS IIIA	Sanfillipo A	*SGSH*	1:86.000-1:114.000	HS	SNC
MPS IIIB	Sanfillipo B	*NAGLU*	1:139.000-1:238.000	HS	SNC
MPS IIIC	Sanfillipo C	*HGSNAT*	1:407.000-1:803.000	HS	SNC
MPS IIID	Sanfillipo D	*GNS*	1:1.000.000-1:1.056.000	HS	SNC
MPS IVA	Morquio A	*GALNS*	1:167.000-1:455.000	KS, CS	Esqueléticas
MPS IVB	Morquio B	*GLB1*	1:714.000	KS, CS	Esqueléticas
MPS VI	Maroteaux-Lamy	*ARSB*	1:235.000-1:666.000	DS, CS	Multisistêmica
MPS VII	Sly	*GUSB*	1:416.000-1:2.111.000	HS, DS, CS	Multisistêmica, SNC
MPS IX	Natowicz	*HYAL1*	ND	AH	Lesões articulares

* Os dados de prevalência refletem o maior e menor valores encontrados nos estudos em Portugal, Holanda e Austrália, revisado por Fuller e colaboradores (2006). ND- não determinado. Abreviações: AH - ácido hialurônico; CS-condroitin sulfato; DS-dermatan sulfato; HS- heparan sulfato; KS-keratan sulfato; SNC- sistema nervoso central.

O diagnóstico definitivo das MPS se dá através da medida da atividade enzimática em leucócitos, fibroblastos ou plasma de pacientes com suspeita clínica. Como testes de triagem podem ser realizadas a medida de GAG urinário e eletroforese de GAG. Ainda, a pesquisa de mutações nos genes envolvidos serve como diagnóstico complementar e para o aconselhamento genético das famílias (Matte et al, 2003). O

diagnóstico ao nascimento só é realizado em casos onde já existe algum familiar afetado, já que neonatos não possuem sinais clínicos evidentes. No entanto, devido ao desenvolvimento de tratamentos recentes, em algumas situações de alta incidência populacional tem-se sugerido a realização de triagem neonatal para algumas MPS, como é o caso da MPS VI, que possui uma alta freqüência na região de Monte Santo, no nordeste brasileiro (Giugliani et al, 2012).

Clinicamente estas doenças se caracterizam por alguns achados em comum, dependendo do substrato acumulado. Desta forma, pacientes com acúmulo de dermatan ou de queratan sulfato (MPS I, II, IV, VI, VII) apresentam deformidades esqueléticas como disostose multiplex e baixa estatura, além de anormalidades cardíacas (dilatação do miocárdio e espessamento das válvulas cardíacas) e nas articulações (rigidez articular, mãos em garra). Por outro lado, o acúmulo de heparan sulfato (MPS I, II, III e VII) parece estar relacionado a alterações no sistema nervoso central, sendo que estes pacientes possuem retardo mental. O acúmulo de condroitin sulfato parece agravar os sintomas já encontrados pelo acúmulo dos demais substratos. Já o acúmulo de ácido hialurônico (MPS IX) foi descrito em poucos pacientes, mas nestes foi observada uma alteração articular semelhante a um processo de artrite (Imundo et al, 2011). Outras características comuns entre as MPS incluem organomegalia, espessamento de traquéia, problemas respiratórios, de dentição, visuais e de audição (Giugliani et al, 2010).

Mecanismos patológicos das mucopolissacaridoses

Acúmulo de GAG e metabólitos secundários

Até poucos anos acreditava-se que o acúmulo de GAG era o responsável direto por todos os sinais clínicos encontrados nas MPS. Hoje se sabe que existem outros mecanismos envolvidos. No entanto algumas manifestações da doença realmente podem ser explicadas pelo simples espessamento de estruturas causado pelo acúmulo de mucopolissacarídeos. Entre estas características, pode-se incluir a pele infiltrada, a hepatomegalia, o espessamento das válvulas cardíacas e algumas alterações nas estruturas da traquéia e dos ouvidos. Outras manifestações, como a hidrocefalia e a compressão espinhal, também podem ser atribuídas pelo acúmulo de GAG nas meninges (Lachman et al, 2010). No entanto, a deficiência no *turnover* de GAG leva a

uma série de alterações em processos celulares que contribuem para a patogênese da doença, que estão resumidos na figura 1.

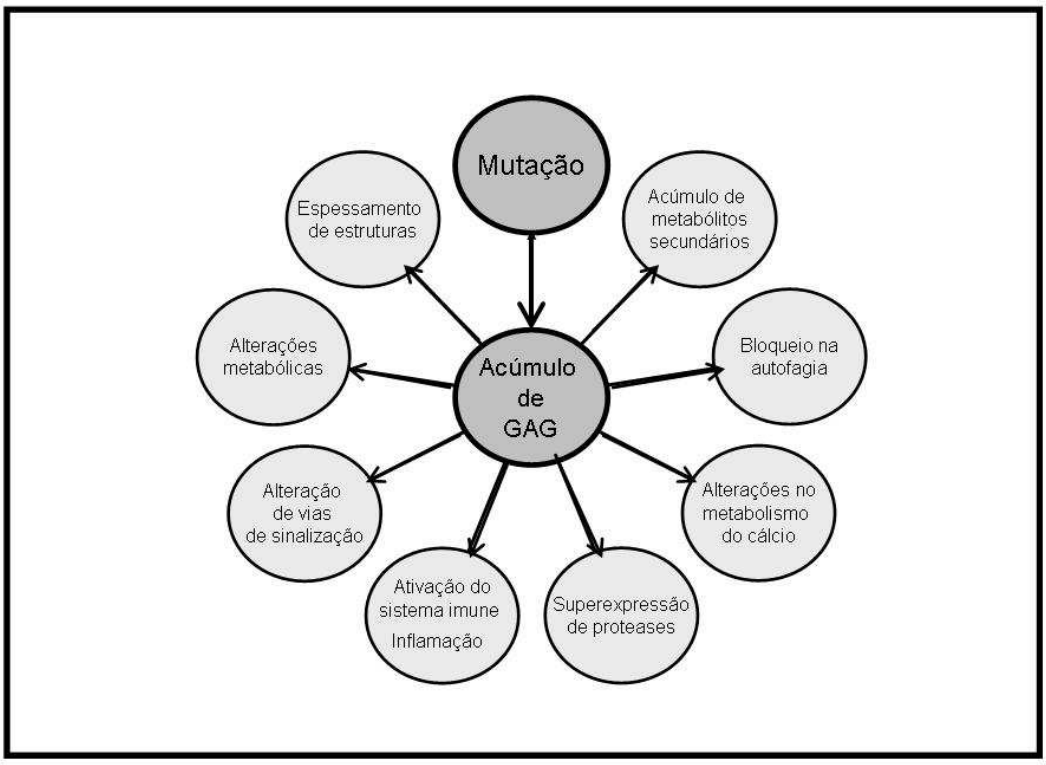

Figura 1: Esquema representando os possíveis mecanismos envolvidos na patogênese das mucopolissacaridoses. A partir da perda de função em alguma enzima lisossômica que degrade GAG por uma mutação, o acúmulo do substrato leva a uma série de alterações em nível celular e tecidual. Os mecanismos patogênicos podem estar relacionados e estudos deverão ser conduzidos nos próximos anos para identificar tais relações.

O acúmulo de metabólitos secundários não-relacionados ao defeito genético primário já foi demonstrado nas mucopolissacaridoses (Ohmi et al, 2011), bem como em outras DL (Cox et al, 2012). Entre as substâncias mais estudadas estão os gangliosídeos GM2 e GM3, que acumulam principalmente no cérebro de pacientes e animais com MPS, e acredita-se que estejam ligados ao processo de neurodegeneração nestas enfermidades. Esta suposição se baseia principalmente no fato de que a não-degradação de GM2 e GM3 leva a duas outras DL (Gangliosidoses GM2 e GM3, respectivamente) que se caracterizam pela rápida neurodegeneração (Cox et al, 2012). Além disso, já está descrito na literatura que um aumento nos níveis de GM3 pode levar à morte de neurônios *in vitro* e *in vivo* em peixe-zebra (Sohn et al, 2006). O mecanismo

de acúmulo de gangliosideos nas MPS ainda não está totalmente esclarecido, mas acredita-se que aconteça por problemas de tráfego destas moléculas devido a alterações na homeostase do cálcio no lisossomo (Lloyd-Evans et al, 2008). Outras substâncias também aparecem acumuladas nas células de pacientes e modelos animais de MPS, incluindo colesterol não esterificado (Mcglynn et al, 2004) e algumas proteínas, como a subunidade C da ATP sintase mitocondrial (Ryazantsev et al, 2007). Porém sua contribuição para a patogênese destas doenças ainda é incerto.

Alteração na homeostase do cálcio e no reticulo endoplasmático

A homeostase do cálcio é outro processo que parece estar desregulado nas MPS. Em estudo recente, Pereira e colaboradores (2010) demonstraram que existe maior liberação de cálcio pela membrana lisossômica e pelo reticulo endoplasmático em esplenócitos de camundongos MPS I. Além disso, a concentração de íons H^+ dentro dos lisossomos era menor nos animais com MPS I, sugerindo que o pH lisossômico também pode estar alterado. Estas anormalidades podem perturbar o tráfego e a atividade de proteínas lisossômicas, levando ao aumento da liberação das catepsinas para fora do lisossomo, o que, por sua vez, pode levar a clivagem de diversos produtos e alterações em vias de sinalização, incluindo apoptose (Boya e Kroemer, 2008).

Alterações na homeostase do cálcio também parecem estar relacionadas a problemas ósseos nas MPS, sendo que cachorros com MPS VII apresentam menor conteúdo de cálcio na epífise de ossos da coluna vertebral, o que pode contribuir para anormalidades mecânicas, incluindo o enrijecimento desta estrutura (Smith et al, 2010). Ainda, processos de calcificação de válvulas cardíacas são comuns em pacientes com diferentes tipos de MPS (Fischer et al, 1999) e contribuem para a perda da funcionalidade das mesmas, embora os mecanismos responsáveis por esta calcificação ainda não estejam esclarecidos.

Por fim, um estudo recente (Mu et al, 2008) utilizou inibidores de canais de cálcio em células de pacientes com diferentes DL, incluindo MPS IIIA, e mostrou que a manipulação dos níveis de cálcio pode aumentar a atividade enzimática em certas mutações. Uma vez que o cálcio é importante para a função do retículo endoplasmático (RE), e alterações na função desta organela já foram demonstradas em diversas DL, os autores sugerem que problemas no tráfego e dobramento de proteínas devido ao mau-funcionamento do RE podem contribuir para a patogênese destas doenças. Ainda, a

partir disso, sugerem que tratamentos com inibidores de canais de cálcio possam ser desenvolvidos, para gerar um dobramento correto da proteína mutada (em casos de mutação de ponto) e restaurar parcialmente a sua atividade.

Aumento na expressão de catepsinas e outras proteases

As catepsinas são proteases sintetizadas como pré-pro-catepsinas e ativadas em pH ácido. As catepsinas B, C, F, H, L, K, O, S, V, W e X são cisteino-proteases, enquanto a catepsina G é uma serina carboxipeptidase e as catepsinas D e E são aspartil-proteases (Kuester et al, 2008). Como proteases lisossômicas, elas possuem importante função proteolítica fisiológica. No entanto, nos últimos anos uma série de outras funções tem sido descritas para estas enzimas (tabela 2). Por exemplo, a catepsina S, que estava descrita na literatura como a única catepsina ativa e estável em pH neutro (Vasiljeva et al, 2005), está envolvida na apresentação de antígenos mediados por MHC classe II (Shi et al, 1999) e na clivagem da proteína príon (Polyaokova et al, 2009). A catepsina K está envolvida na remodelação óssea e sua deficiência leva à picnodisostose (Saftig et al, 1998). As catepsinas D e B estão envolvidas no processo de morte celular mediada por lisossomo em processos fisiológicos como a regressão da glândula mamária após a lactação (Kreuzaler et al, 2011). A desregulação na expressão de catepsinas parece estar envolvida em uma série de processos inflamatórios, incluindo artrite reumatóide e arteriosclerose, além de outros processos, como a invasividade de tumores (Kuester et al, 2008) e a dilatação cardíaca (Ge et al, 2006) (tabela 2).

Nas MPS o aumento na expressão de catepsinas B, S e K foi descrito nos últimos anos na aorta de camundongos MPS I e cachorros com MPS I e VII (Ma et al, 2008; Metcalf et al, 2010). Por possuir atividade elastolítica, sugeriu-se que o aumento de catepsina S possa estar relacionado às quebras na estrutura da elastina encontradas na aorta desses animais.

Um aumento na atividade de catepsina K foi demonstrado em peixe-zebra com mucolipidose, uma DL que acumula GAG pela deficiência na enzima que fosforila as enzimas lisossômicas. Esse aumento foi associado a defeitos na cartilagem destes animais, sendo importante para o metabolismo do colágeno e morfogênese (Petrey et al, no prelo).

Tabela 2: Envolvimento de catepsinas na patogênese de algumas doenças.

Doença	Catepsinas	Evidência em animais	Evidência em humanos
Aterosclerose	K, L e S	Nocaute dos genes produziu fenótipos atenuados em animais apoE$^{-/-}$.	Catepsinas são expressas em células de músculo liso e endotélio e macrófagos em lesões ateroscleróticas.
Câncer e metástases	B, F, H, K, L, V, S e X/Z	Nocautes mostram envolvimento em inflamação associada ao tumor e em angiogênese	Estão superexpressas em diversos carcinomas e são associadas a um pior prognóstico.
Obesidade e diabetes	K, L e S	Deleção de CtsK e L previnem obesidade e melhoram o metabolismo de glicose.	Altos níveis de CtsS foram associados a diabetes.
Artrite reumatóide, osteoartrite	B, L, K, S	Inibição de catepsinas foi benéfica em alguns modelos animais, com algumas divergências.	São expressas em células da sinóvia bem como macrófagos, contribuem para a destruição tecidual.
MPS	B, K, S, Z	Aumento na expressão e atividade na aorta, aumento do mRNA no córtex cerebral	Sem estudos publicados

(Adaptado de Reiser et al, 2010). Abreviações: Cts-catepsina

Ainda, o aumento no mRNA de catepsina B, S e Z já foi demonstrado no cérebro de animais com MPS IIIB, assim como na MPS I (Ohmi et al, 2003), embora a repercussão clinica destes achados nunca tenha sido investigada. O aumento dos níveis de mRNA das catepsinas nas MPS e outras DL pode ser explicado pela ativação do fator de transcrição EB (TFEB), que ocorre na presença de acúmulo de substâncias no lisossomo e tem como alvo genes que controlam a biogênese e função de novos lisossomos (Sardiello et al, 2009). No entanto, esse aumento na transcrição de catepsinas e o aumento na permeabilidade da membrana lisossomal (Pereira et al, 2010)

podem exacerbar os efeitos destas proteases, desencadeando a degradação de substâncias importantes, como a elastina e o colágeno.

Outras proteases também parecem estar superexpressas nas MPS, incluindo as metaloproteinases de matriz (MMP) que são ativas em pH neutro e também possuem uma série de funções. Evidências de superexpressão de MMP-12 na aorta de animais com MPS I e VII (Metcalf et al, 2010), bem como de MMP-2 e MMP-9 nos condrócitos de animais com MPS VI e VII (Simonaro et al, 2005) já foram descritas. No entanto, o mecanismo pelo qual esta expressão aumentada acontece não é conhecido.

Ativação do sistema imune e vias inflamatórias

Até pouco tempo acreditava-se que o acúmulo de GAG se restringia apenas ao interior dos lisossomos. Porém experimentos de co-localização demonstraram sua presença também fora das células (Ohmi et al, 2011). A partir disto, uma das correntes que tentam explicar algumas manifestações das MPS que tem ganhado mais força nos últimos anos é a ativação do sistema imune (principalmente o sistema imune inato) pelos GAG não degradados ou parcialmente degradados (Ausseil et al, 2008). O sistema imune inato engloba as defesas ditas não-especificas do organismo, que não envolvem a formação de anticorpos. Entre estas estão incluídas as células fagocitárias (neutrófilos, células NK e macrófagos) e o sistema complemento.

O sistema complemento é composto por uma série de proteínas que reconhecem diversos ligantes, incluindo glicosaminoglicanos (Zaferani et al, 2011) e desencadeiam uma série de reações de clivagem proteolítica, que tem como pontos finais a liberação de duas anafilotoxinas (C3a e C5a) bem como a formação do complexo de ataque à membrana (MAC), que é formado na parede do organismo invasor e ocasiona sua morte (Janeway et al, 2001). O sistema complemento pode ser ativado por 3 vias diferentes, que estão descritas resumidamente na figura 2.

A via clássica é iniciada pela ligação de uma IgG ou IgM ao antígeno, embora vírus e bactérias gram-negativas também possam ativar esta via. Ocorre então a ativação de C1q, que ativa C1r, que por sua vez ativa C1s, que cliva C4 em C4a e C4b. Este último liga-se ao C2 e após nova clivagem forma C4b2a que serve como C3 convertase para esta via. A ativação de C3, após novas clivagens, forma C4b2a3b, que é a C5 convertase desta via. Ocorre então a liberação de C5a e a formação do MAC, com a ligação do C5b ao C6, C7, C8 e C9 (Holst et al ,2012).

A segunda forma de ativação do sistema complemento é pela via alternativa. Nela, ocorre hidrólise espontânea do componente C3, que se liga à proteína plasmática fator B, que é clivado pelo fator D, que gera C3Bb, que pode clivar mais C3 em C3a e C3b, que novamente se liga ao fator B, formando C3bBb, que após novas clivagens cliva C5 a C5a e C5b, que se liga às demais moléculas formando o MAC (Horst et al, 2011).

A terceira forma de ativação do sistema complemento é pela via das lectinas, que utiliza uma proteína estruturalmente semelhante à C1q da via clássica, chamada lectina ligadora de manose (MBL). Estas se complexam com duas serinas proteases, a MASP-1 e MASP-2, que é ativada para clivar C4 e C2, originando C4b2b, que é a mesma C3 convertase da via clássica (Degn et al, 2011).

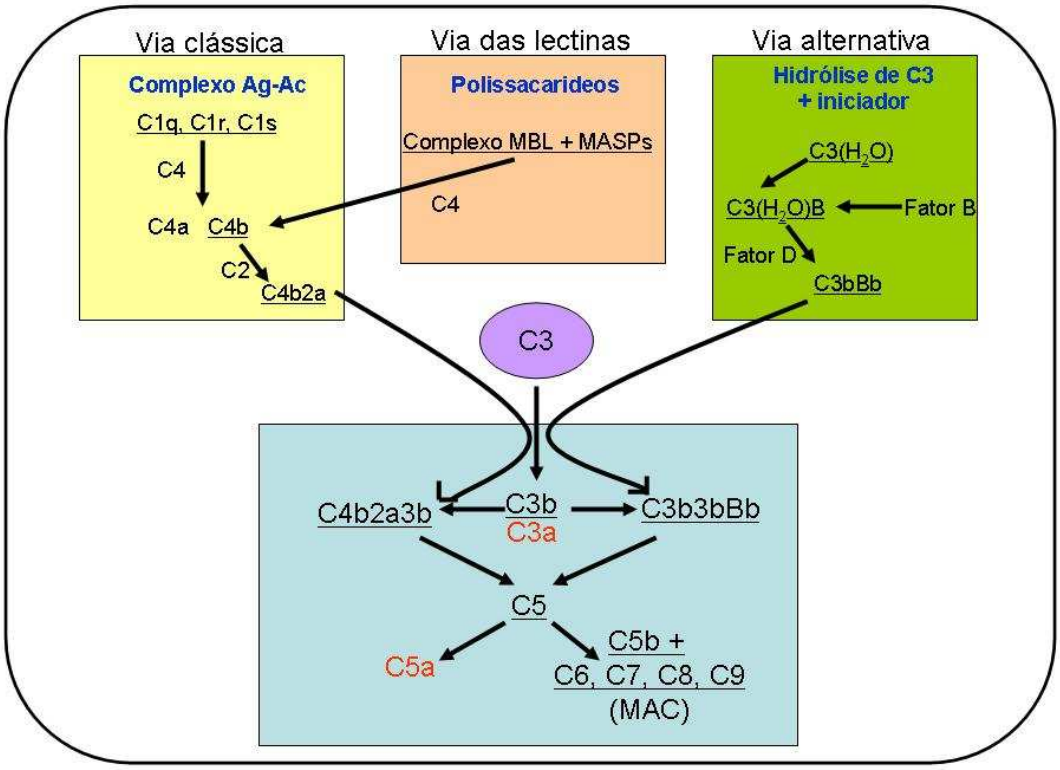

Figura 2: Esquema de vias de ativação do sistema complemento. Escrito em azul encontra-se o principal ativador de cada via. Em vermelho estão indicadas as anafilotoxinas. Embora sejam ativados por mecanismos diferentes, o final da via (conhecido como fase lítica) é comum a todas elas, e o objetivo sempre é formar as anafilotoxinas, que recrutarão células de defesa, e formar o complexo de ataque à membrana, cujo papel é a opsonização da membrana celular do invasor. Abreviaturas: Ac-anticorpo; Ag-Antigeno; MBL- lectina ligadora de manose; MAC- complexo de ataque à membrana; MASP- serina protease associada à manose.

Existem alguns achados inicias que indicam que o sistema complemento possa estar de alguma forma ativado nas MPS. Por exemplo, experimentos de microarray indicam a superexpressão de genes do sistema complemento no córtex cerebral de camundongos com MPS IIIB e MPS I (Ohmi et al 2003), bem como em células da sinóvia de ratos com MPS VI (Simonaro et al, 2008). No entanto, este aspecto nunca foi profundamente investigado.

A ativação do sistema imune em modelos animais de MPS tem sido estudada principalmente no cérebro. Estudos iniciais verificaram um aumento de astrócitos no córtex de animais com MPS I e IIIB (Ohmi et al, 2003). Posteriormente, di Rosário e colaboradores (2009) sugeriram que a patogênese da doença cerebral da MPS IIIB envolvia diversas células do sistema imune, incluindo células T, B e glia. Além disso, demonstraram que células T no baço estavam ativadas nesse modelo animal, e sugeriram um componente auto-imune participando da doença, o que foi reforçado num estudo posterior do mesmo grupo (Killedar et al, 2010). Ainda, ao tratar animais com prednisolona, foram capazes de diminuir a progressão da doença, realmente sugerindo que o sistema imune e a ativação de vias inflamatórias são um componente importante da mesma.

Não só a ativação de células do sistema imune tem sido descrita nas MPS, mas também a liberação de moléculas relacionadas ao processo de inflamação. Diversos trabalhos tem demonstrado elevação dos níveis de fator de necrose tumoral alfa (TNF-α), interleucinas e ativação de vias de transdutores de sinal e ativadores de transcrição (STAT) em diversos órgãos de animais com mucopolissacaridose (Simonaro et al, 2005; Ma et al, 2008; Metcalf et al, 2010), mesmo quando não existe um infiltrado inflamatório tecidual importante.

Para explicar esta ativação de vias inflamatórias, Ausseil et al (2008) realizaram uma série de experimentos, demonstrando que os GAG parcialmente degradados presentes na urina de pacientes com MPS IIIB eram capazes de ativar células da microglia através da via do receptor toll-like tipo IV (TLR-4), e que duplos nocaute (MPS IIIB também nocautes para TLR-4) tinham menores níveis de citocinas inflamatórias. Postulou-se então a hipótese que os GAG não degradados ou parcialmente degradados nas MPS eram capazes de ativar a via do TLR-4.

A via dos TLR está envolvida na defesa do organismo contra patógenos, sendo uma ativadora do sistema imune inato. O TLR especificamente reconhece lipopolissacarídeos presentes na parede de bactérias gram-negativas, sendo capaz de

produzir citocinas inflamatórias a partir da sua ativação (Ausseil et al, 2008). Um segundo estudo foi desenvolvido em camundongos MPS VII, nocautes também para o TLR-4 (duplo nocaute, *Gusb*$^{-/-}$*Tlr4*$^{-/-}$). Estes animais apresentaram ossos longos maiores que os MPS VII, mostrando um papel do TLR também na doença óssea (Simonaro et al, 2010), sugerindo que esta via possa estar envolvida em diversos aspectos das MPS.

Alterações em vias de sinalização

Os GAG possuem uma série de ligantes, sendo capazes de modular diversas citocinas e processos celulares. Dessa forma, é razoável predizer que a não-degradação dos mesmos ou sua degradação incompleta possa influenciar distintos processos e vias de sinalização. Além dos trabalhos já citados que mostram ativação de vias como o TLR-4, outros trabalhos demonstraram alterações em processos celulares distintos. Por exemplo, Pan e colaboradores (2005) provaram que o heparan sulfato parcialmente degradado obtido de pacientes com MPS I era capaz de afetar a ligação do fator de crescimento de fibroblastos tipo 2 (FGF-2) com seu receptor, diminuindo a proliferação e aumentando a morte celular em células multipotentes de pacientes com MPS I.

Um estudo seguinte demonstrou que o heparan sulfato acumulado em células de pacientes com MPS I também leva a uma alteração na via de sinalização da proteína morfogenética óssea 4 (BMP-4), podendo contribuir para anormalidade ósseas encontradas nestas doenças (Khan et al, 2008) .

Ainda, alterações nas vias controladas por cinases, incluindo ativação de janus cinases (JAK1 e JAK 2) e cinase ativadora de mitose (MAPK), bem como alterações nas fosforilação de transdutores de sinal e ativadores de transcrição (STAT-1 e STAT-3) já foram demonstradas em órgãos como ossos e aorta de animais com MPS I e VII (Ma et al, 2008; Metcalf et al ,2010), sugerindo que realmente diversos processos celulares e vias de sinalização possam estar alteradas.

Alterações em outros processos celulares

A não degradação de GAG parece alterar uma série de processos celulares, principalmente os que envolvem funções do lisossomo e metabolismo energético. Um destes processos, que tem sido descrito não só nas MPS, mas também em outras DL, é o processo de autofagia. O processo de autofagia é importante para a degradação de

organelas disfuncionais e obtenção de energia, principalmente no estado de jejum. Em um estudo pioneiro, Settembre e colaboradores (2008) demonstraram que a fusão do lisossomo com o autofagossomo está prejudicada nas DL, o que torna o processo de autofagia falho nestas células. Inicialmente demonstrado em células de pacientes com MPS IIIA, posteriormente identificou-se que outras MPS como a MPS I, II e IIIB também possuem problemas de autofagia (Ohmi et al, 2011).

Ainda, a não degradação de GAG parece levar a uma série de adaptações metabólicas, sendo que animais com MPS I apresentam maior consumo de comida (Woloszynek et al, 2007) e peso após os primeiros meses de vida (Pan et al, 2008). Também em camundongos MPS I, embora a absorção de lipídios seja normal, a deposição de gordura é maior que em animais normais (Woloszynek et al, 2007). Alterações em níveis de aminoácidos sugerem uma alteração no metabolismo intermediário nas MPS, possivelmente porque a manutenção da síntese de GAG num cenário de não-reciclagem e de problemas em processos como a autofagia leva a alterações na utilização de energia pelas células (Woloszynek et al 2009).

Todas as alterações citadas evidenciam que, embora sejam causadas por mutações em um único gene, as repercussões clínicas encontradas nas MPS tem suas origens em múltiplos e complexos processos, e o conhecimento dos mesmos pode levar a tratamentos mais eficientes.

Modelos animais de MPS

Muito sobre os mecanismos patogênicos nas MPS foi descoberto graças aos modelos animais disponíveis. Eles foram, em sua maioria, criados em laboratório através da interrupção do gene de interesse em células-tronco embrionárias. No entanto, alguns modelos animais aconteceram de forma espontânea e foram identificados através de observações fenotípicas e subseqüentemente por confirmação bioquímica e molecular.

Hoje já existem modelos em camundongos para a MPS I (Clarke et al, 1997; Ohmi et al, 2003; Wang et al, 2010); MPS II (Jung et al, 2010); MPS IIIA (Bhaumik et al, 1999); MPS IIIB (Li et al, 1999); MPS IVA (Tomatsu et al, 2005); MPS VI (Evers et al, 1996), MPS VII (Sands e Birkenmeyer, 1993) e MPS IX (Martin et al, 2008). Apenas os modelos de MPS VII e IIIA ocorreram de forma espontânea, sendo o de MPS VII por uma deleção de 1 base, resultando num códon de terminação prematuro.

Outros modelos animais já foram descritos em animais maiores, incluindo ratos (MPS VI) gatos (MPS I, VI) e cachorros (MPS I, IIIA, IIIB e VII), entre outros (Haskins, 2007).

É inegável a importância desta ferramenta no estudo de mecanismos patogênicos, bem como no desenvolvimento de tratamentos. Tomando-se como exemplo a MPS I, já existem 3 modelos animais murinos que mimetizam a doença. O primeiro modelo foi criado em 1997 (Clarke et al, 1997) através da interrupção do éxon 6 do gene da *Idua*. Como resultado, um modelo animal que mimetiza a Síndrome de Hurler foi produzido, com aumento nos níveis de GAG na urina e em diversos tecidos, e atividade indetectável de IDUA. Posteriormente, em 2003, o segundo modelo murino de MPS I foi publicado pelo grupo da Dra Elizabeth Neufeld, na Califórnia (Ohmi et al, 2003). De maneira similar, o gene da *Idua* foi interrompido no éxon 6 com a inserção de um gene de resistência à neomicina em sentido inverso (figura 3), resultando novamente em animais com a síndrome de Hurler, com fenótipo similar ao primeiro modelo desenvolvido. O terceiro modelo murino de MPS I foi recentemente descrito (Wang et al, 2010) e é na verdade um modelo *knock in,* no qual foi inserida a mutação mais comum encontrada em pacientes (W402X) que está associada ao fenótipo mais grave da doença (Síndrome de Hurler). O objetivo dos pesquisadores foi testar terapias que sejam potencialmente eficazes apenas em mutações sem sentido, como o uso de gentamicina visando à tradução alternativa.

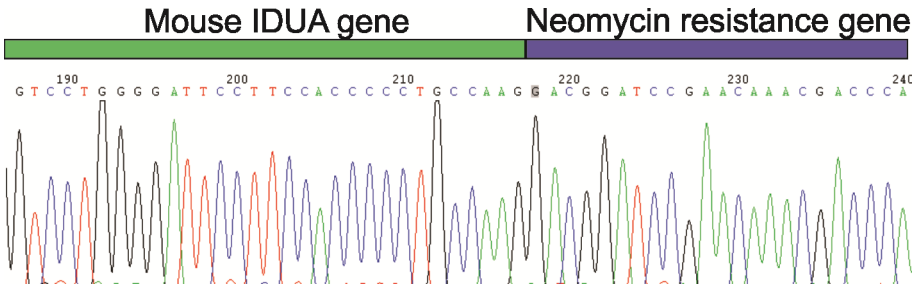

Figura 3: Eletroferograma mostrando o seqüenciamento do gene *Idua* em animais nocaute produzidos pelo grupo da Dra Neufeld (Ohmi et al, 2003). A barra superior em verde representa a seqüência do gene *Idua*, enquanto que a barra roxa representa a posição onde ocorre a interrupção de *Idua* e se inicia a seqüência do gene de resistência a neomicina.

Numa série de trabalhos subseqüentes à criação dos modelos animais, estudos foram realizados focando-se em sua caracterização, mecanismos causadores de doença e desenvolvimento de novas terapias. Estes trabalhos identificaram, por exemplo, que animais com MPS I possuem o miocárdio dilatado bem como redução da fração de ejeção aos 10 meses de idade (Jordam et al, 2005) além de espessamento das válvulas cardíacas (Braulin et al, 2006) e quebras nas fibras de elastina da aorta (Ma et al ,2008). Com relação à doença cerebral, foram descritas a ativação da microglia no córtex (Ohmi et al, 2003) e alterações em comportamentos como memória aversiva (Reolon et al, 2006) e não-aversiva (Pan et al, 2008). Outros trabalhos descreveram alterações ósseas como o espessamento do fêmur, nos olhos (morte de células retininianas e alterações no eletroretinograma) e alterações na função auditiva (Metcalf et al, 2010). Estes animais também foram usados para verificar eficácia de terapias, como por exemplo, a terapia gênica (Osbourne et al, 2011; Wolf et al, 2011a); terapia de reposição enzimática (Boado et al, 2011) e transplante de células-tronco hematopoiéticas (Wolf et al, *in press*).

Por fim, o estudo de modelos animais maiores permite investigar estruturas que são muito pequenas nos camundongos, bem como auxiliam no escalonamento de dose de terapias (Haskins et al, 2007). O presente trabalho focou-se principalmente no estudo das mucopolissacaridoses tipo I e VII, que serão descritas mais detalhadamente a seguir.

Mucopolissacaridose tipo VII

A MPS VII, ou síndrome de Sly, é uma das formas de MPS mais raras, causada pela deficiência de beta-glicuronidase (GUSB). A deficiência de GUSB leva ao acúmulo de heparan, dermatan e condroitin sulfato (Neufeld e Muenzer, 2001). Os sintomas clínicos da MPS VII incluem retardo mental, opacidade de córnea, organomegalia, dilatação aórtica, disostose multiplex, entre outros. Diversos pacientes desenvolvem hydrops fetalis (Venkat-Raman et al, 2006) e morrem ao nascimento ou mesmo durante a gestação, o que causa um subdiagnóstico da doença. Os pacientes com a forma atenuada da doença sobrevivem até o início da vida adulta. O diagnóstico é feito pela medida da atividade enzimática em leucócitos ou fibroblastos cultivados, e até o momento não existe tratamento para a MPS VII, apenas medidas de suporte. Apesar de rara, diversos estudos têm sido desenvolvidos nos modelos murino e canino de MPS VII, uma vez que a doença se apresenta mais rapidamente e de forma mais pronunciada

nestes animais, comparado a outras formas de MPS. Muitos resultados obtidos nos estudos em modelos animais de MPS VII foram confirmados depois em outros modelos (Metcalf et al, 2010), como a MPS I, sugerindo que os modelos animais dessa doença sejam muito úteis para o estudo de mecanismos patogênicos das MPS.

Mucopolissacaridose tipo I

A MPS tipo I é considerada a doença lisossômica prototípica, por apresentar envolvimento progressivo e multisistêmico. Ela é causada por mutações que afetam o gene da alfa-L-iduronidase (*IDUA*), localizado em seres humanos no cromossomo 4 (4p16.3). O gene humano da IDUA possui 14 éxons e um total de 2.1 kb, que originam uma proteína de 653 aminoácidos (Scott et al, 1991). Esta proteína possui um tamanho inicial de 73 kDa, que é processada a uma forma madura de 69 kDa.

A IDUA é uma glicosidase, cuja função é a hidrólise de resíduos ácidos alfa-L-idurônicos dos GAG heparan e dermatan sulfato (figura 4). Os GAG são cadeias polissacarídicas ácidas compostas por repetições de dissacarídeos ligados a um núcleo protéico, que formam os proteoglicanos. O heparan sulfato é composto principalmente por ácido glicurônico e N-acetilglicosaminas, enquanto o dermatan sulfato é formado por ácido-L-idurônico e N-acetilgalactosamina sulfatada (Neufeld and Muenzer, 2001). Após a ação da IDUA, o processo de degradação dos GAG continua através de reações seqüenciais de hidrólise, formando monossacarídeos e sulfato inorgânico (Hopwood e Morris, 1990).

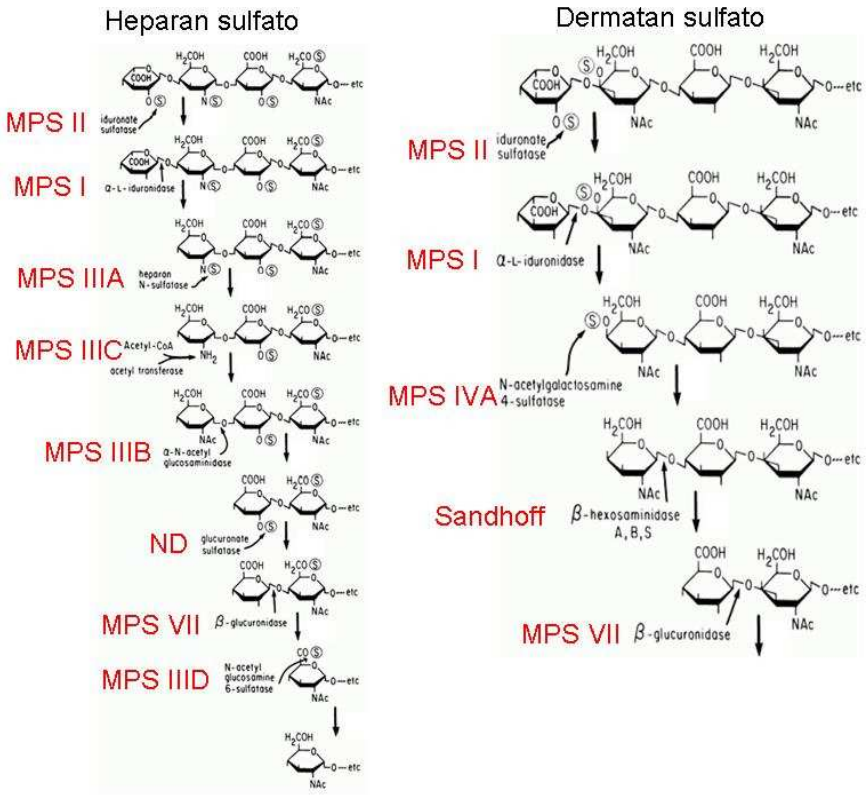

Figura 4: Via de degradação do heparan sulfato e do dermatan sulfato. Em vermelho estão indicadas as doenças causadas pela deficiência de cada enzima. ND- não-determinado. Sandhoff- a doença de Sandhoff é outra DL, também conhecida como gangliosidose GM2. Adaptado de Neufeld e Muenzer (2001).

Esta síndrome possui uma prevalência estimada de 1:75.000 em Portugal e 1:88.000 na Austrália (Fuller et al, 2006). No Brasil não existe um estudo exato de prevalência, mas a rede MPS Brasil (uma rede formada pela parceria de centros brasileiros que atendem pacientes com MPS) já diagnosticou 93 novos casos entre abril de 2004 e dezembro de 2010 (http://www6.ufrgs.br/redempsbrasil/), sendo uma das MPS de maior prevalência no país.

O diagnóstico definitivo de MPS I se dá através da dosagem da atividade de alfa-L-iduronidase em plasma, fibroblastos ou leucócitos. Testes de screening como níveis urinários de GAG também auxiliam no diagnóstico, e podem ser utilizados para acompanhamento de eficácia de tratamento. Geralmente parte-se de uma suspeita pelos sinais clínicos, e após os testes de screening iniciais, realiza-se a medida da atividade enzimática. Pode ainda ser realizada a pesquisa de mutações no gene da IDUA. No entanto, a correlação entre genótipo e fenótipo na MPS I não é 100% precisa, mas geralmente mutações que causam a perda total da atividade enzimática, como mutações

sem sentido, deleções e inserções, levam a um fenótipo mais grave, enquanto mutações de sentido trocado levam a uma atividade residual da enzima e a um fenótipo menos grave. Nos pacientes brasileiros, bem como no resto do mundo, as mutações mais encontradas são mutações que levam a um códon de terminação prematuro (Matte et al, 2003). No Brasil, as mutações mais comuns são a W402X e a P533R.

Embora exista um espectro continuo de fenótipos, os pacientes com MPS I podem ser classificados para fins didáticos e para tomadas de decisões quanto a tratamentos em 3 síndromes, baseados nos seus sinais clínicos: síndrome de Hurler (OMIM # 607014), síndrome de Hurler-Scheie (OMIM # 607015) e Síndrome de Scheie (OMIM # 607016).

A síndrome de Hurler é a forma mais grave de MPS I. Nela, os primeiros sintomas aparecem ao redor de 8 meses de idade e incluem hérnias inguinais, deformidades ósseas e retardo no desenvolvimento mental. Posteriormente outras anormalidades se destacam, e incluem opacificação da córnea, perda de audição devido a problemas de condução e neurosensoriais, e hepatoesplenomegalia. As crianças com síndrome de Hurler também apresentam repetidas infecções pulmonares, causadas por obstrução de vias aéreas. O coração se apresenta dilatado e ocorre espessamento das válvulas cardíacas. Outras anormalidades incluem rigidez articular, baixa estatura e alterações fenotípicas (pele infiltrada, aumento da língua, face característica). Quando não tratados, pacientes com síndrome de Hurler vão à óbito antes dos 10 anos de idade devido a complicações cardíacas ou por infecção respiratória (Neufeld e Muenzer, 2001; Beck, 2003).

Em pacientes com a forma atenuada da MPS I (síndrome de Scheie) não existe retardo mental associado, no entanto anormalidades ósseas, cardíacas e oculares estão presentes. Estes pacientes possuem degeneração de células de retina e glaucoma. Além disso, apresentam comumente apnéia do sono, sendo que em vários casos uma traqueostomia é necessária (Beck, 2003). Ainda, podem apresentar compressão da medula espinhal devido ao acumulo de GAG e espessamento de estruturas (Munoz-Rojas et al, 2008). A sobrevida varia, mas pode chegar até a sexta década de vida.

Pacientes com a forma intermediária (Hurler-Scheie) apresentam alterações somáticas mais precoces e mais graves que os pacientes com a forma Scheie, geralmente sem um envolvimento do sistema nervoso central (Neufeld e Muenzer, 2001).

Tratamentos para a MPS I

Pacientes com MPS I até alguns anos atrás eram tratados apenas com medidas gerais de suporte incluindo fisioterapia (para os problemas articulares e respiratórios), cirurgias (troca de válvulas, síndrome do túnel do carpo, hérnias umbilicais) e medicações, como analgésicos e antibióticos (Valayannopoulos e Wijburg, 2012). No entanto, baseado no conhecimento de que as enzimas lisossômicas podem ser secretadas e captadas por células vizinhas via receptores de manose-6-fosfato, foram desenvolvidos dois principais tratamentos. Estes tratamentos são o transplante de células-tronco hematopoiéticas (TCTH) e a terapia de reposição enzimática (TRE). Além desses, outras abordagens para a MPS I estão sendo testadas em fase experimental ou em ensaios clínicos preliminares, e suas características estão citadas no quadro 1.

O primeiro TCTH realizado com sucesso para MPS I aconteceu no início da década de 1980 (Hobbs et al, 1981). Essa abordagem envolve uma ablação da medula do paciente, seguida por um transplante não autólogo. O racional do TCTH na MPS I é que a reconstituição do sistema hematopoiético permite que as células transplantadas, produtoras da enzima, circulem e a distribuam aos diferentes órgãos e sistemas do corpo. Este é o tratamento de escolha para crianças com a forma mais grave da MPS I que tenham menos de 2 anos de idade, para que se possa preservar as funções neurológicas. No entanto, principalmente em países com o Brasil, isso muitas vezes não é possível devido ao diagnóstico tardio (Vieira et al, 2008).

Embora existam casos de transplante exitoso que demonstrem pouca efetividade em longo prazo na literatura (Grigull et al, 2009), geralmente este tratamento é capaz de prolongar a sobrevida dos pacientes, reduzir a boa parte das alterações somáticas, bem como o dano cognitivo. No entanto, os estudos parecem concordar que alterações esqueléticas, visuais e nas válvulas cardíacas têm pouco beneficio com essa abordagem (Aldenhoven et al, 2008). Ainda, pelo menos 60% dos pacientes desenvolvem algum tipo de complicação referente ao procedimento, incluindo óbito em alguns casos (Boelens et al, 2009).

Quadro 1: Principais tratamentos em uso ou em desenvolvimento para a MPS I.

Tratamento	Principio	Vantagens	Desvantagens	Andamento
Reposição enzimática	Infusão i.v. da enzima recombinante, que é captada pelos tecidos via receptor M6P.	-Reduz manifestações viscerais e melhora qualidade de vida; - Pode ser aplicado intratecal para o tratamento das complicações do SNC.	-Alto custo e formação de anticorpos; -Eficácia limitada em válvulas, ossos; -Necessidade de infusões repetidas; - Não ultrapassa a BHE quando aplicado por via periférica;	Aprovado para uso clínico
Transplante de Células-tronco hematopoiéticas	Transplante não-autólogo de células $CD34^{+}$.	-Eficaz em diversos aspectos da doença. -Atravessa a BHE.	- Quimerismo; -Procedimento arriscado (alta morbidade e mortalidade associadas);	Aprovado para uso clínico
Inibição da síntese de substrato	Uso de moléculas como a genisteína, que inibem a síntese de GAG.	- Atravessa a BHE; - Terapia administrada via oral;	- Eficácia não-comprovada; - Não corrige o problema da não-degradação de GAG;	Aprovado para uso clínico.
Chaperonas farmacológicas	Pequenas moléculas que estabilizam enzimas com mutações de ponto até o lisossomo.	- Tratamento via oral;	-Funciona apenas em pacientes com certas mutações de ponto. - Restabelece apenas função residual;	Estudos pré-clínicos.
Tradução alternativa	Fármacos (como a gentamicina) capazes de substituir um códon de terminação prematuro por um aminoácido aleatório.	- Passa a BHE; - Tratamento por via oral; - Baixo custo;	- Eficácia limitada; - Pode ser usado apenas em mutações sem sentido;	Estudos pré-clínicos;
Terapia gênica	Inserção de uma cópia normal do gene da IDUA usando vetores.	- Tratamento de injeção única; - Mais barato que TRE;	- Mutagênese insercional; - Silenciamento do transgene;	Estudos pré-clínicos;

O segundo tratamento disponível para MPS I é a TRE. Esta terapia foi aprovada pelo FDA em 2003 (Aldurazyme®, Genzyme Corporation e BioMarin Pharmaceutical, USA) e consiste na administração, por via intravenosa, de uma versão recombinante da enzima alfa-L-iduronidase. A administração pode ser semanal (dose de 0.6 mg/kg de peso corporal) ou quinzenal (1.2 mg/kg de peso) (Giugliani et al, 2009). Nos ensaios clínicos, observou-se uma redução no volume do fígado e baço, bem como uma melhora na capacidade pulmonar e diminuição na excreção de GAG na urina (Sifuentes et al, 2007). Outros parâmetros observados em estudos posteriores mostraram resultados mais conflitantes. Enquanto os estudos iniciais relataram estabilização ou melhora nos movimentos articulares (Sifuentes et al, 2007), estudos mais recentes descrevem pouca ou nenhuma melhora na amplitude de movimentos, sugerindo pouca eficácia da TRE sobre o dano articular (Cox-Brinckman et al, 2007; Tylki-Szymanska et al, 2010). Resultados dissonantes também aparecem com relação à função do miocárdio, com alguns trabalhos demonstrando melhoras na função (Clarke et al, 2009; Harada et al, 2011), enquanto outros demonstram pouca eficácia (Sifuentes et al, 2007). No entanto, assim como no TCTH, algumas estruturas, mais notadamente as válvulas cardíacas, os ossos e, por dados em modelos animais, a aorta, não melhoram com a TRE (Sifuentes et al , 2007; Ma et al, 2008; Valayannopoulus et al, 2011). Outro órgão que se acredita não apresentar melhoras com a TRE é o cérebro, uma vez que a enzima não passa a barreira hemato-encefálica. Para contornar esse obstáculo, infusões da enzima pela via intratecal têm sido propostas nos últimos anos, e embora tenham se mostrado seguras, sua eficácia em longo prazo ainda é incerta (Munoz-Rojas et al, 2008). O tratamento com TER intra-venoso precoce conseguiu melhorar o estado clinico de 94% dos pacientes, com redução da incidência de hipertrofia cardíaca de 53% para 17%, e desenvolvimento intelectual normal no primeiro ano de acompanhamento (Wraith et al, 2007). No entanto nunca foi realizada uma comparação sistemática dos benefícios do tratamento precoce com o tratamento iniciado mais tardiamente.

Outros problemas da TRE também devem ser salientados. Entre eles, o custo desta terapia (cerca de meio milhão de reais/ paciente/ano) faz com que os pacientes no Brasil tenham que constantemente entrar na justiça para garantir acesso à enzima, o que é um processo que esbarra em questões burocráticas, e pode determinar períodos de interrupção do tratamento. Além disso, o tratamento de poucos pacientes gera um gasto muito alto ao sistema publico de saúde. A necessidade de infusões repetidas, que afetam a qualidade de vida dos pacientes e de suas famílias também é um problema. Por fim, a

formação de anticorpos contra a enzima, que ocorre em cerca de 90% dos pacientes, leva à diminuição da eficácia da terapia (Brooks et al, 2003). Todas estas limitações e desvantagens têm levado a busca de novas terapias, como a terapia gênica.

Terapia gênica

Conceito

A terapia gênica permite a inserção de material genético em células eucarióticas, aumentando, corrigindo ou inibindo a expressão de genes de interesse. Embora inicialmente desenvolvida para doenças monogênicas, hoje existem protocolos de terapia gênica para as mais diversas doenças, incluindo câncer (Cervantes-García et al, 2008), processos infecciosos (Wayengera, 2011) e doenças neurodegenerativas (Morgenstern et al, 2011), entre outros.

Existem duas principais formas de se realizar terapia gênica. Pode-se fazer uma transferência gênica *in vivo,* na qual o vetor carregando o gene de interesse é inserido no paciente, ou a transferência gênica pode ser realizada *ex vivo* coletando-se as células, modificando-as geneticamente em laboratório, e introduzindo as células modificadas no paciente. Cada uma possui suas vantagens, sendo que a escolha por um ou outro método depende basicamente das características do estudo (tipo de doença, características do vetor, segurança do procedimento). Para a MPS I existem protocolos pré-clínicos que usam a abordagem *in vivo* (Metcalf et al, 2010), bem como *ex vivo* (Visigalli et al, 2011).

O gene de interesse é inserido nas células, juntamente a outras seqüências que garantem a sua funcionalidade, como promotor, sitio de poliadenilação, seqüências *enhancer*, etc. Os dois principais métodos de transferência gênica são vetores virais e os métodos não virais.

Vetores virais

Valendo-se de propriedades obtidas por processos evolutivos, os vírus ainda são a forma mais eficiente de se entregar um transgene a uma célula. Modificações na estrutura dos vírus são necessárias para retirar a sua infectividade e tornar a terapia mais segura. Geralmente o genoma viral é reconstruído através de diferentes plasmídeos

numa linhagem celular empacotadora, que produz então vírus incapazes de se replicar, contendo o transgene de interesse. Estes são purificados e podem ser utilizados *in vitro* ou *in vivo*.

Dentre os diferentes tipos de vírus, os mais utilizados são os adenovírus, os vírus adeno-associados e os retrovírus, embora protocolos baseados em outros tipos de vírus, como os lentivírus (que são da família dos retrovírus) e os vírus herpes-simples, também tenham considerável destaque. A tabela 3 descreve as principais características de cada sistema viral.

Os adenovírus têm como característica uma capacidade de transdução bastante rápida e eficiente, porém, não se integram no genoma da célula, tendo sua expressão reduzida algumas semanas após o tratamento. Devido a estas propriedades, são bastante utilizados em estudos envolvendo tumores (Trask et al, 2000). Os adenovírus são bastante imunogênicos, já tendo sido descrito casos na literatura de óbito de pacientes tratados com este tipo de vetor por uma resposta imune exacerbada (Wilson, 2009). Por suas características, não são os melhores candidatos para uma doença como a MPS I.

Na última década, os vetores baseados em vírus adeno-associados (AAV) tem ganhado espaço devido a características peculiares. São vírus pequenos, da família dos parvovírus (cerca de 5 kb), não-patogênicos, que via de regra não se integram no genoma da célula transduzida, embora isso possa acontecer (Donsante et al, 2007). Porém, eles formam concatâmeros no núcleo, tendo uma expressão sustentada. Recentemente estudos envolvendo o sorotipo AAV2/8 foram capazes de manter níveis terapêuticos de fator IX por pelo menos 6 meses, revertendo o fenótipo hemofílico de pacientes (Nathwani et al, 2011). Estes vetores têm demonstrado uma boa eficácia em modelos animais de MPS I, de forma que são promissores no tratamento desta doença (Elinwood et al, 2011).

Ainda, outra família de vírus bastante atraente para as mucopolissacaridoses são os retrovírus. De estrutura viral mais simples, estes vírus se integram de maneira bastante eficiente no genoma de células em divisão, gerando uma transdução estável. Como principal desvantagem, por se integrar no genoma, podem ativar oncogenes, conforme já descrito em pacientes com imunodeficiência severa combinada (Hacein-Bey-Abina et al, 2008). Devido a estas limitações, alterações na estrutura dos retrovírus têm sido descritas para aumentar a sua segurança. Um construto alternativo é a geração de vetores chamados auto-inativantes (SIN, figura 5). Nesta abordagem, parte da região 3` da porção LTR (*long term repeat*, uma região com atividade promotora e de

enhancer) é deletada. Durante a transcrição reversa, esta deleção é copiada para a região 5`-LTR, retirando a atividade promotora da região LTR e deixando o gene de interesse apenas sob controle do promotor interno (Maetzig et al, 2011). Os retrovírus têm sido amplamente investigados para o tratamento da MPS I em modelos animais caninos (Traas et al, 2007) e murino (Herati et al, 2008; Zheng et al, 2004), tendo sido o vetor que atingiu maiores níveis séricos da enzima. Existe ainda um trabalho que usa um vetor auto-inativante, que também demonstra boa eficácia, embora inferior ao vetor com a porção LTR intacta (Metcalf et al, 2010).

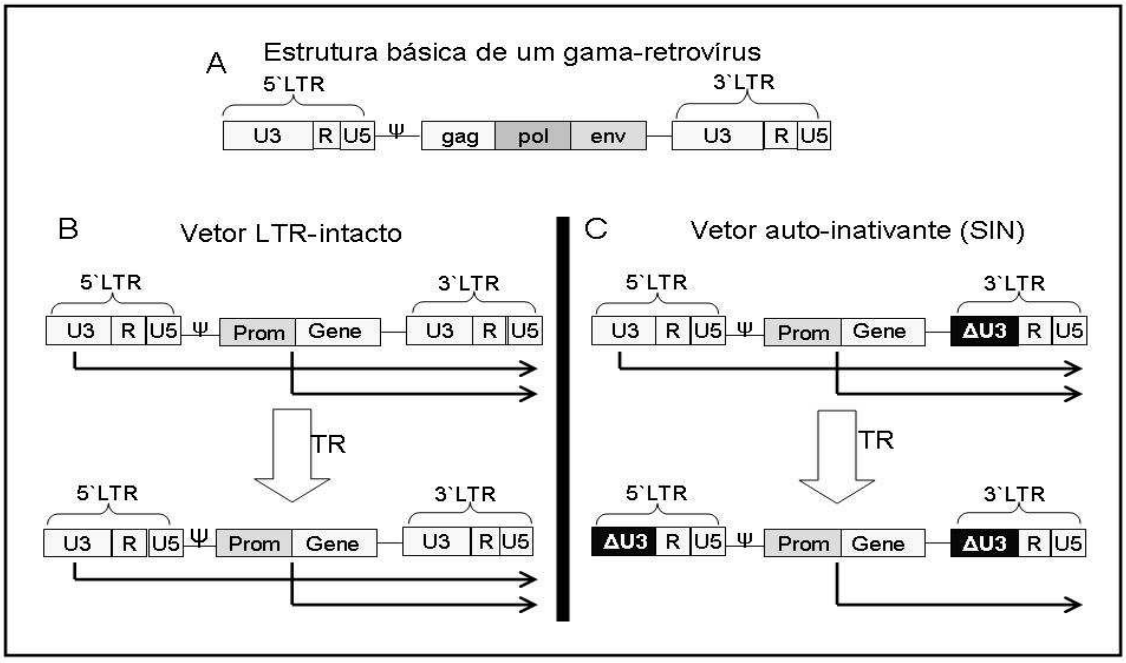

Figura 5: Construtos baseados em retrovírus. A) Esquema do genoma de um gama-retrovírus, contendo as duas LTR (compostas pelas regiões U3, R e U5), o sinal de encapsidação ψ e os genes *gag* (codifica proteínas estruturais), *pol* (polimerase) e *env* (proteínas do envelope viral). Para construir um vetor retroviral, os genes *gag* e *pol* são dados num segundo plasmídeo e o gene *env* num terceiro plasmídeo que não possuem o sinal de encapsidação (não mostrado). O sinal ψ é mantido apenas no plasmídeo que contém o gene de interesse (mostrado em B e C). B) Construto com a LTR intacta. Note que mesmo com a inserção de um promotor (prom) interno, as LTR mantém sua atividade promotora e de *enhancer*, mesmo apos a transcrição reversa (TR), o que pode ativar oncogenes. Os produtos de transcrição são indicados pelas setas escuras. C) A versão auto-inativante do construto (SIN). Neste construto, parte da 3`LTR está deletada (ΔU3). No momento da transcrição reversa esta região é copiada na 5`LTR, inativando-a. Desta forma, a transcrição do gene de interesse fica controlada apenas pelo promotor interno.

Métodos não-virais de transferência gênica

Devido principalmente aos problemas com segurança envolvendo os vetores virais apresentados anteriormente, diversas técnicas envolvendo terapia gênica não-viral tem sido estudadas. Entre as principais, podem ser citados o uso de lipossomas e outras nanoestruturas, bem como o uso de transposons e a encapsulação celular, que são discutidos em detalhes no capitulo de livro *"Non-viral gene therapy approaches for lysosomal storage disorders"* que faz parte do corpo desta tese (ver anexos).

Embora mais seguros, as principais limitações do uso de vetores não-virais para terapia gênica estão relacionadas a sua baixa eficiência de transfecção e ao silenciamento do transgene. Para superar essas desvantagens, diversas técnicas têm sido estudadas, e entre elas destacamos o uso de células encapsuladas.

Nesta abordagem, uma linhagem celular é transfectada *ex vivo* com um plasmideo contendo um gene de interesse, e, após seleção clonal, encapsulada em microesferas poliméricas. Esse polímero deve ser biocompativel e semi-permeável, e entre os principais materiais utilizados, destaca-se o alginato de sódio. As células microencapsuladas liberam grandes quantidades da enzima para o meio extracapsular, podendo ser captadas pelas células deficientes. A abordagem de encapsulação celular previne que as células superexpressando o transgene entrem em contato com células do sistema imune do paciente, permitindo a expressão continuada do transgene por maiores períodos de tempo (Matte et al, 2011).

Estudos prévios relatam o uso de células encapsuladas para a MPS I e MPS II, bem como outras DL (Friso et al, 2005; Matte et al, 2011; Piller-Puciher et al, 2012), com eficácia transitória sobre o acúmulo de GAG. Ainda, estudos de segurança demonstraram a factibilidade do uso das microcapsulas quando implantadas no tecido cerebral de cachorros com MPS (Matte et al, 2011). Portanto, esta abordagem pode ser usada tanto para correção sistêmica, quanto localizada, sozinha ou em combinação com outras terapias. Por todo exposto, esta estratégia se parece promissora para o tratamento de DL, incluindo as MPS.

Tabela 3: Características dos principais vetores utilizados em terapia gênica (adaptado de Walther e Stein, 2000).

Vetor	Tamanho do inserto	Integração	Duração da expressão	Vantagens	Desvantagens
Adenovírus	Até 8kb	Não	Curta	Transdução eficiente	Expressão transitória, imunogênicos
Vírus adeno-associado	≈ 5kb	Raro	Longa	Não patogênico, episssomal, transduz células quiescentes, diferentes sorotipos com tropismos variáveis.	Imunogenicidade, suportam pequenos insertos, dificuldade de produção.
Retrovírus	Até 8kb	Sim	Longa	Integração estável, fácil manipulação do genoma e produção de vírus.	Transduz apenas células em divisão, mutagênese insercional
Lentivírus	Até 10kb	Sim	Longa	Transduz células quiescentes, expressão estável.	Mutagênese insercional.
Vírus Herpes-simples	Até 50kb	Não	Longa no SNC, curta em demais órgãos.	Neurotrópico, comportam grandes insertos.	Risco de recombinação, expressão transitória (exceto no SNC).

OBJETIVOS

Objetivo geral

Esta tese tem como objetivo estudar mecanismos responsáveis pelo fenótipo clínico nas mucopolissacaridoses em órgãos de difícil correção pelas terapias atuais, bem como avaliar novas abordagens para o tratamento destas doenças, baseados em diferentes estratégias de terapia gênica e de reposição enzimática

Objetivos específicos

- Caracterizar a doença cardíaca e valvular em camundongos com MPS I, bem como o possível envolvimento de proteases neste processo.
- Avaliar o papel da MMP-12 e da catepsina S na patogênese da dilatação aórtica em camundongos com MPS VII, bem como o papel do sistema complemento neste processo.
- Caracterizar a progressão da doença articular em camundongos MPS I, estudar mecanismos responsáveis por este aspecto da doença e os efeitos da terapia de reposição enzimática.
- Verificar se camundongos MPS I desenvolvem alterações motoras, bem como idade de início das alterações e possíveis mecanismos para as mesmas.
- Identificar, através de espectrometria de massas, proteínas diferencialmente expressas no hipocampo de camundongos MPS I que possam estar relacionadas à disfunção cognitiva observada nestes animais.
- Produzir cápsulas de alginato contendo células BHK que superexpressem a enzima alfa-L-iduronidase e avaliar a possibilidade de criopreservação destas estruturas.
- Avaliar se o co-cultivo das cápsulas de alginato com fibroblastos de pacientes com MPS I consegue reverter a deficiência enzimática e o acumulo de GAGs nestas células.
- Estudar os efeitos a curto e longo prazo do implante intraperitoneal das células encapsuladas em camundongos MPS I.
- Verificar os efeitos do tratamento por terapia gênica com 2 vetores retrovirais sobre parâmetros comportamentais e histológicos em cérebro e orelha de animais com MPS I; e sobre a aorta de camundongos com MPS VII.
- Comparar a eficácia do tratamento com terapia de reposição enzimática em camundongos MPS I iniciada no início da vida ou em idade adulta.

PARTE II

RESULTADOS

Os resultados da presente tese serão apresentados no formato de 10 artigos científicos. O status de cada manuscrito está apresentado no quadro abaixo.

Manucrito	Status
Heart dilatation in MPS I mice may be mediated by increased cathepsin B activity	A ser submetido para o periódico *Cardiovascular Pathology*
Pathogenesis of aortic dilatation in mucopolysaccharidosis type VII mice may involve complement activation	Publicado na periódico *Molecular Genetics and Metabolism*
Characterization of joint disease in mucopolysaccharidosis type I mice and the effects of enzyme replacement therapy	Submetido ao periódico *Osteoarthritis and Cartilage*
Evidence of a progressive motor dysfunction in MPS I mice	Aceito para publicação no periódico *Behavioural Brain Research*
Shotgun proteomics reveals possible mechanisms for cognitive impairment in Mucopolysaccharidosis type I mice	Manuscrito em preparação para ser submetido para o periódico *Molecular Genetics and Metabolism*
Effects of cryopreservation and hypotermic storage on cell viability and enzyme activity in recombinant encapsulated cells overexpressing IDUA	Publicado no periódico *Artificial Organs*
Recombinant encapsulated cells overexpressing alpha-L-iduronidase correct enzyme deficiency in human mucopolysaccharidosis type I cells.	Publicado no periódico *Cells Tissues Organs*
Intraperitoneal implant of recombinant encapsulated cells overexpressing alpha-l-iduronidase partially corrects visceral pathology in mucopolysaccharidosis type I mice.	Aceito para publicação no periódico *Cytotherapy*
Retroviral vector-mediated gene therapy to MPS I mice improves sensorimotor impairments and other behavioral deficits	Submetido ao periódico *Journal of Inherited Metabolic Disease*
A comparison of enzyme replacement therapy started at birth or at adult age in MPS I mice	Manuscrito em preparação para ser submetido ao periódico *Proceedings of the National Academy os Sciences USA*

Heart dilatation in MPS I mice may be mediated by increased cathepsin B activity

Guilherme Baldo[1,2], Angela Maria Vicente Tavares[1], Fabiana Quoos Mayer[1], Ursula da Silveira Matte[1], Roberto Giugliani[1,2]

1- Gene Therapy Center-Hospital de Clinicas de Porto Alegre, RS, Brazil
2- Post-Graduation Program in Biochemistry-UFRGS

Abstract

Mucopolysaccharidosis type I (MPS I) is a lysosomal disorder characterized by deficiency of alpha-L-iduronidase and storage of undegraded glycosaminoglycans (GAGs). Clinical findings of the disease include heart failure and patients often need valve replacement. It has been shown that at late times MPS I mice develop those abnormalities, but so far there is no study on the progression and pathogenesis of the disease. Therefore, in the present study we evaluated heart and valve function in normal and MPS I male mice from 2 to 8 months of age. Echocardiographic analysis evidenced heart enlargement with progressive reduction in ejection fraction, fractional area change and left ventricle fraction shortening in MPS I myocardium at 6 and 8 months. Other abnormalities included increased aortic diameter at 8 months and a reduction in acceleration/ejection time (AT/ET) ratio of pulmonary artery starting at 6 months, which can indicate pulmonary vascular resistance (PVR). Histological and biochemical analysis confirmed progressive GAG storage from 2 months onwards in myocardium and heart valves, which were also thickened. Collagen content was reduced in MPS I mice valves. Cathepsin B activity was up to 12-fold elevated in MPS I, and could be responsible for the heart dilatation observed. Our results suggest that MPS I mice have a progressive heart failure and valve disease, which may be caused by cathepsin B overexpression.

Introduction

Mucopolysaccharidosys type I (MPS I) is an autosomal recessive disorder due to deficiency of alpha-L-iduronidase (IDUA), a lysosomal enzyme involved in the degradation of glycosaminoglycans (GAG) heparan sulphate and dermatan sulphate (Giugliani et al, 2010).

The disease spectrum varies from the severe Hurler syndrome (OMIM #67014) to the attenuated Scheie syndrome (OMIM # 67016), with intermediate severity patients classified as Hurler-Scheie (OMIM # 67015). The Hurler form presents severe mental retardation in addition to other systemic manifestations (disostosis multiplex, hapetosplenomegaly, corneal clouding, joint stiffness) which are also found in the more attenuated forms of the disease (Munoz-Rojas et al, 2011).

Heart and valve disease is present in all forms of MPS I. It generally develops earlier in Hurler patients (Hirth et al, 2007) compared to patients with the more attenuated forms (Soliman et al, 2007). Accurate data on the frequency of heart disease in MPS I is hard to obtain due to early death in some cases, but it is estimated that at least 60% of MPS I patients develop cardiac and valve abnormalities (Braulin et al, 2011). Myocardial and heart valve thickening are common in all forms of MPS I with some patients developing also systemic or pulmonary hypertension (Dangel, 1998; Chan et al, 2003). Death by congestive heart failure is frequent in Hurler patients, while both phenotypes usually undergo valve replacement (Braulin et al, 2011). MPS I hearts are often dilated, and patients with increased left ventricle dimensions usually have a very poor prognosis (Hirth et al, 2007; van den Broek et al, 2011; Harada et al, 2011).

The animal model of MPS I was created in 2003 by disruption of the IDUA gene with the neomycin resistance gene (Ohmi et al, 2003) and has proven to be a useful model for study of pathogenesis of disease as well as for development of treatment options (Pan et al, 2008; Metcalf et al, 2010). Myocardium abnormalities in MPS I mice were reported at 6 and 10 months, with heart and valves being enlarged and mitral and aortic valves presenting regurgitation at the latest time point (Jordan et al, 2006). Also, the aorta presented reduced elasticity and increased breaks in elastin structure, with an associated increase in the activity of matrix metalloproteinases (MMPs) and cathepsins (Ma et al, 2008).

Cathepsin B (CtsB) is a protease known to mediate a series of processes, including remodeling of extracellular matrix (Reiser et al, 2010; Ge et al, 2006). The

increase in CtsB expression in aortas from MPS VII mice (Baldo et al, 2011) and MPS I and VII dogs (Metcalf et al, 2010) made us hypothesize that heart enlargement in MPS I mice could also be due to increased CtsB. Therefore, we evaluated mice at different ages, aiming to verify the onset of abnormalities in the myocardium and heart valves from these animals as well as to look for mechanisms possibly responsible for the abnormalities observed in hearts and valves of MPS I mice.

Materials and methods

Animals

All animal studies were approved by the authors' institutional ethics review board and MPS I mice on a C57BL/6 background were used. DNA was extracted from MPS I mice ears at 21 days and IDUA genotyping was performed with specific primers by PCR. Heterozygous mice were used for breeding.

Male $IDUA^{-/-}$ mice (referred as MPS I group) and their normal littermate controls ($IDUA^{-/+}$ and $IDUA^{+/+}$, referred from now on as "Normal" group) were the subjects for these experiments. At 3 weeks of age, offspring were separated from the dam, genotyped and housed (2–5 per cage) by sex. Animals were maintained to conventional housing under a 12 h light/12 h dark cycle with controlled temperature (19 ± 1°C) and humidity (50 ± 10%). Echocardiography was performed at 2, 4, 6 and 8 months. In each time point a subset of mice was analyzed for echocardiogram, sacrificed by cervical dislocation, and tissues were collected. The apical portion of the heart was flash frozen in liquid nitrogen and stored at -80ºC for biochemical analysis; the basal portion was fixed in buffered formalin and processed for histopathology.

Some mice (N=10 for Normal and 9 for MPS I) were kept for survival analysis for up to 1 year.

Echocardiographic analysis

Mice were anesthetized with isofluorane and positioned under a controlled temperature bed. Animals were placed in left lateral decubitus position (45° angle) to obtain cardiac images. An EnVisor HD System, Philips Medical (Andover, MA, USA), with a 12–4 MHz transducer was used, at 2 cm depth with fundamental and harmonic imaging. Images were captured by a trained operator with experience in small animal

echocardiography. After the procedure, mice were allowed to recover and monitored for 1h.

Left ventricular dimensions

Left ventricular (LV) diastolic and systolic transverse areas (cm^2) were obtained by 2D tracing the endocardial border at three levels: basal (at the tip of the mitral valve leaflets), middle (at the papillary muscle level) and apical (distal from the papillary muscle but before the final curve cavity). Diastolic and systolic diameters (cm) were obtained by M-MODE and were used as measure of myocardial hypertrophy and dilatation. Final value for each animal was obtained by taking the average of all three planes (Tavares et al., 2010).

LV systolic function

Left ventricular ejection fraction (LVEF) was calculated as: (end diastolic volume− end-systolic volume/ end-diastolic volume)×100; end-diastolic and end-systolic cavity volumes were calculated using Simpson's rule (Mercier et al., 1982).

LV fraction shortening (LVFS) values were obtained using the following equation: LVFS = DD − SD / DD × 100 (diastolic diameter — DD; systolic diameter — SD). Fractional area change (FAC) was calculated as follows: FAC = diastolic area – systolic area / diastolic area (Litwin et al., 1994; Moises et al., 2000).

Cardiac Flows and diastolic function

Evaluations of flow at the mitral, aortic and pulmonary valves were obtained by doppler echocardiography analyzes.

Left Ventricular diastolic function was assessed by E/A ratio, which was determined by ratio of the peak velocity of the E wave (fast filling) by peak velocity of the A wave (slow filling) of the mitral flow.

Performance Myocardial Index (PMI) is defined as the sum of the isovolumic contraction time plus isovolumic relaxation time and isovolumic relaxation time divided by the ejection time, obtained from Doppler recordings of left ventricular inflow and outflow. The index was derived as (a - b)/b, where ‘a’ is the interval between the cessation and the onset of the mitral inflow, and ‘b’ is the ejection time of the left ventricular outflow (Shingu, et al, 2010).

Finally, in the pulmonary valve the measures of the ejection and acceleration time were obtained, as well as their ratio as index of pulmonary vascular resistance (PVR) (Jones et al, 2010).

Final values for all calculations for each animal were based on three transverse planes. Data were recorded in CD for later review and off-line analysis.

Tissue GAG measurement

Total tissue GAG was measured using the dimethyl blue technique. Briefly, samples were homogeneized in acetate buffer, centrifuged for 10 min at 12.000xg, and the supernatant was collected. For the assay, 25µL of supernatant were mixed with dimethyl blue 0.3 M in Tris 2 M and absorbance was read at 530 nm in a spectrophotometer. Protein was measured by the method of Lowry. Results were expressed as percentage of normal levels.

Cathepsin B activity

Cathepsin B activity was performed using the specific substrate Z-Arg-Arg-AMC (Bachem, USA) at 100uM in acetate buffer pH 7.5, as previously described (Baldo et al, 2011). Results were expressed as U/ mg protein. One unit corresponds to 1 nmole of substrate cleaved per hour.

Histopathology

Hearts containing the valves were fixed in buffered formalin and embedded in paraffin according to our hospital`s routine processing. Thin sections (5µm) were stained with hematoxylin/eosin and alcian blue 1%, which stains GAG blue. An adjacent slide was stained with Sirius Red for visualization of collagen content in the heart valves. GAG storage in the myocardium was classified as present or absent, since quantification was performed with biochemical assay.

GAG storage in the heart valves was graded as 0-absent; 1-mild; 2-moderate; and 3- intense. The thickness of the heart valves was measured using the computer software Cell-F. Since in several cases we could not identify which valve specifically was being observed due to their small size, they were analyzed as valves from the left ventricle (aortic + mitral valves) and valves from the right ventricle (tricuspid + pulmonary). That was possible since we observed that in cases were we had both valves,

they had a similar width. Heart valves width were measured at 10 different points and the average was considered the valve thickness. Sections were analyzed by a trained researcher blinded to the groups.

Survival analysis

Ten MPS I mice and 9 normal mice were monitored for up to 1 year to obtain a survival curve. These mice were housed together with their littermates, in the same conditions above described and daily checked by our veterinary.

Statistics

Comparisons between the normal and MPS I mice were performed with student`s t test. A $p< 0.05$ was considered statistically significant. All statistical analyses were performed with the SigmaStat software version 11.0.

Results

Echocardiographic alterations in the myocardium

A battery of parameters were evaluated in Normal and MPS I myocardium from 2 to 8 months of age (table 1). No significant alterations were found at 2 and 4 months. However at 6 months LVEF was reduced in more than 10% in affected animals (60.2% in normals vs 49.5% in MPS I, p=0.008). Similarly, LVFS (36.7% vs 27.1%, p =0.001) and FAC (51.5 vs 42.5, p=0.024) were also reduced. Those differences were also observed at 8 months, when LVEF was 17% reduced in MPS I mice compared to normal (56.1% vs 38.7%, p=0.007). LVFS (39.9% vs 25.3%, p=0.003) and FAC (45.4 vs 31.2, p=0.044) were also reduced, as observed at 6 months.

In addition, analyzes of heart diameter revealed that myocardium from MPS I mice was enlarged at 6 months, with a 28% increase compared to normal mice during systole (0.25 cm vs 0.32 cm, p=0.006), and 10% (0.39 cm vs 0.43 cm, p=0.047), respectively during diastole. The left cavity increase was progressive and reached a 58% increase in systole (p=0.001) and 28% increase in diastole (p=0.02) at 8 months. Aortic root was 31% enlarged at 8 months (0.13 cm in normal vs 0.17 cm in MPS I mice, p=0.028). No differences were observed in wall thickness (not shown) or heart rate at any time.

GAG storage in the myocardium

Storage of GAG in the myocardium could be visualized in histological sections from 2 months old (figure 1B) and were progressive up to 8 months (figure 1C). Cells presenting storage were basically interstitial cells. Storage on myocytes was not observed. GAG levels in MPS I mice at 2 months were 154% of those found in Normal mice ($p=0.104$). At 8 months, GAG levels in MPS I myocardium reached 217% the normal levels ($p=0.01$, figure 1D).

Cathepsin B activity

CtsB activity was measured using the specific substrate Z-Arg-Arg-AMC (figure 2). At 2 months, MPS I myocardium presented a 6-fold increase in CtsB activity compared to normal mice (201 U/mg in MPS vs 33 U/mg in Normal, $p <0.01$). At 8 months, CtsB in MPS I mice was 12-fold higher than in normal mice (217 U/mg in MPS I vs 17.6 U/mg in Normal, $p<0.01$).

Doppler echocardiography

Doppler echocardiography was performed to evaluate heart valves and results are detailed described in table 2. Mitral valve flow was evaluated using 4 parameters. The E wave was reduced at 8 months in MPS I mice (1.22 vs 0.93, $p=0.049$), however the ratio between E wave and A wave was not altered, since both seemed to be reduced in MPS I mice, although A wave results did not reach significance. Other parameters were not altered.

Aortic valve disease was observed at 4 months, where ejection time was increased in MPS I mice (0.078 s vs 0.087 s, $p=0.03$) while the ejected volume (0.13 vs 0.098, $p=0.02$) and the cardiac output were reduced (50.6% vs 36.1%, $p=0.02$). However, those differences were not maintained when analyzing 6 and 8 month-old mice.

The Doppler method was also used to study if MPS I mice develop PVR using parameters obtained at the pulmonary valve. At 6 months, we could observe a reduction in the AT/ET ratio (0.25 vs 0.19, $p=0.033$). At 8 months, not only the AT/ET ratio was once again reduced (0.25 vs 0.15, $p=0.02$), but also the acceleration time *per se* (0.022 vs 0.013, $p=0.027$).

Histological alterations in the heart valves

Heart valves from mice were stained with H-E/Alcian blue for GAG analysis, since they are too small to quantify it using a biochemical assay (figure 3 A-B). We were able to obtain valves with mice from 6 and 8 months, as well as a few mice with 12 months-old that were kept for survival analysis. GAG scores were increased in MPS I mice from 6 months of age, in both valves from left and right ventricle (figure 3C). In addition, measuring the valve thickness in 10 different points revealed that heart valves are thickened in MPS I mice (figure 3D).

Heart valves are mainly composed of collagen, therefore we performed a Sirius red staining, which revealed collagen loss in MPS I mice valves compared to normal mice (figure 4).

Survival analysis

MPS I mice that were maintained for survival analysis started dying at 16 weeks, however most animals died from weeks 30 to 40. Survival after 12 months in MPS I mice was only 44% (4 alive out of 9), while normal littermates had a 100% (10/10) survival ($p<0.01$, figure 5).

Discussion

Heart and valve disease is a frequent feature among MPS I patients, and it leads often to death or to a reduction in the quality of life. Treatments are ineffective or only partially effective in correcting these aspects of the disease (Braulin et al, 2011). Therefore, it is important to study mechanism by which the disease occurs, in order to avoid its progression.

Myocardium disease in mice was not altered until 6 months, when we could evidence a reduction in the contractility, analyzed by 3 different parameters (ejection fraction, fractional area change and shortening fraction). In addition, heart enlargement could be detected by diastolic chamber dilatation. At 8 months, these aspects worsened and we could also observe an increase in aortic root diameter, which indicates aortic dilatation. It was previously show that ascending aortas from MPS I mice are severely dilated from 6 months (Ma et al, 2008), and although we could only observe this increase at 8 months, we believe that the upregulation in cathepsins and matrix metalloproteinases previously observed could also be happening in the present study

(Ma et al, 2008). We did not perform echocardiogram analysis in animals older than 8 months as a previous work (Jordan et al, 2005) because it would be hard to obtain MPS I animals, since they die around 8 months, as seen in the survival curve. Furthermore, when we tried to perform analysis in some MPS I mice older than 8 months, they were not able to recover from the surgery and died from hypothermia.

Looking for possible explanation for the heart dilatation, we decided to measure the activity of cathepsin B in the myocardium, since it has been shown previously to be elevated in hearts from patients with different types of dilated cardiomyopathy (Ge et al, 2006), and it was recently described to be elevated in aortas from MPS I and VII mice and dogs (Ma et al, 2008; Metcalf et al, 2010; Baldo et al, 2011). Cathepsin B expression was found to be upregulated as early as two months and kept elevated at 8 months. The chronic increase in CtsB activity has been shown to lead to remodeling of the extracellular matrix in the myocardium and heart valves, leading to enlargement of the structures (Ge et al, 2006; Schenke-Layland et al, 2009; Reiser et al; 2010). These results suggest that heart dilatation could be mediated by increased CtsB activity.

MPS I patients develop heart valve thickening and consequently regurgitation, often needing valve replacement (Braulin et al, 2011). In the present work we could detect AV alterations as early as 4 months, although the results were not maintained at 6 and 8 months. It is possible that we observed a difference that was not true (false positive) at 4 months, but it is unlikely, since the difference was observed in several parameters, which are complementary. Another explanation is that we lost the animals with worse AV disease due to death or sacrifice, and therefore the surviving ones developed a milder AV disease. Aortic valve was thickened in MPS I as observed by histological analysis, and therefore suggest a valve dysfunction in these mice. In the mitral valve only the E wave was reduced at 8 months, suggesting that the fast filling was impaired. Marked abnormalities in thickness could be detected at 6 and 8 months by histological analysis. A previous work (Jordan et al, 2005) has shown that heart valve regurgitation is present in 10-month old mice, but we could not consistently detect regurgitation in our animals, possibly due to equipment limitation.

Thickening was also seen in the pulmonary valve, where we also found at 6 and 8 months a reduction in the ratio from acceleration and ejection times (AT/ET ratio). The reduction in the AT/ET ratio suggests pulmonary vascular resistance (Mosely et al, in press) which may lead to pulmonary hypertension which is frequently found in patients (Braulin et al, 2011).

Since we found thickening of the heart valves, we hypothesized that extracellular matrix (ECM) could be altered. ECM in heart valves is composed mainly (55% of dry weight) of collagen (Balguid et al, 2007); therefore we performed Sirius-red stain to analyze total collagen content. A reduction in collagen signal was observed in MPS I heart valves. Although we didn't evaluate cathepsin B activity in the valves from MPS I mice due to their small size and difficulty of obtention, our unpublished results in the MPS VII dogs (Baldo et al, unpublished) suggest that cathepsin B is significantly elevated in these structures. Cathepsin B is a known collagenase (Beltran et al, 1992; Sires et al, 1995; Dufour et al, 1996), and therefore it is reasonable to consider that an increase in the expression of cathepsin B and possibly other collagenases could be responsible for the loss of collagen observed. Our results extend the findings from the MPS VII dog model, suggesting that collagen loss in the valves also happens in other types of MPS. These findings together with previous studies suggest that heart valve thickening is an early event, and combined with collagen loss may lead to heart valve dysfunction.

Altogether our results confirm that MPS I mice have a progressive heart and valve disease, which can be detected from 6 months on. Our finding also suggest that heart enlargement in MPS I mice may happen through an increase in CtsB activity, and that CtsB together with possibly other collagenases might be also responsible for the reduction in collagen observed in MPS I heart valves. Since current treatments have shown limited success in treating these structures, based on our findings ancillary therapies might be tested to benefit patients with mucopolysaccharidoses.

References

Baldo G, Wu S, Howe RA, Ramamoothy M, Knutsen RH, Fang J, Mecham RP, Liu Y, Wu X, Atkinson JP, Ponder KP. Pathogenesis of aortic dilatation in mucopolysaccharidosis VII mice may involve complement activation. Mol Genet Metab. 2011;104(4):608-19.

Balguid A, Rubbens MP, Mol A, Bank RA, Bogers AJ, van Kats JP, de Mol BA, Baaijens FP, Bouten CV. The role of collagen cross-links in biomechanical behavior of human aortic heart valve leaflets relevance for tissue engineering. Tissue Eng. 2007; 13(7):1501-11.

Beltrán J, Bonnet M, Ouali A. Comparative action of cathepsins B and L on intramuscular collagen as assessed by differential scanning calorimetry. Meat Sci. 1992;32(3):299-306.

Braunlin EA, Harmatz PR, Scarpa M, Furlanetto B, Kampmann C, Loehr JP, Ponder KP, Roberts WC, Rosenfeld HM, Giugliani R. Cardiac disease in patients with mucopolysaccharidosis: presentation, diagnosis and management. J Inherit Metab Dis. 2011; 34(6):1183-97

Chan D, Li AM, Yam MC, Li CK, Fok TF. Hurler's syndrome with cor pulmonale secondary to obstructive sleep apnoea treated by continuous positive airway pressure. J Paediatr Child Health. 2003; 39(7):558-9.

Dangel JH. Cardiovascular changes in children with mucopolysaccharide storage diseases and related disorders--clinical and echocardiographic findings in 64 patients. Eur J Pediatr. 1998; 157(7):534-8.

Dufour E, Dalgalarrondo M, Hervé G, Goutefongea R, Haertlé T. Proteolysis of type III collagen by collagenase and cathepsin B under high hydrostatic pressure. Meat Sci. 1996; 42(3):261-9.

Ge J, Zhao G, Chen R, Li S, Wang S, Zhang X, Zhuang Y, Du J, Yu X, Li G, Yang Y. Enhanced myocardial cathepsin B expression in patients with dilated cardiomyopathy. Eur J Heart Fail. 2006; 8(3):284-9.

Giugliani R, Federhen A, Rojas MV, Vieira T, Artigalás O, Pinto LL, Azevedo AC, Acosta A, Bonfim C, Lourenço CM, Kim CA, Horovitz D, Bonfim D, Norato D, Marinho D, Palhares D, Santos ES, Ribeiro E, Valadares E, Guarany F, de Lucca GR, Pimentel H, de Souza IN, Correa J Neto, Fraga JC, Goes JE, Cabral JM, Simionato J, Llerena J Jr, Jardim L, Giuliani L, da Silva LC, Santos ML, Moreira MA, Kerstenetzky M, Ribeiro M, Ruas N, Barrios P, Aranda P, Honjo R, Boy R, Costa R, Souza C, Alcantara FF, Avilla SG, Fagondes S, Martins AM. Mucopolysaccharidosis I, II, and VI: Brief review and guidelines for treatment. Genet Mol Biol. 2010; 33(4):589-604.

Harada H, Uchiwa H, Nakamura M, Ohno S, Morita H, Katoh A, Yoshino M, Ikeda H. Laronidase replacement therapy improves myocardial function in mucopolysaccharidosis I. Mol Genet Metab. 2011; 103(3):215-9.

Hirth A, Berg A, Greve G. Successful treatment of severe heart failure in an infant with Hurler syndrome. J Inherit Metab Dis. 2007; 30(5):820.

Hessel MH, Steendijk P, den Adel B, Schutte CI, van der Laarse A. Characterization of right ventricular function after monocrotaline-induced pulmonary hypertension in the intact rat. Am J Physiol Heart Circ Physiol. 2006; 291(5):H2424-30.

Jones JE, Mendes L, Rudd MA, Russo G, Loscalzo J, Zhang YY. Serial noninvasive assessment of progressive pulmonary hypertension in a rat model. Am J Physiol Heart Circ Physiol 2002; 283: 364-371

Jordan MC, Zheng Y, Ryazantsev S, Rozengurt N, Roos KP, Neufeld EF. Cardiac manifestations in the mouse model of mucopolysaccharidosis I. Mol Genet Metab. 2005; 86(1-2):233-43.

Litwin SE, Katz SE, Morgan JP, Douglas PS. Serial echocardiographic assessment of left ventricular geometry and function after large myocardial infarction in the rat. Circulation. 1994; 89(1):345-54.

Ma X, Tittiger M, Knutsen RH, Kovacs A, Schaller L, Mecham RP, Ponder KP. Upregulation of elastase proteins results in aortic dilatation in mucopolysaccharidosis I mice. Mol Genet Metab. 2008; 94(3):298-304.

Metcalf JA, Ma X, Linders B, Wu S, Schambach A, Ohlemiller KK, Kovacs A, Bigg M, He L, Tollefsen DM, Ponder KP. A self-inactivating gamma-retroviral vector reduces manifestations of mucopolysaccharidosis I in mice. Mol Ther. 2010; 18(2):334-42.

Metcalf JA, Linders B, Wu S, Bigg P, O'Donnell P, Sleeper MM, Whyte MP, Haskins M, Ponder KP. Upregulation of elastase activity in aorta in mucopolysaccharidosis I and

VII dogs may be due to increased cytokine expression. Mol Genet Metab. 2010; 99(4):396-407

Mercier JC, DiSessa TG, Jarmakani JM, Nakanishi T, Hiraishi S, Isabel-Jones J, Friedman WF. Two-dimensional echocardiographic assessment of left ventricular volumes and ejection fraction in children. Circulation. 1982; 65(5):962-9.

Moisés VA, Ferreira RL, Nozawa E, Kanashiro RM, Campos O, Andrade JL, Carvalho AC, Tucci PJ. Structural and functional characteristics of rat hearts with and without myocardial infarct. Initial experience with Doppler echocardiography. Arq Bras Cardiol. 2000; 75(2):125-36.

Mosely F, Tavares AMV, Caron-Lienert R, Bello-Klein A. Effects of purple grape juice in the redox-sensitive modulation of right ventricular remodeling in a pulmonary arterial hypertension model. J Cardiovasc Pharmacol. *in press*.

Muñoz-Rojas MV, Bay L, Sanchez L, van Kuijck M, Ospina S, Cabello JF, Martins AM. Clinical manifestations and treatment of mucopolysaccharidosis type I patients in Latin America as compared with the rest of the world. J Inherit Metab Dis. 2011; 34(5):1029-37.

Ohmi K, Greenberg DS, Rajavel KS, Ryazantsev S, Li HH, Neufeld EF. Activated microglia in cortex of mouse models of mucopolysaccharidoses I and IIIB. Proc Natl Acad Sci U S A. 2003; 100(4):1902-7.

Okada M, Harada T, Kikuzuki R, Yamawaki H, Hara Y. Effects of telmisartan on right ventricular remodeling induced by monocrotaline in rats. J Pharmacol Sci. 2009; 111(2):193-200.

Pan D, Sciascia A 2nd, Vorhees CV, Williams MT. Progression of multiple behavioral deficits with various ages of onset in a murine model of Hurler syndrome. Brain Res. 2008; 1188:241-53.

Reiser J, Adair B, Reinheckel T. Specialized roles for cysteine cathepsins in health and disease. J Clin Invest. 2010; 120(10):3421-31.

Schenke-Layland K, Stock UA, Nsair A, Xie J, Angelis E, Fonseca CG, Larbig R, Mahajan A, Shivkumar K, Fishbein MC, MacLellan WR. Cardiomyopathy is associated with structural remodelling of heart valve extracellular matrix. Eur Heart J. 2009; 30(18):2254-65.

Shingu Y, Amorim P, Nguyen TD, Mohr FW, Schwarzer M, Doenst T. Myocardial performance (Tei) index is normal in diastolic and systolic heart failure induced by pressure overload in rats. Eur J Echocardiogr 2010; 11(10): 829-33.

Sires UI, Schmid TM, Fliszar CJ, Wang ZQ, Gluck SL, Welgus HG. Complete degradation of type X collagen requires the combined action of interstitial collagenase and osteoclast-derived cathepsin-B. J Clin Invest. 1995; 95:2089-95.

Soliman OI, Timmermans RG, Nemes A, Vletter WB, Wilson JH, ten Cate FJ, Geleijnse ML. Cardiac abnormalities in adults with the attenuated form of mucopolysaccharidosis type I. J Inherit Metab Dis. 2007; 30(5):750-7.

Tavares AM, da Rosa Araújo AS, Baldo G, Matte U, Khaper N, Belló-Klein A, Rohde LE, Clausell N. Bone marrow derived cells decrease inflammation but not oxidative stress in an experimental model of acute myocardial infarction. Life Sci. 2010; 87(23-26):699-706

van den Broek L, Backx AP, Coolen H, Wijburg FA, Wevers R, Morava E, Neeleman C. Fatal coronary artery disease in an infant with severe mucopolysaccharidosis type I. Pediatrics. 2011; 127(5):e1343-6.

TABLE 1

Table 1: Myocardium parameters analyzed by echocardiography.

Age	2 months			4 months			6 months			8 months		
Parameters	Normal (n=11)	MPS I (n=7)	P value	Normal (n=15)	MPS I (n=9)	P value	Normal (n=17)	MPS I (n=16)	P value	Normal (n=8)	MPS I (n=8)	P value
LVEF (%)	63.1 ± 9.4	60.2 ± 7.4	0.49	66.2 ± 6.6	59.8 ± 12.4	0.12	60.2 ± 8.6	49.5 ± 12.2	0.01	56.1 ± 11.1	38.7 ± 8.8	0.01
LVSF	38.8 ± 8.1	39.1 ± 7.1	0.94	39.5 ± 5.4	42.1 ± 8.2	0.38	36.7 ± 7.4	27.1 ± 6.1	0.01	39.9 ± 5.2	25.3 ± 10.1	0.01
FAC (%)	52.5 ± 11.5	54.5 ± 8.1	0.68	54.2 ± 9.6	53.5 ± 11.0	0.87	51.5 ± 10.4	42.5 ± 11.1	0.02	45.4 ± 14.6	31.2 ± 8.9	0.04
SD (cm)	0.21 ± 0.043	0.21 ± 0.023	0.82	0.23 ± 0.036	0.24 ± 0.043	0.91	0.25 ± 0.053	0.32 ± 0.066	0.01	0.24 ± 0.039	0.38 ± 0.093	0.01
DD (cm)	0.34 ± 0.045	0.34 ± 0.021	0.92	0.38 ± 0.038	0.39 ± 0.052	0.84	0.39 ± 0.05	0.43 ± 0.056	0.04	0.39 ± 0.039	0.50 ± 0.10	0.02
Aortic root (cm)	0.14 ± 0.01	0.14 ± 0.01	0.45	0.15 ± 0.01	0.14 ± 0.02	0.25	0.14 ± 0.02	0.15 ± 0.02	0.63	0.14 ± 0.01	0.17 ± 0.02	0.03
Heart rate (bpm)	448 ± 42	428 ± 35	0.33	383 ± 57	369 ± 61	0.55	384 ± 43	365 ± 53	0.33	374 ± 66	374 ± 33	0.98

TABLE 2

Table 2: Heart valve parameters analyzed by echocardiography.

	Age	2 months			4 months			6 month			8 months		
	Parameter	Normal (n=11)	MPS I (n=7)	P value	Normal (n=15)	MPS I (n=9)	P value	Normal (n=17)	MPS I (n=16)	P value	Normal (n=8)	MPS I (n=8)	P value
Mitral Valve	E wave (cm/s)	1.21 ± 0.15	1.26 ± 0.29	0.66	1.13 ± 0.10	1.04 ± 0.13	0.18	1.18 ± 0.12	1.11 ± 0.11	0.27	1.22 ± 0.11	0.93 ±0.36	0.049
	A wave (cm/s)	0.70 ± 0.15	0.74 ± 0.28	0.73	0.63 ± 0.09	0.59 ±0.12	0.52	0.68 ± 0.07	0.65 ± 0.17	0.66	0.65 ± 0.09	0.53 ± 0.24	0.25
	E/A ratio	1.80 ± 0.27	1.80 ± 0.30	0.98	1.82 ± 0.18	1.80 ± 0.27	0.88	1.78 ± 0.06	1.81 ± 0.5	0.89	1.89 ± 0.29	1.97 ± 0.34	0.67
	Flow time (s)	0.090 ± 0.015	0.089 ± 0.022	0.93	0.089 ± 0.012	0.081 ± 0.0068	0.15	0.082 ± 0.012	0.089 ± 0.018	0.34	0.088 ± 0.021	0.101 ± 0.021	0.21
Aortic Valve	Ejection time (s)	0.085 ± 0.011	0.085 ± 0.010	0.89	0.078 ± 0.0083	0.087 ± 0.010	0.03	0.083 ± 0.0093	0.092 ± 0.014	0.09	0.087	0.084 ± 0.01	0.39
	Ejected Volume (mL)	0.11 ± 0.021	0.12 ± 0.030	0.305	0.13 ± 0.028	0.098 ± 0.022	0.02	0.12 ± 0.026	0.11 ± 0.024	0.61	0.12 ± 0.026	0.11 ± 0.035	0.88
	Cardiac output (mL/min)	47.57 ± 7.02	51.88 ± 9.92	0.34	50.65 ± 12.06	36.10 ± 11.53	0.02	46.37 ± 12.12	41.06 ± 13.03	0.34	46.2 ± 13.3	43.85 ± 14.6	0.77
	PMI	0.31 ± 0.15	0.43 ± 0.15	0.15	0.48 ± 0.20	0.46 ± 0.19	0.87	0.35 ± 0.13	0.41 ± 0.19	0.477	0.32 ± 0.20	0.52 ± 0.11	0.06
Pulmonary Valve	Ejection time (s)	0.086 ± 0.012	0.089 ± 0.008	0.55	0.086 ± 0.009	0.09 ± 0.015	0.49	0.083 ± 0.010	0.09 ± 0.012	0.13	0.088 ± 0.010	0.087 ± 0.0088	0.87
	Acceleration time (s)	0.022 ± 0.005	0.020 ± 0.0029	0.44	0.021 ± 0.0034	0.022 ± 0.0036	0.22	0.02 ± 0.0032	0.017 ± 0.0045	0.11	0.022 ± 0.0074	0.013 ± 0.0025	0.03
	AT/ET ratio	0.26 ± 0.056	0.23 ± 0.046	0.32	0.25 ± 0.047	0.26 ± 0.031	0.56	0.25 ± 0.057	0.20 ± 0.051	0.03	0.25 ± 0.071	0.15 ± 0.038	0.02

Legend: PMI-performance myocardial index; AT/ET ratio- acceleration time/ Ejection time ratio;

Figures

Figure 1: GAG storage in MPS I myocardium. A) Normal mice at 8 months. H-E/Alcian blue stain. B) MPS I mice at 2 months, arrows indicate GAG storage. H-E/alcian blue stain. C) MPS I mice at 8 months, arrows indicate GAG storage. H-E/alcian blue stain. D) Quantification of GAG levels in normal and MPS I mice at 2 and 8 months (n=3-4/group). **p<0.01 compared to normal, Student t test.

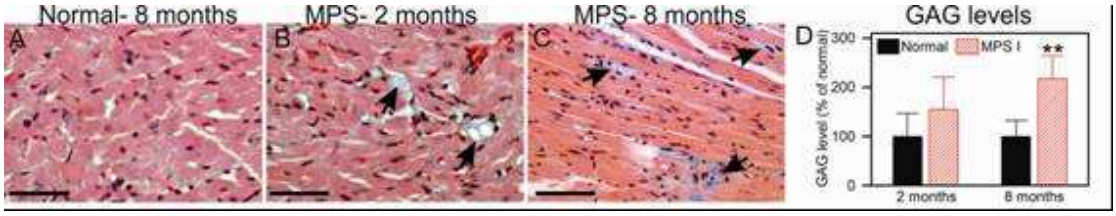

Figure 2: Cathepsin B activity in the myocardium. Cathepsin B activity was measured using the fluorogenic substrate Z-Arg-Arg-AMC at pH 7.5 (n=4/group). Results are expressed as U/mg. One Unit corresponds to 1 nmole of substrate cleaved per hour. **p<0.01, Student`s t test.

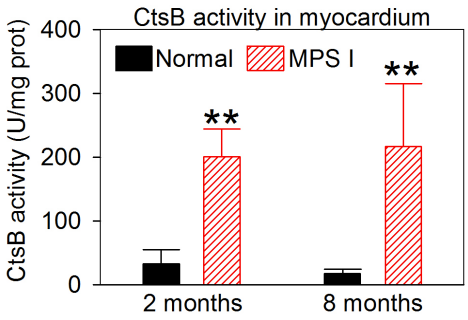

Figure 3: Heart Valves thickening and GAG storage. A) An example of a normal aortic valve at 6 months. B) An example of an aortic valve from a 6-month MPS I mice. C) GAG storage was scored in normal and MPS I heart valves from the left ventricle (LV) and right ventricle (RV) from mice at different ages. D) Thickening of the heart valves was measured in 10 different points and the average value was recorded. The number of animals in each group is indicated in the bars. *p<0.05 and **p<0.01, Student`s t test.

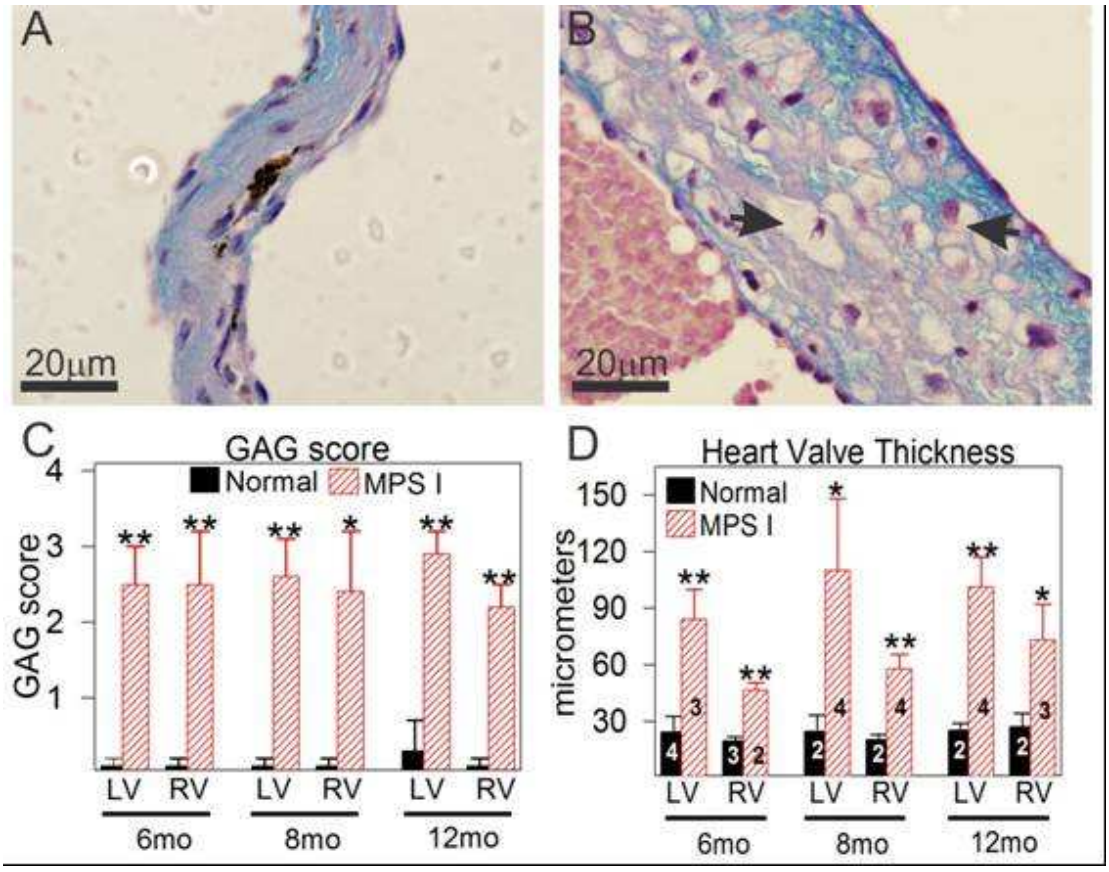

Figure 4: Valve disease: sirius red staining for collagen content. A) Normal 6-months heart valve from the left ventricle. B) MPS I valve at 6 months, showing loss of red signal (collagen content) compared to the Normal. C) Higher magnification of the normal valve. D) Higher Magnification of MPS I valve. E) Results from collagen score for heart valve in normal and MPS I mice. The number of animals is each group is indicated in the bars. * p< 0.05.

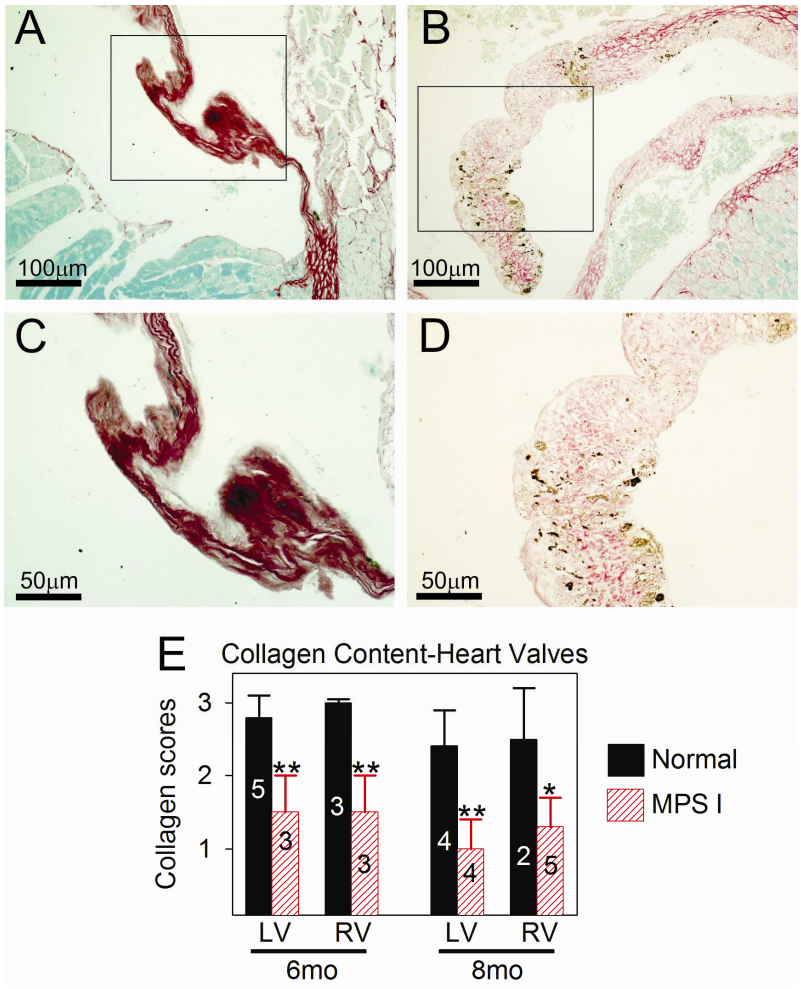

Figure 5: Survival curve in normal and MPS I mice for 12 months.

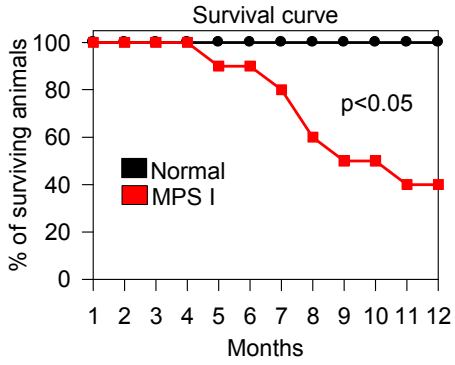

Molecular Genetics and Metabolism 104 (2011) 608–619

Contents lists available at SciVerse ScienceDirect

Molecular Genetics and Metabolism

journal homepage: www.elsevier.com/locate/ymgme

Pathogenesis of aortic dilatation in mucopolysaccharidosis VII mice may involve complement activation

Guilherme Baldo [a], Susan Wu [a], Ruth A. Howe [a], Meera Ramamoothy [a], Russell H. Knutsen [b], Jiali Fang [a], Robert P. Mecham [b], Yuli Liu [a], Xiaobo Wu [a], John P. Atkinson [a], Katherine P. Ponder [a,c,*]

[a] Department of Internal Medicine, Washington University School of Medicine, St. Louis, MO, USA
[b] Department of Cell Biology, Washington University School of Medicine, St. Louis, MO, USA
[c] Biochemistry and Molecular Biophysics, Washington University School of Medicine, St. Louis, MO, USA

ARTICLE INFO

Article history:
Received 8 July 2011
Received in revised form 16 August 2011
Accepted 17 August 2011
Available online 24 August 2011

Keywords:
Mucopolysaccharidosis VII
Cathepsin S
Matrix metalloproteinase 12
Complement system
Aortic dilatation
Gene therapy

ABSTRACT

Mucopolysaccharidosis VII (MPS VII) is due to mutations within the gene encoding the lysosomal enzyme β-glucuronidase, and results in the accumulation of glycosaminoglycans. MPS VII causes aortic dilatation and elastin fragmentation, which is associated with upregulation of the elastases cathepsin S (CtsS) and matrix metalloproteinase 12 (MMP12). To test the role of these enzymes, MPS VII mice were crossed with mice deficient in CtsS or MMP12, and the effect upon aortic dilatation was determined. CtsS deficiency did not protect against aortic dilatation in MPS VII mice, but also failed to prevent an upregulation of cathepsin enzyme activity. Further analysis with substrates and inhibitors specific for particular cathepsins suggests that this enzyme activity was due to CtsB, which could contribute to elastin fragmentation. Similarly, MMP12 deficiency and deficiency of both MMP12 and CtsS could not prevent aortic dilatation in MPS VII mice. Microarray and reverse-transcriptase real-time PCR were performed to look for upregulation of other elastases. This demonstrated that mRNA for complement component D was elevated in MPS VII mice, while immunostaining demonstrated high levels of complement component C3 on surfaces within the aortic media. Finally, we demonstrate that neonatal intravenous injection of a retroviral vector encoding β-glucuronidase reduced aortic dilatation. We conclude that neither CtsS nor MMP12 are necessary for elastin fragmentation in MPS VII mouse aorta, and propose that CtsB and/or complement component D may be involved. Complement may be activated by the GAGs that accumulate, and may play a role in signal transduction pathways that upregulate elastases.

1. Introduction

Mucopolysaccharidoses (MPS) are a group of 11 diseases caused by mutations in genes that encode lysosomal enzymes that degrade glycosaminoglycans (GAGs) [1]. MPS is associated with accumulation of GAGs throughout the body and multisystemic disease. The focus of this project was to better understand the pathogenesis of aortic disease in MPS using the murine model of MPS VII, which is an autosomal recessive disease due to β-glucuronidase (GUSB) deficiency (Online Mendelian Inheritance in Man #253220). An elegant model for the pathogenesis of MPS involves the binding of GAGs to Toll-like Receptor 4 (TLR4), which upregulates cytokines such as tumor necrosis factor α (TNFα), Ccl4 (MIP-1β), and interleukin 6 (IL-6), which in turn upregulate destructive proteases [2–4]. Adult humans with attenuated MPS I have aortas that are 122% of normal diameter [5] and reduced elasticity [6], while one patient with MPS VII required an aortic graft [7]. Mice with MPS I [8–10] and MPS VII [11], cats with MPS I and MPS VI [12], and dogs with MPS I [13–15] and MPS VII [14,16,17] also have aortic dilatation.

Elastin represents 30% of the dry weight of the aorta [18]. Tropoelastin monomers are secreted and then crosslinked into elastic fibers in a process that involves elastin binding protein, extracellular matrix microfibrils, and crosslinking enzymes [19]. Elastin was fragmented in the ascending aorta of humans, mice, and dogs with MPS I, and in humans and dogs with MPS VII [10,13,20–22]. Hinek et al. demonstrated that exogenous administration of dermatan sulfate, a GAG that accumulates in many types of MPS, reduced elastin binding protein levels and inhibited elastin assembly *in vitro*, and proposed that reduced assembly caused elastin defects in MPS I [23]. Alternatively,

Abbreviations: MPS, mucopolysaccharidosis; Cts, cathepsin; MMP, matrix metalloproteinase; GUSB, β-glucuronidase; GAGs, glycosaminoglycans; TLR4, toll-like receptor 4; TNFα, tumor necrosis factor alpha; IL-6, interleukin 6; M6P, mannose 6-phosphate; ERT, enzyme replacement therapy; RV, retroviral vector; PBS, phosphate buffered saline; VVG, Verhoeff Van Gieson; AMC, 7-amino-4-methylcoumarin; IDUA, α-L-iduronidase; TBS, tris-buffered saline; BP, blood pressure; STAT3, signal transducer and activator of transcription 3.

* Corresponding author. Department of Internal Medicine, Washington University School of Medicine, 660 South Euclid Avenue, St. Louis, MO 63110, USA. Fax: +1 314 362 8813.
E-mail address: kponder@dom.wustl.edu (K.P. Ponder).

1096-7192/$ – see front matter © 2011 Elsevier Inc. All rights reserved.
doi:10.1016/j.ymgme.2011.08.018

we reported in MPS I mice and dogs and in MPS VII dogs [10,14] that elastin fragmentation was temporally associated with increases in RNA and enzyme activity for two elastases, cathepsin S (CtsS) and matrix metalloproteinase 12 (MMP12), which contribute to aortic aneurisms in mouse models [24,25], and proposed that degradation was the major factor leading to elastin fragmentation. Although collagen is another important extracellular matrix protein of the aorta, collagen fibrils appeared to be relatively intact with histochemical stains in MPS I and MPS VII dogs [14].

Hematopoietic stem cell transplantation can reduce clinical manifestations of MPS, as hematopoietic cells migrate into tissues and secrete mannose 6-phosphate (M6P)-modified enzyme that can be taken up via the M6P receptor by nearby cells [26]. This has reduced, but not prevented, accumulation of GAGs, elastin fragmentation, and/or dilatation of the aorta in MPS VII mice [27] and dogs [16], MPS VI rats [28], and MPS I dogs [15] and cats [29]. Enzyme replacement therapy (ERT) involves intravenous (IV) injection of M6P-modified enzyme that can diffuse to organs and be taken up via the M6P receptor [30,31], although ERT is not available for MPS VII. ERT had little effect on lysosomal storage accumulation in aortic smooth muscle cells in MPS VI cats [32]. Gene therapy is also being tested in animal models [33]. One approach involves neonatal IV injection of a retroviral vector (RV) expressing the appropriate enzyme, which results in transduction of liver cells and secretion of enzyme into blood [33–35]. This reduced aortic dilatation, but MPS I mice required very high expression for a full therapeutic effect [8–10], and MPS VII dogs developed aortic dilatation after 5 years [14].

The data that CtsS and MMP12 are upregulated in MPS aortas led us to hypothesize that deletion of CtsS and/or MMP12 might reduce elastin fragmentation. To test this hypothesis, $CtsS^{-/-}$ and $MMP12^{-/-}$ mice were crossed with MPS VII ($GUSB^{-/-}$) mice and the effect upon the aorta diameters was determined. In addition, microarray analysis was performed to determine if other genes that could contribute to aortic dilatation were upregulated. The results demonstrate that CtsS and MMP12 are not essential for aortic dilatation, but a related cathepsin, CtsB, may contribute. These studies also demonstrate that the complement system may directly result in elastin fragmentation, or may indirectly contribute by induction of signal transduction pathways that result in upregulation of elastases.

2. Materials and methods

Reagents were from Sigma-Aldrich Chemical (St. Louis, MO) unless otherwise stated.

2.1. Animals

National Institutes of Health (NIH) guidelines for the care and use of animals in research were followed. MPS VII [27], CtsS-deficient [36], and MMP12 deficient [37] mice were all in a C57BL/6 background. Some MPS VII mice were injected IV with 1×10^{10} transducing units/kg of the RV designated hAAT-cGUSB-WPRE [38] at 2 to 3 days after birth to enable them to survive and breed. Genotyping for MPS VII mice used a SNP assay on tail DNA with a forward primer (5′ CCATAGTCATGATACCAAGAAAAGTAGCT-3′), a reverse primer (5′-TGACTATTCTGACCTCAGTGTGTGA-3′), a wild-type minor-groove binding probe labeled with Vic (5′-TTGTCTTAGGCCCCGTACGT-3′; the underlined C represents the position deleted in the MPS VII mouse), a mutant minor groove binding probe labeled with FAM (5′-TTGTCTTAGGCCC-GTACGT-3′) and a One-Step Plus PCR machine (Applied Biosystems; Foster City, CA). PCR for the wild-type CtsS allele used the primers 5′-CTTGAAGGGCAGCTGAAGCTG-3′ (forwards) and 5′-GTAGGAAGCGTCTGCCTCTAT-3′ (reverse), and PCR for the mutant CtsS allele used the primers 5′-CTCTGTGTAGCCTGGAATTC-3′ (forwards) and 5′-CTAAAGCGCATGCTCCAGACTGCC-3′ (reverse) [36] with analysis of the C_T using SYBR green real-time PCR of DNA. MMP12 mice genotyping PCR used a forward primer common to the wild-type and mutant MMP12 alleles (5′-CCCTCGATGTGGA GTGCCCG-3′), a reverse primer specific for the PGK-neo cassette (5′-AAGAACGGAGCCGGTTGGCG-3′), and a reverse primer specific for the MMP12 wild-type allele (5′-ACTTGCCCTGAGCACCCCCT-3′), with gel electrophoresis used to identify wild-type (337 bp) or mutant (460 bp) alleles.

2.2. Measurement of aortic diameter and histopathology

Mice were anesthetized with 120 mg/kg ketamine/40 mg/kg xylazine in phosphate buffered saline (PBS) at pH 7.4. For some animals, aortic compliance was assessed, in which the outer diameter of isolated aortas was determined at different internal pressures [39]. For histopathology, ascending aortas obtained from 1 to 2 mm from the aortic valve were fixed with buffered formalin, embedded in paraffin, and 6 μm sections were stained with Verhoeff Van Gieson (VVG) stain. For biochemical analyses, animals were perfused with 20 ml of PBS, and the aorta from just above the aortic valve to just before the first branch was cleaned of surrounding fat. To test the effect of gene therapy, the width of dissected ascending aortas was measured after gently pressing it against a surface.

2.3. RNA analysis

Frozen ascending aortas were homogenized in Trizol for 30 s with a hand-held homogenizer (Kimble-Kontes; Vineland, NJ), and RNA was isolated using a Qiagen column. Reverse transcription (RT) was performed on 1 μg of DNase I-treated RNA with an oligo (dT) 20 primer using a Superscript III kit (Invitrogen Corp., Carlsbad, CA) in 20 μl, followed by real-time PCR on 0.4 μl of each cDNA sample using SYBR green reagents from Applied Biosystems [10]. Primer sequences are in our previous publication [10] or in Supplementary Table 1. The percentage of a test RNA to that of β-actin was calculated by subtracting the cycle to reach the threshold (C_T) for a gene from the C_T for a separate assay using β-actin primers to determine the ΔC_T, and the formula: percent β-actin $= (100)\times 2^{\Delta CT}$. The percent β-actin for MPS animals was divided by the percent β-actin in normal animals to determine the ratio of the gene in MPS to normal mice.

For microarray, RNA was reverse transcribed with primers with a T7 RNA polymerase binding site, amplified with T7 RNA polymerase with fluorescently-labeled deoxynucleotides, and hybridized to an Illumina bead microarray (Mouse8, version 2). Expression analysis was performed with ParTek software (St. Louis, MO). Pathway analysis was performed with GeneGo interactions software (https://portal.genego.com/cgi/data_manager.cgi; St. Joseph, MI).

2.4. Enzyme and GAG assays

For the GUSB, α-L-iduronidase (IDUA), and cathepsin assays, frozen aortas were homogenized with the hand-held homogenizer in 100 mM sodium acetate pH 5.5 containing 2.5 mM ethylenediaminetetraacetic acid, 0.1% Triton X-100, and 2.5 mM dithiothreitol, and centrifuged at 10,000 *g* for 5 min at 4 °C. The protein concentration was determined with the Bradford assay (BioRad Laboratories, Hercules CA). For the MMP12 and GAG assays, extracts were homogenized in the neutral buffer provided with the MMP12 kit with 0.1% Triton-X.

GUSB and IDUA assays were performed with the extracts prepared at pH 5.5 using the fluorogenic substrates 4-methylumbelliferyl-β-L-glucuronide (Sigma-Aldrich, St. Louis, MO) for GUSB and 4-methylumbelliferyl-α-L-iduronide (Toronto Research Chemicals, North York, Canada) for IDUA and a Fluoroskan Ascent microplate fluorometer (Thermo Electron, Milford, MA) as previously described [9]. One unit of enzyme converts 1 nmol of substrate to product per hour at 37 °C. GAG content was determined in the samples obtained

at neutral pH using the commercial kit Blyscan (Biocolor, Carrickfergus, UK) using 30 μg of protein from each sample as described [10].

For the general cathepsin assay, 1 μg or less of the supernatant was incubated with 100 μM benzyloxycarbonyl-L-phenylalanyl-L-arginine-7-amido-4-methylcoumarin (Z-Phe-Arg-AMC) from Anaspec (San Jose, CA) at pH 7.5 in 100 mM sodium acetate with 2.5 mM ethylenediaminetetraacetic acid, 0.01% Triton X-100, and 2.5 mM dithiothreitol in a microtiter plate at 37 °C for 1 h [10]. The amount of product was determined by excitation at 355 nm and emission at 460 nm using kinetic readings and comparison with 7-amino-4-methylcoumarin (AMC) standards from Anaspec. One unit (U) of enzyme released 1 nmol of product per hour at 37 °C. The CtsB assay used the same extracts, the substrate Z-Arg-Arg-AMC (Bachem, Torrance, CA) at pH 7.5, and the same wavelengths as for the general cathepsin assay. CtsK activity was measured at pH 7.5 with 10 μM of the substrate 2-aminobenzoic acid-HPGGPQ-N-(2,4-dinitrophenyl)-ethylenediamine (Abz-HPGGPQ-EDDnp) from Anaspec, which is cleaved by CtsK but not other cathepsins, and 2-aminobenzoic acid was the standard. The CtsD assay was performed at pH 4 with 10 μM of the substrate 7-methoxycoumarin-4-acetyl (Mca)-Gly-Lys-Pro-Ile-Leu-Phe-Phe-Arg-Leu-Lys-2,4 nitrophenyl (Dnp)-D-Arg-NH2, which can also be cleaved by CtsE, with Mca-Pro-Leu-OH (Enzo Life Sciences) as the standard. CtsK and CtsD assays were read at 320 nm for excitation and 420 nm for emission. Inhibitors were from Calbiochem (San Diego, CA) and included the CtsS inhibitor Z-FL-COCHO (#219393), the CtsK inhibitor I [1,3-Bis (N-carbobenzoyloxy-L-leucyl) amino acetone; #219377] and the CtsB inhibitor Ac-Leu-Val-Lysinal (#219385). Samples were incubated with the inhibitor for 10 min prior to starting the assay. Additional assays were performed with human recombinant purified CtsB [R&D systems, Minneapolis, MN; specific activity 150 nmol of substrate cleaved per hour (U)/μg protein], CtsK (Enzo Life Sciences, Farmington, NY; 90 U/μg protein), CtsL (R&D systems; 900 U/μg protein), CtsS (R&D systems; 18 U/μg protein) and with CtsH purified from human liver (Enzo Life Sciences; 61 U/μg protein). An MMP12 assay kit (SensolyteTM 490 MMP12) was obtained from Anaspec for which the substrate can also be cleaved by MMP1, 2, 3, 8, and 13 and was performed as described previously with ~5 μg of extract in 100 μl reactions [10].

2.5. Immunostaining

Immunostaining for STAT3 that was phosphorylated at tyrosine 705 was performed as described previously [10]. For C3 immunostaining, frozen sections of aorta in optimal cutting temperature compound were fixed with formalin for 10 min at room temperature, and washed 3 times with TBS (Tris-buffered saline; 50 mM Tris pH 7.6, 150 mM NaCl, 0.1% Triton X-100). Endogenous peroxidase was inhibited with 0.6% H_2O_2 in water for 30 min. Samples were washed 3 times with TBS, and then preincubated with blocking buffer (TBS with 10% horse serum) for 30 min at room temperature. A goat-anti-mouse antibody specific for C3 (MP Biomedicals #55474, Solon, OH) was incubated overnight at 4 °C at a 1:100 dilution in blocking buffer, and then washed 3 times with TBS. A horse-radish peroxidase-conjugated horse anti-goat IgG (Vector Laboratories, Burlingame CA) was incubated at a 1:100 dilution for 1 h at RT in blocking buffer, and samples were washed 3 times with TBS. Samples were developed with 0.7 mg/ml 3,3′-diaminobenzidine with 0.7 mg/ml urea for 5 min.

2.6. Statistics

The Student's t test compared values between 2 groups, and ANOVA with Tukey post-hoc analysis compared values between 3 or more groups using Sigma Stat software (Systat Software, Inc., Point Richmond, CA).

3. Results

3.1. Aortic dilatation in MPS VII mice

A goal of this study was to determine if deficiency in other genes could reduce aortic dilatation in MPS animals. We chose to study mice, as animals with deficiency of our candidate genes, CtsS and MMP12, were available. We had previously demonstrated in MPS I mice that aortic dilatation was severe at 6 months, but was only mild at 3 months [10]. Since aortic disease was more severe in MPS VII dogs than in MPS I dogs [14], we postulated that disease might similarly develop more quickly in MPS VII mice than in MPS I mice, which would allow for earlier analysis for a protective effect of other genes. Others had demonstrated with echocardiography that MPS VII mice had ascending aorta internal diameters that were 158% of normal at 5 months [11], but evaluation at earlier ages was not performed. As shown in Fig. 1A, isolated aortas from male MPS VII mice had mild dilatation at 1.5 months of age, when the outer diameter was 1.6 ± 0.1 mm at 75 mm Hg, which was 122% of the value of 1.3 ± 0.02 mm Hg found in normal mice ($p<0.001$). At 3 months (Fig. 1B), the outer diameter of male MPS VII mouse aortas was markedly dilated at 2.7 ± 0.2 mm at 75 mm Hg, which was 208% of the value of 1.3 ± 0.04 mm Hg found in normal mice at the same age ($p<0.001$). In contrast, the left carotid diameter was only slightly dilated at 109% of normal ($p=0.02$) and the abdominal aorta was 98% of normal (not significant) at 3 months in MPS VII mice (data not shown), demonstrating that arterial disease was more severe in the ascending aorta than in other blood vessels. At 3 months, normal mice had systolic and diastolic blood pressures (BP) of 106 ± 3 and 75 ± 3 mm Hg, respectively, while MPS VII mice had an elevated systolic BP of 146 ± 14 mm Hg, and a reduced diastolic BP of 60 ± 4 mm Hg ($p<0.001$ for MPS VII *vs.* normal mice for both systolic and diastolic BP; data not shown).

Histological evaluation of the ascending aorta demonstrated normal elastin structure at 3 months in normal mice (Fig. 1C), near-normal structure at 1.5 months in MPS VII mice (Fig. 1D), and marked elastin fragmentation at 3 months in MPS VII mice (Fig. 1E). In addition, there was increased phosphorylation at tyrosine 705 of STAT3 at 3 months in the nuclei of MPS VII mice (Fig. 1G) as compared with normal mice (Fig. 1F). Furthermore, analysis of RNA levels at 3 months (Fig. 1H) demonstrated that elastin levels were near-normal at 2.1 ± 1.9-fold normal (not significant *vs.* normal), collagen Iα1 levels were near-normal at 1.9 ± 1.5-fold normal (not significant), MMP12 levels were elevated at 6.8 ± 4.9-fold normal ($p=0.02$), and CtsS mRNA was elevated at 4.8 ± 2.3-fold normal ($p=0.004$). mRNA for osteopontin (SPP1), a protein that can activate MMPs by non-proteolytic mechanisms and plays a role in signal transduction, was markedly elevated at 28 ± 25.6-fold normal ($p=0.03$). In addition, mRNA for MMP3, an inhibitor of MMPs (TIMP1), cathepsin B (CtsB), cathepsin D (CtsD), cathepsin L (CtsL), and the MMP-activating enzyme urokinase plasminogen activator (uPA) were also significantly elevated, although the magnitude was not as high. These data demonstrate that aortic dilatation is due to elastin fragmentation in the MPS VII mouse model, which in turn is associated with upregulation of CtsS and MMP12 mRNA. In addition, there was upregulation of other genes and phosphorylation of the transcription factor STAT3 that mimic closely what occurs in the MPS I mouse model [10], suggesting that the pathogenesis is similar. Since aortic dilatation was severe by 3 months in MPS VII mice, analysis at 3 months or later should be informative.

3.2. Effect of CtsS or MMP12 deficiency on aortic dilatation in MPS VII mice

MPS VII ($GUSB^{-/-}$) mice on a C57BL/6 background were crossed with $CtsS^{-/-}$ or $MMP12^{-/-}$ mice on C57BL/6 backgrounds, and the

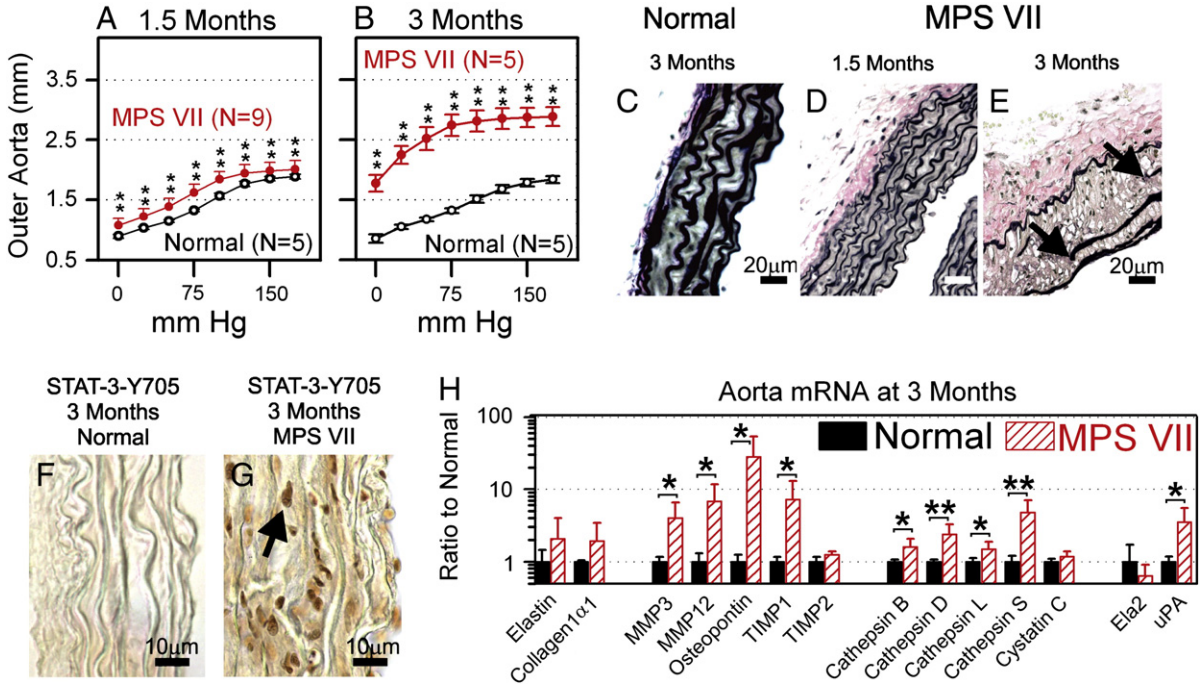

Fig. 1. Evaluation of MPS VII aortas. A and B. Compliance curves. Aortas were isolated from normal ($GUSB^{+/-}$, +/+ for other genes) or MPS VII ($GUSB^{-/-}$, +/+ for other genes) males at 1.5 or 3 months of age, and the average outer diameter of the aorta at the indicated mm Hg ± SD was determined. The Student's t-test was used to compare values in the 2 groups at each pressure, and ** indicates a p value < 0.01. C–E. Elastin stain. Sections of fixed ascending aortas were stained with VVG, which stains elastin a dark color, at the indicated age. The arrows indicate the edges of fragmented elastin fibers in the MPS VII mouse, size bars indicate 20 μm. For all panels, the intima is located on the right side, and the adventitia is on the left side. F and G. Immunostain for tyrosine-phosphorylated STAT3. Frozen sections were stained for the presence of STAT3 that was phosphorylated at tyrosine 705. The arrow identifies the dark nucleus of a positive cell in the MPS VII mouse. Bars indicate 10 μm. H. mRNA levels at 3 months. RNA was isolated from aortas at 3 months of age, and real-time PCR was used to compare levels of genes in normal (N = 6) and MPS VII (N = 5) mice after normalization to β-actin levels. Abbreviations are TIMP for tissue inhibitor of metalloprotease, ELA2 for neutrophil elastase, and uPA for urokinase plasminogen activator.

F1 offspring were then crossed to generate mice that were deficient in one or both genes. During breeding, some $GUSB^{-/-}$ mice were injected with 1×10^{10} transducing units/kg of the RV designated hAAT-cGUSB-WPRE, which contains the canine GUSB cDNA, and was previously demonstrated to result in high expression of GUSB in liver cells, high serum GUSB activity, and the ability to survive and breed long-term [38]. Aortas from RV-treated MPS VII mice were not included in analyses for mice of a particular genotype, as treatment reduced aortic dilatation. Mice from the $GUSB^{-/-}$ $CtsS^{-/-}$ colony were then crossed with mice from the $GUSB^{-/-}$ $MMP12^{-/-}$ colony to generate mice that were deficient in GUSB, CtsS, and MMP12.

Compliance studies were performed on aortas from 3 month-old male mice. Fig. 2A shows that none of the aortas were dilated in normal mice, while all of the aortas from purebred MPS VII mice (black lines in Fig. 2B) were dilated. Interestingly, some of the $GUSB^{-/-}$ mice that were $CtsS^{+/+}$ and $MMP12^{+/+}$ that had been crossed through the $Cts^{-/-}$ colony (red lines in panel 2B) had relatively normal diameters, while others were dilated. This suggests the presence

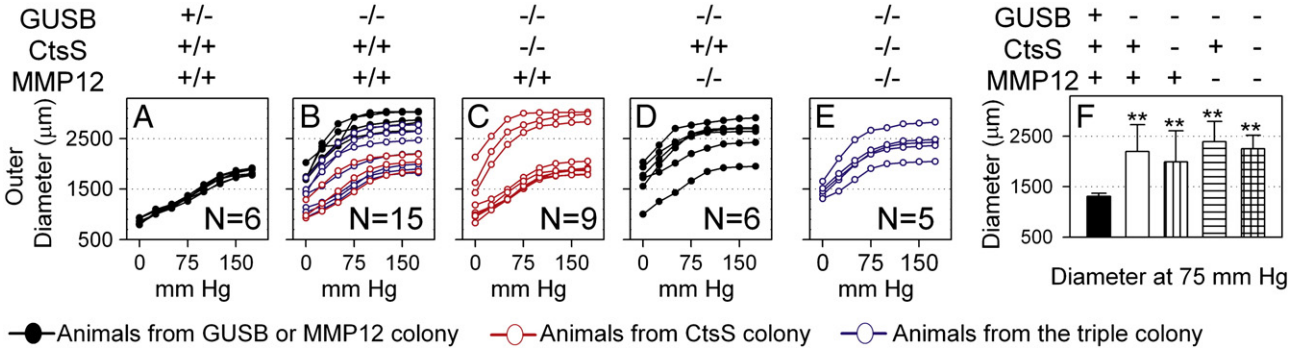

Fig. 2. Effect of CtsS and/or MMP12 deficiency on aortic dilatation in MPS VII mice. Aortas were isolated from male mice at 3 months of age, and the outer diameter was determined at the indicated mm Hg of internal pressure. Each line represents a single animal. Black lines represent animals that were never crossed through the CtsS colony, which were derived from either the original MPS VII colony or MPS VII mice that were crossed with MMP12-deficient mice. Red lines represent animals derived from a cross of the MPS VII and the $CtsS^{-/-}$ mice. Blue lines represent animals that were derived from a triple cross of $GUSB^{-/-}$, $CtsS^{-/-}$, and $MMP12^{-/-}$ mice. A. Normal. Phenotypically normal mice ($GUSB^{+/-}$ $CtsS^{+/+}$ $MMP12^{+/+}$) were analyzed. B. MPS VII mice. $GUSB^{-/-}$ $CtsS^{+/+}$ $MMP12^{+/+}$ mice were analyzed C. MPS VII mice with CtsS deficiency. MPS VII mice that were also deficient in CtsS ($GUSB^{-/-}$, $CtsS^{-/-}$, $MMP12^{+/+}$) were analyzed. D. MPS VII mice with MMP12 deficiency. MPS VII mice that also deficient in MMP12 ($GUSB^{-/-}$, $CtsS^{+/+}$, $MMP12^{-/-}$) were analyzed. E. MPS VII mice with CtsS and MMP12 deficiency. MPS VII mice that were also deficient in CtsS and MMP12 ($GUSB^{-/-}$, $CtsS^{-/-}$, $MMP12^{-/-}$) were analyzed. F. Average aortic diameter. The average outer aortic diameter ± SD at 75 mm Hg was determined from the compliance curves in panels A to E. Statistical comparisons were performed between normal mice and other groups; ** indicates a p value < 0.01.

of an independently-segregating gene in the CtsS colony that can provide protection from aortic dilatation. Similarly, some of the MPS VII mice derived from the triple colony (cross of GUSB$^{-/-}$ CtsS$^{-/-}$ mice or related genotypes with GUSB$^{-/-}$ MMP12$^{-/-}$ mice or related genotypes) that were CtsS$^{+/+}$ and MMP12$^{+/+}$ (blue lines in Fig. 2B) had near-normal diameters, while others were dilated to a varying extent.

GUSB$^{-/-}$ CtsS$^{-/-}$ mice (Fig. 2C) showed marked variability between individual mice, with some mice exhibiting near-normal diameters, and others showing marked dilatation. GUSB$^{-/-}$ CtsS$^{-/-}$ mice with near-normal aortic diameters tended to be found early in the breeding strategy when the representation of the CtsS colony was high and derived from particular parents, while animals of the same genotype with dilated aortas were usually found later in breeding and to derive from different parents. The genetic data are consistent with the presence of an independently-segregating gene in the CtsS colony that conferred protection from aortic dilatation when present in a homozygous recessive state, although the identification of this putative gene remains unknown. GUSB$^{-/-}$ MMP12$^{-/-}$ mice aortas were consistently dilated, although one animal was less severe than the others (Fig. 2D). GUSB$^{-/-}$ CtsS$^{-/-}$ MMP12$^{-/-}$ mice (Fig. 2E) all had dilated aortas.

Average aortic diameters ± SD at 75 mm Hg for each of these groups are shown in Fig. 2F. Aortic diameters from GUSB$^{-/-}$ CtsS$^{-/-}$ mice, GUSB$^{-/-}$ MMP12$^{-/-}$ mice, or GUSB$^{-/-}$ CtsS$^{-/-}$ MMP12$^{-/-}$ mice were not statistically different from GUSB$^{-/-}$ mice without additional deficiencies, and all MPS VII groups were statistically different from normal mice. We conclude that deficiency of CtsS, MMP12, or both cannot prevent aortic dilatation in MPS VII mice.

3.3. Effect of gene therapy on functional and biochemical abnormalities in the aorta

The effect of gene therapy on aortic dilatation in MPS VII mice was determined. Some MPS VII mice received IV injection of an RV expressing GUSB at 2–3 days after birth. This resulted in high GUSB activity in serum, as shown in Fig. 3A. Values in individual animals varied from 182 to 4042 U/ml, which is consistent with our previous results showing marked variation in individual RV-treated mice [38]. Aorta diameters were measured after exsanguination with no internal application of pressure. RV-treated MPS VII mice had improvement of aortic diameters to 1.6 ± 0.3 mm at 6 months of age (Fig. 3B; 113% normal but not significant *vs.* normal). Aorta GUSB activity increased to 195 ± 108 U/mg in RV-treated mice (Fig. 3C), which was 5.0-fold the value in normal mice ($p<0.001$), and was 325-fold the value in untreated MPS VII mice ($p<0.001$). Elevation of other lysosomal enzymes generally occurs in lysosomal storage diseases, and normalization of this elevation is a good biochemical marker of correction of disease. Indeed, IDUA activity (Fig. 3D) was 22-fold normal in MPS VII mice ($p<0.001$), and RV-treated mice had a reduction in IDUA activity to 15% of that found in untreated MPS VII mice ($p<0.001$), although it remained elevated at 3-fold normal (not significant *vs.* normal). Similarly, GAGs (Fig. 3E) were elevated in MPS VII mouse aortas to 111-fold normal ($p=0.01$), and were reduced in RV-treated aortas to 5% of the value in untreated MPS VII mice ($p=0.04$), although they remained 6-fold normal. The failure to achieve complete biochemical correction is likely responsible for the fact that RV-treated MPS VII mice had modest dilatation of the aorta at 10 months at 2.2 ± 0.5 mm, which was 155% ($p=0.01$) of the value of 1.4 ± .02 mm in the normals (Fig. 3B), demonstrating that gene therapy was not fully effective at preventing aortic disease long term.

3.4. Cathepsin enzyme activity in aortas

We focused on the role of CtsS in aortic dilatation despite the fact that mRNAs for other cysteine cathepsins were elevated in MPS VII aortas. This was because CtsS was reported to be the only cysteine cathepsin that was active at neutral pH [40,41], which is the pH expected outside of the cell where elastin resides, and a CtsS inhibitor markedly reduced enzyme activity in MPS I mice [10]. The failure of CtsS deficiency to protect MPS VII mice from aortic dilatation led us to test the assumption that other cathepsins are inactive at neutral pH. Supplementary Fig. 1 shows the activity of purified cathepsins against different substrates and inhibitors at pH 7.5. CtsB, CtsH, CtsK, and CtsS maintained activity at pH 7.5 against the fluorogenic peptide Z-Phe-Arg-AMC that can be cleaved by all enzymes at lower pH, although CtsL was inactive at pH 7.5. This result differs from the literature, which suggested that CtsB and CtsK were inactive at neutral pH [40,41]. The CtsB inhibitor was reasonably specific for CtsB, as 96% of the activity was inhibited at 100 nM, while CtsH and CtsK

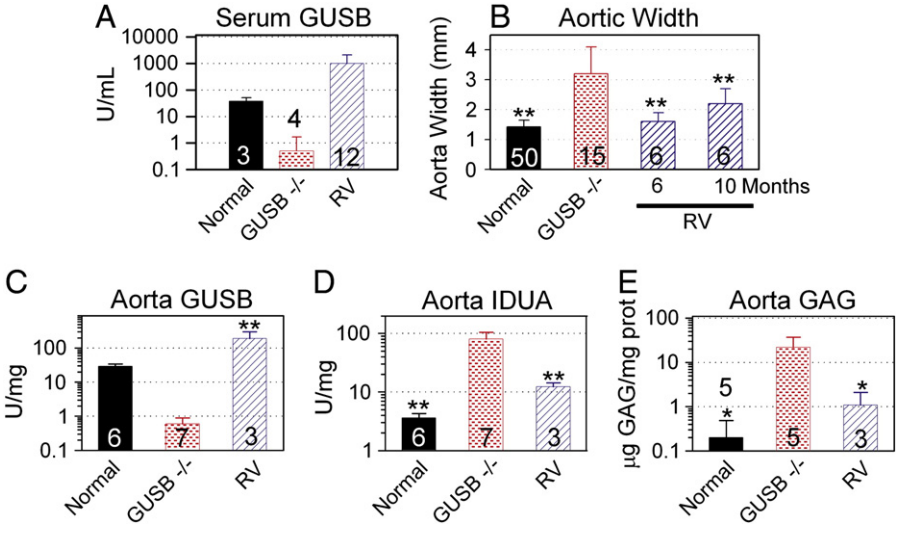

Fig. 3. Effects of gene therapy on aortic abnormalities. Some MPS VII mice were injected IV with 1×10^{10} transducing units/kg of the RV designated hAAT-cGUSB-WPRE at 2–3 days after birth, while other mice were untreated. A. Serum GUSB activity. GUSB activity was determined at 2 to 6 months of age for normal, untreated MPS VII, and RV-treated MPS VII mice for the indicated number of animals. B. Aortic width. Aortas were dissected and the width was measured at 6 months of age for normal and MPS VII mice, and at 6 months or 10 months as indicated for RV-treated MPS VII mice. C and D. Aorta GUSB and IDUA activity. Extracts prepared at pH 5.5 were tested for GUSB and IDUA activity. E. GAG levels. Extracts prepared at pH 7.5 were tested for GAG levels. Values were compared using ANOVA with Tukey post-hoc analysis, and * represents $p\leq0.05$ and ** represents $p\leq0.01$ as indicated above the bars for comparison with values in untreated MPS VII mice.

activity were at most modestly reduced at this concentration. The CtsK-specific inhibitor was relatively specific for CtsK, although it had modest activity against CtsB (50% inhibition) at 1000 nM. However, the CtsS inhibitor was quite promiscuous, inhibiting CtsB, CtsK, and CtsL almost as effectively as CtsS.

The ability of extracts from aortas of MPS VII mice with or without deficiency of CtsS to cleave cathepsin substrates is shown in Fig. 4. Extracts from GUSB$^{-/-}$ CtsS$^{+/+}$ aortas had high activity against Z-Phe-Arg-AMC at pH 7.5 (4838 ± 777 U/mg), which was 7-fold the value in normal mice of 678 ± 159 U/mg ($p = 0.01$), as shown in Fig. 4A. Surprisingly, extracts from GUSB$^{-/-}$ CtsS$^{-/-}$ mice also had very high activity against Z-Phe-Arg-AMC at pH 7.5 at 5377 ± 2354 U/mg, which was 111% of the value in purebred MPS VII mice.

To further investigate the identity of the cathepsin responsible for the activity in extracts from GUSB$^{-/-}$ CtsS$^{-/-}$ mice, specific inhibitors of cathepsins and other substrates were used. Fig. 4B demonstrates that the CtsB inhibitor reduced overall activity of both GUSB$^{-/-}$Cts$^{+/+}$ and GUSB$^{-/-}$CtsS$^{-/-}$ extracts *vs.* Z-Phe-Arg-AMC by 95%, suggesting that CtsB was the major cathepsin responsible for activity, while the CtsK inhibitor had a modest effect, which could be due to some activity against CtsB (see Supplementary Fig. 1). Z-Arg-Arg-AMC is a substrate that is specific for CtsB, as shown in Supplementary Fig. 1. As shown in Fig. 4C, aortic extracts from GUSB$^{-/-}$ Cts$^{+/+}$ and GUSB$^{-/-}$ CtsS$^{-/-}$ had 2049 ± 847 and 1580 ± 898 U/mg vs. Z-Arg-Arg-AMC, which were 8-fold and 6-fold, respectively, the value of 251 ± 54 in normal aortas. The lower activity of these extracts against Z-Arg-Arg-AMC as compared with Z-Phe-Arg-AMC is consistent with the fact that purified CtsB has only 61% as much activity against Z-Arg-Arg-AMC as against Z-Phe-Arg-AMC.

The data shown above suggest that CtsB is the major enzyme responsible for cathepsin activity in MPS VII mice. It is possible, however, that some other cathepsin is active at neutral pH, and that this is difficult to detect due to the high CtsB activity. CtsK is a very important enzyme, as it maintains activity at pH 7.5 (Supplementary Fig. 1), it has elastin-degrading activity [42], and is activated by chondroitin sulfate [43], which is one of the GAGs that accumulates in MPS VII. A CtsK substrate was obtained that was not cleaved by CtsB or CtsS to an appreciable extent, although it was cleaved by CtsL 1% as efficiently as CtsK (data not shown). Activity with this CtsK substrate was elevated in GUSB$^{-/-}$Cts$^{+/+}$ or in GUSB$^{-/-}$ CtsS$^{-/-}$ mice to 16.5 ± 3.3 U/mg and 16.9 ± 5.6 U/mg, respectively, which was 2.2-fold the value of 7.4 ± 4 U/mg in normal mice (Fig. 4D). Although activity was significantly elevated in the MPS VII mice ($p = 0.019$ vs. normal), the CtsK activity was <0.1% of the CtsB activity on a U/mg basis.

CtsD is an aspartyl protease that can activate other cathepsins such as CtsB [44], although it has no activity against substrates that are cleaved by cysteine cathepsins. CtsD activity at pH 4.0 (Fig. 4E) was 9.5- and 11.2-fold normal in GUSB$^{-/-}$CtsS$^{+/+}$ and GUSB$^{-/-}$ CtsS$^{-/-}$ mice, respectively, suggesting a mechanism for activation of CtsB.

We conclude that CtsS does not play an important role in aortic dilatation in MPS VII, and that the major cysteine cathepsin that is upregulated is CtsB, which is generally believed to have low, albeit detectable, activity against elastin [50]. Although there was some increase in CtsK activity, which is a known elastase, this activity was

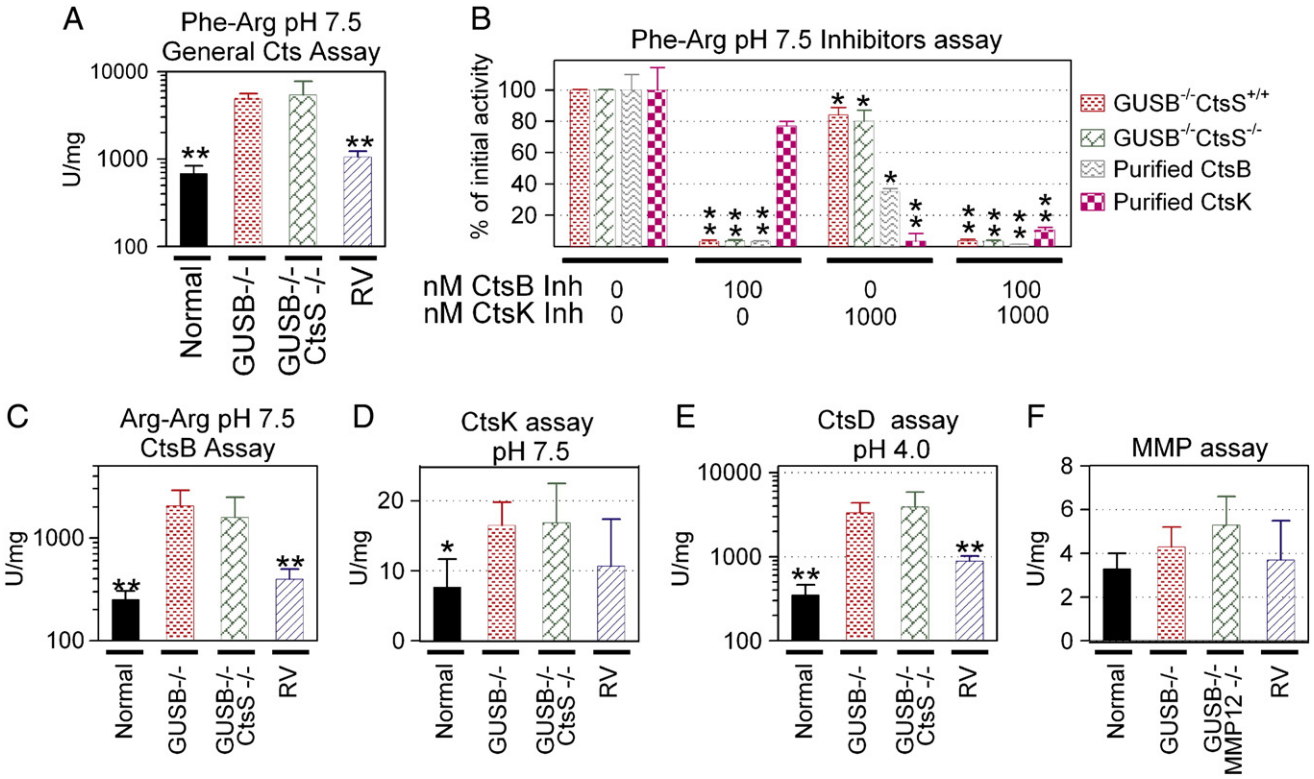

Fig. 4. Cathepsins and MMP assays. Aortas from normal mice, GUSB$^{-/-}$ CtsS$^{+/+}$ mice (labeled GUSB$^{-/-}$ on the figure), GUSB$^{-/-}$ CtsS$^{-/-}$ mice, or RV-treated MPS VII mice (RV) were homogenized at pH 5.5 for cathepsin assays, while aortas from normal mice, GUSB$^{-/-}$ MMP12$^{+/+}$ mice (labeled GUSB$^{-/-}$ on figure), GUSB$^{-/-}$ MMP12$^{-/-}$ mice, or RV-treated MPS VII mice (RV) were homogenized at pH 7.5 for the MMP assay. A. Total cathepsin activity at pH 7.5. Samples were incubated with the non-specific substrate Z-Phe-Arg-AMC (Phe-Arg) at pH 7.5, and the activity in U/mg determined. B. Effect of inhibitors on activity against Z-Phe-Arg at pH 7.5. Samples from GUSB$^{-/-}$ CtsS$^{+/+}$ mice, samples from GUSB$^{-/-}$ CtsS$^{-/-}$ mice with dilated aortas, purified CtsB (0.15 U), or purified CtsK (0.15 U) were incubated with the non-specific Z-Phe-Arg-AMC substrate with and without inhibitors of CtsB and CtsK at the indicated concentration, and the activity relative to that present in samples that did not receive an inhibitor was determined. C. CtsB activity at pH 7.5. Samples were incubated with the CtsB-specific substrate Z-Arg-Arg-AMC (Arg-Arg) at pH 7.5. D. CtsK activity at pH 7.5. Samples were incubated with a CtsK-specific substrate. E. CtsD activity at pH 4.0. Activity for CtsD was determined using a CtsD substrate. F. MMP activity. MMP activity was determined using a commercial kit. For panel B, values in samples that were treated with an inhibitor were compared with values for samples that did not receive the inhibitor using the Student's t test. For other panels, values in other groups were compared with values in untreated MPS VII mice using ANOVA with Tukey post-hoc analysis. * represents $p \leq 0.05$ and ** represents $p \leq 0.01$.

very low. It was difficult to assess CtsH activity, as no specific assay was identified.

3.5. MMP12 activity

MMP12 was a good candidate for an enzyme that could degrade elastin in MPS VII aortas, as it is a known elastase, its mRNA was 7-fold normal at 3 months in MPS VII mice, its enzyme activity was elevated in MPS I mouse aortas [10] and in MPS I and MPS VII dog aortas [14], and its deficiency reduced aortic dilatation in one model [24]. Ascending aorta extracts from MPS VII mice were tested for MMP12 activity using a fluorogenic substrate that can be cleaved by MMP12. This demonstrated that MMP12 activity was not elevated in MPS VII mice at 6 months of age (Fig. 4F). This substrate can be cleaved by other MMPs, as demonstrated by the fact that extracts from MMP12-deficient mice still had activity in this assay. The failure of MMP12 deficiency to prevent dilatation of MPS VII aortas demonstrates that this enzyme does not play a major role in this model.

3.6. RNA analysis in MPS VII mice

The above studies demonstrate that deficiency of both CtsS and MMP12 cannot prevent aortic dilatation in MPS VII mice. We therefore used microarray analysis of RNA from the aorta of normal mice ($GUSB^{+/-}$ $CtsS^{+/+}$ $MMP12^{+/+}$) and MPS VII mice with aortic dilatation ($GUSB^{-/-}$ $CtsS^{+/+}$ $MMP12^{+/+}$) to attempt to identify other genes whose protein products might contribute to aortic dilatation. Samples were isolated at 6 months of age, when aortic disease was well-established. Table 1 summarizes the genes in various categories whose expression was upregulated (≥2.5-fold normal) or downregulated (≤0.4-fold normal) in a statistically significant fashion (p value ≤0.01) after comparison of values in normal with those in MPS VII mice. Supplementary Table 2 shows values for all up- and down-regulated genes, which are sorted into different categories. In addition, all microarray data were uploaded to the GEO microarray data base (GSE30657), and values for genes whose expression was not significantly altered can be found there. Some categories of genes are discussed below, while others simply appear in Table 1 or Supplementary Table 2. Finally, a list of all elastases that were interrogated is in Supplementary Table 3, while a list of all complement components that were interrogated is in Supplementary Table 4.

GeneGo software was used to determine if the changes in gene expression observed in MPS VII aortas resemble those that occur in other processes, networks, or diseases, using a level of upregulation of 2.5-fold normal, and a p value ≤0.01. The most upregulated process was the immune system process, with 62 genes upregulated out of 1617 genes that were put into this category by the software (not all of which are regulated at the transcriptional level), with a p value for significant upregulation of 2×10^{-27}. The most upregulated process network was inflammation of the complement system, with 12 genes upregulated out of 73 genes that were put into this pathway, for a p value of 2×10^{-11}. The most upregulated disease was rheumatoid arthritis, with 58 genes upregulated out of 941 that were placed in this category, for a p value of 6×10^{-25}.

3.7. RNA for extracellular matrix proteins

Extracellular matrix protein mRNAs that were evaluated include elastin and collagen, genes that are necessary for their assembly, and miscellaneous extracellular matrix genes. Elastin mRNA was not altered, while the elastin-associated protein fibulin 2 (Fbln2) mRNA was modestly elevated at 3.1-fold normal in the MPS VII aorta, as shown in Table 1 and in Supplementary Table 2. Some extracellular matrix proteins were reduced. For example, mRNA for procollagen C-endopeptidase enhancer 2 (Pcolce2), which enhances processing of types I and II procollagens, was 0.3-fold normal. Finally, mRNA for optican (Optc), a protein that affects collagen fibrils in the eye, was markedly reduced at 0.15-fold normal. We conclude that elastin fragmentation was probably not due to downregulation of mRNA for elastin or elastin-associated proteins, but there were a few abnormalities in genes associated with collagen assembly.

3.8. RNA for elastases

A major hypothesis of this project was that a protease that can degrade elastin was upregulated in the aorta of MPS VII mice. According to GeneGo interactions software and the national library of medicine (http://www.ncbi.nlm.nih.gov/pubmed/) gene category, elastin can be cleaved by at least 28 different proteases. Supplementary Table 3 lists all known elastases that were interrogated on the microarray regardless of their expression level. mRNA was significantly higher in MPS VII than in normal mice for cathepsin L (6.2-fold), complement component D (CFD, 4.0-fold normal; 16,645 fluorescent units (FU/) spot in normal mice; p = 0.006), MMP12 (3.6-fold normal) and cathepsin K (CtsK; 2.8-fold normal). In addition, mRNAs for some other elastases were elevated on the microarray, but were not ≥2.5-fold normal or did not achieve a p value ≤0.01 for comparison of the 2 groups. These include MMP2, CtsS, CtsB, CtsH, and legumain (Lgmn), which is a cysteine protease that is induced by LPS whose substrates are poorly characterized. mRNA for several other elastases were not significantly altered, as summarized in Supplementary Table 3.

3.9. RNA for genes of the complement system

Complement components play important roles in the innate and the acquired immune response, and activation of the complement pathway can result in upregulation of destructive proteases. As noted above, the process network that most resembles the changes in gene expression observed in MPS VII aortas was the complement system, with a p value of 2×10^{-11}. In addition, there is one report that CFD (also called adipsin or endogenous vascular elastase) can cleave elastin [45], and CFD were very abundant in the normal aorta and elevated to 4.0-fold normal in MPS VII mice (p = 0.006). Genes of the complement system that were upregulated on the microarray are shown on Table 1 and on page 2 of Supplementary Table 2. In addition, values for all complement genes that were interrogated on the microarray are shown in Supplementary Table 4.

Activation of the complement system may occur by 3 different pathways [46]. The classical pathway involves binding of IgG or IgM to a complex containing the C1 complex (containing C1q, C1r, and C1s), which can then cleave C4 and then C2 to generate C3 convertase, which in turn can activate C3 to C3a and C3b by proteolytic cleavage. C1 (6.1-fold normal for the most upregulated component), C4 (3.4-fold normal), and C2 (2.5-fold normal) were all upregulated in MPS VII aortas. A second pathway of complement activation is the alternative pathway, which can be initiated by spontaneous decay of C3 to C3a and C3b, or by generation of C3b from other pathways. This involves cleavage of complement component B of a C3bB complex by CFD, after which the C3bBb complex can cleave additional C3, while properdin (CFP) stabilizes the C3bBb complex and protects it from regulation by complement inhibitors. CFD was elevated to 4-fold normal, while CFP was 1.9-fold normal. A third pathway for complement activation involves the lectin pathway, in which mannose-binding lectin (MBL) or a ficolin binds to carbohydrates such as mannose or N-acetyl glucosamine that results in activation of MBL-associated serine proteinase 1 (MASP1) or MASP2, which in turn activate complement. Ficolin A (FcnA) was 2.7-fold normal. Cleavage of C3 can result from all three pathways of complement, and generates an anaphylatoxin (C3a) and C3b. C3b can initiate formation of the membrane attack complex as well as generate another anaphylatoxin, C5a. Although mRNA for none of these downstream components or receptors for anaphylatoxins were upregulated in the MPS VII aorta, they

Table 1
Genes differentially expressed in the MPS VII aorta. RNA was extracted from normal (N = 3) or MPS VII (N = 3) aortas at 6 months of age and a microarray was performed. Genes were considered significantly upregulated (≥2.5-fold Normal) or downregulated (≤0.4-fold Normal) when p was <0.01. The gene symbol is shown here. Supplementary Table 2 shows the gene symbol, the ratio of the signal in MPS VII to normal mice, the signal for each probe for normal mice, and the p value for comparison of MPS VII with normal mice.

Classification	Upregulated (>2.5-fold normal)	Downregulated (<0.4-fold normal)
Extracellular matrix proteins	Spp1, Reln, Fbln2, Tnc	Vit, Tnxb, Cyr61, Npnt, Pcolce2, Omd, Optc
Proteases	Ctsl, Dpep2, Mmp3, Mmp12, Lgmn, Napsa, Ctsk, Ctsa, Cpxm2	Dpp10, Phex
Protease Inhibitors	Fetub, Timp4	Serpine2, Wfdc1
Complement system	C1qc, C1qb, C1qa, CFD, C4, Fcna, C2	None
Lectins	Clec4d, Clec4n, Lgals3, CD83, Mrc1	Clec3b
Toll-like receptor and TNFα signaling	Trem2, Tlr13, Tnfaip2, Tyrobp, CD14, Lcp1, Tnfaip8l2, Litaf	None
Fc Immunoglobulin receptors	Ms4a7, Fcgr4, Fcgr3, Fcgr2b, Fcer1g, Msr2, Lilrb4	None
Chemokines or growth factors	Ccl21c, Igfbp2, Ccl4, Igfbp3, Cxcr4, Pdgfb, Ngfb, Cx3cl1, Agtr1a, Il10ra, Cxcl16, Igf1	Igf2, Ltbl4, Bmp3, Cytl1, Bmpr1b
Kinases or kinase binders	Rps6ka1, Tec, Btk, Pbk, Fes, Ptk2b	Prkaa2
Phosphatases	Ptpre, Inpp5d	Pitpnm3, Ppm1e, Dusp8, Dusp1, Ppp1r1b
G protein-associated proteins	Gpr176, Gpr109a, Ednrb, Gpr34, Gpr81, Gng2, Cnr2, Gpr97	Ngef, Rgs4
Cytoskeletal proteins, integrins, cell adhesion	Lpxn, Myo1f, Nckap1l, Myo7a, Emcn, Vcam1, Icam1, Unc93b1, Cotl1, Arhgdib, Rai14, Svep1, Gja4, Arhgap25, Vill, Itgb7, Pcdh1, Lasp1,Tpm3, Cldn5, Thbs1, Arhgap22, Was, Arhgap30	Cnn1, Pdlim4, Pdlim3, Slmap, Scin, Wasf1, Mcam, Tmem47, Myoz2, Thsd4, Unc5c, Sema5a, Dtna, Tppp3, Sgca, Xirp1, Des, Amigo2, Bves, Actg2, Tcap
Wnt pathway	Sprf1, Wisp1, Wisp2	Wif1, Cxxc4
Lipid metabolism	Pld3, Ptgds, Pld4, Agpat2,	Dgkg
Transcription factors	Cebpa, Elk3	Crtc3, Creb5, Zfp281, Id1, Myocd, Atf3, Fos
Miscellaneous signal transduction proteins	Gpnmb, Lat2, Ccnd1, Rerg, Xlr4a, Emr1, Cd84, Ly9, Havcr2, Nrn1, Ly86, Sirpa, CD52, H2-Ab1, Ncf4, Insig1, CDC20, Cd74, H2-Eb1, Irs3, Fst	Gucy1a3, Retnla, Rab9b
Lysosomal or peroxisomal proteins	Cd68, Lyz2, Lyz, Laptm5, Atp6ap2	Hyal1, Gusb
Proteoglycans	Sdc3	Acan
Glycosynthesis-related enzymes or proteins in ER or Golgi	Chst1, Ugt1a10, Renbp, Mfng, Uap1l1, Man2a1, Gal3st1	Pigz
Vesicle transport	Scg2, Stab1, Rftn1, Syngr1	Syngr3, Rtn2, Cav3, Stx1a, Sorl1, Kalrn
Ubiquitination	None	Fbxl13, Fbxo30, Hspa1a
Neurodegeneration	Sncg	Npy1r
Apoptosis	Arl11, Cidec, Bid	None
DNA/RNA metabolism	Apobec1, Fus	Rbm8a, Hdac5, Brip1
Metabolism	Cyp2e1, Car3, Ddah1, Cyp2f2, Hbb-b2, Trf, Apoe, Acaa2, Car5b, Htatip2, Mup2, Mgst1, Aldh3b1, Akr1c12, Hk3, Eno1, Cp, Chpt1, Cyp1b1, Cyp4f18, Tcn2, Pdhb, Idh1, Cryz	Bdh1, Stc2, Agpat5, Pgm5, Vldlr, Adh7,Noxo1
Solute or water transporters	Slc15a3, Slc40a1, Slc11a1, Slco2a1, Abcc3, Slc7a10, Slc27a1, Slc13a4, Aqp7, Slc16a4	None
Ion channels	Ttyh2, Hvcn1, Atp1b1, Fxyd6	Atp1b2, Kcnk1, Kcnab1
Miscellaneous function	None	Hspa2, Olfml2b, Hspa1l
Unclear function	MsA46d, Evi2a, Tmem176b, Art4, Klhl6, Mlana, Lrrc33,	Tspan11, Stbd1, Crispld2, Fam171b, Vstm2b, Fam107a, Scube3

were expressed, and thus poised to respond to upstream events. Of the complement inhibitors, complement factor H was reduced to 0.64-fold in MPS VII mice, while others were not significantly affected, and were generally expressed at fairly low levels except for CD59, which is an inhibitor of the late stages of complement.

3.10. Signal transduction molecules

As one hypothesis for the mechanism of disease in MPS VII is that GAGs bind to the TLR4 and induces inflammatory signals, genes of the TLR pathway or downstream signaling molecules are shown in Supplementary Table 2. Although TLR4 was not elevated in MPS VII mice, it was moderately abundant, and thus could respond to GAGs. In addition, mRNA for proteins CD14, which associates with the TLR4 was 4.0-fold normal. Finally, genes that are upregulated by TLR signaling such as TREM2 (10.8-fold normal) and its associated protein, Tyrobp (DAP12 = 4.1-fold normal) were elevated, as were several other proteins that are known to be induced by TLR or TNFα signaling.

Receptors for immunoglobulins can act synergistically with TLR receptors or with complement in signal transduction, and can activate many of the same downstream molecules [47]. Many mRNAs for genes that encode Fc receptors were markedly elevated, as shown in Supplementary Table 2. Fc receptors were also elevated in MPS VI synovial cells [3].

Complement receptors, TLRs, and Fc receptors can all result in alteration of mRNA for cytokines, growth factors, intracellular signal transduction proteins, or proteins that bind to these proteins. Genes for such proteins whose expression was altered in MPS VII mouse aorta are shown in Supplementary Table 2. Ccl21 is the most highly upregulated cytokine at 35.5-fold normal, while the cytokine Cxcl4 (MIP-1β) was 10.3-fold normal, and is a gene that is upregulated in many models of MPS. The increase in angiotensin II receptor, type 1, a receptor for angiotensin II, to 2.9-fold normal, was of interest, as inhibitors of this receptor such as losartan can reduce elastin fragmentation in Marfan Syndrome mice [48]. Genes that were downregulated included latent transforming growth factor beta binding protein 4 (0.4-fold normal), bone morphogenetic protein 3 (BMP3; 0.3-fold normal), and BMP receptor, type IB (0.2-fold normal).

3.11. Immunohistochemsitry for C3

Aortas were tested for deposition of C3 (Fig. 5), since several genes of the complement system were upregulated in MPS VII aortas on the microarray. MPS VII aortas had a strong positive signal in the media, which was localized at the edge of GAG deposits and to a lesser extent along the edge of elastin fibers. Although normal mice had some C3 deposition in the intima and adventitia, there was little signal in the media. These data confirmed that the complement system was

activated in the MPS VII aortas, and suggest that it occurs at sites of GAG deposits.

3.12. Real-time PCR for complement genes

Real-time reverse transcriptase analysis of expression of complement genes (Fig. 6) confirmed elevation of genes in MPS VII aortas that were found on the microarray. For example, CFD was elevated at 34.6 ± 27.3-fold normal and was very abundant at 4.5-fold the level of β-actin, while properdin was 3.7 ± 2.4-fold normal. In addition, there was upregulation of mRNA for genes related to the classical pathway such as C1qa (11.5 ± 2.4-fold normal), C2 (6.4 ± 2.7-fold normal), C4 (11.1 ± 8.2-fold normal), and the lectin pathway such as FcnA (9.5 ± 5.4-fold normal), MASP1 (0.01% β-actin; not detectable in normal) and MASP2 (0.3% β-actin; not detectable in normal). Furthermore, genes related to downstream events of complement pathways were also elevated in MPS VII aortas, including C3 (4.0 ± 2.5-fold normal) and C5 (0.005% β-actin signal; undetectable in normal). Finally, regulators of complement were either significantly reduced (CFH) or moderately increased (CFI, CD55) in MPS VII as compared with normal mice.

4. Discussion

Aortic dilatation in MPS is important, as it will likely result in aortic dissection and possibly death as patients live longer after treatment with HSCT or ERT. Identification of the pathogenesis of elastin fragmentation might lead to the identification of a drug that would prevent this from occurring in patients. We favor the hypothesis that degradation of elastin is the most important mechanism responsible for elastin fragmentation, as MPS VII aortas had minimal amounts of lysosomal storage material, relatively normal elastin, and only minimal dilatation at 6 weeks of age, when elastin formation is believed to be largely completed [19]. Elastin fragmentation then developed in conjunction with progressive accumulation of lysosomal storage material, suggesting that degradation was involved. It remains possible that elastin assembly contributes to abnormal elastin structure, as proposed by Hinek et al. for MPS I [23]. The present work focused on the role of elastin, as collagen fibers were not overtly abnormal in MPS VII aortas (data not shown) or in MPS I or MPS VII aortas [14].

4.1. CtsS and MMP12 deficiency do not prevent elastin fragmentation in MPS VII aorta

A hypothesis of this project was that CtsS and/or MMP12 played pivotal roles in the elastin fragmentation that is likely responsible for the dilatation that occurs in MPS VII aortas. This hypothesis was clearly wrong, as deficiency of CtsS, MMP12, or both could not prevent aortic dilatation in MPS VII mice. In the case of CtsS deficiency, biochemical analyses demonstrated that the elevation in cysteine proteinase activity that we had previously attributed to CtsS in MPS I mice [10] and in MPS I and MPS VII dogs [14] was still present in GUSB$^{-/-}$ CtsS$^{-/-}$ mice, suggesting that another cathepsin was responsible. There are 11 lysosomal cysteine cathepsins, all of which are primarily destined for the lysosome but can also be secreted [49]. Further biochemical analyses demonstrated that this cathepsin activity in MPS VII aortas was primarily due to CtsB activity based upon efficient cleavage of a CtsB-specific substrate (Z-Arg-Arg-AMC) and inhibition with a CtsB-specific inhibitor at 100 nM. However, CtsB is believed to have relatively low activity against elastin [50], although it remains possible that the very high CtsB activity observed could have sufficient elastin-degrading activity to result in damage over time. One interesting feature was the fact that CtsB activity was markedly elevated at 8-fold normal, while CtsB mRNA was only 1.5-fold normal. It is possible that an activator of CtsB was upregulated, and indeed, the enzyme activity for the aspartyl protease CtsD that can activate CtsB by cleavage [44] was elevated to 10-fold normal. It is also possible that CtsK activity contributed to elastin fragmentation, as CtsK RNA and enzyme activity were 2.8- and 2.2-fold normal, respectively, and CtsK is known to be a potent elastase, although the activity appeared to be very low. Although CtsL mRNA was elevated at 6.2-fold normal, it is unlikely to be important, as the levels of RNA were very low, and CtsL is inactive at neutral pH. Although it is possible that CtsH contributes to elastin degradation, as its mRNA was 1.5-fold normal, we were unable to test its activity due to the absence of a specific assay. Finally, legumain is a poorly

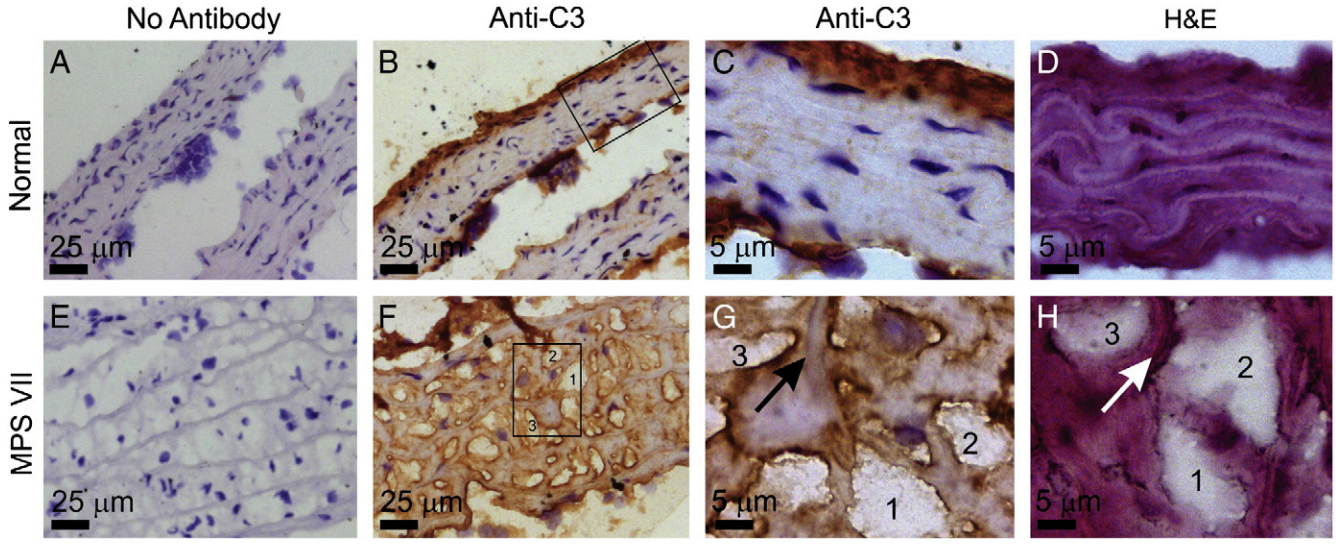

Fig. 5. Immunostain for C3. Aortas were from a normal (panels A–D) and an MPS VII (panels E–H) aorta isolated at 6 months. Frozen sections underwent immunostaining without the addition of the anti-C3 first antibody (panels A and E; No Antibody), or with the addition of the anti-C3 first antibody (panels B–C and F–G; Anti-C3) as detailed in the Materials and methods section, and were counterstained with hematoxylin. Panels D and H received hematoxylin and eosin staining only (H&E). The boxes in panels B and F are the regions that are shown at higher power in panels C and G, respectively. Panels G and H represent adjacent sections of the same region of the MPS VII aorta, where 3 separate deposits of GAGs are numbered 1, 2, or 3, and the arrow identifies an elastin fiber. The brown color indicates a positive signal for C3, and nuclei appear blue. Size bars are indicated in each panel. The adventitia is at the top of all low magnification panels.

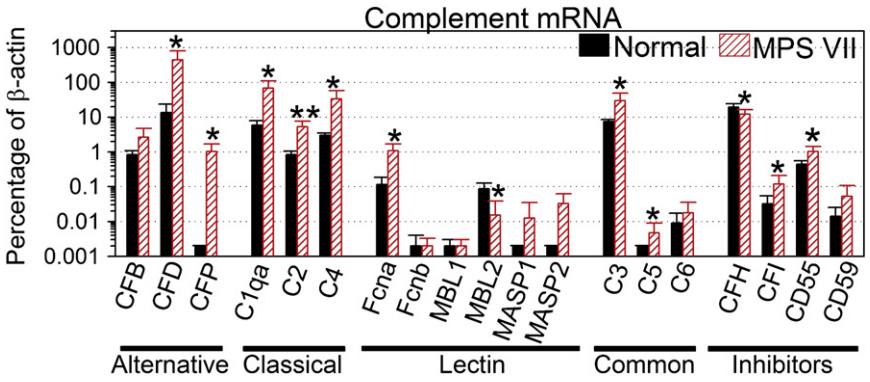

Fig. 6. mRNA for complement genes. RNA was extracted from normal (N = 4) and MPS VII (N = 6) mice at 6 months of age and used for reverse transcriptase real-time PCR to assess complement gene mRNA levels. Results are shown as the percentage of β-actin. Genes with expression lower than 0.002% of β-actin were considered not present and are shown as 0.002% in the figure. *$p<0.05$ or **$p<0.01$ for comparison of values in MPS VII with those in normal mice using Student's t test. Abbreviations include Fcna for ficolin A, Fcnb for ficolin B, MBL for mannose-binding lectin, MASP for mannan-binding lectin associated serine protease, CD55 for decay accelerating factor, and CD59 for protectin.

characterized cysteine protease whose mRNA was elevated to 2.9-fold normal.

MMP12 was clearly not necessary for aortic dilatation, as deficiency of MMP12 did not prevent aortic dilatation in MPS VII mice. This was likely due to the fact that MMP12 activity was only 1.5-fold normal in $GUSB^{-/-}$ mice at 6 months, and was not statistically different from values in normal mice, or from values in $GUSB^{-/-}$ $MMP12^{-/-}$ mice despite the fact that MMP12 mRNA was 6.8 ± 4.9-fold normal at 3 months, and was 3.6-fold normal at 6 months. This discrepancy may reflect the fact that MMP12 needs to activated by proteolytic cleavage. The matrix metalloproteinase (MMP) family has at least 20 members, of which MMP-2, -7, -8, -9, -10, -12, and -14 have elastase activity [51], and of which MMP2 and MMP8 can cleave the peptide that was used in our MMP12 assay. Thus, although MMP2 mRNA was modestly elevated at 2-fold normal in the microarray, it is unlikely that MMP2 contributes to elastin fragmentation, as upregulation of MMP2 enzyme activity should have been detected in this enzyme assay.

4.2. Possible role of another gene involved in aortic dilatation in MPS VII

An interesting feature of this study was the fact that some $GUSB^{-/-}$ $CtsS^{+/+}$ $MMP12^{+/+}$ mice that derived from breeding through the CtsS colony did not have dilated aortas. We hypothesize that this was due to an independently-segregating gene that initiated from the $CtsS^{-/-}$ colony that conferred protection from aortic dilatation when present in an autosomal recessive state. The $CtsS^{-/-}$ mice were generated in 129 mice whose subtype was not specified, and then backcrossed with C57BL/6 mice. Interestingly, 129/SvEv mice are less susceptible to formation of aortic aneurisms in one model of disease than are C57BL/6 mice [52], which is consistent with the presence of a gene that confers protection from aortic dilatation in 129/SvEv mice. Although there were no differences in cathepsin activity between $GUSB^{-/-}Cts^{+/+}MMP12^{+/+}$ mice with dilated aortas and $GUSB^{-/-}Cts^{+/+}MMP12^{+/+}$ with non-dilated aortas, MPS VII mice from the CtsS colony with unexpectedly-small aortas had reduced mRNA levels of cytokines as compared with MPS VII mice with dilated aortas (data not shown). We are currently trying to map the gene that reduces aortic dilatation in MPS VII mice and derives from the CtsS colony.

4.3. Possible role of complement in aortic dilatation

The absence of a major effect of CtsS and/or MMP12 deficiency on aortic dilatation in MPS VII mice led us to use microarray to look for other elastases that might play a role. CFD was intriguing, as it was very abundant in the microarray at 16,645 FU/spot in normal mice, and was elevated to 4.0-fold normal (60,202 FU/spot) in MPS VII aortas. Real-time reverse transcriptase PCR confirmed it to be elevated compared to normal (28-fold) and to be very abundant at 3.7-fold the level of β-actin. CFD was originally cloned as endogenous vascular elastase, a factor present in lung that could degrade elastin in a model of lung damage [45], and has also been cloned as adipsin, a gene expressed in fat cells. Although it was puzzling at the time that recombinant CFD did not cleave elastin, it is now clear that CFD needs to be activated by cleavage of 5 amino acids from the N-terminus, and that this cleavage is absolutely dependent on MASP1/3, an enzyme of the lectin pathway of complement [53,54]. CFD is very low in serum and abundant in adipocytes, but was not previously known to be expressed in aorta. Interestingly, we found that complement was strongly activated in aortas of MPS VII mice, as C3 was present at high levels on surfaces of the aorta media, although it is unclear if this occurs via the lectin, alternative, or classical pathway of complement. Analysis of mRNA with real-time RT-PCR demonstrates that several components were expressed in the aorta of MPS VII mice, many of which were increased as compared with normal mice. A role for complement proteins has previously been reported for the development of aneurisms in an elastase-injury model [55], while mRNA for complement genes was upregulated in the brains of MPS I and MPS III mice [56] and synovial cells of MPS VI rats [3]. Complement can be activated via the classical or the lectin pathways by carbohydrates [46], raising the possibility that the GAGs that accumulate in MPS VII directly activate complement.

4.4. Role of signal transduction in MPS VII aorta

This paper identifies several signal transduction pathways that are upregulated in MPS VII aortas, and may be potential targets for inhibition in the future. First, the JAK–STAT pathway appears to be activated by phosphorylation, as shown in Fig. 1, where STAT3 was phosphorylated at tyrosine 705 in MPS VII aortas. That could be due to a variety of pathways including the TLR4 pathway. Evidence for activation of the TLR4 pathway include the marked upregulation of osteopontin, TREM2 and its binding partner Tyrobp, as well as numerous other genes. There was a marked upregulation of several Fc receptors, and these are known to interact with TLR to augment signaling [47]. Finally, the complement pathway was clearly activated, as C3 was very abundant on the surface of cells in the MPS VII aorta. C3a and C5a, which are degradation products of C3 and C5, respectively, and are known to synergize with TLR4 in signal transduction [57].

4.5. Effects of gene therapy

MPS VII mice that received neonatal gene therapy with an RV vector expressing canine GUSB had normal aortic diameters and marked,

but not complete, improvements in biochemical abnormalities at 6 months. However, some aortic dilatation was observed at 10 months, suggesting that gene therapy was not fully corrective, which likely reflects poor diffusion of GUSB in the interior of the relatively avascular aorta. We observed a similar outcome in the dog MPS VII model [14], which developed aortic dilatation at 5 years after neonatal gene therapy. These results highlight the importance of searching for the mechanisms responsible for the pathogenesis of aortic disease, as some ancillary therapy may be needed to prevent this manifestation.

4.6. Implications and further directions

These data demonstrate that CtsS and MMP12 are not essential for elastin fragmentation, and hence would not be good targets for drug inhibition in attempts to prevent aortic dilatation. A candidate for another elastase is CFD, as this is a known elastase, is very abundant, and there is evidence of complement activation in the MPS VII aortas. CtsB and CtsK are also candidates, although CtsB has low elastase activity, while CtsK levels were relatively low. It is also possible that there are other enzymes with elastase activity that are upregulated in the aorta. These studies also illustrate the activation of complement as well as other signal transduction pathways that are almost certainly critical for the upregulation and/or activation of destructive proteases, and may be targets for drug inhibition.

Supplementary materials related to this article can be found online at doi:10.1016/j.ymgme.2011.08.018.

Acknowledgments

This work was supported by the MPS Society and the National Institutes of Health (HD061879 awarded to KPP, and R01 AI041592 and U19 AI070489 awarded to JPA). Histology was supported by P30 DK52574 from the NIH. GB received support from the Conselho Nacional de Desenvolvimento Cientifico-CNPg Brazil, grant number 200584/2010-3. We thank Robert Thompson and John Curci (Washington University St. Louis) for the generous gift of CtsS and MMP12 deficient mice, Paul W. Bigg for helpful comments on the manuscript, and Doug Tollefsen for help with enzyme assays.

References

[1] E.F. Neufeld, J. Muenzer, The mucopolysaccharidoses, in: C.R. Scriver, A.L. Beaudet, W.S. Sly, D. Valle (Eds.), Metabolic and Molecular Basis of Inherited Disease, McGraw Hill, New York, 2001, pp. 3421–3452.
[2] J. Ausseil, N. Desmaris, S. Bigou, R. Attali, S. Corbineau, S. Vitry, M. Parent, D. Cheillan, M. Fuller, I. Maire, M.T. Vanier, J.M. Heard, Early neurodegeneration progresses independently of microglial activation by heparan sulfate in the brain of mucopolysaccharidosis IIIB mice, PLoS One 3 (2008) 1–11.
[3] C.M. Simonaro, M. D'Angelo, X. He, E. Eliyahu, N. Shtraizent, M.E. Haskins, E.H. Schuchman, Mechanism of glycosaminoglycan-mediated bone and joint disease: implications for the mucopolysaccharidoses and other connective tissue diseases, Am. J. Pathol. 172 (2008) 112–122.
[4] C.M. Simonaro, Y. Ge, E. Eliyahu, X. He, K.J. Jepsen, E.H. Schuchman, Involvement of the Toll-like receptor 4 pathway and use of TNF-alpha antagonists for treatment of the mucopolysaccharidoses, Proc. Natl. Acad. Sci. U. S. A. 107 (2010) 222–227.
[5] O.I. Soliman, R.G. Timmermans, A. Nemes, W.B. Vletter, J.H. Wilson, F.J. ten Cate, M.L. Geleijnse, Cardiac abnormalities in adults with the attenuated form of mucopolysaccharidosis type I, J. Inherit. Metab. Dis. 30 (2007) 750–757.
[6] A. Nemes, R.G. Timmermans, J.H. Wilson, O.I. Soliman, B.J. Krenning, F.J. ten Cate, M.L. Geleijnse, The mild form of mucopolysaccharidosis type I (Scheie syndrome) is associated with increased ascending aortic stiffness, Hear. Vessel. 23 (2008) 108–111.
[7] A.L. Beaudet, N.M. Ferrante, G.D. Ferry, B.L. Nichols, C.E. Mullins, Variation in the phenotypic expression of beta-glucuronidase deficiency, J. Pediatr. 86 (1975) 388–394.
[8] Y. Liu, L. Xu, A.K. Hennig, A. Kovacs, A. Fu, S. Chung, D. Lee, B. Wang, R.S. Herati, O. J. Mosinger, S.-R. Cai, K.P. Ponder, Liver-directed neonatal gene therapy prevents cardiac, bone, ear, and eye disease in mucopolysaccharidosis I mice, Mol. Ther. 11 (2005) 35–47.
[9] J.A. Metcalf, X. Ma, B. Linders, S. Wu, A. Schambach, K.K. Ohlemiller, A. Kovacs, M. Bigg, L. He, D.M. Tollefsen, K.P. Ponder, A self-inactivating gamma retroviral vector reduces manifestations of mucopolysaccharidosis I in mice, Mol. Ther. 18 (2010) 334–342.
[10] X. Ma, M. Tittiger, R.H. Knutsen, A. Kovacs, L. Schaller, R.P. Mecham, K.P. Ponder, Upregulation of elastase proteins results in aortic dilatation in mucopolysaccharidosis I mice, Mol. Genet. Metab. 94 (2008) 298–304.
[11] J.C. Woloszynek, A. Kovacs, K.K. Ohlemiller, M. Roberts, M.S. Sands, Metabolic adaptations to interrupted glycosaminoglycan recycling, J. Biol. Chem. 23 (2009) 29684–29691.
[12] M.M. Sleeper, C.M. Kusiak, F.S. Shofer, P. O'Donnell, C. Bryan, K.P. Ponder, M.E. Haskins, Clinical characterization of cardiovascular abnormalities associated with feline mucopolysaccharidosis I and VI, J. Inherit. Metab. Dis. 31 (2008) 424–431.
[13] A.M. Traas, P. Wang, X. Ma, M. Tittiger, L. Schaller, P. O'donnell, M.M. Sleeper, C. Vite, R. Herati, G.D. Aguirre, M. Haskins, K.P. Ponder, Correction of clinical manifestations of canine mucopolysaccharidosis I with neonatal retroviral vector gene therapy, Mol. Ther. 15 (2007) 1423–1431.
[14] J.A. Metcalf, B. Linders, S. Wu, P. Bigg, P. O'Donnell, M.M. Sleeper, M.P. Whyte, M. Haskins, K.P. Ponder, Upregulation of elastase activity in aorta in mucopolysaccharidosis I and VII dogs may be due to increased cytokine expression, Mol. Genet. Metab. 99 (2010) 396–407.
[15] R.E. Gompf, R.M. Shull, M.A. Breider, J.A. Scott, G.C. Constantopoulos, Cardiovascular changes after bone marrow transplantation in dogs with mucopolysaccharidosis I, Am. J. Vet. Res. 51 (1990) 2054–2060.
[16] C. Sammarco, M. Weil, C. Just, S. Weimelt, C. Hasson, T. O'Malley, S.M. Evans, P. Wang, M.L. Casal, J. Wolfe, M. Haskins, Effects of bone marrow transplantation on the cardiovascular abnormalities in canine mucopolysaccharidosis VII, Bone Marrow Transplant. 25 (2000) 1289–1297.
[17] M.M. Sleeper, B. Fornasari, N.M. Ellinwood, M.A. Weil, J. Melniczek, T.M. O'Malley, C.D. Sammarco, L. Xu, K.P. Ponder, M.E. Haskins, Gene therapy ameliorates cardiovascular disease in dogs with mucopolysaccharidosis VII, Circulation 110 (2004) 815–820.
[18] M.A. Cattell, J.C. Anderson, P.S. Hasleton, Age-related changes in amounts and concentrations of collagen and elastin in normotensive human thoracic aorta, Clin. Chim. Acta 245 (1996) 73–84.
[19] S.M. Mithieux, A.S. Weiss, Elastin, Adv. Protein Chem. 70 (2005) 437–461.
[20] M.D. Jordan, Y. Zheng, S. Ryazantsev, N. Rozengurt, K.P. Roos, E.F. Neufeld, Cardiac manifestations in the mouse model of mucopolysaccharidosis I, Mol. Genet. Metab. 86 (2005) 233–243.
[21] V.G. Renteria, V.J. Ferrans, W.C. Roberts, The heart in the hurler syndrome: gross, histologic and ultrastructural observations in five necropsy cases, Am. J. Cardiol. 38 (1976) 487–501.
[22] E. Braunlin, S. Mackey-Bojack, A. Panoskaltsis-Mortari, J.M. Berry, R.T. McElmurry, M. Riddle, L.Y. Sun, L.A. Clarke, J. Tolar, B.R. Blazar, Cardiac functional and histopathologic findings in humans and mice with mucopolysaccharidosis type I, Pediatr. Res. 59 (2006) 27–32.
[23] A. Hinek, S.E. Wilson, Impaired elastogenesis in Hurler disease: dermatan sulfate accumulation linked to deficiency in elastin-binding protein and elastic fiber assembly, Am. J. Pathol. 156 (2000) 925–938.
[24] G.M. Longo, S.J. Buda, N. Fiotta, W. Xiong, T. Griener, S. Shapiro, B.T. Baxter, MMP-12 has a role in abdominal aortic aneurysms in mice, Surgery 137 (2005) 457–462.
[25] G.K. Sukhova, Y.-O. Zhang, J.-H. Pan, Y. Wada, T. Yamamoto, M. Naito, T. Kodama, S. Tsimikas, J.L. Witztum, M.L. Lu, Y. Sakara, M.T. Chin, P. Libby, G.P. Shi, Deficiency of cathepsin S reduces atherosclerosis in LDL receptor-deficient mice, J. Clin. Invest. 111 (2003) 897–906.
[26] E.A. Braunlin, N.R. Stauffer, C.H. Peters, J.L. Bass, J.M. Berry, J.J. Hopwood, W. Krivit, Usefulness of bone marrow transplantation in the Hurler syndrome, Am. J. Cardiol. 92 (2003) 882–886.
[27] E.H. Birkenmeier, J.E. Barker, C.A. Vogler, J.W. Kyle, W.S. Sly, B. Gwynn, B. Levy, C. Pegors, Increased life span and correction of metabolic defects in murine mucopolysaccharidosis type VII after syngeneic bone marrow transplantation, Blood 78 (1991) 3081–3092.
[28] C.M. Simonaro, M.E. Haskins, T. Kunieda, S.M. Evans, J.W. Visser, E.H. Schuchman, Bone marrow transplantation in newborn rats with mucopolysaccharidosis type VI: biochemical, pathological, and clinical findings, Transplantation 63 (1997) 1386–1393.
[29] N.M. Ellinwood, M.A. Colle, M.A. Weil, M.L. Casal, C.H. Vite, S. Wiemelt, C.W. Hasson, T.M. O'Malley, X. He, U. Prociuk, L. Verot, J.R. Melniczek, A. Lannon, G.D. Aguirre, V.W. Knox, S.M. Evans, M.T. Vanier, E.H. Schuchman, S.U. Walkley, M.E. Haskins, Bone marrow transplantation for feline mucopolysaccharidosis I, Mol. Genet. Metab. 91 (2007) 239–250.
[30] M. Sifuentes, R. Doroshow, R. Hoft, G. Mason, I. Walot, M. Diament, S. Okazaki, K. Huff, G.F. Cox, S.J. Swiedler, E.D. Kakkis, A follow-up study of MPS I patients treated with laronidase enzyme replacement therapy for 6 years, Mol. Genet. Metab. 90 (2007) 171–180.
[31] E.A. Braunlin, J.M. Berry, C.B. Whitley, Cardiac findings after enzyme replacement therapy for mucopolysaccharidosis type I, Am. J. Cardiol. 98 (2006) 416–418.
[32] D. Auclair, J.J. Hopwood, D.A. Brooks, J.F. Lemontt, A.C. Crawley, Replacement therapy in mucopolysaccharidosis type VI: advantages of early onset of therapy, Mol. Genet. Metab. 78 (2003) 163–174.
[33] K.P. Ponder, M.E. Haskins, Gene therapy for mucopolysaccharidosis, Expert. Opin. Biol. Ther. 7 (2007) 1333–1345.
[34] K.P. Ponder, J.R. Melniczek, L. Xu, M.A. Weil, T.M. O'Malley, P.A. O'Donnell, V.W. Knox, G.D. Aguirre, H. Mazrier, N.M. Ellinwood, M. Sleeper, A.M. Maguire, S.W. Volk, R.L. Mango, J. Zweigle, J.H. Wolfe, M.E. Haskins, Therapeutic neonatal hepatic gene therapy in mucopolysaccharidosis VII dogs, Proc. Natl. Acad. Sci. U. S. A. 99 (2002) 13102–13107.

[35] L. Xu, M.E. Haskins, J.R. Melniczek, C. Gao, M.A. Weil, T.M. O'Malley, P.A. O'Donnell, H. Mazrier, N.M. Ellinwood, J. Zweigle, J.H. Wolfe, K.P. Ponder, Transduction of hepatocytes after neonatal delivery of a Moloney murine leukemia virus based retroviral vector results in long-term expression of beta-glucuronidase in mucopolysaccharidosis VII dogs, Mol. Ther. 5 (2002) 141–153.
[36] G.P. Shi, G.K. Sukhova, M. Kuzuya, Q. Ye, J. Du, Y. Zhang, J.H. Pan, M.L. Lu, X.W. Cheng, A. Iguchi, S. Perrey, A.M. Lee, H.A. Chapman, P. Libby, Deficiency of the cysteine protease cathepsin S impairs microvessel growth, Circ. Res. 92 (2003) 493–500.
[37] J.P. Shipley, R.L. Wesselschmidt, D.K. Kobayashi, T.J. Ley, S.d. Shapiro, Metaloelastase is required for macrophage-mediated proteolysis and matrix invasion in mice, Proc. Natl. Acad. Sci. U. S. A. 93 (1996) 3942–3946.
[38] L. Xu, R.L. Mango, M.S. Sands, M.E. Haskins, N.M. Ellinwood, K.P. Ponder, Evaluation of pathological manifestations of disease in mucopolysaccharidosis VII mice after neonatal hepatic gene therapy, Mol. Ther. 6 (2002) 745–758.
[39] J.E. Wagenseil, N.L. Nerurkar, R.H. Knutsen, R.J. Okamoto, D.Y. Li, R.P. Mecham, Effects of elastin haploinsufficiency on the mechanical behavior of mouse arteries, Am. J. Physiol. Heart Circ. Physiol. 289 (2005) H1209–H1217.
[40] S. Jordans, S. Jenko-Kokalj, N.M. Kühl, S. Tedelind, W. Sendt, D. Brömme, D. Turk, K. Brix, Monitoring compartment-specific substrate cleavage by cathepsins B, K, L, and S at physiological pH and redox conditions, BMC Biochem. 10 (2009) 23.
[41] O. Vasiljeva, M. Dolinar, J.R. Pungercar, V. Turk, B. Turk, Recombinant human procathepsin S is capable of autocatalytic processing at neutral pH in the presence of glycosaminoglycans, FEBS Lett. 579 (2005) 1285–1290.
[42] M. Novinec, R.N. Grass, W.J. Stark, V. Turk, A. Baici, B. Lenarcic, Interaction between human cathepsins K, L, and S and elastins: mechanism of elastinolysis and inhibition by macromolecular inhibitors, J. Biol. Chem. 282 (2007) 7893–7902.
[43] Z. Li, Y. Yasuda, W. Li, M. Bogyo, N. Katz, R.E. Gordon, G.B. Fields, D. Brömme, Regulation of collagenase activities of human cathepsins by glycosaminoglycans, J. Biol. Chem. 279 (2004) 5470–5479.
[44] J.W. van der Stappen, A.C. Williams, R.A. Maciewicz, C. Paraskeva, Activation of cathepsin B, secreted by a colorectal cancer cell line requires low pH and is mediated by cathepsin D, Int. J. Cancer 67 (1996) 547–554.
[45] L. Zhu, D. Wigle, A. Hinek, J. Kobayashi, C. Ye, M. Zuker, H. Dodo, F.W. Keeley, M. Rabinovitch, The endogenous vascular elastase that governs development and progression of monocrotaline-induced pulmonary hypertension in rats is a novel enzyme related to the serine proteinase adipsin, J. Clin. Invest. 94 (1994) 1163–1171.
[46] C. Speth, W.M. Prodinger, R. Wurzner, H. Stoiber, M.P. Dierich, Complement, in: William E. Paul (Ed.), Fundamental Immunology (0-7817-6519-6, 978-0-7817-6519-0), Wolters Kluwer/Lippincott Williams & Wilkins, 2008, pp. 1048–1107.
[47] L.B. Ivashkiv, Cross-regulation of signaling by ITAM-associated receptors, Nat. Immunol. 10 (2009) 340–347.
[48] J.P. Habashi, J.J. Doyle, T.M. Holm, H. Aziz, F. Schoenhoff, D. Bedja, Y. Chen, A.N. Modiri, D.P. Judge, H.C. Dietz, Angiotensin II type 2 receptor signaling attenuates aortic aneurysm in mice through ERK antagonism, Science 332 (2011) 361–365.
[49] D. Bromme, S. Wilson, Role of cysteine cathepsins in extracellular proteolysis, in: W.C. Parks, R.P. Mecham (Eds.), Extracellular Matrix Degradation (Biology of Extracellular Matrix), Springer, New York, 2011, pp. 23–51.
[50] R.W. Mason, D.A. Johnson, A.J. Barrett, H.A. Chapman, Elastinolytic activity of human cathepsin L, Biochem. J. 233 (1986) 925–927.
[51] B. Fingleton, MMPs as therapeutic targets—still a viable option? Semin. Cell Dev. Biol. 19 (2008) 61–68.
[52] R.W. Thompson, J.A. Curci, T.L. Ennis, D. Mao, M.B. Pagano, C.T. Pham, Pathophysiology of abdominal aortic aneurysms: insights from the elastase-induced model in mice with different genetic backgrounds, Ann. N. Y. Acad. Sci. 1085 (2006) 59–73.
[53] N.K. Banda, M. Takahashi, B. Levitt, M. Glogowska, J. Nicholas, K. Takahashi, G.L. Stahl, T. Fujita, W.P. Arend, V.M. Holers, Essential role of complement mannose-binding lectin-associated serine proteases-1/3 in the murine collagen antibody-induced model of inflammatory arthritis, J. Immunol. 185 (2010) 5598–5606.
[54] M. Takahashi, Y. Ishida, D. Iwaki, K. Kanno, T. Suzuki, Y. Endo, Y. Homma, T. Fujita, Essential role of mannose-binding lectin-associated serine protease-1 in activation of the complement factor D, J. Exp. Med. 207 (2010) 29–37.
[55] M.B. Pagano, H.F. Zhou, T.L. Ennis, X. Wu, J.D. Lambris, J.P. Atkinson, R.W. Thompson, D.E. Hourcade, C.T. Pham, Complement-dependent neutrophil recruitment is critical for the development of elastase-induced abdominal aortic aneurysm, Circulation 119 (2009) 1805–1813.
[56] K. Ohmi, D.S. Greenberg, K.S. Rajavel, S. Ryazantsev, H.H. Li, E.F. Neufeld, Activated microglia in cortex of mouse models of mucopolysaccharidoses I and IIIB, Proc. Natl. Acad. Sci. U. S. A. 100 (2003) 1902–1907.
[57] G. Hajishengallis, J.D. Lambris, Crosstalk pathways between Toll-like receptors and the complement system, Trends Immunol. 31 (2010) 154–163.

Characterization of joint disease in mucopolysaccharidosis type I mice and the effects of enzyme replacement therapy

Patricia Gnieslaw de Oliveira[1*], Guilherme Baldo[2,3*], Fabiana Quoos Mayer[3], Barbara Martinelli[3], Luise Meurer[4], Roberto Giugliani[2,3], Ursula Matte[3], Ricardo Machado Xavier[1]

1 Programa de pós-graduação em medicina: ciências medicas Universidade Federal do Rio Grande do Sul, RS, Brazil.
2 Programa de pós-graduação em Ciências Biológicas: Bioquímica- Universidade Federal do Rio Grande do Sul, RS, Brazil.
3 Centro de Terapia Gênica- Hospital de Clinicas e Porto Alegre, RS, Brazil
4 Serviço de Patologia- Hospital de Clinicas de Porto Alegre, RS, Brazil

*Both authors contributed equally to this work.

Author's emails:

Patricia Gnieslaw de Oliveira- patty22@pop.com.br
Guilherme Baldo- guibaldo@g.com.br
Fabiana Quoos Mayer- bimmayer@gmail.com
Barbara Martinelli- barbaramartinelli@hotmail.com
Luise Meurer- meurerl@hcpa.ufrgs.br
Roberto Giugliani-rgiugliani@hcpa.ufrgs.br
Ursula Matte- umatte@hcpa.ufrgs.br
Ricardo Machado Xavier- rmaxavier@hcpa.ufrgs.br

Corresponding Author:

Ricardo Machado Xavier, PhD, Hospital de Clínicas de Porto Alegre,

Serviço de Reumatologia, Rua Ramiro Barcellos, 2350, sala 645

Zip code 90035-003 - Porto Alegre, Brasil.

Fone: 55-51-21018340

Fax: 55-51-33313834

Abstract

Introduction: Mucopolysaccharidosis type I (MPS I) is a lysosomal disorder caused by deficiency of alpha-L-iduronidase, which leads to storage of the glycosaminoglycans heparan sulphate and dermatan sulphate. Patients with MPS I present destructive changes in their joints in a process not well understood. The MPS I animal model is a useful tool to study the disease pathogenesis; however the changes in the MPS I joints were never investigated. This work aimed to describe the joint disease progression in the murine model of MPS I, and the effect of treatment with enzyme replacement therapy (ERT). **Methods:** Normal (wild type) and untreated MPS I mice were killed at different time points (from 2 to 12 months). In addition, some MPS I mice were treated with ERT and sacrificed at 6 months. The knee joints were collected and hematoxylin and eosin staining was used to evaluate the articular architecture. Safranin-O staining was used to analyze proteoglycans (PGs) content. In addition we analyzed the expression of matrix-degrading metalloproteinases (MMPs), MMP-2 and -9, by immunohistochemistry. **Results and Conclusion:** We observed progressive joint alterations from 6 months, including presence of synovial inflammatory infiltrate, destruction and thickening of the cartilage extracellular matrix and PGs depletion. Also, we observed an increase in the expression of MMP-2 and -9, which could explain the degenerative changes. We also investigated the effect of ERT when started at 2 months, which showed no benefits, suggesting that the poorly vascularized cartilage is difficult to reach, and an ancillary therapy might be needed for patients.

Keywords: alpha-L-iduronidase; mucopolysaccharidosis type I; joint disease; matrix mettalloproteinases; osteoarthritis.

Running title: Joint disease in MPS I mice

1. Introduction

Mucopolysacharidoses (MPS) are a group of lysosomal storage disorders characterized by mutation in enzymes involved in the degradation of glycosaminoglycans (GAGs). Joint disease is present in most forms of mucopolysacharidosis, including MPS I[1].

MPS I occur due to deficiency of the enzyme alpha-L-iduronidase (IDUA), which is involved in degradation of heparan sulphate and dermatan sulphate. As consequence, these two undegraded GAGs accumulate in the lysosomes and extracellular space and lead to the clinical manifestations observed. Bone and joint disease in MPS I patients is characterized by abnormal cartilage and bone development, short stature, dysostosis multiplex, and degenerative joint disease[2].

Treatments available for MPS I are hematopoietic stem cell transplantation (HSCT) and enzyme replacement therapy (ERT). Patients who received HSCT before 2 years of age had some improvements in joint mobility, but hip subluxation and kyphosys eventually progressed[3]. In a cohort of patients under ERT for at least 52 weeks, it was observed that the treatment was only able to slow the progression of the symptons, when evaluating range of motion in upper extremities[4]. Thus, although the reports are still not conclusive, they suggest that existing therapies can reduce, but do not completely prevent, joint and bone disease in MPS I.

The animal model of MPS I was created in the last decade by disruption of the *Idua* gene[5] and it has been proven to be a valuable tool for the study of different aspects of the pathogenesis of MPS I[5, 6]. The MPS I mice have been shown to present joint disease at late stages in life[7], but a complete description of the disease was never reported.

Therefore, in the present work we created a score to characterize the histological abnormalities in the MPS I mice knee joints. It allowed us to systematically study the age of onset of joint disease, as well as its progression. In addition, based on the results from the histological analysis, we tried to find possible mechanisms responsible for the disease. Finally, we verified if intravenous ERT was effective in preventing this complication of MPS I.

2. Material and Methods

2.1 Animals

All animal studies were approved by the authors' institutional review board and MPS I mice (knockout for the alpha-L-iduronidase gene) on a C57BL/6 background (kindly donated by Dr Elizabeth Neufeld) were used. MPS I mice were identified by

PCR reaction. Male $IDUA^{-/-}$ mice (referred as MPS I group) and their normal littermate controls ($IDUA^{-/+}$ and $IDUA^{+/+}$, referred from now on as "Normal" group) were the subjects for these experiments. Heterozygous mice were used for breeding. Number of mice ranged from 6 to 11 each time point.

At 3 weeks of age, offspring were separated from the dam, genotyped and housed (2–5 per cage) by sex. Animals were maintained to conventional housing under a 12 h light/12 h dark cycle with controlled temperature (19 ± 1°C) and humidity (50 ± 10%). Mice were sacrificed at 2, 4, 6, 8 or 12 months. Both female and male mice were analyzed.

2.2 ERT treatment

MPS I male mice (n=8) were treated with an intravenous injection of 1.2 mg/kg of Laronidase® (Genzyme, USA) every 2 weeks, which is the same dose and regimen proven to be effective in clinical trials[8]. ERT was started at 2 months. The injections were made via the tail vein. Treated animals were sacrificed at 6 months.

2.3 Histological analysis

Mouse knees from both rear legs were collected and placed in buffered formalin from 24h to up to 1 week, then were decalcified with EDTA 14% for up to 1 week. Paraffin sections (7μm thickness) were made and stained with Hematoxilin/Eosin (HE) for articular architecture and Safranine-O for proteoglycans (PGs) content.

Joint disease was scored to evaluate MPS I joints and effect of treatment with ERT taking in consideration the following abnormalities analyzed with HE staining: presence of inflammatory infiltrate: 0- absent, 1- present; bone and cartilage resorption: 0-absent, 1- mild, 2- moderate, 3- severe; integrity (damage) of articular surface: 0-absent, 1- present; fibrocartilaginous bridge: 0- absent, 1- present; fibrocartilaginous proliferation: 0- absent, 1- mild, 2- moderate, 3- severe. The maximum score is 12.

When analyzing the Safranin-O slides for proteoglycan content on the cartilage we used the following semi-quantitative scoring parameters: 0- Normal staining of non-calcified cartilage, 1- Decreased but not complete loss of Safranin-O staining over 1-100 % of the articular surface, 2- Complete loss of Safranin-O staining in the non-calcified cartilage extending to <25% of the articular surface, 3- Complete loss of Safranin-O staining in the non-calcified cartilage extending to 25-50% of the articular surface, 4- Complete loss of Safranin-O staining in the non-calcified cartilage extending to 50-75% of the articular surface, 5- Complete loss of Safranin-O staining in the non-calcified cartilage extending to >75% of the articular surface[9]. In all cases both legs

were analyzed by the pathologist blindly, and the scores were obtained from the leg considered to be the worst one.

2.4 Growth plate alterations

The length of growth plates from Normal and MPS I mice were measured using the Photoshop computer program. To obtain the images, photos from HE slides were taken at 20X magnification and assembled to a single picture. The length of the growth plate was measured in 6 distinct points and the average was obtained for each animal.

2.5 Expression of matrix mettalloproteinases

Immunohistochemistry for matrix metalloproteinase type 2 (MMP-2) was performed using the first antibody from Abbiotec (San Diego, CA) in a 1:200 dilution. For the MMP-9 the first antibody was purchased from Santa Cruz and a 1:200 dilution was performed. Incubation with the primary antibodies was performed overnight at 4^{o}C. Secondary antibody conjugated to peroxidase was incubated (antibody multi-species from DAKO, USA) in a 1:1000 dilution for 1h. Samples were developed with DAB. Quantification was performed using the software ImageProPlus. Results were expressed as fold-normal.

2.6 Statistical analysis

Results for general score, growth plate abnormalities, and immunohistochemistry were compared using t test. When comparing groups with the treatment, ANOVA and Tukey were performed. All analyses were performed using the software SigmaStat version 3.1.

3. Results

3.1 Time course of histological alterations

No abnormalities were observed in the joint of MPS I mice at 2 or 4 months (data not shown). MPS I mice presented progressive alterations that can be visualized in figure 1, and are described in more details below.

Alterations in MPS I mice joints could become detectable at 6 months. At this stage 66% (4 out of 6) of MPS I mice presented mild inflammatory infiltrate compared to normal group with the same age. Fibrocartilaginous proliferation was present in 66%

(4/6) of MPS I mice, with 3 of them having a mild alteration. Cartilage resorption was mild and present in only 2/6 mice. Bone resorption was rare and mild at this time point, with only 1 mice presenting it. Uneven articular surface was found in all animals at this age. Average score for MPS I mice at 6 months was 3.3 ± 1.5 versus 0.5 ± 0.7 in normal mice (p=0.01, figure 1). Proteoglycan depletion was mild at this stage.

The joints alterations were even more pronounced at 8 and 12 months and also presented proteoglycans and collagen depletion in the cartilage matrix and underlying bone throughout the development of the disease. At 8 months, inflammatory infiltrate was still mild, but present in 91% of MPS I mice (10/11), other parameters were also present in almost all mice, and included fibrocartilaginous proliferation, irregularities at articular surface, and cartilage resorption. Bone resorption was present in only 1 mice. Average score for MPS I mice was 4.3 ± 2.4 and for normal mice it was 0.3 ± 0.8 (p =0.01, figure 1).

At 12 months more striking differences were observed, including bone resorption being present in 50% of MPS I mice (4/8). Inflammatory infiltrate was still mild, but present in 88% of mice. Other parameters were also more proeminent. Average score for MPS I mice was 6.6 ± 3.1 versus 0.8 ± 0.8 in normal mice (p=0.01, figure 1).

Loss of cartilage proteoglycan content was progressive with age (6 - 12 months of ages, figure 2). Overall, the joint disease in these mice appears as a GAG accumulation and articular cartilage matrix abnormalities with a significant increase in the volume of extracellular matrix, causing further destruction of the joints in a process that resembles osteoarthritis and not rheumatoid arthritis, as previously described in MPS VII and VI[10]. Interestingly, the articular lesions observed were asymmetric and the worst joint was analyzed. No inflammatory cells were observed in normal mice at any age.

3.2 Growth plate alterations

It has been shown previously that there were no differences in the size of growth plates at 3 weeks in MPS I mice, as opposite of MPS VII mice[11], however we decided to investigate if the growth plate abnormalities found at histological level could alter its size later in life, since MPS I patients have short stature. No differences were found at any of the times analyzed in the length of the growth plate (data not shown).

3.3 MMP-2 and MMP-9 Expression

Using specific antibodies, we detected expression of MMP-2 and MMP-9 in normal and MPS I samples. Pictures were taken and positive signal was quantified using the software ImageProPlus.

MMP-2 expression was upregulated in MPS I mice (figure 3). At 6 months, the expression of this collagenase in MPS I mice was already 2-fold normal, with a borderline p value (p=0.1). At 8 and 12 months, MMP2 was found to be 1.6 and 2.3-fold normal values (p=0.025 and 0.013, respectively)

In a similar pattern, MMP-9 expression was also found to be elevated in MPS I mice. At 6 and 8 months, its levels were 1.4 and 1.2 fold normal (not significant). At 12 months MMP-9 expression in MPS I mice was found to be 1.9-fold normal (p= 0.019, figure 3). The areas with increased MMP-2 and 9 seem to correlate with the places were we found loss of proteoglycan stain.

3.4 Enzyme replacement therapy

Enzyme replacement therapy was able to correct visceral organ pathology, reducing GAG storage in liver, lung and kidney (data not shown). However it was not able to correct the joint abnormalities observed in MPS I mice, obtaining an average score similar to those found in untreated mice (figure 4). We used the score from HE slides, where untreated mice presented an average score of 3.3 ± 1.5 and ERT mice presented a similar average score value (2.7 ± 3.0), which was much higher than normal mice (0.5 ± 0.7).

4. Discussion

The pathogenesis of joint disease in the mucopolysaccharidosis is a very important aspect that deserves studies focused on disease pathogenesis, since current available treatments have shown modest results in correcting this complication [3,4].

Here we have shown that MPS I mice present a progressive disease that in some of its histological aspects resembles osteoarthritis, which is different from what Simonaro et al (2008) have described for MPS VI[10]. Using a microarray approach in MPS VI rats, it was shown that several genes that have been previously shown to be differentially expressed in rheumathoid arthritis were also elevated on MPS VI synovial cells[10]. Those included genes related to inflammation as well as upregulation of destructive proteases. Our findings suggest that an inflammatory process is indeed occurring, although mild. Degradation of proteoglycans is also present, but

histologically, the process in MPS I mice resembles the one found in osteoarthritis, which agrees with observations found in the mouse MPS IX model[12].

Collagenases known as matrix metalloproteinases (MMPs), including MMP-2 and MMP-9, have been shown to be present in injured cartilage. MMP-2 has been shown to be upregulated in MPS VII mouse aortas[13] at the mRNA level, as well as in patients with osteoarthritis[14]. Importantly, MMP-2 is the most active MMP against collagen type II, which is the main collagen in the cartilage[15] and have a broad spectrum of substrates, including collagen types I, IV, VII, X and XI, proteoglycans and elastin[16]. MMP-9 is another gelatinase, known for its ability to degrade a series of substrates, which includes elastin, proteoglycans, laminin, and fibronectin[16]. Those facts made us look for expression of MMP-2 and MMP-9 in the joints, which showed to be upregulated in affected mice. We conclude that upregulation of MMP-2, MMP-9 and possibly other destructive proteases might be contributing for joint disease in MPS I.

The growth plate width did not show significant differences in the analyzed times. Previous papers analyzing MPS I and VII growth plates have shown a reduction in the growth plate and increase in the apoptosis of chondrocytes in the MPS VII mice, but not in MPS I[11]. Our results strengthen those findings.

ERT is available for patients since 2003, and the results of ERT on joints of MPS I patients seem to point to a moderate effect. Here we used the same dose of ERT applied to patients, in the same regimen[8] and we verified no benefits on the joint disease of MPS I mice. A recent study on MPS I dogs[17] was able to show improvements in the growth plate only in the animals treated with a high-dose of ERT. As the ERT is a very expensive medication which can also develop neutralizing antibodies[18], other routes of delivery or ancillary therapies should be considered for MPS patients.

5. Conclusion

In conclusion, our results suggest that MPS I mice present a progressive joint disease characterized by mild inflammation, bone and cartilage resorption, irregular cartilage surface and depletion of proteoglycans, possibly caused by upregulation of destructive proteases such as MMP-2 and MMP-9. Furthermore, ERT was not able to correct the abnormalities observed, which highlights the important of studies on the pathogenesis of joint disease in MPS I, since patients may not get a complete benefit from current treatments.

6. List of abbreviations

MPS I –mucopolysaccharidosis type I
IDUA- alpha-L-iduronidase
MMP-2- matrix metalloproteinase type 2
MMP-9- matrix metalloproteinase type 9
PGs- proteoglycans
ERT- enzyme replacement therapy

7. Competing of interests

Authors declare that they have no competing of interests.

8. Authors contribution

All authors were involved in drafting the article or revising it critically for important intellectual content, and all authors approved the final version to be published. Dr Xavier had full access to all of the data in the study and takes responsibility for the integrity of the data and the accuracy of the data analysis.

9. Aknowledgements

This work was partially supported by CNPq (Conselho Nacional de Desenvolvimento Científico e Tecnologico), CAPES (Coordenação de Aperfeiçoamento de Pessoal de Nível Superior) and FIPE (Fundação de Incentivo à Pesquisa do Hospital de Clínicas de Porto Alegre).

10. Figures

Figure 1- A) Joint sections representative from a normal mouse and MPS I mice at different ages. Arrows indicate alterations found in MPS I mice, including invasion of the surrounding tissue to the articular cavity. Note also the irregular articular surface that MPS I mice develop over time. B) Results from histological scores obtained in normal and MPS I mice joints at 6, 8 and 12 months (n=6-11). **p= 0.01, Using Student`s t test.

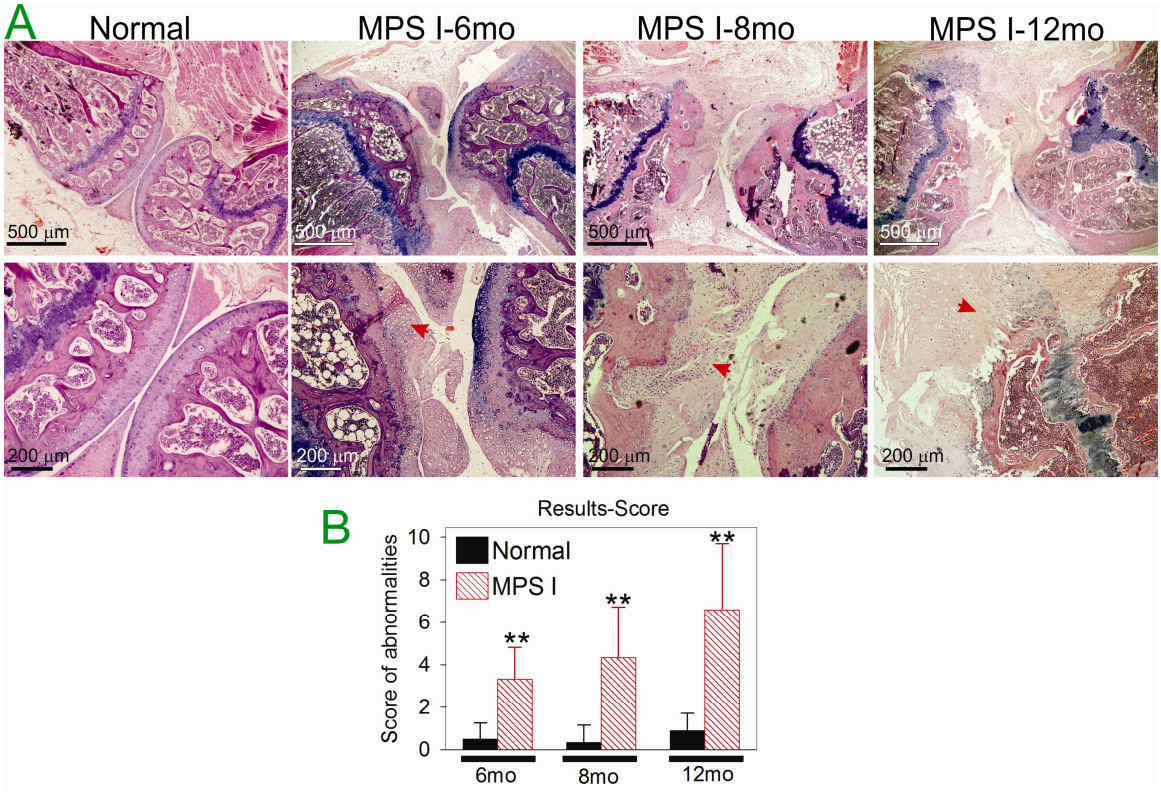

Figure 2: Loss of proteoglycan (PG) content in MPS I mice evidenced using Safranin-O stain. A) An example of representative sections of a Normal, a 6-month and a 12-month old MPS I mice. Showing progressive loss of PG. Arrowheads indicate normal staining, while yellow arrows indicate areas presenting loss of Safranin-O stain. B) Results from histological scores obtained in Safranin-O stain in normal and MPS I mice joints at 6, 8 and 12 months. **p= 0.01, Using Student`s t test.

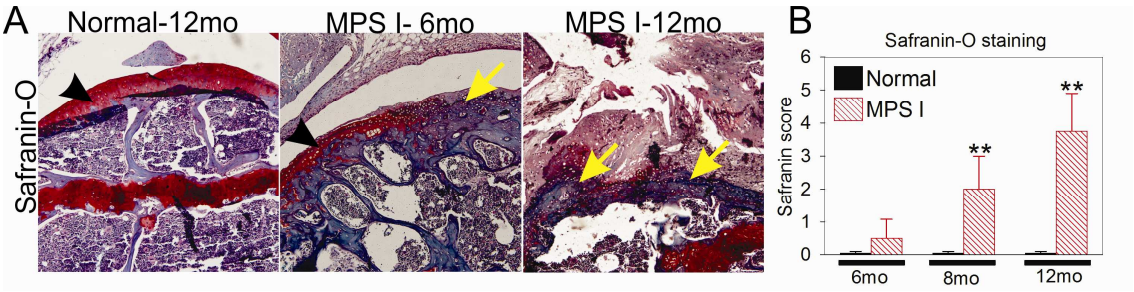

Figure 3: Immunohistochemistry for matrix mettalloproteinases quantified by appropriate software. A-C) MMP-2 expression D-F) MMP-9 expression. * p<0.05, t-test.

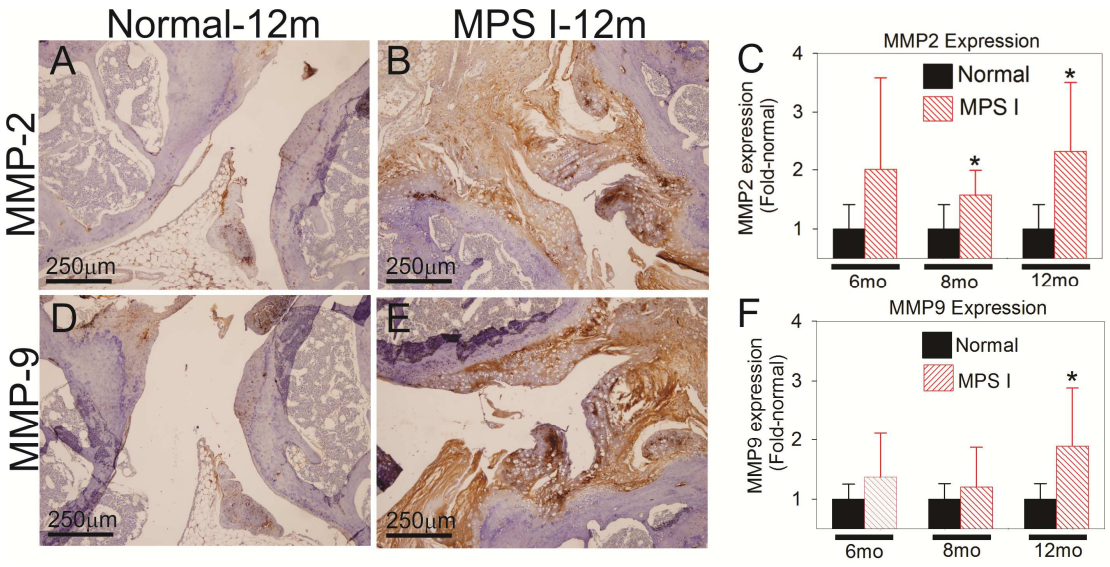

Figure 4: Treatment with ERT. Scores from normal, MPS I and ERT mice showing no improvement in joint histological aspect after treatment at 6 months of age. p< 0.05 compared to normal.

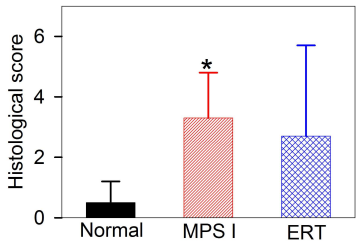

11. References

1. Giugliani R, Federhen A, Muñoz Rojas MV, Vieira TA, Artigalás O, Pinto LL, et al. Enzyme replacement therapy for mucopolysaccharidoses I, II and VI: recommendations from a group of Brazilian F experts. Rev Assoc Med Bras. 2010; 56: 271-7.

2. Pastores GM, Meere PA. Musculoskeletal complications associated with lysosomal storage disorders: Gaucher disease and Hurler-Scheie syndrome (mucopolysaccharidosis type I). Curr Opin Rheum 2005; 17: 70–78.

3. Field RE, Buchanan JAF, Copplemans MGJ, Aichroth PM: Bone-marrow transplantation in Hurler's syndrome. Bone Joint Surg. Br. 1994; 76: 975–981.

4. Tylki-Szymanska A, Marucha J, Jurecka A, Syczewska M, Czartoryska B. Efficacy of recombinant human alpha-L-iduronidase (laronidase) on restricted range of motion of upper extremities in mucopolysaccharidosis type I patients. J Inherit Metab Dis. 2010; 33:151-7.

5. Ohmi K, Greenberg DS, Rajavel KS, Ryazantsev S, Li HH, Neufeld EF. Activated microglia in cortex of mouse models of mucopolysaccharidoses I and IIIB. Proc Natl Acad Sci U S A. 2003; 100:1902-7.

6. Ma X, Tittiger M, Knutsen RH, Kovacs A, Schaller L, Mecham RP, Ponder KP. Upregulation of elastase proteins results in aortic dilatation in mucopolysaccharidosis I mice. Mol Genet Metab. 2008; 94: 298-304.

7. Mango RL, Xu L, Sands MS, Vogler C, Seiler G, Schwarz T, et al. Neonatal retroviral vector-mediated hepatic gene therapy reduces bone, joint, and cartilage disease in mucopolysaccharidosis VII mice and dogs. Mol Genet Metab. 2004; 82:4-19.

8. Giugliani R, Rojas VM, Martins AM, Valadares ER, Clarke JT, Góes JE, et al. A dose-optimization trial of laronidase (Aldurazyme) in patients with mucopolysaccharidosis I. Mol Genet Metab. 2009; 96:13-9.

9. Schmitz N, Laverty S, Kraus VB, Aigner T. Basic methods in histopathology of joint tissues. Osteoarthritis and Cartilage 2010; 18: S113-S116.

10. Simonaro CM, D'Angelo M, He X, Eliyahu E, Shtraizent N, Haskins ME, Schuchman EH. Mechanism of glycosaminoglycan-mediated bone and joint disease: implications for the mucopolysaccharidoses and other connective tissue diseases. Am J Pathol. 2008; 172: 112-22.

11. Metcalf JA, Zhang Y, Hilton MJ, Long F, Ponder KP. Mechanism of shortened bones in mucopolysaccharidosis VII. Mol Genet Metab. 2009; 97: 202-11.

12. Martin DC, Atmuri V, Hemming RJ, Farley J, Mort JS, Byers S, Hombach-Klonisch S, Csoka AB, Stern R, Triggs-Raine BL. A mouse model of human mucopolysaccharidosis IX exhibits osteoarthritis. Hum Mol Genet. 2008; 17: 1904-15.

13. Baldo G, Wu S, Howe RA, Ramamoothy M, Knutsen RH, Fang J, et al. Pathogenesis of aortic dilatation in mucopolysaccharidosis VII mice may involve complement activation. Mol Genet Metab. 2011, 104: 608-19.

14. Kevorkian L, Young DA, Darrah C, Donell ST, Shepstone L, Porter S, et al. Expression profiling of metalloproteinases and their inhibitors in cartilage. Arthritis Rheum. 2004; 50:131-41.

15. Zhen EY, Brittain IJ, Laska DA, Mitchell PG, Sumer EU, Karsdal MA, Duffin KL. Characterization of metalloprotease cleavage products of human articular cartilage. Arthritis Rheum. 2008; 58:2420-31.

16. Shapiro SD. Matrix metalloproteinase degradation of extracellular matrix: biological consequences. Current opinion in cell biology 1998; 10:602-8

17. Dierenfeld AD, McEntee MF, Vogler CA, Vite CH, Chen AH, Passage M, et al. Replacing the enzyme alpha-L-iduronidase at birth ameliorates symptoms in the brain and periphery of dogs with mucopolysaccharidosis type I. Sci Transl Med. 2010;**2**: 60ra89.

18. Dickson P, Peinovich M, McEntee M, Lester T, Le S, Krieger A, et al. Immune tolerance improves the efficacy of enzyme replacement therapy in canine mucopolysaccharidosis I. J Clin Invest. 2008; 118: 2868-76.

Evidence of a progressive motor dysfunction in Mucopolysaccharidosis type I mice

Guilherme Baldo[1,2], Fabiana Quoos Mayer[1,3], Barbara Martinelli[1], Anna Dilda[1], Fabiola Meyer[4], Katherine Parker Ponder[5], Roberto Giugliani[1,2,3] and Ursula Matte[1,3]

1- Gene Therapy Center- Research Center- Hospital de Clinicas de Porto Alegre, Brazil

2- Post-Graduation Program in Biological Sciences: Biochemistry-UFRGS, Brazil

3- Post-Graduation Program in Genetics and Molecular Biology-UFRGS, Brazil

4- Animal Facility-Research Center-Hospital de Clinicas de Porto Alegre, Brazil

5- Internal Medicine- Washington University in Saint Louis, USA

Corresponding author:

Roberto Giugliani, MD, PhD

Gene Therapy Center

Hospital de Clinicas de Porto alegre

Rua Ramiro Barcelos, 2350

Bairro Rio Branco, Porto Alegre, RS, Brazil

90035-903

Phone: +55-51-3359-8838

Fax: +55-51-3359-8010

Abstract

Mucopolysaccharidosis (MPS) type I or Hurler syndrome is a lysosomal storage disorder characterized by deficiency of alpha-L-iduronidase (IDUA), intracellular storage of glycosaminoglycans (GAGs) and progressive neurological pathology, whose mechanisms are not completely understood. The MPS I mouse model provides an opportunity to study the pathological aspects of this disorder and to determine the efficacy of novel therapies. Previous works demonstrated a series of abnormalities in MPS I mice behavior, but so far some important brain functions have not been addressed. Therefore, in the present study we aimed to determine if MPS I mice have motor abnormalities, and at what age they become detectable. MPS I and normal male mice from 2 to 8 months of age were tested in open-field for locomotor activity, hindlimb gait analysis and hang wire performance. We were able to detect a progressive reduction in the crossings and rearings in the open field test and in the hang wire test in MPS I mice from 4 months, as well as a reduction in the gait length at 8 months. Histological examination of 8-month old mice cortex and cerebellum revealed storage of GAGs in Purkinje cells and neuroinflammation, evidenced by GFAP immunostaining. However TUNEL staining was negative, suggesting that neuronal death does not occur. Our findings suggest that MPS I mice have a progressive motor dysfunction, which is not caused by loss of neuron cells but might be related to a neuroinflammatory process.

Key words: mucopolysaccharidosis type I; hang wire; open field; gait; neuroinflammation.

Abbreviations:

MPS – mucopolysaccharidosis;

IDUA- alpha-L-iduronidase;

GAG- glycosaminoglycans;

GFAP- glial fibrilarry acid protein;

TUNEL- terminal deoxynucleotidyl transferase dUTP nick end labeling.

BP- base pairs

1. Introduction

Mucopolysaccharidosis type I (MPS I, OMIM #607014, #607015, and #607016) is an autosomal recessive lysosomal disorder due to deficiency of alpha-L-iduronidase (IDUA, EC 3.2.1.76) and storage of partially degraded glycosaminoglycans (GAGs) heparan sulphate and dermatan sulphate within the lysosomes. The severe form of the disease manifests progressive central nervous system deterioration, and symptoms include mental dullness and hypoactivity [1].

The MPS I animal model was created by disruption of the IDUA gene [2] and has proved to be a good model of the severe form of the disease, being useful in the study of pathological mechanisms and treatment options [3, 4]. Previous studies reported impairment in both aversive and non-aversive memory tasks [5] and acoustic startle behaviors in these mice [6]. Nevertheless, important aspects of brain function such as motor activity showed conflicting results in these two studies.

In addition, previous works reported activation of glial cells in the cortex [2] and storage of undegraded material, which include glycosaminoglycans and GM3 ganglioside [7]. Also, it is possible that oxidative stress may play a role in the process [8]. However, the mechanism of neurological deficit in MPS I mice are not fully understood.

Better understanding the abnormalities in these mice and the onset of the pathological manifestations is imperative to study mechanisms by which disease occurs as well as to evaluate treatments. Therefore we conducted a study in MPS I mice from 2 to 8 months to evaluate if they develop motor deficits and anxiety and, if so, at what age these alterations can be detectable.

2. Materials and Methods

2.1 Animals

All animal studies were approved by the authors' institutional review board and MPS I mice on a C57BL/6 background (kindly donated by Dr Elizabeth Neufeld, UCLA) were used [2]. The MPS I mice carry a disrupted version of the **Idua** gene that contains the neomycin resistance gene inserted in the opposite orientation in exon 6 (supplementary fig 1A) and could be detected by PCR after DNA extraction from ear tissue, using the following primers: Forward 5'-GAGACTTGGAATGAACCAGAC-3'

and ReverseA 5'-ATAGGGGTATCCTTGAACTC-3' and ReverseB 5'-GTTCTTCTGAGGGGATCGG-3'. Normal mice amplify a sequence of 514 base pairs (bp) and MPS I mice amplify a 321 bp fragment (supplementary figure 1B). Heterozygous mice were used for breeding.

Male *Idua*$^{-/-}$ mice (referred as MPS I group) and their normal littermate controls (*Idua*$^{-/+}$ and *Idua*$^{+/+}$, referred from now on as Normal group) were the subjects for these experiments. Heterozygous mice had no differences in behavior studies compared to I*dua*$^{+/+}$ mice (data not shown). At 3 weeks of age, offspring were separated from the dam, genotyped and housed (2–5 per cage) by sex. Animals were maintained in conventional housing under a 12 h light/12 h dark cycle with controlled temperature (19 ± 1°C) and humidity (50 ± 10%). Mice were examined in behavior tests every other month for 4 test periods beginning at 2 months of age. Each test was performed with a 24h interval from the previous one, in the following order: open field, elevated plus maze, hang wire and gait test. Mice were weighted at 21 days, 2, 4, 6 and 8 months.

2.2 Urinary GAGs measurement

Urine was collected at 1, 2, 4, 6 and 8 months and GAG measurement was performed using the Dimethyl blue assay based on our previous study [9] with small modifications. Briefly, 25 uL of urine was mixed with 2 mL of freshly prepared dimethyl blue solution (Dymethyl blue 0.3 mol/L with 2 mol/L Tris) and absorbance was read at 530 nm. Creatinine was measured spectrophotometrically using the picric acid method. Results were expressed as μg GAGs/mg creatinine.

2.3 Elevated plus maze

Anxiety was analyzed by the elevated plus maze test [10]. It consisted of two open arms and two enclosed arms, 65 cm length × 5 cm wide and walls of 15 cm height with an open roof, assayed so that the two arms were opposite to each other, resulting in a plus shape. The maze was elevated to a height of 50 cm and mice were placed in the center of the maze, facing one of the open arms. Mice were observed for 5 minutes, and the number of entries and time spent in the open and closed arms were measured. In this test, animals with a reduction in anxiety spend more time on the open (unprotected) arms.

2.4 Open field test

Locomotor and exploratory activities were accessed using an open field test [11]. The test consisted of a square arena (52 × 52 cm) with 60 cm high walls. The floor was divided into 16 squares by parallel and intersecting lines, obtaining four centered squares and 12 peripheral squares. Mice were placed in one of the corners of the open field and (a) ambulation (total number of crossings), and (b) exploratory behavior (rearings) were observed during 5 min for both control and MPS I animals. The percentage of crossings in the center squares compared to the total crossings and number of fecal pellets were also analyzed as additional tests for anxiety.

2.5 Gait analysis

Hind-limb gait was determined with a footprint test, as previously described for the MPS III mice [12]. Animals had their paws painted with non-toxic ink and were placed at the beginning of a well-lit runway approximately 50 cm long and 12 cm wide, with walls of 15 cm height, and allowed to move towards the end of the runway. Once dried, the average distance between footprints was determined for both left and right hind-limbs and gait length for each limb was determined. In addition, a line perpendicular to the direction of movement from one foot to the other (supplementary figure 2) was drawn, to determine gait width. The average of at least three lengths and five widths was taken for each run. The first and last two strides were discarded due to alterations in speed in the beginning and in the end of the runway.

2.6 Hang wire test

This test was used as a measure of neuromuscular strength. Animals were placed by the forelimbs on a stainless steel bar (30 cm length, 2mm in diameter, and elevated 30 cm from the surface) at a point midway between the supports and observed for 60 s. Three consecutive trials were performed, with a 60s interval between trials. The amount of time spent hanging was recorded and scored from 1 to 5 (5 as the best) according to the following scheme: 1, hung onto the bar with two forepaws; 2, in addition to 1, attempted to climb onto the bar; 3, hung onto the bar with two forepaws and one or both hind paws; 4, hung onto the bar with all four paws with tail wrapped around the bar; 5, escaped to one of the supports [13, 14].

2.7 Histological analysis

Eight-month normal and MPS I mice (n=4-5 each group) were anesthetized with ketamine and xylasine and perfused with saline solution. Brains were collected; the cortex and cerebellum were isolated and fixed in buffered formalin. Thin cross sections were submitted to routine histological processing, stained with toluidine blue and analyzed for storage in Purkinje cells (cerebellum), cortical neurons and glial cells (cortex). Immunohistochemistry for glial fibrillary acidic protein (GFAP) was performed using specific antibody (Dako Cytomation, Polyclonal Rabbit anti-GFAP) and a secondary antibody conjugated to horseradish peroxidase. Slides were analyzed by a researcher blinded to the groups, counting positive cells in 5 high-power fields (40X). TUNEL staining was performed to analyze cell death by routine histological procedure.

2.8 Statistical Analysis

All values were expressed as mean ± SD. Behavioral data was analyzed using Student's **t**-test; significance level was chosen at $\mathbf{P} < 0.05$. All statistical analyses were carried out by using SigmaStat software version 11.0.

3. Results

3.1 General aspects

The MPS I mice showed no abnormalities at birth, and the body weight was not different from normal mice at weaning (day 21). From the fourth week on, the facial bones started to appear abnormal, with the normal mice having a more lean aspect than the MPS I mice. Also, the MPS I mice weighted significantly more than the normal mice from 2 months on (Figure 1A). GAG excretion was significantly higher in the urine from MPS I mice by 1 month of age (figure 1B). From 4 months on, MPS I mice started to become hypoactive and docile (showing no aggressive behavior), being easier to catch in the cage, compared to normal mice.

3.2 Anxiety tests

We could not observe differences in any of the anxiety tests performed. Both normal and MPS I mice presented similar patterns on the elevated plus maze test (figure

2). Also, no differences were observed in the number of crossings to the central squares and on the number of fecal pellets on the open field test (data not shown).

3.3 Open field test

MPS I and normal mice had no detectable differences at 2 months. However, the number of crossings and rearings at 4 months in *Idua* knockout mice were 33% and 25% reduced, respectively ($p<0.05$). The reduction in both parameters was progressive and reached 53% and 59% at 8 months ($p<0.01$, figure 3).

3.4 Hang wire

Alterations in the time spent on the wire could be observed at second and third trials performed at 4 months, and were consistently observed at all trials at 6 and 8 months, as shown in figure 4. MPS I mice usually fell by difficulties on hanging onto the wire, while the few normal mice that fell, usually did in attempting to climb to one of the edges (supplementary videos 1 and 2). Therefore, we decided to score the performance in some animals, based on a previous report [14]. When the score (ranked from 1 to 5, with 5 as the best) was analyzed, we could observe consistent differences from 6 months-old. At this time, normal mice had an average score of 4.2 ± 0.6 on the first trial, and 3.7 ± 0.9 on the third one. Both were superior to scores obtained by MPS I mice (3.2 ± 1.3, $p<0.05$ and 1.5 ± 0.8 $p<0.05$ respectively). Those differences were even more accentuated at 8 months (4.0 ± 0.7 and 3.8 ± 0.7 for Normal vs 2.2 ± 1.7 and 1.3 ± 0.7 for MPS I in the first and third trials, with $p <0.05$).

3.5 Gait analysis

The average gait length and width are shown in figure 5. MPS I mice presented no alterations in gait width at any of the ages analyzed. However, a marked reduction in gait length was observed in MPS I mice at 8 months ($p<0.01$). Independent analysis from left and right paws showed similar results (reduction in 19% and 15% of gait lenght, respectively), and thus confirmed the consistency of the analysis.

3.6 Histological analysis

Since differences were noted in all motor tests at 8-months, animals were sacrificed at this age and cortex and cerebellum were isolated and processed for histological analysis. Toluidine blue staining revealed storage of undegraded GAGs in

Purkinje cells, shown as white vacuoles inside the cytoplasm (figure 6B), and also on neurons and glial cells in the cortex (figure 6D). Normal mice did not have those features (figures 6A and C). TUNEL staining was negative in normal and MPS I brains (supplementary figure 3), suggesting that apoptosis of neurons is not responsible for the neurological impairment observed. MPS I mice (figure 7) showed more GFAP positive cells than normal mice (2-fold normal in cerebellum and 5.7-fold normal in cortex, $p<0.05$ in both cases) who were located throughout the brain structures analyzed, indicating activation of glial cells and neuroinflammation in both cortex and cerebellum.

4. Discussion

Previous studies have shown behavioral abnormalities in MPS I mice, with special emphasis on memory impairment [5, 6]. However, characterization of the motor deficits in this model has shown contradictory results. The present study sought to expand upon these initial observations describing motor dysfunction in the MPS I model, trying to establish the time-course of the development of these abnormalities.

The open field task was used here as a measure of locomotor and exploratory activities. While in the study published by Reolon *et al* [5] MPS I mice analyzed at 5 to 7 months of age showed only differences in rearing, a study performed by Pan *et al* [6] described that MPS I mice were hypoactive from early stages in life, being noticed as early as 2 months. We were able to clearly demonstrate that MPS I mice are less active than normal mice from 4 months-old onwards, evidencing a motor dysfunction in these mice.

The hang wire test is not only a measure of neuromuscular strength and fine motor skills, but also of cerebellar function [13]. The MPS I mice showed difficulty in holding onto the wire and fell more quickly from 6-months onwards, although in the 2nd and 3rd trials at 4 months it was possible to observe some differences. Alterations in gait are also usually associated to abnormalities in cerebellar function [13]. Gait analysis suggest impairment of cerebellar function in the MPS I mice only at 8 months, which is about the time MPS I mice start to die. This is an interesting finding, since cerebellar function was never studied in severe MPS I patients with an advanced disease process, possibly because other brain abnormalities such as mental retardation may underlie the ataxia phenotype and/or the patients die before developing it. However, as improvements verified after enzyme replacement therapy are leading patients to better

quality of life [15] and a possible increase in life spam, it is possible that impairment in cerebellar function may develop in these patients and could be clinically relevant.

A previous study reported motor abnormalities in MPS IIIa mice [12], a disease resulting from Sulphamidase (EC 3.10.1.1) deficiency, which blocks exclusively the degradation of heparan sulphate. However, both MPS IIIa patients and mice exhibit hyperactivity, while the MPS I human and mice are hypoactive. Whether this difference is due to the presence of undegraded dermatan sulphate in MPS I or because of the step at which heparan sulphate degradation is blocked still remains unknown [16].

Post-mortem studies in MPS I mice have shown widespread accumulation of undegraded GAGs in the brain [17]. Here, we confirm those findings, showing storage in the cortex and cerebellum, two brain regions responsible for motor function. In addition, increased expression of GFAP in these areas evidences a neuroinflammatory process that can contribute to the neurological deficit observed [18]. The activation of glial cells has been previously shown in the MPS I mouse cortex [2], but this was never described to occur in the cerebellum. However, storage and inflammation are not leading to cell death, as shown by TUNEL staining. Therefore, the behavioral deficits found in MPS I mice seem to be not due to neuron death, but more likely to happen because of a neuronal dysfunction. These results raise the question whether blocking inflammation could prevent or delay SNC disease in MPS I mice and humans, as recently described for MPS IIIa mice [19].

In summary, these findings and the behavioral analysis suggest that motor deficits are present in this animal model, while anxiety is not altered. It is worth noticing that MPS I mice develop a progressive multisystemic disease which includes bone and joint alterations [20], and that could be influencing motor tasks. However, the battery of tests applied here strongly suggest that MPS I mice have impaired motor skills rather than other limitations. Hopefully these tests can provide additional methods for measuring functional improvement after administration of novel therapies.

5. Acknowledgements

We would like to thank Elisabeth Neufeld (UCLA, USA) for the generous gift of MPS I mice. This work was supported by grants from Conselho Nacional de Desenvolvimento Cientifico- CNPq and Fundo de Incentivo a Pesquisa do Hospital de Clinicas de Porto Alegre (FIPE-HCPA).

6. References

[1] Jardim LB, Villanueva MM, de Souza CF, Netto CB. Clinical aspects of neuropathic lysosomal storage disorders. J Inherit Metab Dis. 2010; 33: 315-29.

[2] Ohmi K, Greenberg DS, Rajavel KS, Ryazantsev S, Li HH, Neufeld EF. Activated microglia in cortex of mouse models of mucopolysaccharidoses I and IIIB. Proc Natl Acad Sci U S A. 2003;100: 1902-7.

[3] Ma X, Tittiger M, Knutsen RH, Kovacs A, Schaller L, Mecham RP, Ponder KP. Upregulation of elastase proteins results in aortic dilatation in mucopolysaccharidosis I mice. Mol Genet Metab. 2008; 94: 298-304.

[4] Metcalf JA, Ma X, Linders B, Wu S, Schambach A, Ohlemiller KK, Kovacs A, Bigg M, He L, Tollefsen DM, Ponder KP. A self-inactivating gamma-retroviral vector reduces manifestations of mucopolysaccharidosis I in mice. Mol Ther. 2010; 18: 334-42.

[5] Reolon GK, Braga LM, Camassola M, Luft T, Henriques JA, Nardi NB, Roesler R. Long-term memory for aversive training is impaired in Idua(-/-) mice, a genetic model of mucopolysaccharidosis type I. Brain Res. 2006; 1076: 225-30.

[6] Pan D, Sciascia A 2nd, Vorhees CV, Williams MT. Progression of multiple behavioral deficits with various ages of onset in a murine model of Hurler syndrome. Brain Res. 2008; 1188: 241-53.

[7] Garcia-Rivera MF, Colvin-Wanshura LE, Nelson MS, Nan Z, Khan SA, Rogers TB, Maitra I, Low WC, Gupta P. Characterization of an immunodeficient mouse model of mucopolysaccharidosis type I suitable for preclinical testing of human stem cell and gene therapy. Brain Res Bull. 2007; 74: 429-38.

[8] Reolon GK, Reinke A, de Oliveira MR, Braga LM, Camassola M, Andrades ME, Moreira JC, Nardi NB, Roesler R, Dal-Pizzol F. Alterations in oxidative markers in the cerebellum and peripheral organs in MPS I mice. Cell Mol Neurobiol. 2009; 29: 443-8.

[9] Baldo G, Matte U, Artigalas O, Schwartz IV, Burin MG, Ribeiro E, Horovitz D, Magalhaes TP, Elleder M, Giugliani R. Placenta analysis of prenatally diagnosed patients reveals early GAG storage in mucopolysaccharidoses II and VI. Mol Genet Metab. 2011; 103: 197-8.

[10] Pinheiro SH, Zangrossi H Jr, Del-Ben CM, Graeff FG. Elevated mazes as animal models of anxiety: effects of serotonergic agents. An Acad Bras Cienc. 2007; 79: 71-85.

[11] Langford-Smith A, Malinowska M, Langford-Smith KJ, Wegrzyn G, Jones S, Wynn R, Wraith JE, Wilkinson FL, Bigger BW. Hyperactive behaviour in the mouse model of mucopolysaccharidosis IIIB in the open field and home cage environments. Genes Brain Behav. 2011; 10: 673-82.

[12] Hemsley K, Hopwood JJ. Development of motor deficits in a murine model of mucopolyssaccharidosis type IIIA. Behavioral Brain Research 2005; 158: 191-199.

[13] Alonso I, Marques JM, Souza N, Sequeiros J, Olsson IAS, Silveira I. Motor and cognitive deficits in the heterozygous leaner mouse, a Cav2.1 voltage-gated Ca2+ channel mutant. Neurobiology of Aging 2008; 29: 1733–1743.

[14] Takahashi E, Niimi K, Itakura C. Motor coordination impairment in aged heterozygous rolling Nagoya, Cav2.1 mutant mice. Brain Research 2009; 1279: 50-57.

[15] Sifuentes M, Doroshow R, Hoft R, Mason G, Walot I, Diament M, Okazaki S, Huff K, Cox GF, Swiedler SJ, Kakkis ED. A follow-up study of MPS I patients treated with laronidase enzyme replacement therapy for 6 years. Mol Genet Metab. 2007; 90: 171-80.

[16] Węgrzyn G, Jakóbkiewicz-Banecka J, Narajczyk M, Wiśniewski A, Piotrowska E, Gabig-Cimińska M, Kloska A, Słomińska-Wojewódzka M, Korzon-Burakowska A,

Węgrzyn A. Why are behaviors of children suffering from various neuronopathic types of mucopolysaccharidoses different? Med Hypotheses. 2010; 75: 605-9.

[17] Chung S, Ma X, Liu Y, Lee D, Tittiger M, Ponder KP. Effect of neonatal administration of a retroviral vector expressing alpha-L-iduronidase upon lysosomal storage in brain and other organs in mucopolysaccharidosis I mice. Mol Genet Metab. 2007; 90: 181-92.

[18] Wynne AM, Henry CJ, Godbout JP. Immune and behavioral consequences of microglial reactivity in the aged brain. Integr Comp Biol. 2009; 49: 254-66.

[19] Arfi A, Richard M, Gandolphe C, Bonnefont-Rousselot D, Thérond P, Scherman D. Neuroinflammatory and oxidative stress phenomena in MPS IIIA mouse model: the positive effect of long-term aspirin treatment. Mol Genet Metab. 2011; 103: 18-25.

[20] Russell C, Hendson G, Jevon G, Matlock T, Yu J, Aklujkar M, Ng KY, Clarke LA. Murine MPS I: insights into the pathogenesis of Hurler syndrome. Clin Genet. 1998; 53: 349-61.

7. Figure legends

Figure 1: Body weight (panel A) and urinary GAGs (panel B) in normal (n=3-5) and MPS I (n=5-7) mice. *p<0.05 and ** p<0.01, student t test.

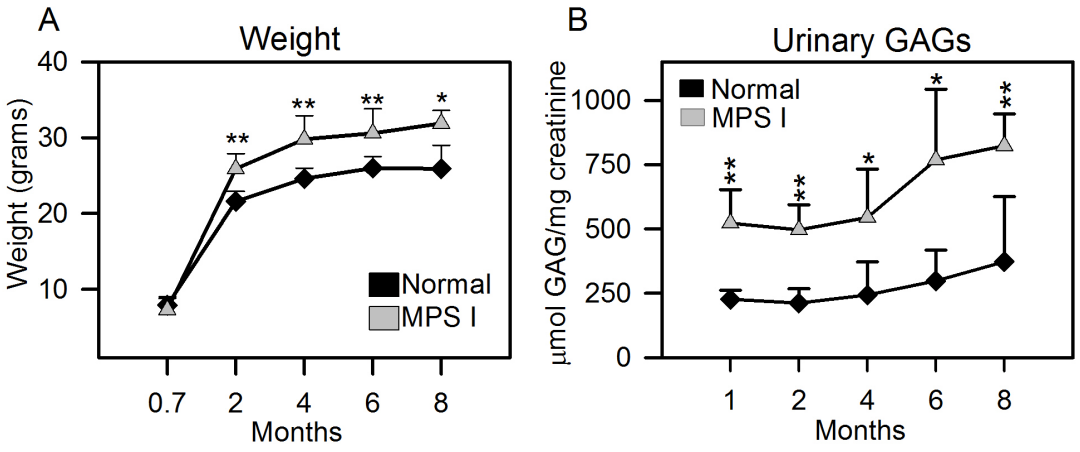

Figure 2: Results from plus maze test, performed as a measure of anxiety. A) The number of entries in the open and closed arms as well as B) the time (in seconds) spent on them was recorded during 5 minutes. No differences were observed between normal and MPS I mice from 2 to 8 months. OA- open arms; CA-closed arms. N= 5-9 animals per group. Abbreviations: mo-months

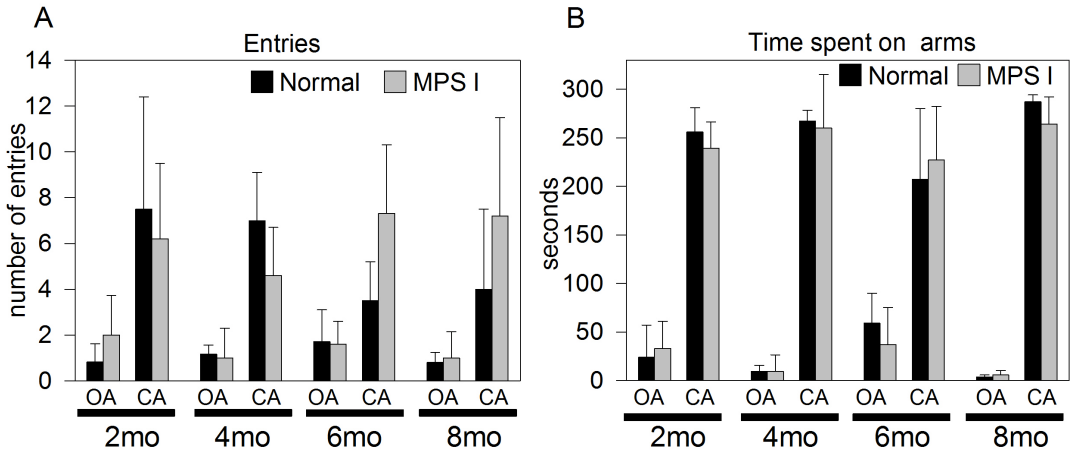

Figure 3: Results from open field test. MPS I and normal mice were submitted to the test for 5 minutes. A) The number of crossings (locomotor activity) and B) rearings (exploratory behavior) were compared at each age. The number of animals can be seen in the bars, and p value is presented above them for each comparison. Statistical analysis was performed using Student`s t test. *p<0.05 and ** p<0.01. Abbreviations: mo-months.

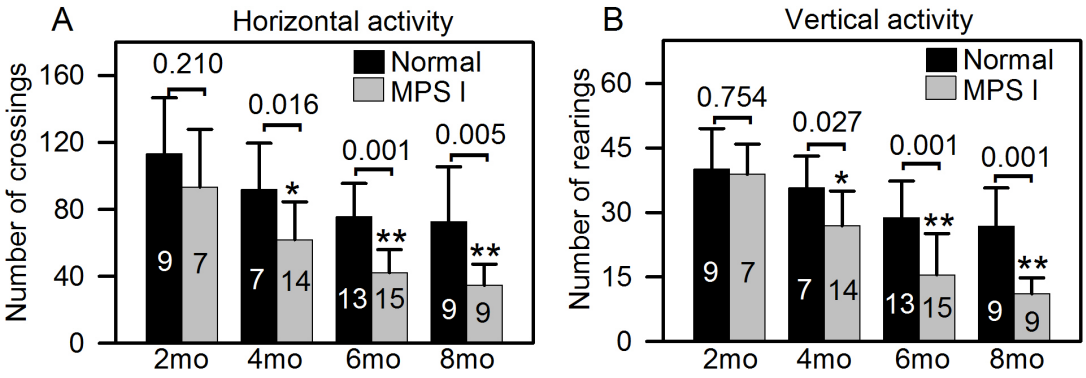

Figure 4: Results from hang wire test. This test was used to evaluate motor coordination and muscular strength. The animals were placed in a suspended wire, and observation was carried for up to 60 seconds, in 3 consecutive trials analyzing A) time spent hanging on the wire and B) scoring the performance (score from 1 to 5, with 5 as the best). The number of mice analyzed at each time point is indicated in the bars. P values are indicated on the figure, Student t test.

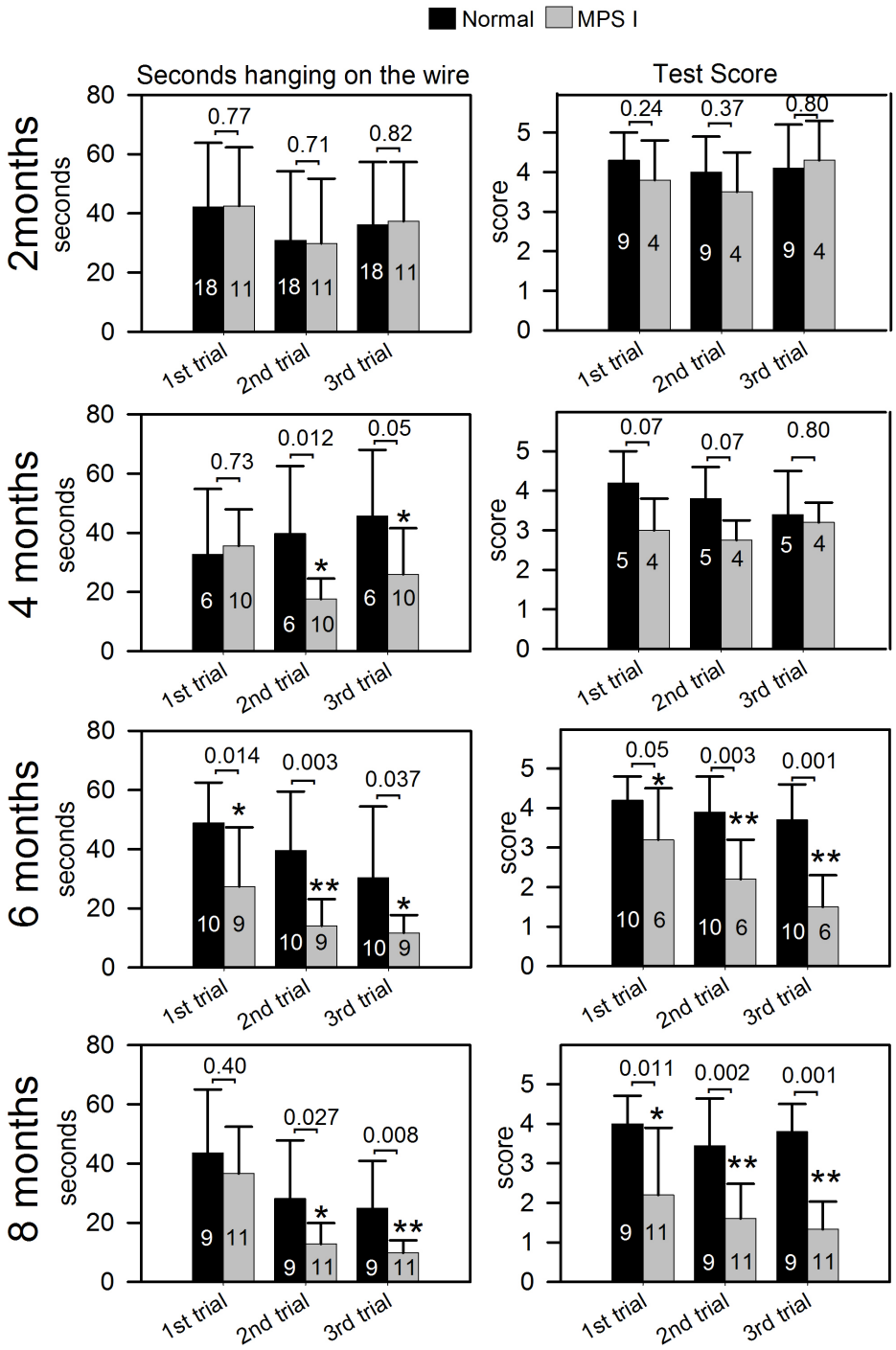

Figure 5: Gait analysis was used to evaluate cerebellar function. The animals had their paws painted with ink and were allowed to walk on a runway with a blank paper on the floor. The length of their right (R) and left (L) steps and the width (W) were measured as described in the materials and methods session. The number of animals at each time point is indicated in the bars. Statistics were performed by Student`s T test. **p<0.01 compared to normal.

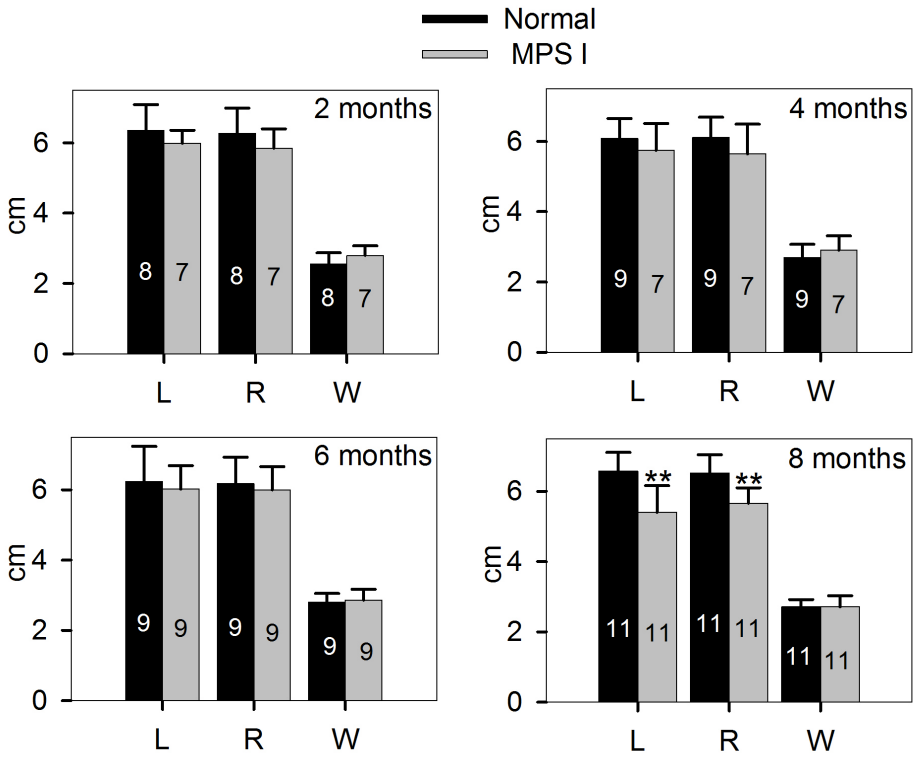

Figure 6: Toludidine blue staining for analysis of GAG storage in 8-month mice. A) Purkinje cell from normal mice B) Purkinje cell from MPS I mice containing vacuoles with storage material. C) Cortex from normal mice. D) Cortex from MPS I mice revealing storage in neurons (arrows) and glial cells (arrow heads).

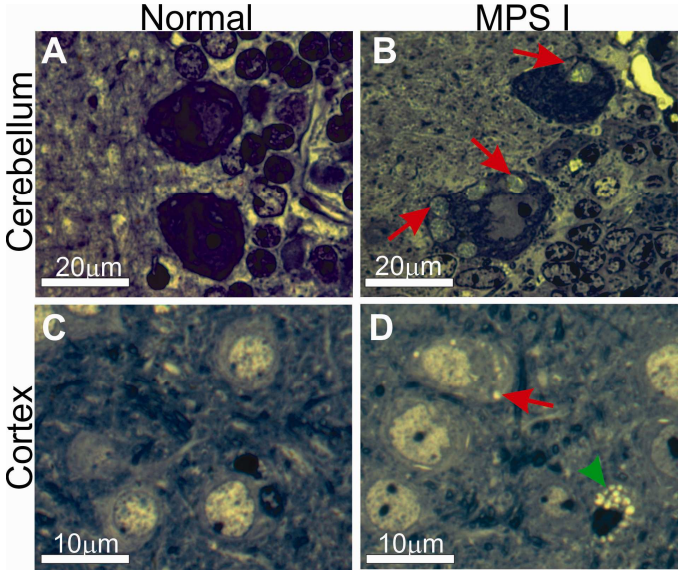

Figure 7: Glial fibrilary acidic protein (GFAP) immunohistochemistry. Representative sections from 8-month normal (A and D) and MPS I (B and E) mouse brains. Number of positive cells were counted in 5 fields (40X magnification) in mouse cerebellum (C) and cortex (F). Arrows indicate some cells positive for GFAP immunohistochemistry, evidencing glial activation in MPS I mice. * p< 0.05; ** p< 0.01 Student t test.

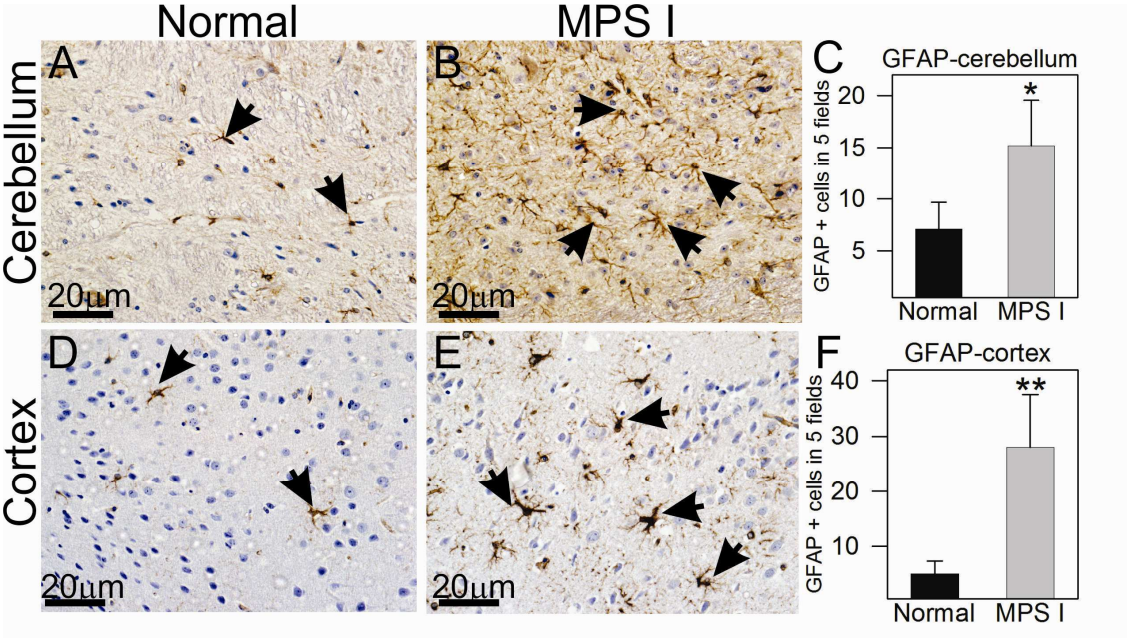

8. Supplementary material

Supplementary figure 1: Genotyping. A) Sequencing of a MPS I mice, indicating the position where the neomycin gene was inserted. B) Example of genotyping by PCR and vizualization of PCR products n 1.5% agarose gel. Normal mice amplify a 514bp fragment and MPS I mice a 321bp. Genotypes are indicated in yellow.

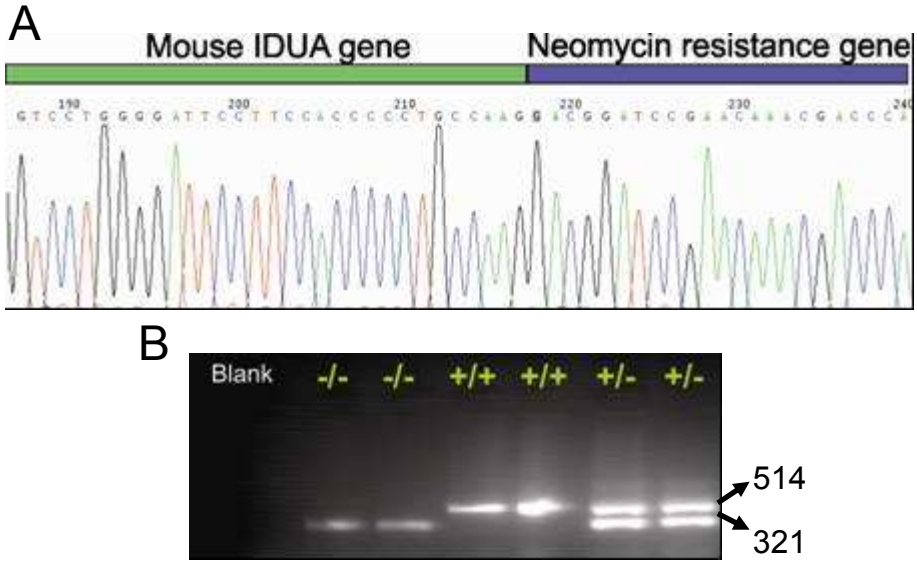

Supplementary figure 2: Example of gait analysis. At least 3 right (R) and left (L) steps were analyzed, as well as at least 5 widths (W), measured as indicated in the figure.

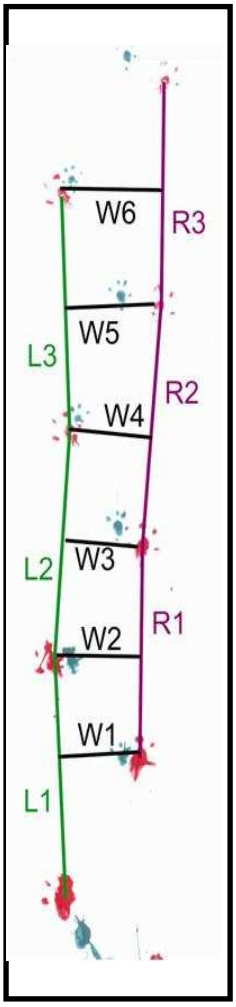

Supplementary figure 3: TUNEL staining in cerebellum and cortex from normal and MPS I mice at 8 months, showing no apoptosis in the groups.

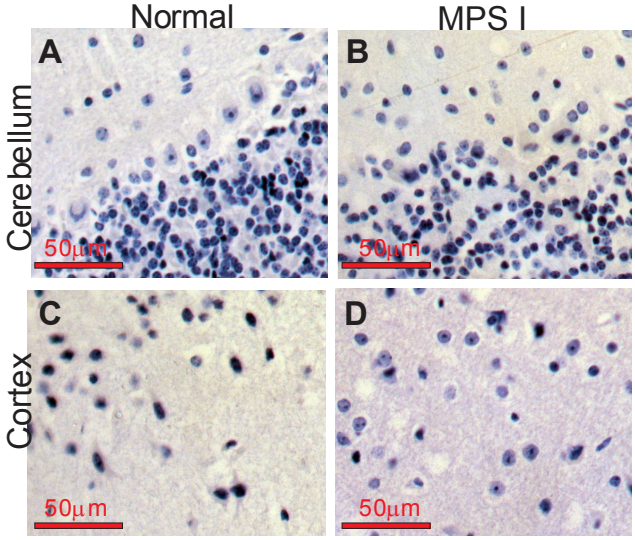

Shotgun proteomics reveals possible mechanisms for cognitive impairment in Mucopolysaccharidosis type I mice

Guilherme Baldo[1,2], Daniel Macedo Lorenzini[3], Diogenes Santiago Santos[3], Fabiana Quoos Mayer[1,4], Sandrine Vitry[5], Stephanie Bigou[5], Jean Michael Heard[5], Katherine Parker Ponder[6], Ursula Matte[1], Roberto Giugliani[1,2,3]

[1]Gene Therapy Center-Hospital de Clinicas de Porto Alegre, RS,Brazil
[2]Post Graduation program in Biochemistry,-UFRGS, Porto Alegre, RS, Brazil
[3]Centro de Pesquisas em Biologia Molecular e Funcional, Instituto Nacional de Ciência e Tecnologia em Tuberculose, Pontifícia Universidade Católica do Rio Grande do Sul, RS, Brazil
[4]Post Graduation program in Genetics and Molecular Biology,-UFRGS, Porto Alegre, RS, Brazil
[5]Pasteur Institute, Paris, France
[6]Internal Medicine- Hematology-Washington University Saint Louis, USA

Abstract

Mucopolysaccharidosis type I (MPS I) is due to deficient alpha-L-iduronidase (IDUA) which leads to storage of undegraded glycosaminoglycans (GAG). The severe form of the disease is characterized by mental retardation of unknown etiology. Trying to unveil the mechanisms that lead to cognitive impairment in MPS I, we studied alterations in the proteome from MPS I mouse hippocampus. Eight-month old mice presented GAG storage in neurons and glial cells, and impaired aversive and non-aversive memory. Shotgun proteomics was performed and 296 proteins were identified. Of those, 32 were diferentially expressed. We found elevation in proteins such as cathepsin D and cathepsin B, however their increase did not lead to cell death in MPS I brains. Glial fibrilary acid protein (GFAP) was markedly elevated, and immunohistochemistry confirmed a neuroinflammatory process that could be responsible for neuron dysfunction. We didn't observe any differences in ubiquitin expression, as well as in other proteins related to protein folding, suggesting that the ubiquitin system is working properly. Finally, we observed alterations in several proteins involved in synaptic plasticity, including overexpression of post synaptic density-95 (PSD-95) and reduction of microtubule-associated proteins A and B. These results together suggest that the cognitive impairment in MPS I mice is not due to cell death, but rather to neuron dysfunction caused by multiple processes, including neuroinflammation and alterations in synaptic plasticity.

Keywords: Mucopolysaccharidosis type I; brain disease; PSD-95; cathepsin; ubiquitin; GFAP.

1. Introduction

Mucopolysaccharidosis type I (MPS I) is a lysosomal storage disorder due to alpha-L-iduronidase (IDUA, EC 3.2.1.76) deficiency. The lack of IDUA activity leads to multisystemic accumulation of the glycosaminoglycans (GAG) heparan and dermatan sulphate (Giugliani et al, 2010). Patients with the severe form, called Hurler syndrome (OMIM, #601414), develop mental retardation and cognitive decline from first years of life. It is believed that patients with the attenuated forms, known as Hurler-Sheie (OMIM, #601415) and Scheie (OMIM, #601416) syndromes, do not present brain abnormalities, although a recent study suggest that at least 10% of these patients have mild to moderate impairments in cognitive function (Thomas et al 2010).

The etiology of neurological dysfunction in MPS I is unclear. The creation of the MPS I mouse model (Ohmi et al, 2003) allowed major findings on the pathogenesis of brain disease. Neurons and glial cells accumulate GAGs (Baldo et al, submitted), and storage of other substances such as gangliosides have also been reported (Walkley, 2004). Activation of glial cells has been reported in the cortex and cerebellum (Ohmi et al, 2003; Baldo et al, submitted) as well as alterations in oxidative status (Reolon et al, 2009).

These abnormalities are concomitant with alterations in behavioral parameters. Previous studies suggest that, among other abnormalities, MPS I mice show impaired behavior in tests involving memory skills, including failure to habituate in the repeated open field test (Hartung et al, 2004; Pan et al, 2008) and impairment in long-term memory for aversive training (Reolon et al, 2006). Also, results from Morris water maze tests have shown contradictory results, with some studies reporting abnormalities (Wolf et al, 2011) while other studies found inconsistent results (Pan et al, 2008).

These findings evidence that the mechanisms that lead to cognitive impairment in MPS I are very complex, possibly involving multiple dysfunctional processes. Therefore in the present work we compared the proteome of normal and MPS I mouse hippocampus, aiming to evidence possible mechanisms responsible for brain dysfunction in MPS I mice.

2. Materials and methods

2.1 Animals and study design

All animal studies were approved by the authors' institutional review board (Study #09420) and MPS I mice on a C57BL/6 background (kindly donated by Dr Elizabeth Neufeld) were used. The MPS I mice carry a disrupted version of the *Idua* gene and could be detected by PCR after DNA extraction from ear tissue, using the following primers Forward 5'-GAGACTTGGAATGAACCAGAC-3' and ReverseA 5'-ATAGGGGTATCCTTG AACTC-3' and ReverseB 5'-GTTCTTCTGAGGGGATCGG-3'. Heterozygous mice were used for breeding.

Idua$^{-/-}$ mice (referred as MPS I group) and their normal littermate controls (I*dua*$^{-/+}$ and *Idua*$^{+/+}$, referred from now on as "Normal" group) were the subjects for the experiments. At 3 weeks of age, offspring were separated from the dam, genotyped and housed (2–5 per cage) by gender. Animals were maintained to conventional housing under a 12 h light/12 h dark cycle with controlled temperature (19 ± 1°C) and humidity (50 ± 10%). We examined mice in behavior tests at 6 and 8 months, all behavior studies were performed between 2:00 pm and 6:00pm.

2.2 Behavior studies

All behavior and proteomic studies were performed in 6 to 8-months male mice. Normal and MPS I mice were submitted to 2 different tests to evaluate memory.

The inhibitory avoidance test in rodents is a widely used animal model of aversively motivated learning and memory (Reolon et al, 2006). The inhibitory avoidance training box was a 50 × 25 × 25-cm acrylic box whose floor consisted of parallel stainless steel bars (1 mm diameter) spaced 1 cm apart (Insight, Sao Paulo, Brazil). Animals were placed on a platform, and their latency to step-down on the grid with all four paws was recorded with the device. In the training trial, immediately after stepping down on the grid, animals were given a 0.5 mA, 2 s footshock. In retention test sessions, carried out 24 h (long-term memory retention) after training, no footshocks were given and a maximum of 180 s was imposed in the step-down latency. The differences between retention test and training trial step-down latencies were used as memory retention scores (Reolon et al, 2006).

Non-aversive memory was accessed using a repeated open field test. The test consisted of a square arena 13 × 13 cm^2 with 60 cm high walls. The floor was divided into 16 squares by parallel and intersecting lines, obtaining four centered squares and 12 periphery squares. Mice were placed in one of the corners of the open field and (a) ambulation (total number of crossings), and (b) rearings were observed during a 5 min exposure period for both control and MPS I animals. Test was repeated 30 and 60 min after the first test and results from the first and third trial were compared, as reported (Pan et al, 2008).

2.3 Samples collection and GAG staining

Eight-month old MPS I and normal mice were perfused with 20 mL of PBS, and brains were removed and fixed in PBS with 4% paraformaldehyde and 2% glutaraldehyde. Pieces of brain were embedded in plastic, and 1 μm-thick sections of the hippocampus were stained with toluidine blue as described (Ma et al 2007) to analyze GAG storage in neurons and glial cells.

2.4 Comparative proteome analysis

Hippocampus from 8-month normal (n=5) and MPS I(n=5) male mice were isolated and flashly frozen in liquid nitrogen, and stored in -80^{o}C freezer. Subsequently, the pieces were homogeneized in PBS using a dismembrator and proteins were extracted with TCA 10% and cold acetone.

The total protein extracts were individually subjected to analysis by mass spectrometry to identify differentially expressed proteins. The protein extracts were incubated in 0.1% Rapigest (Waters) and 50 mM Ammonium bicarbonate pH 8 for 2 min at 100°C for protein denaturation, and treated with 5 mM dithiothreitol (DTT) for 30 min at 60 °C to reduce disulfide bonds. Free sulfhydryl bonds were alkylated with 15 mM iodoacetamide (IAA) for 30 min at room temperature. A total of 100 μg of protein was digested with 2 μg of trypsin (Sigma, St Louis, USA) for 1 h at 37 °C. The digestion was quenched and the Rapigest hydrolyzed by the addition of HCl to a final concentration of 100 mM and incubating the sample at 37 °C for 45 min. The tryptic digest was separated on a homemade column (solid phase Kinetex C18 of 2.6um particles, 0.15X100mm) using a nanoUPLC (nanoLC Ultra 1D plus, Eksigent, USA)

and eluted directly to a nanospray ion source connected to a hybrid mass spectrometer (LTQ-XL and LTQ Orbitrap Discovery, Thermo, USA). The flow rate was set to 1 μL/min, using a gradient from 10-40% acetonitrile/0.1% formic acid over 1 hour, and the mass spectrometer was set to acquire one MS survey scan for the m/z range of 400–1800 (30000 resolution) and MS/MS spectra for the five most intense ions from the survey scan during the gradient. In MS survey, the preview mode for FTMS master scan was turned on, and only doubly and triply charged ions were selected for MS/MS. An isolation mass window of 15 ppm was used for the precursor ion selection, and a normalized collision energy of 35% was used for the fragmentation. Dynamic exclusion lasting for 30 sec was used to acquire MS/MS spectra from low intensity ions.

For database searching, tandem mass spectra were extracted by Proteome Discoverer 1.0 (Thermo Fisher Scientific, San Jose, CA, USA; version 1.0.43.0), and all MS/MS samples were analyzed using Sequest set to search ipi.MOUSE (v3.72, 56958 entries) assuming the digestion by trypsin. Sequest was searched with a fragment ion mass tolerance of 0.80 Da and a parent ion tolerance of 10.0 PPM. Iodoacetamide derivative of cysteine was specified in Sequest as a fixed modification. Oxidation of methionine was specified in Sequest as a variable modification. Scaffold (version Scaffold_3.1.2, Proteome Software Inc., Portland, OR) was used to validate MS/MS based peptide and protein identifications.

Peptide identifications were accepted if they could be established at greater than 95.0% probability as specified by the Peptide Prophet algorithm (Keller et al, 2002). Protein identifications were accepted if they could be established at greater than 80.0% probability and contained at least 2 identified peptides. Protein probabilities were assigned by the Protein Prophet algorithm (Nesvizhskii et al, 2003). Proteins that contained similar peptides and could not be differentiated based on MS/MS analysis alone were grouped to satisfy the principles of parsimony.

2.5 Western Blots

Western blotts were performed as previously described (Hocquemiller et al, 2010). Antibodies were used as follows: mouse mAb IgG1 anti-LAMP1 (clone H4A3, 1:200, SouthernBiotech, Birmighan, AL, USA), rabbit IgG anti-GAP43 (1:500; Abcam, Cambridge, MA), polyclonal anti-Calnexin (1:1000, Stressgen, Victoria, Canada), rabbit polyclonal anti-Ubiquitin (1:500, Dako, Glostrup, Denmark), rabbit anti-Synaptophysin

(1:200, Synaptic system), anti-PSD95 (1:2000, Affinity BioReagents, Rockfort, IL, USA), anti-actin (1:2000, Sigma, St Louis, MO, USA) Secondary antibodies conjugated to alexafluor or DyLightTM were from molecular probes (Invitrogen) and Jackson ImmunoResearch Laboratories (West Grove, PA, USA). Signal intensities were measured with the LAS-1000CH Luminescent photofilm LTD system, piloted by the IR-LAS-Pro software (Fuji). Specific signal values were normalized relative to the actin signal.

2.6 Enzyme assays

For the cathepsin assays, frozen mouse forebrains were homogenized with the hand-held homogenizer in 100 mM sodium acetate pH 5.5 containing 2.5 mM ethylenediaminetetraacetic acid (EDTA), 0.1% Triton X-100, and 2.5 mM dithiothreitol (DTT), and centrifuged at 10,000 g for 5 minutes at 4^{O}C. The protein concentration was determined with the Bradford assay (BioRad Laboratories, Hercules CA).

The cathepsin B (CtsB) assay was performed using the extracts and the substrate Z-Arg-Arg-AMC (Bachem, Torrance, CA) at pH 7.5. The amount of product was determined by excitation at 355 nm and emission at 460 nm using kinetic readings and comparison with 7-Amino-4-methylcoumarin (AMC) standards from Anaspec. One unit (U) of enzyme released 1 nmole of the product per hour at 37^{O}C (Baldo et al, 2011).

The cathepsin D (CtsD) assay was performed at pH 4 with 10 μM of the substrate 7-methoxycoumarin-4-acetyl(Mca)-Gly-Lys-Pro-Ile-Leu-Phe-Phe-Arg-Leu-Lys-2,4-nitrophenyl (Dnp)-D-Arg-NH2 with Mca-Pro-Leu-OH (Enzo Life Sciences, USA) as the standard. CtsD assay was read at 320 nm for excitation and 420 nm for emission (Baldo et al, 2011).

The caspase-3 assay was performed incubating the protein extracts with 50 μM of the substrate AC-DEVD-AMC (Enzo Life Sciences, Farmingdale, NY) in buffer (10mM HEPES at pH 7.5, 50mM NaCl and 8mM dithiothreitol). The substrate is cleaved mainly by caspase-3 but also by caspase-1, -4, -7 and -8. The samples were incubated at 37 ^{o}C for 5 h and fluorescence (Kreuzaler et al, 2011) was measured using a Fluoroskan Ascent microplate fluorometer (Thermo Electron, Milford, MA) with excitation at 355 nM and at emission 460 nM.

2.7 Immunohistochemistry and TUNEL stain

Immunohistochemistry for glial fibrillary acidic protein (GFAP) was performed using specific antibody (Dako Cytomation, Polyclonal Rabbit anti-GFAP) and a secondary anti-rabbit IgG antibody conjugated to horseradish peroxidase according to our previous work (Baldo et al, *in press*). Slides were analyzed by a researcher blinded to the groups, counting positive cells in 5 high-power fields (40X).

TUNEL staining was performed to analyze cell death using the kit ApopTag® (Millipore, USA) according to manufacturer's instructions. Sections were counterstained with hematoxylin. A small intestine biopsy was used as a positive control.

2.8 Statistics

Normal and MPS I mice were compared using the Student t test. A P value less than 0.05 was considered statistically significant. Statistical analysis was performed using the software SigmaStat version 3.1.

3. Results

3.1 Behavior abnormalities and GAG storage

Small vacuoles could be observed in neurons and glial cells from MPS I mice hippocampus (figure 1A) at 8 months. Also, we could observe abnormalities in the repeated open field test, with normal mice showing 66% of crossings and 70% of rearings in the third trial compared to the first trial, while MPS I mice failed to habituate, having 83% of crossings ($p=0.035$ vs normal) and 121% of rearings ($p=0.014$ vs normal) in the third trial (figure 1B).

When the inhibitory avoidance test was performed, we observed that while in the training trial there was not a significant difference between normal and MPS mice ($p=0.29$, data not shown) in the test trial long-term aversive memory was impaired in MPS I mice, since they stepped down from the platform significantly faster than normal mice ($p=0.039$, Mann-Whitney test), indicating failure in remembering the aversive stimulus (figure 1C).

3.2 Proteomic alterations in MPS I hippocampus

Using a proteomics approach, we were able to identify 296 proteins in normal and MPS I mice. Thirty two proteins were found to be differentially expressed (13 proteins were upregulated in MPS I mice, while 19 were downregulated). Table 1 includes protein differentially expressed and proteins with borderline statistics ($0.05<p<0.10$).

The lysosomal CtsD (7.5-fold normal) and prosaposin (5.7-fold) were the 2 most upregulated proteins. GFAP was also upregulated (4.6-fold normal), suggesting neuroinflammation, as it is a marker of glial cells. Another marker of glial cells which was upregulated was the astrocyte-specific glutamine synthethase (1.2-fold). Other proteins found elevated in MPS I mice were MAPK1 (2.9-fold) which mediates cell signaling processes, as well as neuromodulin (also known as GAP-43) which was 2.3-fold normal and mediates growth of dendrites, and calnexin (3.6-fold), which has an important role in protein folding.

Several proteins involved in vesicle transport, including AP-2 complex subunit beta (0.37-fold), syntaxin-1A (0.42-fold), amphiphysin (0.44-fold), complexin-2 (0.6-fold) and synaptophysin (0.61-fold) were downregulated. Proteins from the 14-3-3 family, involved in multiple signaling pathways, were also reduced. The most downregulated protein was microtubule-associated protein 1B (0.21-fold), and very interestingly other proteins also involved in synaptic maturation and plasticity followed the same pattern (microtubule-associated protein 1A and copine-6 were both 0.41-fold normal).

3.3 Cathepsins activity and evaluation of cell death in MPS I mouse brain

Since CtsD and CtsB are involved in apoptosis and lysosomal-mediated cell death, we decided to confirm the proteomics results using fluorescent assays to measure cathepsin activity in the hippocampus from 8-month old mice (figure 2A). CtsD activity was markedly elevated (5.7-fold normal, $p<0.01$) in MPS I hippocampus as well as CtsB (2.1-fold, $p=0.048$).

Despite elevation in cathepsins activitiy, surprisingly we could not observe any consistent sign of cell death in MPS I mice hippocampus. Caspase-3 assay result showed similar activity in both groups (figure 2B). TUNEL stain was also negative in both groups, suggesting that cell death does not occur (figure 2C).

3.4 Assessment of neuroinflammation

Neuroinflammation was detected in MPS I mice counting cells positive for GFAP, a marker of glial cells. MPS I mice had significant more GFAP-positive cells spread throughout the hippocampus (figure 3A and B). The quantification of positive cells confirmed the increase observed (figure 3C) and are in agreement with results from the proteomic analysis.

3.5 Western blot analysis

Since the proteomic analysis suggested that multiple abnormalities were present in MPS I mice brains, we performed western blots trying to identify processes that are likely to be involved in the pathogenesis of the disease. Western blot results are summarized in figure 4.

First of all, we looked for expression of key proteins involved in synapses formation and maturation. We observed a very small and non-significant reduction in synaptophysin levels in MPS I mice (84% normal levels, $p=0.35$). On the other hand, expression of PSD-95 was elevated to 159% normal ($p=0.048$), suggesting an elevation in the levels of this protein.

We quantified the expression of GAP-43, that is involved in neurite growth, and it was not different between normal and MPS I mice. On the other hand, the lysosomal associated membrane protein (LAMP1), a marker of the lysosomal membrane was found to be 4105% normal ($p=0.001$).

We next aimed to verify if proteins involved in protein folding and degradation were altered. We tested calnexin and ubiquitin, and we didn't find consistent differences between groups. Ubiquitin expression was barely detectable in both groups (data not shown).

4. Discussion

MPS I patients with the severe form of the disease develop cognitive impairment within first years of life through mechanisms that are still unknown. Based on that, the goal of this study was to detect proteins that are differentially expressed in MPS I mice hippocampus and could be responsible for the clinical symptoms.

GAG storage could be detected in histological sections in both neurons and glial cells at 8 months. Furthermore, behavioral tests confirmed previous results (Pan et al, 2008; Reolon et al, 2006), showing consistent abnormalities at 8 months of age. Therefore we decided to analyze differences in protein profile at this time point.

Previous studies have shown that in cases of lysosomal dysfunction the transcription factor EB (TFEB) activates the transcription of several lysosomal enzymes, including cathepsin D, cathepsin B and prosaposin (Sardiello et al, 2009) which gives a possible explanation for these proteins to be upregulated in MPS I hippocampus. Furthermore, the elevation in CtsD and CtsB has been reported as mediators of apoptosis and lysosomal-mediated cell death (Ceccariglia et al, 2011; Kreuzaler et al, 2011). Therefore we investigated if these processes were occurring in MPS I mice hippocampus. Surprisingly, cell death was not detected in MPS I mice brains by TUNEL or caspase-3 activity, suggesting that the mechanism that lead to cognitive decline in MPS I mice is caused mainly by a neuronal dysfunction rather than neuron death. These results confirm our previous observations that cell death was not occurring in other brain areas, such as the cerebellum and cortex (Baldo et al, *in press*). Based on these findings, our subsequent experiments aimed to unravel possible mechanisms of neuronal dysfunction.

Overexpression of GFAP suggested that a neuroinflammatory process could be present in MPS I mouse hippocampus, and results from IHQ confirmed that. The activation of glial cells was previously shown in MPS I cortex and cerebellum (Ohmi et al, 2003; Baldo et al, *in press*) and seems to correlate with disease progression (Baldo et al, *in press*). It is known that activation and proliferation of glial cells occurs in several neurodegenerative diseases and it is related to impaired neuronal function (Kawashita et al, 2009; Li et al, 2011). The pro-inflammatory cytokines, chemokines and the components of the complement system released by glial cells can disrupt nerve terminals activity causing dysfunction and loss of synapses, which correlates with memory decline in other neurodegenerative diseases (Agostinho et al, 2010). These results combined with our previous observations suggest that glial activation occurs throughout the brain, and raise questions if anti-inflammatory drugs could reduce brain abnormalities in MPS I, as shown for other mucopolysaccharidosis (Arfi et al, 2011).

GAP-43 was also found to be upregulated in the proteomics study, as well as its mRNA was shown to be elevated in the aorta of MPS VII mice (Baldo et al, 2011) and marginally (1.5-fold) in the hippocampus of MPS I mice at 6-months (Martinelli,

personal communication). Previous studies conducted in MPS IIIB cortex suggest that overexpression of this protein lead to inefficient neurite growth (Hocquemiller et al, 2010) and therefore could be participating in the pathogenesis of MPS I as well. However our western blot results failed in confirming the increase in GAP-43 levels, suggesting that the increase is marginal, if any, and probably does not have a major role in cell dysfunction in MPS I.

An increase in the chaperone calnexin could suggest that protein folding was not occurring properly and proteins could be degraded by the ubiquitin system. Therefore we analyzed protein expression of calnexin and ubiquitin by western blot. They did not show any difference, suggesting that, unlike other lysosomal storage disorders (Bifscha et al, 2007), the protein folding and the ubiquitin system is functioning properly in MPS I brain.

Several proteins linked to synapse plasticity were shown to be altered in MPS I mice. Due to their importance, we decided to look for expression of synaptophysin and PSD-95, although the last one was not found in our proteomic study. Synaptophysin is the most abundant protein in the synaptic vesicle membrane, and previous experiments have shown that it was reduced in MPS IIIB brain cortex due to excessive degradation by the proteosomal system (Vitry et al, 2009). Despite a 40% reduction in the proteomic study, our western blot results suggest a smaller and non-significant reduction, and we conclude that the process observed in MPS IIIB brains is not occurring in MPS I mice.

PSD-95, a synaptic scaffolding protein, is the most abundant post-synaptic protein (Zhang and Lisman, 2012), and plays important roles in the regulation of dendritic spine morphology and glutamate receptor signaling (Sweet et al, 2011a). It has several functions, but its overexpression results in less organized microtubules at dendritic branch points and decreased dendritogenesis (Sweet et al, 2011b). It didn't escape us that at least 2 proteins involved in microtubules formation and organization (microtubule-associated proteins A and B), which are also involved in dentritic spine formation and dendritogenesis (Szebenyi et al, 2005; Tortosa et al, 2011) and who can interact with PSD-95 (Reese et al, 2007) are markedly downregulated, and that these 3 proteins could act together in impairing synaptic plasticity.

Altogether, our results suggest that the cognitive deficits observed in MPS I mice are not caused by neuron death. However, important processes such as neuroinflammation and impaired synaptic plasticity might be causing a neuronal dysfunction, and the loss of memory observed. The results obtained with the present

work suggest that multiple mechanisms acting together are involved in the pathogenesis of cognitive dysfunction in MPS I.

5. Acknowledgements

The authors would like to thank Elizabeth Neufeld (UCLA, CA) for the generous gift of MPS I mice and Paulo Mascarello Bisch (UFRJ, Brazil) for helpful discussion regarding the proteomic experiments. This work was supported by Conselho Nacional de Desenvolvimento Cinetifico (CNPq) and Fundo de Incentivo a Pesquisa do HCPA (FIPE-HCPA).

6. References

Arfi A, Richard M, Gandolphe C, Bonnefont-Rousselot D, Thérond P, Scherman D. Neuroinflammatory and oxidative stress phenomena in MPS IIIA mouse model: the positive effect of long-term aspirin treatment. Mol Genet Metab. 2011; 103(1):18-25.

Agostinho P, Cunha RA, Oliveira C. Neuroinflammation, oxidative stress and the pathogenesis of Alzheimer's disease. Curr Pharm Des. 2010; 16(25):2766-78.

Baldo G, Meyer FQ, Martinelli B, Dilda A, Meyer F, Ponder K, Giugliani R, Matte U. Evidence of a progressive motor dysfunction in Mucopolysaccharidosis type I mice. Behavioral Brain Research, *in press*.

Baldo G, Wu S, Howe RA, Ramamoothy M, Knutsen RH, Fang J, Mecham RP, Liu Y, Wu X, Atkinson JP, Ponder KP. Pathogenesis of aortic dilatation in mucopolysaccharidosis VII mice may involve complement activation. Mol Genet Metab. 2011; 104(4):608-19.

Bifsha P, Landry K, Ashmarina L, Durand S, Seyrantepe V, Trudel S, Quiniou C, Chemtob S, Xu Y, Gravel RA, Sladek R, Pshezhetsky AV. Altered gene expression in cells from patients with lysosomal storage disorders suggests impairment of the ubiquitin pathway. Cell Death Differ. 2007; 14(3):511-23

Ceccariglia S, D'Altocolle A, Del Fa' A, Pizzolante F, Caccia E, Michetti F, Gangitano C. Cathepsin D plays a crucial role in the trimethyltin-induced hippocampal neurodegeneration process. Neuroscience. 2011; 174:160-70.

Giugliani R, Federhen A, Rojas MV, Vieira T, Artigalás O, Pinto LL, Azevedo AC, Acosta A, Bonfim C, Lourenço CM, Kim CA, Horovitz D, Bonfim D, Norato D, Marinho D, Palhares D, Santos ES, Ribeiro E, Valadares E, Guarany F, de Lucca GR, Pimentel H, de Souza IN, Correa J Neto, Fraga JC, Goes JE, Cabral JM, Simionato J, Llerena J Jr, Jardim L, Giuliani L, da Silva LC, Santos ML, Moreira MA, Kerstenetzky M, Ribeiro M, Ruas N, Barrios P, Aranda P, Honjo R, Boy R, Costa R, Souza C, Alcantara FF, Avilla SG, Fagondes S, Martins AM. Mucopolysaccharidosis I, II, and VI: Brief review and guidelines for treatment. Genet Mol Biol. 2010; 33(4):589-604.

Hartung SD, Frandsen JL, Pan D, Koniar BL, Graupman P, Gunther R, Low WC, Whitley CB, McIvor RS. Correction of metabolic, craniofacial, and neurologic abnormalities in MPS I mice treated at birth with adeno-associated virus vector transducing the human alpha-L-iduronidase gene. Mol Ther. 2004; 9(6):866-75.

Hocquemiller M, Vitry S, Bigou S, Bruyère J, Ausseil J, Heard JM. GAP43 overexpression and enhanced neurite outgrowth in mucopolysaccharidosis type IIIB cortical neuron cultures. J Neurosci Res. 2010; 88(1):202-13.

Kawashita E, Tsuji D, Kawashima N, Nakayama K, Matsuno H, Itoh K. Abnormal production of macrophage inflammatory protein-1alpha by microglial cell lines derived from neonatal brains of Sandhoff disease model mice. J Neurochem. 2009; 109(5):1215-24.

Keller A, Nesvizhskii AI, Kolker E, Aebersold R. Empirical statistical model to estimate the accuracy of peptide identifications made by MS/MS and database search. Anal Chem. 2002; 74(20):5383-92.

Kreuzaler PA, Staniszewska AD, Li W, Omidvar N, Kedjouar B, Turkson J, Poli V, Flavell RA, Clarkson RW, Watson CJ. Stat3 controls lysosomal-mediated cell death in vivo. Nat Cell Biol. 2011; 13(3):303-9

Li C, Zhao R, Gao K, Wei Z, Yin MY, Lau LT, Chui D, Hoi Yu AC. Astrocytes: implications for neuroinflammatory pathogenesis of Alzheimer's disease. Curr Alzheimer Res. 2011; 8(1):67-80.

Ma X, Liu Y, Tittiger M, Hennig A, Kovacs A, Popelka S, Wang B, Herati R, Bigg M, Ponder KP. Improvements in mucopolysaccharidosis I mice after adult retroviral vector-mediated gene therapy with immunomodulation. Mol Ther. 2007; 15(5):889-902.

Nesvizhskii AI, Keller A, Kolker E, Aebersold R. A statistical model for identifying proteins by tandem mass spectrometry. Anal Chem. 2003; 75(17):4646-58.

Ohmi K, Greenberg DS, Rajavel KS, Ryazantsev S, Li HH, Neufeld EF. tivated microglia in cortex of mouse models of mucopolysaccharidoses I and IIIB. Proc Natl Acad Sci U S A. 2003; 100(4):1902-7

Pan D, Sciascia A 2nd, Vorhees CV, Williams MT. Progression of multiple behavioral deficits with various ages of onset in a murine model of Hurler syndrome. Brain Res. 2008; 1188:241-53.

Reese ML, Dakoji S, Bredt DS, Dötsch V. The guanylate kinase domain of the MAGUK PSD-95 binds dynamically to a conserved motif in MAP1a. Nat Struct Mol Biol. 2007; 14(2):155-63.

Reolon GK, Braga LM, Camassola M, Luft T, Henriques JA, Nardi NB, Roesler R. Long-term memory for aversive training is impaired in Idua(-/-) mice, a genetic model of mucopolysaccharidosis type I. Brain Res. 2006; 1076(1):225-30.

Reolon GK, Reinke A, de Oliveira MR, Braga LM, Camassola M, Andrades ME, Moreira JC, Nardi NB, Roesler R, Dal-Pizzol F. Alterations in oxidative markers in the cerebellum and peripheral organs in MPS I mice. Cell Mol Neurobiol. 2009; 29(4):443-8.

Sardiello M, Palmieri M, di Ronza A, Medina DL, Valenza M, Gennarino VA, Di Malta C, Donaudy F, Embrione V, Polishchuk RS, Banfi S, Parenti G, Cattaneo E, Ballabio A. A gene network regulating lysosomal biogenesis and function. Science. 2009; 325(5939):473-7.

Szebenyi G, Bollati F, Bisbal M, Sheridan S, Faas L, Wray R, Haferkamp S, Nguyen S, Caceres A, Brady ST. Activity-driven dendritic remodeling requires microtubule-associated protein 1A. Curr Biol. 2005; 15(20):1820-6.

Sweet ES, Tseng CY, Firestein BL. To branch or not to branch: How PSD-95 regulates dendrites and spines. Bioarchitecture. 2011; 1(2):69-73.

Sweet ES, Previtera ML, Fernández JR, Charych EI, Tseng CY, Kwon M, Starovoytov V, Zheng JQ, Firestein BL. PSD-95 alters microtubule dynamics via an association with EB3. J Neurosci. 2011b; 31(3):1038-47.

Thomas JA, Beck M, Clarke JT, Cox GF. Childhood onset of Scheie syndrome, the attenuated form of mucopolysaccharidosis I. J Inherit Metab Dis. 2010; 33(4):421-7

Tortosa E, Montenegro-Venegas C, Benoist M, Härtel S, González-Billault C, Esteban JA, Avila J. Microtubule-associated protein 1B (MAP1B) is required for dendritic spine development and synaptic maturation. J Biol Chem. 2011; 286(47):40638-48.

Vitry S, Ausseil J, Hocquemiller M, Bigou S, Dos Santos Coura R, Heard JM. Enhanced degradation of synaptophysin by the proteasome in mucopolysaccharidosis type IIIB. Mol Cell Neurosci. 2009; 41(1):8-18.

Walkley SU. Secondary accumulation of gangliosides in lysosomal storage disorders. Semin Cell Dev Biol. 2004; 15(4):433-44

Wolf DA, Lenander AW, Nan Z, Belur LR, Whitley CB, Gupta P, Low WC, McIvor RS. Direct gene transfer to the CNS prevents emergence of neurologic disease in a murine model of mucopolysaccharidosis type I. Neurobiol Dis. 2011; 43(1):123-33.

Zhang P, Lisman JE. Activity-dependent regulation of synaptic strength by PSD-95 in CA1 neurons. J Neurophysiol. 2012 Feb;107(4):1058-66.

7. Tables

Table 1: Results from proteomic analysis. Hippocampus from five normal and MPS I mice had their proteome analyzed as describe in methods section, and results were compared using the software Scaffold. In the list we present proteins that were statistically different or with borderline results, their fold-change (ratio between MPS and normal levels), the p value and a brief description of the protein function or process involved in.*P<0.05, Student`s t test.

Protein Name	Symbol	IPI	Ratio MPS/Nl	P value	Protein function
Cathepsin D	Ctsd	IPI00111013	7.56	0.019*	Protease
Prosaposin	Psap	IPI00321190	5.67	0.0008*	Sphingolipid metabolism
Cathepsin B	Ctsb	IPI00113517	5.05	0.10	Protease
Isoform 1 of Glial fibrillary acidic protein	Gfap	IPI00117042	4.58	0.000017*	Neuroinflammation
Calnexin	Canx	IPI00119618	3.59	0.038*	ER- Protein folding
Cell cycle exit and neuronal differentiation protein 1	Cend1	IPI00122826	3.49	0.028*	Neuronal maturation
Mitogen-activated protein kinase 1	Mapk1	IPI0011966	2.88	0.045*	Signal transduction
Microtubule-actin crosslinking factor 1b	Macf1b	IPI00884482	2.68	0.094	Microtubule dynamics
Neuromodulin	Gap43	IPI00128973	2.33	0.045*	Neurite growth
Histone H2B type 1-F/J/L	Hist1h2bn	IPI00114642	1.94	0.0038*	DNA binding
Isoform 1 of Tenascin-R	Tnr	IPI00227126	1.93	0.054	Synaptic plasticity
11 kDa protein	?	IPI00329998	1.69	0.059	Unknown
Putative uncharacterized protein	?	IPI00467841	1.56	0.012*	Unknown
Glutamate dehydrogenase 1, mitochondrial	Glud1	IPI00114209	1.50	0.059	Glutamate metabolism
Peptidyl-prolyl cis-trans isomerase	Fkbp1a	IPI00554989	1.45	0.0023*	Synaptic plasticity
Creatine kinase B-type	Ckb	IPI00136703	1.32	0.048*	Energy metabolism
Isoform SNAP-25b of Synaptosomal-associated protein 25	Snap25	IPI00125635	1.29	0.084	Regulation of neurotransmitter release
Phosphatidylethanolamine-binding protein 1	Pebp1	IPI00137730	1.27	0.079	Modulation of cholinergic synapses
Aconitate hydratase, mitochondrial	Aco2	IPI00116074	1.23	0.033*	Energy metabolism
Glutamine synthetase	Glul	IPI00626790	1.22	0.034*	Glutamate metabolism
Putative uncharacterized protein Camk2a	Camk2a	IPI00420725	0.80	0.056	Calcium metabolism
Cofilin-1	Cfl1	IPI00890117	0.80	0.086	Actin organization
Thy-1 membrane glycoprotein	Thy1	IPI00109727	0.77	0.094	Neurite outgrowth

Isoform 1 of 14-3-3 protein theta	Ywhaq	IPI00408378	0.73	0.0086*	Regulation of signaling pathways
14-3-3 protein gamma	Ywhag	IPI00230707	0.72	0.059	Regulation of signaling pathways
V-type proton ATPase subunit d 1	Atp6v0d1	IPI00313841	0.72	0.1	ATPase
Isoform Long of 14-3-3 protein beta/alpha	Ywhab	IPI00230682	0.69	0.026*	Regulation of signaling pathways
Succinate dehydrogenase [ubiquinone] flavoprotein subunit, mitochondrial	Sdha	IPI00230351	0.66	0.089	Krebs cycle
Synaptophysin	Syp	IPI00123505	0.61	0.039*	Synaptic plasticity
Complexin-2	Cplx2	IPI00111501	0.60	0.047*	Formation and exocytosis of synapses vesicles
Plasma membrane calcium ATPase 1	Atp2b1	IPI00556827	0.56	0.035*	Calcium metabolism
Isoform 1 of Rab GDP dissociation inhibitor beta	Gdi2	IPI00122565	0.55	0.038*	Trafficking between organelles
Acetyl-CoA acetyltransferase, mitochondrial	Acat1	IPI00154054	0.52	0.04*	Energy metabolism
76 kDa protein	Plbd2	IPI00113584	0.51	0.0039*	Phospholipase
Isoform 1 of Adenylate kinase isoenzyme 1	Ak1	IPI00128209	0.51	0.08	Tau phosphorilation
Isoform 1 of Neurochondrin	Ncdn	IPI00331299	0.48	0.034*	Neurite outgrowth
Isoform 1 of Protein NDRG2	Ndrg2	IPI00136134	0.48	0.08	Neurogenesis
Isoform A of 1-phosphatidylinositol-4,5-bisphosphate phosphodiesterase beta-1	Plcb1	IPI00130045	0.48	0.051	Acethylcoline receptor signaling
Alpha-internexin	Ina	IPI00135965	0.45	0.0048*	Neurogenesis
Amphiphysin	Amph	IPI00400180	0.44	0.018*	Exocytosis in synapses
Syntaxin-1A	Stx1a	IPI00131618	0.42	0.014*	Role in neurotransmitter exocytosis
Isoform 1 of Microtubule-associated protein 1A	Mtap1a	IPI00408909	0.41	0.0052*	Dendrite growth
Copine-6	Cpne6	IPI00129451	0.41	0.012*	Role in synaptic plasticity
Visinin-like protein 1	Vsnl1	IPI00230418	0.40	0.052	Calcium metabolism

Adenylyl cyclase-associated protein 1	Cap1	IPI00137331	0.39	0.0014*	Filament dynamics
Isoform 1 of C-terminal-binding protein 1	Ctbp1	IPI00128155	0.38	0.057	Maintain Golgi structure
RAP1, GTP-GDP dissociation stimulator 1 isofrm b	Rap1gds1	IPI00310972	0.37	0.025*	Cell signaling
Isoform 1 of AP-2 complex subunit beta	Ap2b1	IPI00119689	0.37	0.0035*	Clathrin adaptor
NADH dehydrogenase [ubiquinone] flavoprotein 1, mitochondrial	Ndufv1	IPI00130460	0.23	0.022*	ATP synthesis
microtubule-associated protein 1B	Mtap1b	IPI00896700	0.21	0.0065*	Synaptic maturation

8. Figure Legends

Figure 1. Characterization of hippocampus abnormalities in MPS I mice. A and B) Toluidine blue stain in 8-month normal (A) and MPS I (B) mouse hippocampus indicates GAG storage in both neurons (arrowheads) and glial cells (arrows). C) Long term memory for aversive training in 6-8 months mice. Results are shown as median and percentile 25 and 75. N= 18 for normal and 13 for MPS I. *P<0.05 versus normal. C) Repeated open field test in 6-8 months mice. N= 13 for Normal and 16 for MPS I. *P<0.05, Student`s t test.

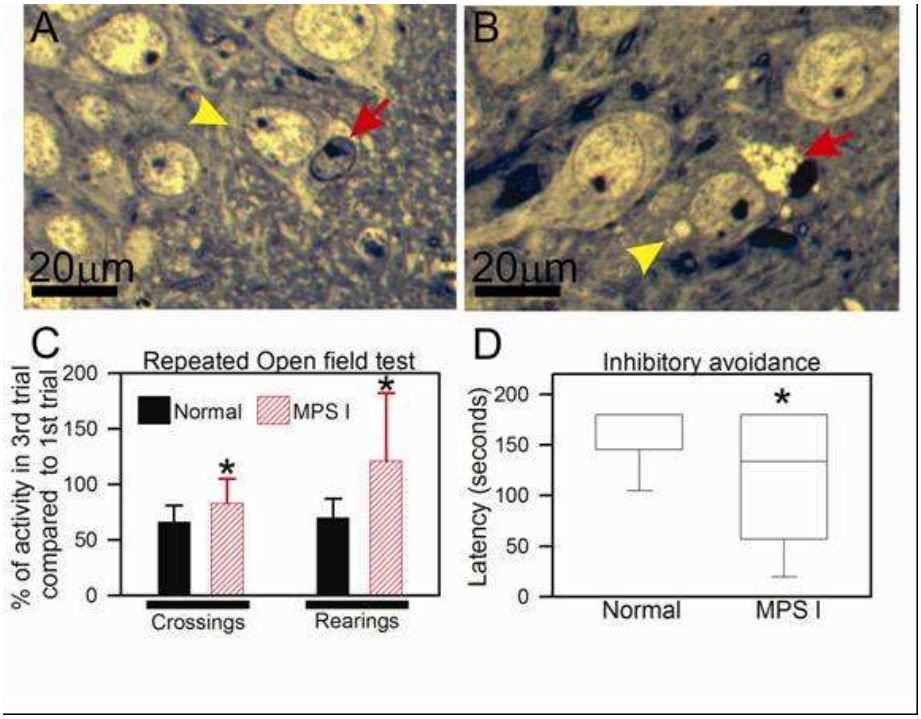

Figure 2) Cell death does not occur in MPS I mice hippocampus. A) Cathepsin D (CtsD) and cathepsin B (CtsB) activities in 8-month mice. N=5-6/ group. B) Caspase-3 activity. C and D) TUNEL stain in (C) Normal and (D) MPS I mice. Despite the increase in cathepsin activity, no cell death could be detectable in MPS I mice. *P<0.05 and **P<0.01, Student`s t test.

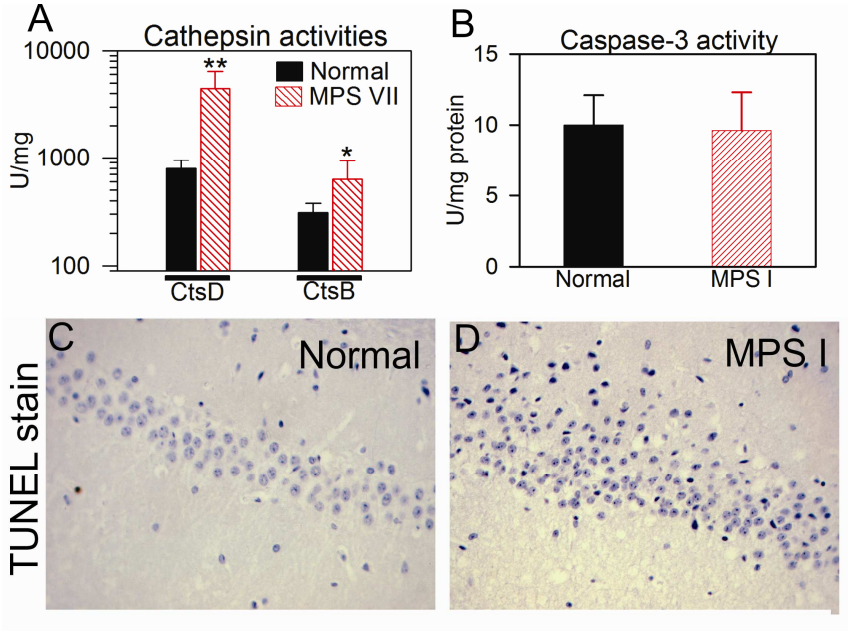

Figure 3) Assessment of neuroinflammation. A and B) Representative sections of a 8-month Normal (A) and MPS I (B) mouse hippocampus stained for GFAP. C) Results from quantification of GFAP-positive cells in 5 high-power (40X) fields. * P<0.05, Student`s t test.

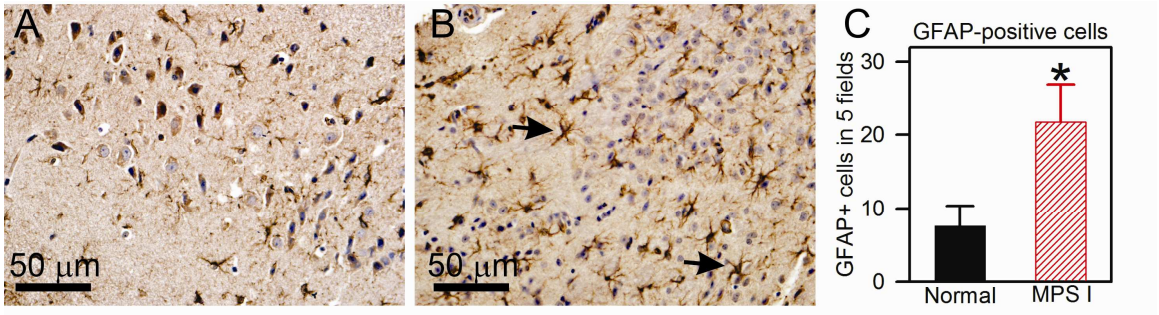

Figure 4) Western Blot analysis. Under each graph, a representative western blot from the protein being tested and the internal control (actin) is shown. A) Proteins involved in synaptic plasticity. B) Calnexin expression. C) GAP-43 expression. D) LAMP-1 expression. Ubiquitin was also tested but expression was not detectable. *P<0.05 and **P<0.01, Student`s T test.

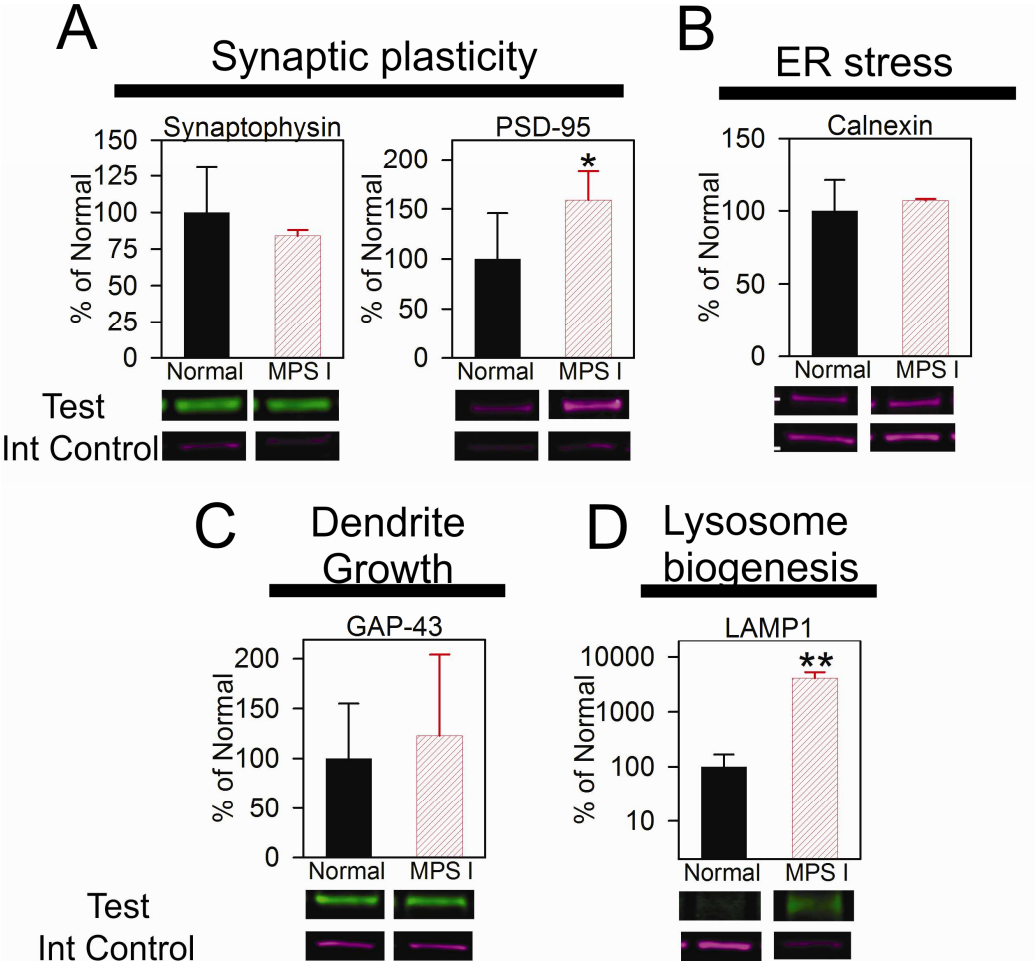

Effects of Cryopreservation and Hypothermic Storage on Cell Viability and Enzyme Activity in Recombinant Encapsulated Cells Overexpressing Alpha-L-Iduronidase

*Fabiana Quoos Mayer, *†Guilherme Baldo, *Talita Giacomet de Carvalho, *‡Valeska Lizzi Lagranha, *‡Roberto Giugliani, and *Ursula Matte

*Centro de Terapia Gênica, Centro de Pesquisas, Hospital de Clínicas de Porto Alegre; †Programa de Pós-Graduação em Ciências Biológicas: Bioquímica, Universidade Federal do Rio Grande do Sul; and ‡Programa de Pós Graduação em Genética e Biologia Molecular, Universidade Federal do Rio Grande do Sul, Porto Alegre, RS, Brazil

Abstract: Here, we show the effects of cryopreservation and hypothermic storage upon cell viability and enzyme release in alginate beads containing baby hamster kidney cells overexpressing alpha-L-iduronidase (IDUA), the enzyme deficient in mucopolysaccharidosis type I. In addi-tion, we compared two different concentrations of alginate gel (1% and 1.5%) in respect to enzyme release from the beads and their shape and integrity. Our results indicate that in both alginate concentrations, the enzyme is released in lower amounts compared with nonencapsulated cells. Alginate 1% beads presented increased levels of IDUA release, although this group presented more deformities when compared with alginate 1.5% beads. Importantly, both encapsulated groups presented higher cell viability after long cryopreservation period and hypothermic storage. In addition, alginate 1.5% beads presented higher enzyme release after freezing protocols. Taken together, our findings suggest a benefic effect of alginate upon cell viability and functionality. These results may have impor-tant application for treatment of both genetic and nonge-netic diseases using microencapsulation-based artificial organs. **Key Words:** Mucopolysaccharidosis type I—Gene therapy—Cell encapsulation—Cryopreservation—Hypothermic storage.

Mucopolysaccharidosis I (MPS I, OMIM #607014) is an autosomal recessive disorder caused by a defi-ciency of alpha-L-iduronidase (IDUA; EC 3.2.1.76), which causes storage of its substrates, dermatan sulfate and heparan sulfate (1). Current treatments for this disease are hematopoietic stem cell transplantation (HSCT) and enzyme replacement therapy (ERT), both of which are limited in their effects due to different factors. HSCT presents high morbidity and mortality and it is difficult to find a compatible donor (2). ERT does not correct the neurological symptoms as the enzyme is not able to cross the blood-brain barrier (3).

These hurdles have led researchers to develop new treatment approaches for MPS I and other related diseases (4,5), such as nonautologous somatic gene therapy, in which a cell line genetically modified to deliver a therapeutic product can be implanted in patients (6). The problem of graft rejection can be circumvented through immunoprotection with algi-nate beads. This approach has been recently applied to several situations, including MPS I and other lyso-somal storage disorders (7,8). However, it implies the need of creating reservoirs of beads to rapidly obtain the cells for transplant after a diagnosis.

The aim of this work was to evaluate the effect of cryopreservation and hypothermic storage upon cell viability and enzyme activity in alginate beads over-expressing IDUA. In addition, we compared two dif-ferent concentrations of alginate in respect to enzyme release from the beads and their shape and integrity.

MATERIALS AND METHODS

Experimental design

We performed two different encapsulated groups: Cap 1.5% (beads produced in sodium alginate at 1.5% w/v) and Cap 1% (beads produced with sodium alginate at 1% w/v). In both groups, the number of repetitions was the same ($n = 5$ wells) at different time points (30 and 90 days of cryopreservation and 24 h after hypothermic storage). All groups were analyzed before and after freezing. Control group consisted of baby hamster kidney (BHK) clones overexpressing IDUA that were not submitted to the encapsulation process ($n = 5$ wells).

Transfection of BHK cells

BHK cells were grown to about 90–95% conflu-ence in Dulbecco's Modified Eagle's Medium (DMEM) (LGC Biotecnologia, São Paulo, SP, Brazil) supplemented with 10% fetal bovine serum (FBS) (Gibco, Grand Island, NY, USA), 1% penicillin/ streptomycin (Gibco), and 2 mM L-glutamine (Gibco). The IDUA cDNA was inserted in the pREP9 plasmid (Invitrogen, Carlsbad, CA, USA) according to Camassola et al. (9) and the pR-IDUA (pREP9 plasmid with IDUA cDNA cloned down-stream the multicloning site) vector was obtained. Transfection using Lipofectamine (Invitrogen) was

doi:10.1111/j.1525-1594.2009.00880.x

Received December 2008; revised June 2009.

Address correspondence and reprint requests to Dr. Ursula Matte, Centro de Terapia Gênica, Hospital de Clínicas de Porto Alegre, Rua: Ramiro Barcelos 2350, Porto Alegre 90035-903, RS, Brazil. E-mail: umatte@hcpa.ufrgs.br

Fabiana Quoos Mayer and Guilherme Baldo both contributed equally for the manuscript.

performed for introduction of pR-IDUA vector into BHK cells. Stable clone selection was performed with 400 μg/mL of Geneticin (Invitrogen). The clones were isolated and IDUA activity was measured in the supernatant for selection of clones that were overexpressing the enzyme. A clone overexpressing IDUA was expanded using half dose of Geneticin (Invitrogen). Cells were grown under standard tissue culture conditions for later encapsulation.

Beads production and characterization

Procedures were carried out as previously described by our group (10,11) under sterile conditions. Briefly, 5 ∞ 10^5 cells/mL were mixed with 1% or 1.5% sodium alginate (Sigma-Aldrich, St. Louis, MO, USA) and extruded through an Encapsu-lation Unit, type J1 (Nisco, Zurich, Switzerland), attached to JMS Syringe Pump (Singapore). Droplets were sheared off with an air flow of 3.5 L/min deliv-ered to the tip of a 27-G needle and the rate of infusion was 40 mL/h. The droplets fell into a bath of 125 mM $CaCl_2$ and ionically cross-linked with Ca^{2+} to form solid spherical hydrogel beads containing embedded cells. In each well, beads were produced from a volume of 400 μL of cell suspension (2 ∞ 10^5 cells). The resulting beads were maintained under normal tissue culture conditions (DMEM supple-mented with 10% FBS at 37°C and 5% CO_2) for 24 h and then submitted to further procedures.

To analyze the morphology of the beads obtained with different alginate concentrations, we counted at least 500 beads under a light microscope (4∞ magnification), and classified imperfections as tailed beads, conjoined beads, or beads with irregular surface.

Enzyme assay

IDUA activity assay was performed using a fluorimetric assay where the enzyme activity is measured by the amount of substrate cleaved in 1 hour by 1 mL of media.The substrate (4-methylumbellyferyl-alpha-L-iduronide, Glycosynth, Warrington, Cheshire, UK) is an artificial substrate cleaved exclusively by IDUA (12). This test was performed in all groups before freezing or hypothermic storage and 24 h after thawing. Results were expressed as nmol/h/mL DMEM.

Cryopreservation of free and encapsulated cells

Beads were maintained in culture for 24 h. After this period, the media was collected and stored at −20°C to measure prefreezing enzyme activity. DMEM (1.5 mL) supplemented with 20% FBS and 10% DMSO was added to the beads and then they were rapidly placed into 1.8 mL freezing vials (Corning, New York, NY, USA). These vials were placed on a freezing chamber containing isopro-panol, which led to a gradual diminution of the tem-perature (−1°C/min) in a −80°C freezer for 12 h, and then the vials were placed in liquid nitrogen.

The media from nonencapsulated BHK clones was also collected 24 h after cells had been seeded (2 ∞ 10^5 cells/well). Cells were then trypsinized and submitted to the same freezing protocol.

Cell or beads thawing was performed 30 and 90 days after freezing. Vials were kept at 37°C warm bath and rapidly plated on 6-well dishes with DMEM to avoid toxicity due to DMSO. The cells and beads were washed twice with DMEM and kept in culture for 24 h.After this period, the media was collected for enzyme assay, and alginate beads were dissolved using a 100-mM sodium citrate solution for cell counting and viability.

Hypothermic storage of free and encapsulated cells

Beads were maintained in culture for 24 h after encapsulation, then the media was collected and replaced by fresh DMEM supplemented with 10% FBS and 10 mM N-2-hydroxyethylpiperazine-N′-2-ethanesulfonic (HEPES). Cells were kept at hypothermic controlled temperature (4°C) for 24 h, then the media was changed and beads were once again placed into 6-well plates containing 1.5 mL DMEM supplemented with 10% FBS for 24 h at 37°C and 5% CO_2.After this period, media was collected and beads were dissolved using a 100-mM sodium citrate solu-tion for cell counting and viability.

Nonencapsulated cells were plated at same concentration and the media was collected after 24 h. Cells were then trypsinized and centrifuged for 800 ∞ g for 10 min and stored as the other groups for 24 h. After that, cells were seeded in 6-well plates and 24 h later, media was collected, cells were trypsinized, and viability test was performed.

Cell viability

Cell viability was analyzed 24 h after beads production (before freezing) and 24 h after thawing or after hypothermic preservation. Alginate beads were dissolved using 100 mM sodium citrate solution. Cells were then centrifuged at 800 ∞ g for 10 min and diluted in phosphate buffer saline solution. Viability was assessed through the trypan blue exclusion tech-nique and analyzed under an optical microscope. Results were expressed as percentage of viable cells.

Statistical analysis

Statistical analysis were performed using Statistical Package for Social Sciences (SPSS, version 13.0, Chicago, IL, USA) using analysis of variance and

Tukey's test post hoc. Statistical differences among groups were considered for a $P < 0.05$. Differences between the encapsulated groups were analyzed using Student's *t*-test for unpaired samples. Data are presented as mean and standard deviation.

RESULTS

Clone obtention

We obtained 13 clones overexpressing IDUA. Protein overexpression ranged from twofold to almost 3000-fold the levels before transfection (data not shown). Clones overexpressing the enzyme main-tained their initial morphology. The clone with the highest enzyme level (341 nmol/h/mL) was chosen to perform subsequent experiments.

Beads characterization and enzyme release before freezing or storage

The beads' size was measured using ImageProPlus software (Media Cybernetics, Bethesda, MD, USA) in 30 beads and results indicate a mean size of 400 é 99 μm. Before freezing and storage, beads' morphology was verified and the number of beads presenting tails, conjoined beads, and beads with irregular surface were evaluated (Fig. 1). Cap 1% group presented more problems in morphology, mainly the presence of tailed beads as compared with Cap 1.5% group ($P < 0.001$). These features were not corrected when air flow was increased or reduced (data not shown). Summary of our findings are shown in Table 1.

TABLE 1. *Percentage of morphologic imperfections on alginate beads*

	Beads morphology	% deformed beads
Cap 1.5%	Conjoined	5.8 ± 3.9
	Tailed	8.8 ± 4.6
	Irregular surface	5.5 ± 3.0
Total		20.1 ± 3.0
Cap 1%	Conjoined	12.0 ± 4.9
	Tailed	26.0 ± 5.4*
	Irregular surface	7.2 ± 2.9
Total		45.2 ± 3.0*

Five hundred beads were analyzed per group.
*$P < 0.001$ compared with Cap 1.5% group. Student's *t*-test for unpaired samples.

Cell viability 24 h after encapsulation was 91.10 é 2.62% for Cap 1.5% group and 93.09 é

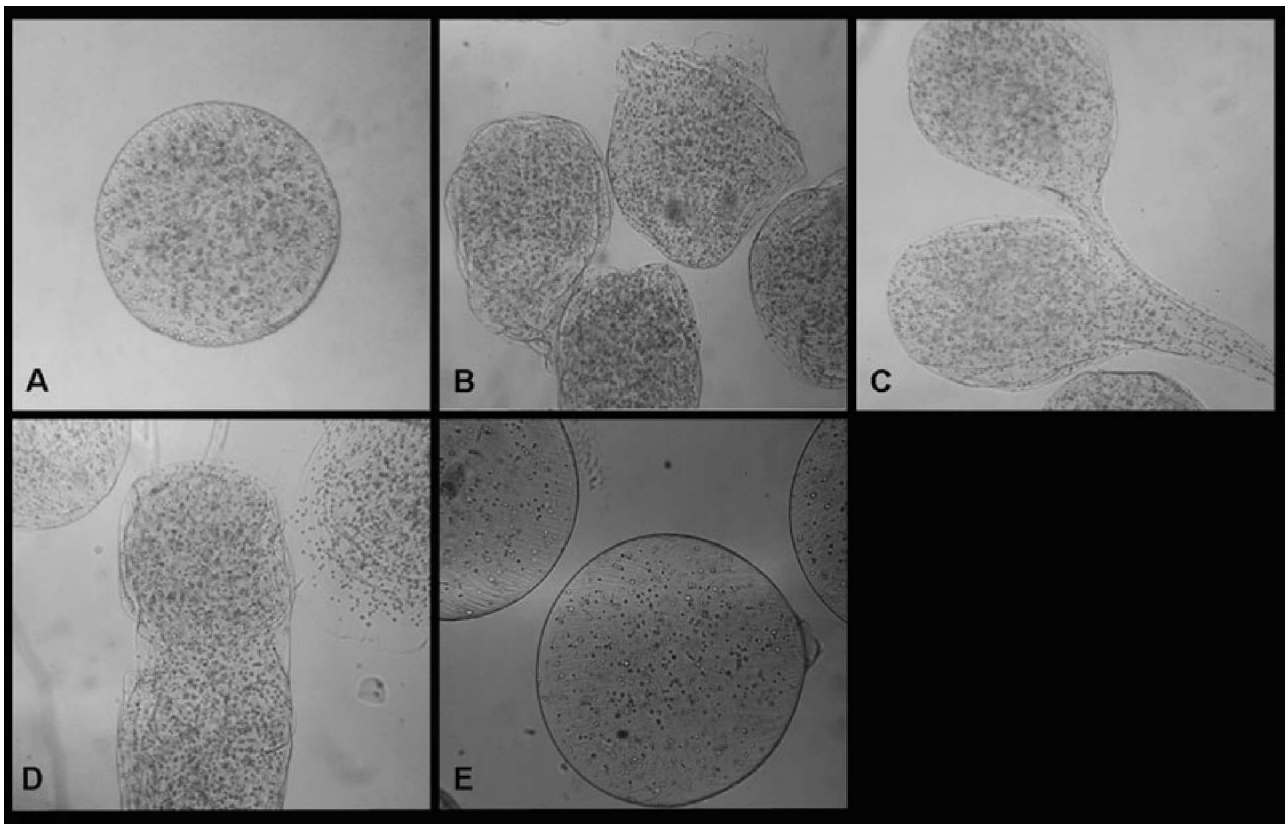

FIG. 1. Morphologic features of the alginate beads. (A) Normal morphology, with round-shaped beads. (B) Alginate beads with an irregular surface. (C) Tailed beads. (D) Conjoined beads. (E) Alginate beads after freezing procedure. Magnification—4∞.

4.60% for Cap 1% group. Nonencapsulated cells presented similar values at 24 h (95.21 é 1.83%) ($P = 0.333$ when compared with Cap 1.5% group and $P = 0.715$ when compared with Cap 1% group), indi-cating that cell viability was not altered by the encap-sulation process.

Enzyme release to the extracapsular media was also performed 24 h after encapsulation. When com-pared with nonencapsulated cells (which presented an enzyme activity of 207.0 nmol/h/mL), enzyme release was reduced approximately four times for Cap 1% group (47.75 nmol/h/mL, $P < 0.001$ com-pared with nonencapsulated cells) and about nine times for Cap 1.5% group (22.87 nmol/h/mL, $P < 0.001$ compared with nonencapsulated and $P = 0.003$ compared with Cap 1% group).

Cell viability after freezing

Control group presented a progressive reduction in cell viability after cryopreservation, with 76% cell death after 90 days. Both encapsulated groups had an initial reduction in cell viability after 30 days (54.5 and 63.2% for Cap 1% and Cap 1.5% groups, respec-tively) but differently from control group, these viability levels were maintained after 90 days (48.6 and 56.3% for Cap 1% and Cap 1.5% groups, respec-tively) (Fig. 2A). No gross alterations were observed in the beads after thawing (Fig. 1E).

Cell viability after 24 h of hypothermic storage was reduced in control group compared with prior values ($P = 0.022$) but not in Cap 1% or Cap 1.5% groups ($P = 0.136$ and $P = 0.652$, respectively) (Fig. 2B).

IDUA release after storage

Enzyme activity was measured 24 h after encapsu-lation and 24 h after thawing (or hypothermic storage). We expressed after-thawing results as per-centage from the prefreezing activity.

We were able to show that while enzyme activity did not change in the control group over time, Cap 1.5% group present the highest enzyme activity 90 days after cryopreservation ($P = 0.024$ compared with control group) (Table 2). Cap 1% group pre-sented a similar pattern to Cap 1.5% group with a tendency to be statistically different from control group after 90 days ($P = 0.057$). These data suggest a benefic effect of alginate gel upon cell function.

In hypothermic preservation experiments, control group presented no alteration in enzyme activity after storage, despite a small reduction in cell viability. Cap 1% group presented a small but not significant reduction in enzyme activity, while surpris-ingly, Cap 1.5% group presented values for IDUA activity threefold the prestorage levels ($P < 0.001$)

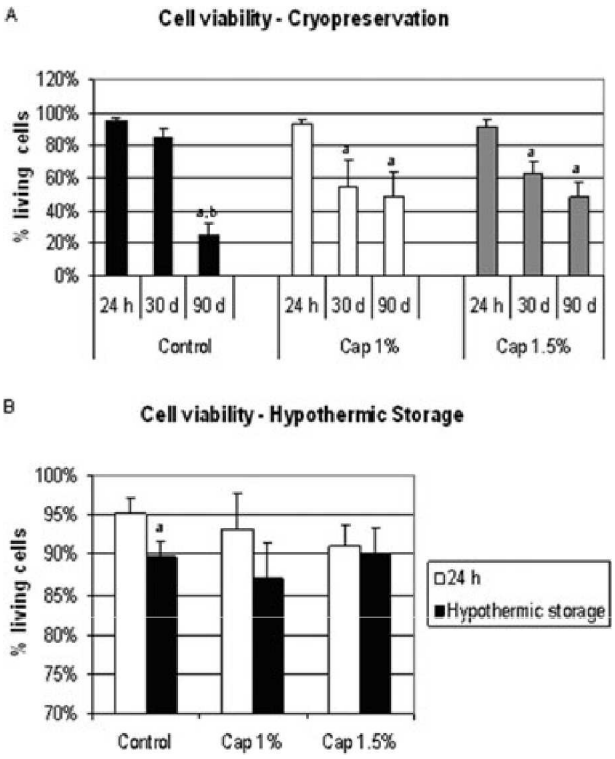

FIG. 2. (A) Cell viability analyzed by trypan blue exclusion method 24 h after encapsulation and 30 and 90 days after cryopreserva-tion ($n = 5$/group). $^{a}P < 0.05$ compared with 24 h, $^{b}P < 0.05$ com-pared with 30 days within the same group. One way ANOVA and Tukey post hoc. (B) Cell viability before and 24 h after hypothermic storage. $^{a}P = 0.022$ compared with the prestorage value within the same group. Student's *t*-test for unpaired samples. All results are expressed as mean and standard deviation.

(Table 2). These data also support a benefic effect of alginate upon cell viability and function after hypo-thermic storage.

DISCUSSION

Mucopolisaccharidosis type I is considered the prototypical lysosomal storage disorder. Current treatments are not able to correct all disease symp-toms (3); thus, new therapeutic approaches are being developed. Promising results of preclinical studies were obtained by encapsulating cells that over-express lysosomal enzymes (8). Such therapies will require protocols for rapidly obtaining a large number of functional modified cells.

In our study,we obtained a BHK clone overexpress-ing IDUA almost 3000-fold the normal levels.This cell line was chosen based on clinical phase I studies using encapsulated cell therapy (13). Two alginate concen-trations (1% and 1.5%) were tested for encapsulation purposes. The Cap 1% group presented higher enzyme release after 24 h when compared with the

TABLE 2. *Enzyme activity after 24 h of hypothermic storage and 30 and 90 days after cryopreservation*

	24 h (Hypothermic storage)	30 days	90 days
Control	109.42 ± 61.62	228.03 ± 69.76	58.86 ± 52.36
Cap 1%	74.18 ± 18.99	186.53 ± 83.17	452.86 ± 298.86
Cap 1.5%	314.72 ± 77.88*	540.91 ± 606.90	560.62 ± 290.97†

Results (n = 5/group) are expressed as percentage from prefreezing activity.
* $P < 0.001$ and † $P = 0.024$ compared with the control group within the same time point. One-way ANOVA and Tukey post hoc.

Cap 1.5% group; however, we observed an increased number of imperfections in the beads with 1% algi-nate. Changing the air flow was not able to correct these characteristics and still maintained an adequate beads size. King et al. (14) and Peirone et al. (15) showed that a homogeneous spherical shape influ-ences cell growth inside the beads,diminishing the risk of cell extravasation and beads disruption. This parameter is especially important to avoid the risk of immune activation after implanting the beads in the host organism (16).The small beads' size is also impor-tant to avoid cell death in the beads' core due to the lack of oxygen and nutrient diffusion (17).

Our results from cryopreservation studies show that cell viability 30 days postfreezing is barely decreased in the control group, while both encapsu-lation protocols lead to approximately 40% of cell death. These results indicate that, as shown by other groups (18), the encapsulation process may lead to a cell stress and loss of viability. Interestingly, cell viability results 24 h after encapsulation did not differ among the groups. A hypothesis is that although cell encapsulation does not lead to an initial cell death, it debilitates cells within the beads (18), leading to a higher cell death after 30 days of cryopreservation. Analyzing longer cryopreservation period (90 days), we noticed that cell death increased in control group but maintained similar levels to 30 days in both encapsulated groups. These results indi-cate that cell encapsulation is able to protect cells from long-term cryopreservation injury. Similar results were obtained by Aoki et al. (19), which found no decrease in the viability of encapsulated hepato-cytes 90 days after cryopreservation.

Control group did not show statistical difference in IDUA activity through time, while 90 days after cryopreservation, Cap 1.5% group demonstrated an increase in enzyme release to the extracapsular media and the Cap 1% group showed a similar pattern. One could suppose this increase to be caused by enzyme released from dead cells inside beads. However, enzyme activity from the superna-tant of free BHK clones killed by hypotonic shock was only two- to threefold higher than in live cells media (data not shown). An alternative explanation is that the alginate structure may be hampered by the cold, what would have increased the pore size and allowed for higher enzyme release. Neverthe-less, our results are strengthened by previous studies showing that although freezing procedures kill a considerable number of cells, the remaining viable cells retain their proliferative and metabolic capacity (20).

Hypothermic storage results also suggest a benefic effect from alginate on cell viability. Both encapsu-lated groups did not differ in this parameter 24 h after cold storage. On the other hand, control group presented a discrete but significant diminution in per-centage of viable cells.A similar effect was verified by Mahler et al. (18) after encapsulation and hypother-mic storage of hepatocytes. Interestingly, enzyme activity increased significantly only in the Cap 1.5% group, which may suggest that the benefits from algi-nate gel depend on its concentration.

Both cryopreservation and hypothermic storage in free cells lead to membrane damage, resulting in decreased cell viability and inducing bleb formation (21). During conventional storage conditions, the cell membrane is no longer stabilized by an extracellular matrix and this contributes to the fragilization of the outer cytoskeletal structure (22). Alginate gel avoids cell pelleting and might contribute to a stabilization of cell plasma membranes, and thus limits conse-quences of both the osmotic shock and mechanical stress during the successive pipetting. In addition, alginate gel acts as a three-dimensional scaffold for recombinant BHK cells and thus favors their survival and function (18).

Our results in the present study show that both hypothermic storage at 4°C and cryopreservation at −196°C induce cell death and that this can be signifi-cantly reduced after cell entrapment within alginate gel beads. To our knowledge, this is the first study that evaluates both storage conditions on recombinant cells for gene therapy purposes. Importantly, these results can be useful to a number of other cell types and situations, suggesting they may have important future applications in related research fields.

CONCLUSIONS

Taken together, our findings suggest a benefic effect of the encapsulation process upon cell viability and functionality. These results may have important application for treatment of both genetic and nonge-netic diseases using microencapsulation-based artifi-cial organs.

Acknowledgments: The authors are grateful to Melissa Camassola and Nance Nardi (Universidade Federal do Rio Grande do Sul, Brazil) for providing pR-IDUA plasmid.This work was supported by Insti-tutos do Milênio—Gene Therapy Network (CNPq/ MCT), and FIPE—HCPA. Fabiana Quoos Mayer is recipient of a scholarship from FAPERGS, Guil-herme Baldo and Valeska Lagranha from CAPES and CNPq.

REFERENCES

1. Neufeld EF, Muenzer J. The mucopolysaccharidosis. In: Scriver CR, Beaudet AL, Sly WS, Valle D, eds. *The Metabolic and Molecular Bases of Inherited Disease*, 8th Edition. New York: McGraw-Hill, 2001;3421–52.
2. Bonfim C, Koliski A, Bitencourt M, et al. Stem cell transplantation for inborn errors of metabolism: a single center experi-ence in 20 patients. *Acta Bioquím Clin Latinoam* 2007;1:52.
3. Pastores GM, Arn P, Beck M, et al. The MPS I registry: design, methodology, and early findings of a global disease registry for monitoring patients with mucopolysaccharidosis type I. *Mol Genet Metab* 2007;91:37–47.
4. Muñoz-Rojas MV, Vieira T, Costa R, et al. Intrathecal enzyme replacement therapy in a patient with mucopolysaccharidosis type I and symptomatic spinal cord compression. *Am J Med Genet* 2008;146A:2538–44.
5. Balestrin RC, Baldo G, Vieira MB, et al. Transient high-level expression of beta-galactosidase after transfection of fibro-blasts from GM1 gangliosidosis patients with plasmid DNA. *Braz J Med Biol Res* 2008;41:283–8.
6. Hortelano G, Al-Hendy A, Ofosu FA, Chang PL. Delivery of human factor IX in mice by encapsulated recombinant myo-blasts: a novel approach towards allogeneic gene therapy of hemophilia B. *Blood* 1996;87:5095–103.
7. Barsoum C, Milgram W, Mackay W, et al. Delivery of recom-binant gene product to canine brain with the use of microencapsulation. *J Lab Clin Med* 2003;142:399–412.
8. Ross CDJ, Bastedo L, Maier SA, Sands MS, Chang PL. Somatic gene therapy of a lysosomal storage disease, muco-polisacharidosis VII, with microencapsulated recombinant cells. *Hum Gene Ther* 2000;11:2117–27.
9. Camassola M, Braga LM, Delgado-Cañedo A, et al. Nonviral in vivo gene transfer in the mucopolysaccharidosis I murine model. *J Inherit Metab Dis* 2005;28:1035–43.
10. Bressel T, Paz AH, Baldo G, Cirne-Lima EO, Matte U, Pereira MLS. An effective device for generating alginate micro-capsules. *Genet Mol Biol* 2008;31:136–40.
11. Lagranha VL, Baldo G, de Carvalho TG, et al. In vitro correc-tion of ARSA deficiency in human skin fibroblasts from metachromatic leukodystrophy patients after treatment with microencapsulated recombinant cells. *Metab Brain Dis* 2008;23:469–84.
12. Hopwood JJ, Muller V, Smithson A, Baggett N. A fluorometric assay using 4-methylumbelliferyl alpha-L-iduronide for the estimation of alpha-L-iduronidase activity and the detection of Hurler and Scheie syndromes. *Clin Chim Acta* 1979;92:257–65.
13. Bloch J, Bachoud-Lévi AC, Déglon N, et al. Neuroprotective gene therapy for Huntington's disease, using polymer-encapsulated cells engineered to secrete human ciliary neu-rotrophic factor: results of a phase I study. *Hum Gene Ther* 2004;15:968–75.
14. King A, Sandler S, Andersson A. The effect of host factors and beads composition on the cellular overgrowth on implanted alginate beads. *J Biomed Mater Res* 2001;57:374–83.
15. Peirone MA, Delaney K, Kwiecin J, Fletch A, Chang PL. Delivery of recombinant gene product to canines with nonau-tologous microencapsulated cells. *Hum Gene Ther* 1998;9:195– 206.
16. Ponce S, Orive G, Hernández R, et al. Chemistry and the bio-logical response against immunoisolating alginate-polycation beads of different composition. *Biomaterials* 2006;27:4831–9.
17. Bazou D, Coakley WT, Hayes AJ, Jackson SK. Long-term viability and proliferation of alginate-encapsulated 3-D HepG2 aggregates formed in an ultrasound trap. *Toxicol in Vitro* 2008;22:1321–31.
18. Mahler S, Desille M, Frémond B, et al. Hypothermic storage and cryopreservation of hepatocytes: the protective effect of alginate gel against cell damages. *Cell Transplant* 2003;12:579– 92.
19. Aoki T, Koizumi T, Kobayashi Y, et al. A novel method of cryopreservation of rat and human hepatocytes by using encapsulation technique and possible use for cell trans-plantation. *Cell Transplant* 2005;14:609–20.
20. Read TA, Stensvaag V, Vindenes H, Ulvestad E, Bjerkvig R, Thorsen F. Cells encapsulated in alginate: a potential system for delivery of recombinant proteins to malignant brain tumours. *Int J Dev Neurosci* 1999;17:653–63.
21. Rauen U, Polzar B, Stephan H, Mannherz HG. Cold-induced apoptosis in cultured hepatocytes and liver endothelial cells: mediation by reactive oxygen species. *FASEB J* 1999;13:155– 68.
22. McKay GC, Henderson C, Goldie E, Connel G, Westmoreland C, Grant MH. Cryopreservation of rat hepatocyte monolayers: cell viability and cytochrome P450 content in post-thaw cultures. *Toxicol in Vitro* 2002;16:1671–9.

Original Paper

Cells Tissues Organs

Cells Tissues Organs 2012;195:323–329
DOI: 10.1159/000327532

Accepted after revision: March 15, 2011
Published online: July 19, 2011

Recombinant Encapsulated Cells Overexpressing Alpha-L-Iduronidase Correct Enzyme Deficiency in Human Mucopolysaccharidosis Type I Cells

Guilherme Baldo [a, c] Fabiana Quoos Mayer [a, d] Maira Burin [b]
Joaquín Carrillo-Farga [e] Ursula Matte [a, d] Roberto Giugliani [a, c, d]

[a] Gene Therapy Center and [b] Medical Genetics Service, Hospital de Clinicas de Porto Alegre, and Post Graduation Programs in [c] Biochemistry and [d] Genetics and Molecular Biology, Universidade Federal do Rio Grande do Sul, Porto Alegre, Brazil; [e] Institute of Hemopathology, México City, México

Key Words

Mucopolysaccharidosis type I ₃ Cell encapsulation ₃ Cryopreservation ₃ Gene therapy ₃ Mannose-6-phosphate receptor

Abstract

Mucopolysaccharidosis I (MPS I) is an autosomal recessive lysosomal storage disease due to deficient α-L-iduronidase (IDUA) activity. It results in the accumulation of the glycosaminoglycans (GAGs) heparan and dermatan sulfate and leads to several clinical manifestations. Available treatments are limited in their efficacy to treat some aspects of the disease. Thus, new approaches have been studied for the treatment of MPS I. Here, we tested the ability of recombinant baby hamster kidney cells transfected with human IDUA cDNA in correcting skin fibroblasts from MPS I patients in vitro. Our results showed an increase in IDUA activity in MPS I fibroblasts after 15, 30 and 45 days of coculture with the capsules. Cytological analysis showed a marked reduction in GAG storage within MPS I cells. Enzyme uptake by the fibroblasts was blocked in a dose-dependent manner with mannose-6-phosphate (M6P), indicating that cells use the M6P receptor to internalize the recombinant enzyme. Capsules were effective in correcting MPS I cells even after a 12-month period of cryopreservation. Taken together, our results indicate that cell encapsulation is a potential approach for treatment of MPS I. This approach becomes particularly interesting as a complementary approach, since the capsules could be implanted in sites which current treatments available are not able to reach. Future studies will focus on the efficacy of this approach in vivo.

Abbreviations used in this paper

BHK	baby hamster kidney
ERT	enzyme replacement therapy
GAGs	glycosaminoglycans
IDUA	α-L-iduronidase
M6P	mannose-6-phosphate
MPS I	mucopolysaccharidosis type I

Introduction

Mucopolysaccharidosis I (MPS I, OMIM No. 607014) is an autosomal recessive lysosomal storage disease due to deficient −-L-iduronidase (IDUA; EC 3.2.1.76) activity and results in the accumulation of the glycosaminogly-cans (GAGs) heparan and dermatan sulfate. It leads to sev-eral clinical manifestations including stiff joints, coarse facial features, visual impairment, deafness, cardiac valve disease and mental retardation [Martins et al., 2009].

Available treatments for MPS I patients include enzyme replacement therapy (ERT) and hematopoietic stem cell transplantation. Both are limited in their effect since intravenous ERT does not cross the blood-brain barrier, thus not correcting the neurological disease, and hematopoietic stem cell transplantation needs to be per-formed early in life and is associated with high morbidity and mortality [Lange et al., 2006].

Despite some advances, delivery of the enzyme into organs which are difficult to reach is still one of the major challenges. In this context, cell encapsulation is an interesting option, since isolation of cells in polymers such as calcium alginate prevents contact of host immune cells with the genetically engineered cells, and these devices can be surgically implanted in situ and deliver constant amounts of the enzyme for prolonged periods of time, as a somatic non-autologous gene therapy approach [Orive et al., 2004]. Taking that into account, we developed a proof-of-concept study verifying the ability of semi-permeable alginate microcapsules with modified cells that secrete large amounts of IDUA to correct in vitro skin fibroblasts from MPS I patients. We also tested mechanisms of enzyme uptake into cells and the possibility of using the capsules after cryopreserving them for 12 months.

Material and Methods

Transfection of Baby Hamster Kidney Cells

Baby hamster kidney (BHK) cells were transfected by lipofection using pR-IDUA cDNA, as we have previously described [Mayer et al., 2010]. Stable clone selection was performed with 400 0g/ml of Geneticin^{TM} (Invitrogen, USA). The clones were isolated and IDUA activity was measured in the supernatant for a selec-tion of clones that were overexpressing the enzyme. A clone over-expressing IDUA was expanded using half the dose of Geneticin. Cells were grown under standard tissue culture conditions for later encapsulation.

Cell Encapsulation

Cells were mixed with 1.5% sodium alginate (Sigma-Aldrich, USA) in DMEM (Invitrogen) at 5 ! 10^5 cells/ml and extruded through a encapsulation unit, type J1 (Nisco, Switzerland), attached to a JMS Syringe Pump (Singapore). Droplets were sheared off with an air flow of 3.5 l/min delivered to the tip of a 27-gauge needle, and the rate of infusion was 40 ml/h [Bressel et al., 2008; Lagranha et al., 2008]. The droplets fell into a bath of 125 mM $CaCl_2$ and ionically cross-linked with Ca^{2+} to form solid spherical hydrogel beads containing embedded cells. In each well, capsules were produced from a volume of 400 0l of cell suspension, thus containing 2 ! 10^5 cells. Cell encapsulation was carried out under sterile conditions. The resulting capsules were maintained in 6-well plates under normal tissue culture conditions (DMEM supplemented with 10% FBS at 37°C and 5% CO_2), with medium changed twice a week.

Cell Viability and Counting

To estimate cell growth and viability, capsules (n = 3–5 wells/group) were dissolved with sodium citrate (Sigma-Aldrich) 40 mM, and cells were counted every week for 1 month after encapsulation. Cell viability (expressed as percentage of viable cells) and counting (number of cells) was performed using the Trypan blue exclusion test. The supernatant was collected from 3 wells at 24 h, 1, 2 and 4 weeks after encapsulation to determine IDUA secretion from the capsules.

Capsules and MPS I Fibroblast Coculture

Skin fibroblasts from patients biochemically diagnosed with MPS I were obtained from the Medical Genetics Service at Hospital de Clínicas de Porto Alegre and were expanded in DMEM, 10% FBS (Cultilab, Brazil), 1% penicillin/streptomycin, at 37°C in a humidified 5% CO_2 incubator. Fibroblasts (2 ! 10^5 cells) were seeded in 6-well plates and 24 h later cocultured with the obtained capsules (2 ! 10^5 encapsulated cells) in the same culture condi-tions described. The medium was changed twice a week and fi-broblasts were collected after 2, 4 and 6 weeks of coculture (n = 3–6 wells/time). For fibroblast collection, the medium was aspi-rated, and each well was carefully washed with 2 ml of PBS to re-move the microcapsules. After removing the capsules, cells were trypsinized, centrifuged and stored in a –20°C freezer for the en-zyme assay.

Enzyme Assay

The IDUA activity assay was performed using a fluorimetric assay [Hopwood et al., 1979]. Results were expressed as nmol/h/ ml DMEM in the supernatant and as nmol/h/mg protein in the fibroblasts. Protein content was measured by the method of Lowry.

Analysis of Intracellular GAG Storage

GAG storage was analyzed in untreated fibroblasts as well as in cells cocultured for 45 days using Wright's staining (Sigma-Aldrich). Cells were cultured for 6 weeks, fixed in methanol and stained according to Carrillo-Farga et al. [1997]. Results were analyzed by a trained pathologist, blinded to the treatment groups. Pictures were taken with an Olympus photomicroscope (model AX70) and Olympus DP70, 12MP digital camera.

Mechanism of Enzyme Uptake by Cells

Since most lysosomal enzymes are taken up by the mannose or the mannose-6-phosphate (M6P) receptors, capsules and MPS I fibroblasts were cocultured for 24 h in the presence of mannose or M6P (0.5 or 1.5 mM, respectively; Sigma-Aldrich). Cells were

harvested and IDUA activity in fibroblasts was measured and re-sults were compared to a control group (cocultured cells in the absence of both sugars).

Cryopreservation and Thawing of Encapsulated Cells

In another experiment, capsules (2 ! 10^5 cells/well, n = 4 wells) produced were maintained in culture for 24 h and DMEM (1.5 ml) supplemented with 20% FBS, and 10% DMSO was added to the capsules, and they were rapidly placed into 1.8-ml freezing vials. These vials were placed in a freezing chamber containing isopropanol which led to a gradual decrease in temperature (–1°C/ min) in a –80°C freezer for 12 h. After that, vials were placed in liquid nitrogen. After 12 months, capsules were thawed, kept in culture for 24 h (10% FBS in DMEM) and then cocultured with MPS I fibroblasts at the same conditions as described above to verify if encapsulated cells could be efficiently cryopreserved and still be able to cross-correct MPS I cells.

Ethics and Statistics

Differences among groups were determined using the Statisti-cal Package for Social Sciences (SPSS, version 16.0). Student's t test or one-way ANOVA and the post-hoc Tukey test were used for statistical analysis depending on the experiment, with p ! 0.05 being considered statistically significant. The study was approved by the Ethics Committee of Hospital de Clínicas de Porto Alegre (study No. 05-516). As the study was performed on unidentified samples, the ethics committee waived the need for informed con-sent.

Results

Growth, Viability and Enzyme Release from Encapsulated Cells

We were able to obtain a clone that overexpresses IDUA. Capsules produced were round shaped, with en-trapped cells inside (fig. 1a). We evaluated the kinetics of cell growth, viability and enzyme release from the cap-sules for 4 weeks. The doubling time of the encapsulated cells was reached after 4 weeks of treatment. Cell viabil-ity remained always above 90%, with no modifications over time (fig. 1b). Enzyme release was lower 24 h after encapsulation (16.2 8 8.0 nmol/h/ml), increased after the first week (78.8 8 38.7 nmol/h/ml; p = 0.066) and remained almost constant until the 4th week (89.1 8 20.0 nmol/h/ml; p = 0.032; fig. 1c).

Coculture of Encapsulated Cells Reestablish IDUA Activity in MPS I Fibroblasts

Next, we analyzed if the enzyme released from the capsules could be taken up by IDUA-deficient skin fibro-blasts. Ratios of 1:5, 1:1 and 5:1 of fibroblasts/encapsu-lated clones were tested in a pilot study (24 h of coculture), and we found a similar increase in enzyme activity at all

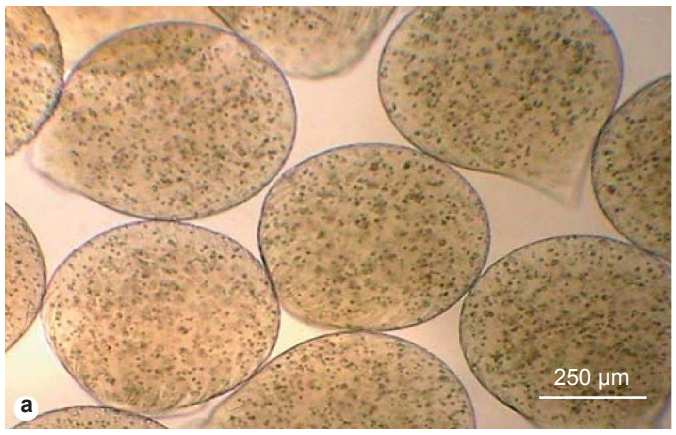

Fig. 1. Characteristics of the capsules produced. **a** Round-shaped morphology of the alginate microcapsules containing cells over-expressing IDUA. **b** Cell growth and viability in the capsules in the first 4 weeks in vitro. **c** IDUA release from the capsules mea-sured in the supernatant 24 h, 1, 2 and 4 weeks after capsule pro-duction. *p ! 0.05 compared to 24 h, ANOVA and Tukey post hoc test.

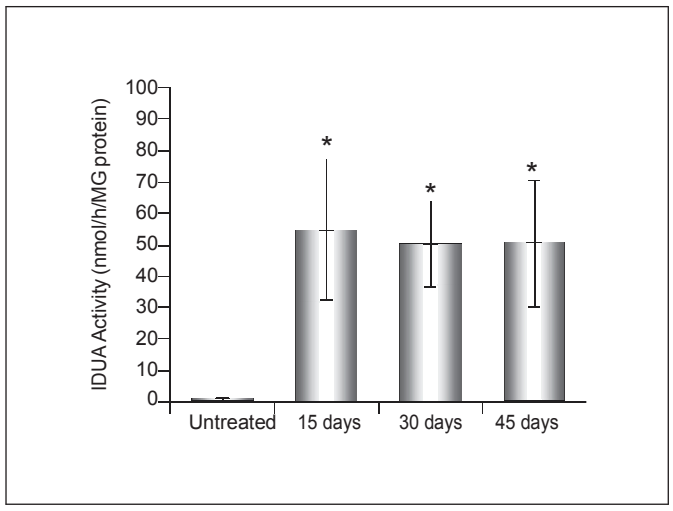

Fig. 2. IDUA activity in nmol/h/mg protein in MPS I fibroblasts (n = 3–6 wells/time) after different time periods of coculture with microcapsules. *p ! 0.05 compared to untreated cells, ANOVA and Tukey post hoc test. IDUA activity in normal fibroblasts is 60–120 nmol/h/mg protein.

ratios (data not shown). Therefore, we chose a 1: 1 ratio to perform the long-term experiments. IDUA activity in un-treated cells was almost zero (0.53 8 0.28 nmol/h/mg protein), while a marked increase (95- to 103-fold the un-treated values) could be observed after 2, 4 and 6 weeks of coculture (p ! 0.01, compared to untreated cells). Dif-ferences among treatment times were not observed (fig.2).

Reversal of GAG Storage in MPS I Cells

MPS-I-treated and -untreated cells were maintained for 45 days, fixed and analyzed for GAG content using Wright's staining. Numerous punctuated cherry-red structures could be visualized in the untreated cells, cor-responding to lysosomes with undegraded GAGs (fig. 3a, b). Those structures were not seen in treated cells (fig. 3c, d), indicating that the enzyme was not only taken up, but reached the lysosomes and had activity over the unde-graded material.

Recombinant IDUA Is Taken Up by the M6P Receptor

We next analyzed the mechanism of enzyme uptake by the skin fibroblasts. When adding M6P to the media, a progressive decrease in IDUA uptake by the cells could be observed compared to the control group (cocultured cells without M6P in the media), being statistically sig-nificant at an 1.5-mM dose (p = 0.03). We were not able to detect differences in enzyme uptake when adding man-nose to the media, indicating that the uptake of the en-zyme produced by the capsules is M6P receptor depen-dent (fig.4).

Cryopreserved Capsules Are Able to Correct Enzyme Deficiency

We have previously shown that encapsulated cells overexpressing IDUA can be effectively cryopreserved, maintaining cell viability around 55% and still secrete significant amounts of enzyme [Mayer et al., 2010]. Therefore, we aimed to verify if after a long cryopreserva-tion period (1 year) the cells could still secrete the enzyme and correct MPS I fibroblasts. Enzyme activity in MPS I fibroblasts after 15 days of coculture was significantly higher than in untreated ones (p ! 0.01; fig.5), indicating that cells are viable and secreting the enzyme, which is being taken up by the deficient cells. Cell viability was 64.5 8 5.5%.

Discussion

Treatment options currently available for MPS I have been shown to be very ineffective in treating some aspects of the disease, including the aorta, bone, joint and brain [Ma et al., 2008; Wraith, 2009]. Reaching these organs is imperative to improve the quality of life in MPS I pa-tients. Therefore, new or complementary approaches must be developed. In the last years, some alternatives to intrathecal ERT have emerged as a complementary ap-proach [Munoz-Rojas et al., 2008], but its efficacy is still uncertain, and the need of repeated infusions still per-sists.

In this study, we produced microcapsules that secrete high amounts of IDUA and correct the enzyme deficien-cy of human MPS I skin fibroblasts after coculture. We have chosen to transfect BHK cells with the pR-IDUA plasmid since this cell line has been successfully used in clinical trials for Huntington's disease [Bloch et al., 2004], in which cells were implanted in 1 ventricle of pa-tients for up to 6 months. Besides, the glycosylation pat-tern is similar to humans. On the other hand, the pR-IDUA plasmid is a pREP9-derived construction, which is a nonintegrative vector capable of autonomous repli-cation in recipient cells [Yang et al., 1996]. The plasmid led to a stable production and secretion of IDUA from the capsules on the period analyzed. This is an impor-tant aspect since the use of a non-viral vector is safer when compared to cell transduction with viral vectors

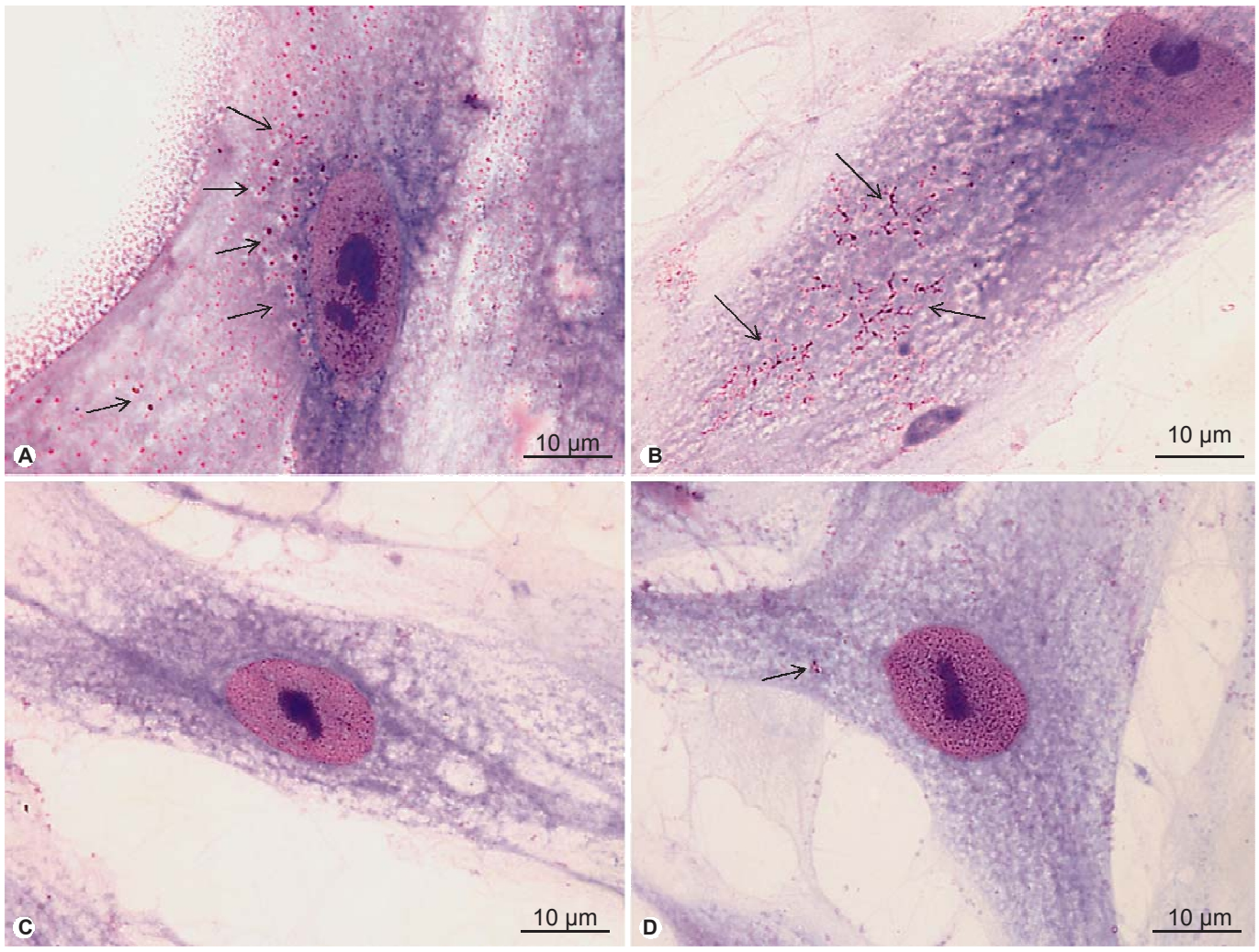

Fig. 3. GAG storage in MPS I fibroblasts before (**a**, **b**) and after 45 days of coculture with the capsules (**c**, **d**) us-ing Wright staining. GAGs are shown as abundant magenta (metachromatic) dots within the MPS cells, almost undetectable in the treated fibroblasts (arrows).

previously used to correct lysosomal storage disorders [Nakama et al., 2006]. Although a surgical procedure would be required for capsule implantation, it potential-ly provides benefits for much longer than a regular in-tratechal ERT, which was performed in patients once a month.

Cells within the capsules grew much slower than free BHK cells, reaching its doubling time after 4 weeks in vitro, versus less than 24 h in free BHK cells [Charp et al., 1983]. The growth delay probably occurs due to a re-duced space for the entrapped cell within the capsule and is of major importance, since cell overgrowth can damage the capsule structure and could lead to cell extravasations from the biomaterial [Lagranha et al., 2008]. Future studies will focus on evaluating the growth rate of the encapsulated cells in vivo. Enzyme activity pre-sented elevated levels at all times analyzed except for 24 h, probably because the encapsulation process debili-tates the cells, which recover their metabolic activity af-ter a few days in culture. Another possibility is that al-though the enzyme is being constantly produced, it might take a little longer for a relatively high molecular weight enzyme as IDUA (69 kDa) to escape from the cap-sule pores.

Our results show that the enzyme could be incorporated into MPS I fibroblasts via M6P receptors in a dose-

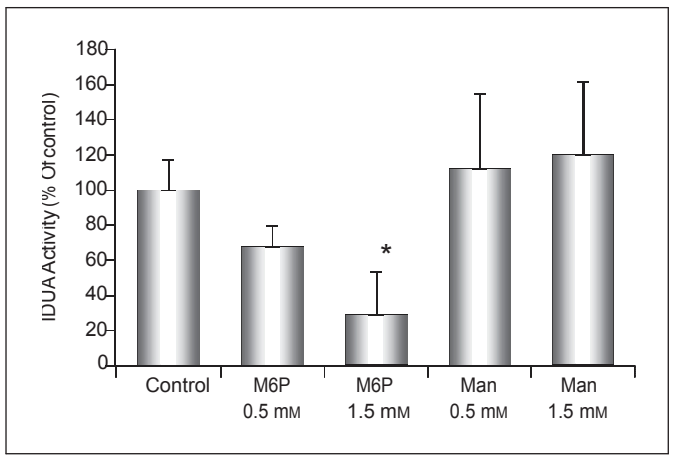

Fig. 4. Mechanism of IDUA entry in the MPS I fibroblasts. Cells were treated with 0.5 or 1.5 mM of mannose (Man) or M6P. IDUA activity was measured 24 h after coculture with the capsules. Results are expressed as percentage of activity compared to the con-trol group (cocultured cells without adding any of the sugars; n = 4–5 wells/group). *p ! 0.05 compared to the control and mannose groups, ANOVA and Tukey post hoc test.

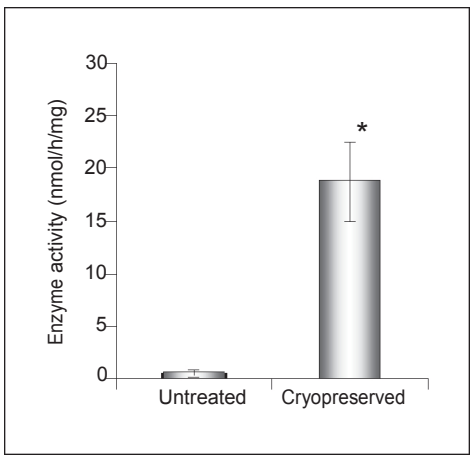

Fig. 5. IDUA activity in MPS I patient fibroblasts treated for 2 weeks with capsules previously cryopreserved for 12 months and untreated cells (n = 4 wells/group). Activity was expressed as nmol/h/mg protein. *p ! 0.01 compared to the untreated group, Student's t test.

dependent manner. Previous reports have shown that the recombinant enzyme commercially available for ERT is taken up mainly by M6P, although mannose receptors also play a small role in this process [Tsukimura et al., 2008]. In our study, we were not able to verify any inhibi-tion in enzyme uptake when mannose was added to the media. Although our results seem to point to a unique mechanism of enzyme uptake in fibroblasts, we cannot exclude the possibility that a percentage of the enzyme could also be taken up by the mannose receptor in other cell types, since distribution of the mannose and the M6P receptor and their relative abundance in tissues affect which cells will be targeted by the available enzyme [Sands et al., 2001]. Also, the extent to which the oligosac-charides are processed from high mannose to complex-type oligosaccharides might lead to an enzyme uptake by one or the other receptor [Sly et al., 2006].

GAG analysis showed a reduction in the accumulated substrate within cells, and together with results from IDUA activity, it confirms that the enzyme produced by the BHK cells is being taken up and processed into its mature form, transported to lysosomes, reducing storage within cells.

Going one step further, for this approach to be clinically relevant, it would be necessary to create reservoirs of capsules to rapidly obtain the cells for transplant after a diagnosis. Therefore, we verified if the capsules produced could be cryopreserved and still retain their ability to correct MPS I cells after thawing. Cross-correction of MPS I fibroblasts was achieved, although the enzyme lev-els were only about 40% from those obtained in freshly made capsules. Our cell viability results indicate a cell loss of 35%, suggesting that the lower level of enzyme ob-tained could be mostly due to cell death within the cap-sules, but also due to a reduction in the levels of enzyme released from the remaining cells.

In this study, we were able to produce a clone that over-expresses IDUA and, after encapsulation in alginate mi-crocapsules, corrects MPS I human skin fibroblasts. These capsules can be surgically implanted in sites which are difficult to reach such as the brain of animal models and could then be tested in clinical trials, hopefully turn-ing into a new approach for the treatment of MPS I and other lysosomal storage disorders.

Aknowledgements

This work was supported by CNPq-Gene Therapy Network and FIPE-HCPA. G.B. and F.Q.M. are recipients of CNPq scholar-ships.

References

Bloch, J., A.C. Bachoud-Lévi, N. Déglon, J.P. Lefaucheur, L. Winkel, S. Palfi, J.P. Nguyen, C. Bourdet, V. Gaura, P. Remy, P. Brugières, M.F. Boisse, S. Baudic, P. Cesaro, P. Hant-raye, P. Aebischer, M. Peschanski (2004) Neuroprotective gene therapy for Hunting-ton's disease, using polymer-encapsulated cells engineered to secrete human ciliary neurotrophic factor: results of a phase I study. Hum Gene Ther *15:* 968–975.

Bressel, T., A.H. Paz, G. Baldo, E.O. Cirne-Lima, U. Matte, M.L.S. Pereira (2008) An effective device for generating alginate microcap-sules. Genet Mol Biol *31:* 136–140.

Carrillo-Farga, J., M.A. Acosta-Barreda, M.E. Gomez-Ruiz, E. Monterrubio, R. Pérez-Landa (1997) El diagnóstico de enfermedades lisosomales hereditarias por morfología de células hematopoyéticas. Rev Mex Patol Clin *44:* 222–232.

Charp, P.A., R.J. Kinders, T.C. Johnson (1983) G2 cell cycle arrest induced by glycopeptides isolated from the bovine cerebral cortex. J Cell Biol *97:* 311–316.

Hopwood, J.J., V. Muller, A. Smithson, N. Baggett (1979) A fluorometric assay using 4-methy-lumbelliferyl alpha-L-iduronide for the esti-mation of alpha-L-iduronidase activity and the detection of Hurler and Scheie syndromes. Clin Chim Acta *92:* 257–265.

Lagranha, V.L., G. Baldo, T.G. de Carvalho, M. Burin, M.L. Saraiva-Pereira, U. Matte, R. Giugliani (2008) In vitro correction of ARSA deficiency in human skin fibroblasts from metachromatic leukodystrophy pa-tients after treatment with microencapsulat-ed recombinant cells. Metab Brain Dis *23:* 469–484.

Lange, M.C., H.A. Teive, A.R. Troiano, M. Bitencourt, V.A. Funke, D.C. Setúbal, J. Zanis Neto, C.R. Medeiros, L.C. Werneck, R. Pasquini, C.M. Bonfim (2006) Bone marrow transplantation in patients with storage diseases: a developing country experience. Arq Neuropsiquiatr *64:* 1–4.

Ma, X., M. Tittiger, R.H. Knutsen, A. Kovacs, L. Schaller, R.P. Mecham, K.P. Ponder (2008) Upregulation of elastase proteins results in aortic dilatation in mucopolysaccharidosis I mice. Mol Genet Metab *94:* 298–304.

Martins, A.M., A.P. Dualibi, D. Norato, E.T. Takata, E.S. Santos, E.R. Valadares, G. Porta, G. de Luca, G. Moreira, H. Pimentel, J. Coel-ho, J.M. Brum, J. Semionato Filho, M.S. Kerstenetzky, M.R. Guimarães, M.V. Rojas, P.C. Aranda, R.F. Pires, R.G. Faria, R.M. Mota, U. Matte, Z.C. Guedes (2009) Guide-lines for the management of mucopolysac-charidosis type I. J Pediatr *155:* S32–S46.

Mayer, F.Q., G. Baldo, T.G. de Carvalho, V.L. La-granha, R. Giugliani, U. Matte (2010) Effects of cryopreservation and hypothermic stor-age on cell viability and enzyme activity in recombinant encapsulated cells overexpress-ing alpha-L-iduronidase. Artif Organs *34:* 434–439.

Munoz-Rojas, M.V., T. Vieira, R. Costa, S. Fagondes, A. John, L.B. Jardim, L.M. Vedolin, M. Raymundo, P.I. Dickson, E. Kakkis, R. Giugliani (2008) Intrathecal enzyme replacement therapy in a patient with mucopolysaccharidosis type I and symptomatic spinal cord compression. Am J Med Genet A *146A:* 2538–2544.

Nakama, H., K. Ohsugi, T. Otsuki, I. Date, M. Kosuga, T. Okuyama, N. Sakuragawa (2006) Encapsulation cell therapy for mucopolysaccharidosis type VII using genetically engineered immortalized human amniotic epi-thelial cells. Tohoku J Exp Med *209:* 23–32.

Orive, G., R.M. Hernández, A. Rodríguez Gascón, R. Calafiore, T.M. Chang, P. de Vos, G. Hortelano, D. Hunkeler, I. Lacík, J.L. Pedraz (2004) History, challenges and perspectives of cell microencapsulation. Trends Biotechnol *22:* 87–92.

Sands, M.S., C.A. Vogler, K.K. Ohlemiller, M.S. Roberts, J.H. Grubb, B. Levy, W.S. Sly (2001) Biodistribution, kinetics, and efficacy of highly phosphorylated and non-phosphory-lated beta-glucuronidase in the murine model of mucopolysaccharidosis VII. J Biol Chem *276:* 43160–43165.

Sly, W.S., C. Vogler, J.H. Grubb, B. Levy, N. Gal-vin, Y. Tan, T. Nishioka, S. Tomatsu (2006) Enzyme therapy in mannose receptor-null mucopolysaccharidosis VII mice defines roles for the mannose 6-phosphate and man-nose receptors. Proc Natl Acad Sci USA *103:* 15172–15177.

Tsukimura, T., Y. Tajima, I. Kawashima, T. Fukushige, T. Kanzaki, T. Kanekura, M. Ikekita, K. Sugawara, T. Suzuki, T. Togawa, H. Sakuraba (2008) Uptake of a recombinant human alpha-L-iduronidase (laronidase) by cultured fibroblasts and osteoblasts. Biol Pharm Bull *31:* 1691–1695.

Wraith, J.E. (2009) Enzyme replacement therapy for the management of the mucopolysac-charidoses. Int J Clin Pharmacol Ther *47:* S63–S65.

Yang, R.Y., D.K. Hsu, F.T. Liu (1996) Expression of galectin-3 modulates T-cell growth and apoptosis. Proc Natl Acad Sci USA *93:* 6737– 6742.

Cytotherapy, 2012; Early Online: 1–8

informa
healthcare

Intraperitoneal implant of recombinant encapsulated cells overexpressing alpha-L-iduronidase partially corrects visceral pathology in mucopolysaccharidosis type I mice

GUILHERME BALDO[1,2], FABIANA QUOOS MAYER[1,3], BARBARA MARTINELLI[1], FABIOLA SCHONS MEYER[4], MAIRA BURIN[5], LUISE MEURER[6], ANGELA MARIA VICENTE TAVARES[7], ROBERTO GIUGLIANI[1,2,3,5] & URSULA MATTE[1,3]

[1]*Centro de Terapia Gênica–Hospital de Cliniças de Porto Alegre, RS, Brazil,* [2]*Programa de Pos-Graduacao em Ciencias Biologicas: Bioquimica, UFRGS, RS, Brazil,* [3]*Programa de Pós–Graduação em Genética e Biologia Molecular, UFRGS, RS, Brazil,* [4]*Unidade de Experimentação Animal, Hospital de Clinicas de Porto Alegre, RS, Brazil,* [5]*Serviço de Genética Medica–Hospital de Clinicas de Porto Alegre, RS, Brazil,* [6]*Unidade de Patologia Experimental, Hospital de Clinicas de Porto Alegre, RS, Brazil, and* [7]*Programa de Pós–Graduação em Fisiologia, UFRGS, RS, Brazil*

Abstract

Background aims. Mucopolysaccharidosis type I (MPS I) is characterized by deficiency of the enzyme alpha-L-iduronidase (IDUA) and storage of glycosaminoglycans (GAG) in several tissues. Current available treatments present limitations, thus the search for new therapies. Encapsulation of recombinant cells within polymeric structures combines gene and cell therapy and is a promising approach for treating MPS I. *Methods.* We produced alginate microcapsules containing baby hamster kid-ney (BHK) cells overexpressing IDUA and implanted these capsules in the peritoneum of MPS I mice. *Results.* An increase in serum and tissue IDUA activity was observed at early time-points, as well as a reduction in GAG storage; however, cor-rection in the long term was only partially achieved, with a drop in the IDUA activity being observed a few weeks after the implant. Analysis of the capsules obtained from the peritoneum revealed inflammation and a pericapsular fibrotic process, which could be responsible for the reduction in IDUA levels observed in the long term. In addition, treated mice developed antibodies against the enzyme. *Conclusions.* The results suggest that the encapsulation process is effective in the short term but improvements must be achieved in order to reduce the immune response and reach a stable correction.

Key Words: *alginate microcapsules, cell encapsulation, cell therapy, gene therapy, Hurler syndrome, mucopolysaccharidosis type I*

Introduction

Mucopolysaccharidosis type I (MPS I) is a lysosomal storage disorder caused by mutations in the gene that encodes the enzyme alpha-L-iduronidase (IDUA), which is involved in the degradation of the glycosaminoglycans (GAG) heparan sulfate and dermatan sulfate, leading to multisystemic abnormalities (1). Among the current treatments available for MPS I, hematopoietic stem cell transplantation (HSCT), which needs to be performed early in life, is only partially effective (2) and is associated with morbidity and mortality (3). Enzyme replacement therapy (ERT) is another option, but the enzyme does not reach several organs affected by the disease, including the brain and heart valves (4). Also, the high cost of ERT and the need for weekly infusions indicates the need for better therapies for this condition, which could be used alone or in combination with the existing therapies (5). Both ERT and HSCT are based on the properties of lysosomal enzymes, to be secreted and taken up by neighboring cells via the mannose-6-phosphate (M6P) receptor. Based on that, gene therapy has been developed in pre-clinical studies (6) but no clinical trials have been conducted so far.

Cell encapsulation is an interesting approach for treating lysosomal storage disorders. with this approach, genetically modified cells that overexpress the enzyme are encapsulated into semi-permeable microcapsules, which can then be implanted into different sites in the host organism. The enzyme produced can be secreted and taken up by deficient cells using the M6P recep-tor, and cross-correct neighboring tissues (7). We have recently developed a baby hamster kidney (BHK) cell line that overexpresses IDUA (8). We have demonstrated that the enzyme is processed correctly and taken up by neighboring cells via the M6P receptor, correcting MPS I patients' fibroblasts *in vitro* (9). In

Correspondence: **Roberto Giugliani**, PhD, Centro de Terapia Gênica, Hospital de Clinicas de Porto Alegre, Ramiro Barcelos, 2350, 90035–903, Porto Alegre, RS, Brazil. E-mail: rgiugliani@hcpa.ufrgs.br

(Received 11 January 2012; accepted 27 February 2012)

the present work we implanted the capsules in the peritoneum of MPS I mice, aiming to verify whether short- and long-term correction could be achieved by this approach *in vivo*.

Methods

Animals

The study was approved by the authors' institutional ethics review boards (project number 08 - 658), and MPS I mice (knockout for the Idua gene) on a C57BL/6 background (kindly donated by Dr E. Neufeld, UCLA, Los Angeles, CA, USA) were used (10). At 3 weeks of age, offspring were separated from the dam, housed (2–5/cage) by sex and genotyped by polymerase chain reaction (PCR). Animals were maintained in conventional housing under a 12-h light/12-h dark cycle with controlled temperature (19 é 1°C) and humidity (50 é 10%). At the time of death, serum was collected by retro-orbital puncture and mice were killed by cervical dislocation.The num-ber of mice in each group varied from three to 16, depending on the parameters, as described below.

Experimental design

Three main groups were evaluated for long-term experiments. In one, 1 month-old male Idua $^{-/-}$ mice were anesthetized with inhaled isofluorane and, after a small incision was made in the abdomen, 1×10^6 encapsulated cells/g body weight were suspended in 1 mL saline buffer and placed in the peritoneal cavity (referred to as the CAPS group). The procedure was repeated at 3 and 5 months of age and capsules were replaced each time. Male untreated Idua $^{-/-}$ mice (referred to as the MPS I group), and their normal littermate controls (Idua $^{+/+}$, referred to as the nor-mal group), comprised the other groups evaluated. Mice were killed at 6 months of age and serum and organs were collected for analysis.

Additional groups were used to address specific issues. A small group of mice ($n = 3$) was implanted with the capsules and killed 24 h later and compared with untreated MPS I and normal mice, to analyze the short-term uptake of the enzyme by the tissues. Another group of animals ($n = 3$) was treated with capsules for 90 days without replacing them, and serum was col-lected after 1, 7, 30 and 90 days of treatment to analyze the serum IDUA over time. A third group of three ani-mals was killed 1 month after treatment (at 2 months of age) to visualize the GAG content in the liver.

Capsule production

We have already described in detail the produc-tion of a BHK cell line transfected with the plasmid pR-IDUA, which overexpresses the enzyme IDUA, and the method for encapsulation of these cells (8). Briefly, cells were mixed with 1.5% sodium alginate (#A2158; Sigma-Aldrich, St Louis, MO, USA) in Dulbecco's modified Eagle medium (DMEM) and extruded thr-ough an encapsulation unit, type J1 (Nisco, Zurich, Switzerland) attached to JMS syringe pump. Droplets were sheared off with an air flow of 3.5 L/min delivered to the tip of a 27-G needle; the rate of infusion was 40 mL/h.The droplets fell into a bath of 125 mM $CaCl_2$ and ionically cross-linked with Ca^{2+} to form solid spheri-cal hydrogel beads containing embedded cells (11,12). In each well capsules were produced from a volume of 500 µL cell suspension, containing the appropriate number of cells to inject in each mouse (1×10^6 cell/g body weight). Cell encapsulation was carried out under sterile conditions. The resulting capsules were main-tained under normal tissue culture conditions [DMEM supplemented with 10% fetal bovine serum (FBS) at 37°C and 5% CO_2] for 24 h prior to administration, to remove any possibility of contamination.

Echocardiographic analysis

Mice were anesthetized with isofluorane and posi-tioned on a controlled temperature bed. They were placed in a left lateral decubitus position (45° angle) to obtain cardiac images. An EnVisor HD System (Philips Medical, Andover, MA, USA), with a 12–13 MHz transducer, was used, at 2 cm depth with fun-damental and harmonic imaging. Images were cap-tured by a trained operator with experience in small animal echocardiography. The following parameters were analyzed in normal ($n = 16$), MPS I ($n = 15$) and CAPS ($n = 5$) mice: ejection fraction, fractional area change and shortening fraction, as described elsewhere (13). After the procedure, mice were allowed to recover and monitored for 1 h.

IDUA activity

Tissues were homogenized with a dismembrator in distilled water, centrifuged, and the supernatant col-lected for assay. An IDUA activity assay was performed, incubating the protein extracts with the fluorescent substrate 4-methylumbelliferyl-alpha-L-iduronide (Glycosynth, Warrington, UK) at 37°C for 1 h (14) in pH 3.5 formate buffer. Results were calculated as nmol/h/mL in serum and nmol/h/mg protein in the tis-sues, and shown as a percentage of normal activity. Pro-tein content was measured using the Lowry method.

GAG measurement

Tissues were homogenized in phosphate buffer, pH 6.5, containing 300 µg/mL papain. GAG levels were

measured using the dimethyl blue technique. Briefly, 25 µL supernatant were mixed with freshly prepared dimethyl blue solution (dymethyl blue 0.3 mol/L with 2 mol/L Tris) and absorbance was read at 530 nm. Results were expressed as µg GAG/mg protein.

Histologic analysis

Livers from 2-month-old mice were collected and fixed in buffered formalin. From 6-month-old mice livers, lungs, kidneys and hearts were isolated and systematically divided into two pieces. One was flash frozen in liquid nitrogen for biochemical analysis and the other portion was fixed in buffered formalin. Thin cross-sections were submitted to routine histologic processing, stained with Hematoxylin-Eosin (H-E)/Alcian blue and analyzed. We also analyzed the capsules collected from 6-month-old mice using H-E, Sirius red (for collagen content) and von Kossa (for calcium content) stains, according to routine techniques.

Antibody assay

To measure whether mice developed antibodies against the enzyme, we performed an enzyme-linked immunosorbent assay (ELISA). Briefly, a 96-well ELISA plate was coated with 4 µg/mL recombinant IDUA enzyme (Aldurazyme®; Genzyme, Boston, MA, USA) overnight at 4°C in acid phosphate-buffered saline (PBS), pH 5.8. The plate was then blocked with 3% bovine serum albumin (BSA) in acid PBS for 2 h. Serum samples (diluted 1:50) were added and incubated for 2 h, following a 3-h incubation with a secondary antibody anti-mouse IgG (Sigma-Aldrich). Detection was performed with 3,3′,5,5′-tetramethylbenzidine (TMB; Sigma-Aldrich) for 5 min, according to the fabricant instructions. The reaction was stopped with H_2SO_4 1 M and absor-bance was read at 450 nm.

Statistics

For statistical analysis, SigmaStat version 11.0 was used. Results were compared using ANOVA and Tukey, Mann–Whitney or Student's *t*-test, as indicated. A Pearson test was used for correlation analysis. A *P*-value less than 0.05 was considered statistically significant.

Results

Long-term outcomes

At 6 months, MPS I mice presented the features that are the hallmarks of the animal model, including thick head bones, gibbous, increased weight (31.4 é 3.6 g, *n* ³ 7, versus 26 é 1.5 g in the normal mice, *n* ³ 15; *P* § 0.01) and infiltrated skin. Treated mice were only partially corrected, with intermediate average weight (30.6 é 2.3 g, *n* ³ 6; *P* ³ 0.84 compared with MPS) and improvements in the general aspect of the skin (Figure 1). However, skeletal abnormalities such as the gibbous remained unaltered.

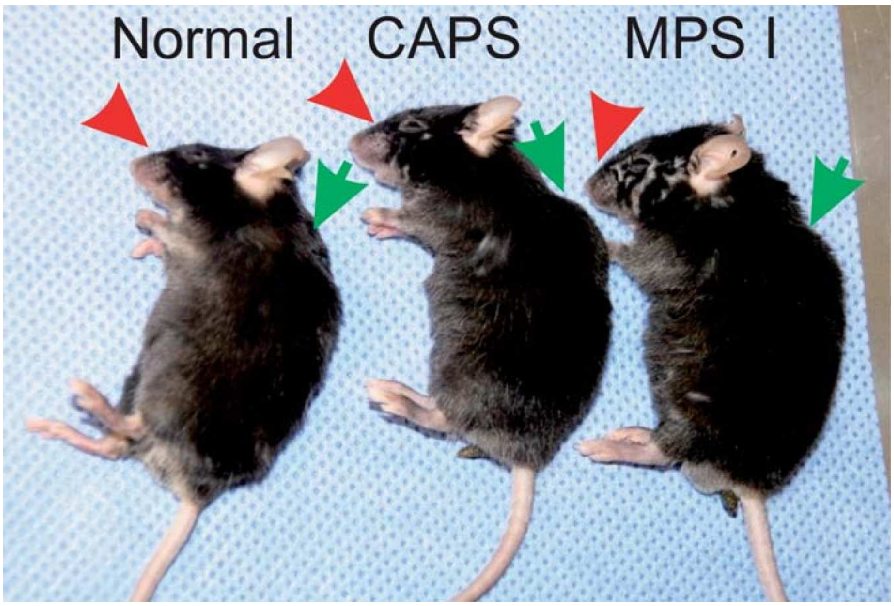

Figure 1. Aspect of normal (left), untreated MPS I mouse (right) and MPS I mouse treated with alginate microcapsules (CAPS, middle) at 6 months. Note that features in MPS I mice such as gibbous (arrows) is not corrected in treated mice, while infiltrated skin (arrowheads) is partially corrected.

Tissue GAG was measured at 6 months of age and showed an average reduction of 24% in the liver (P = 0.501), 26% in the kidney (P = 0.034) and heart (P = 0.490), and less than 10% in the lung (P = 0.960) in treated mice compared with untreated ones. In all cases, GAG levels were intermediate between untreated mice and normal mice; however, the difference was statistically significant only in the kidney (Figure 2A).

IDUA levels at 6 months (Figure 2B) were detectable at very low levels in the liver (an aver-age of 3-fold of the untreated levels, P = 0.056) and heart (1.8-fold of normal, P = 0.01, compared with untreated MPS I mice), and therefore they were not investigated in other organs. There was an inverse correlation (R^2 = 0.82, P = 0.035) between GAG lev-els in the liver and the residual IDUA activity found at 6 months in this organ (Figure 2C). Histologic analysis confirmed that tissues were only partially corrected, with some cells with GAG storage still present (Figure 3).

Echocardiographic analysis at 6 months revealed a reduction in the contractility of the MPS I myo-cardium, with reduced ejection fraction, shortening fraction and fractional area change. Treated animals presented similar values to untreated MPS I mice (Table I), indicating that, even though IDUA activity in the heart was higher in treated mice, abnormali-ties in the MPS I heart in the long term were not corrected.

Short-term results

Because we observed only a partial correction at 6 months, we performed another set of experiments to verify whether this approach could be efficient in the short term. To verify whether the enzyme released from the capsules into the peritoneal space was reaching the circulation and being taken up by the tissues, we used an additional small group of MPS I mice (n = 3) in which we implanted the microcapsules and killed the animals 24 h later. Our results showed that the IDUA levels were increased in the liver (an average of 15-fold of the untreated mice, P = 0.037), kidney (120-fold, P = 0.036), lung (3-fold, P = 0.028), spleen (9-fold, P = 0.006) and heart (3.4-fold, P = 0.05), but not in the brain (cerebellum and cortex), compared with untreated mice. However, the increase in the enzyme activity observed did not reach normal IDUA levels in any organ but the kidney (Figure 4A).

As these results seemed encouraging, three MPS I mice were injected with the capsules and serum was collected at different time-points. Twenty-four hours after treatment, serum IDUA could already be detected in treated mice. Activity peaked at 7 days; however, after 30 and 90 days it returned to unde-tectable levels, suggesting that for some reason the expression of IDUA was only transient (Figure 4B). Serum IDUA levels in untreated mice were unde-tectable.

To verify whether this temporary increase in IDUA activity was able to reduce GAG storage, three animals were killed 30 days after capsule implant (at 2 months of age). The livers of treated mice pre-sented a normal histologic aspect, while in untreated MPS I mice GAG storage was observed, mainly in Kupfer cells (Figure 5).

Analysis of capsules and antibody formation

To verify possible reasons for the apparent loss of expression observed at 6 months, the capsules were collected at the time of death and stained with H-E. Histologic analysis revealed that cells inside the cap-sules maintained their shape and integrity, suggest-ing that cell death does not occur (Figure 6A,B). However, Sirius red staining revealed a fibrotic layer

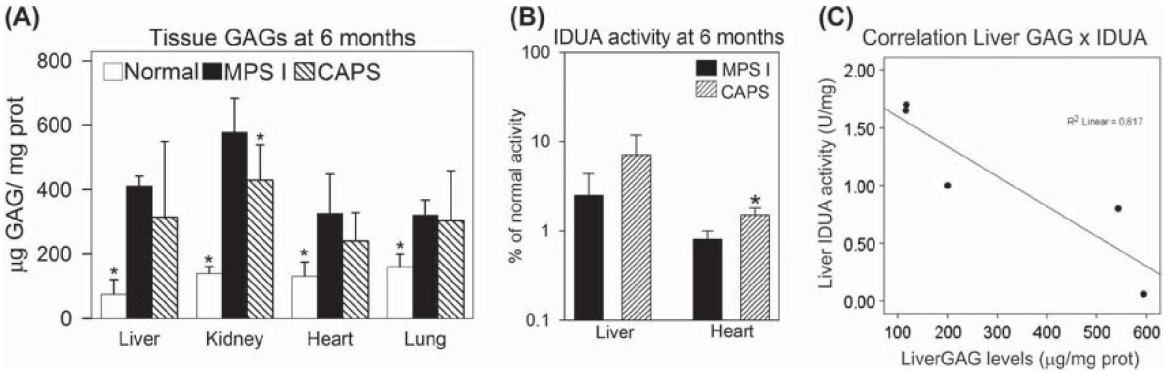

Figure 2. Results from long-term treatment. (A) Tissue GAG content measured at 6 months, n = 5–6/group. P § 0.05 compared with MPS I group, Student's t-test or Mann–Whitney test. (B) IDUA activity in tissues from 6-month old mice, n = 4–6/group. P § 0.05 compared with MPS I group, Student's t-test. (C) GAG levels in the liver showed an inverse correlation with the residual IDUA activity found in this tissue (P = 0.035, Pearson test).

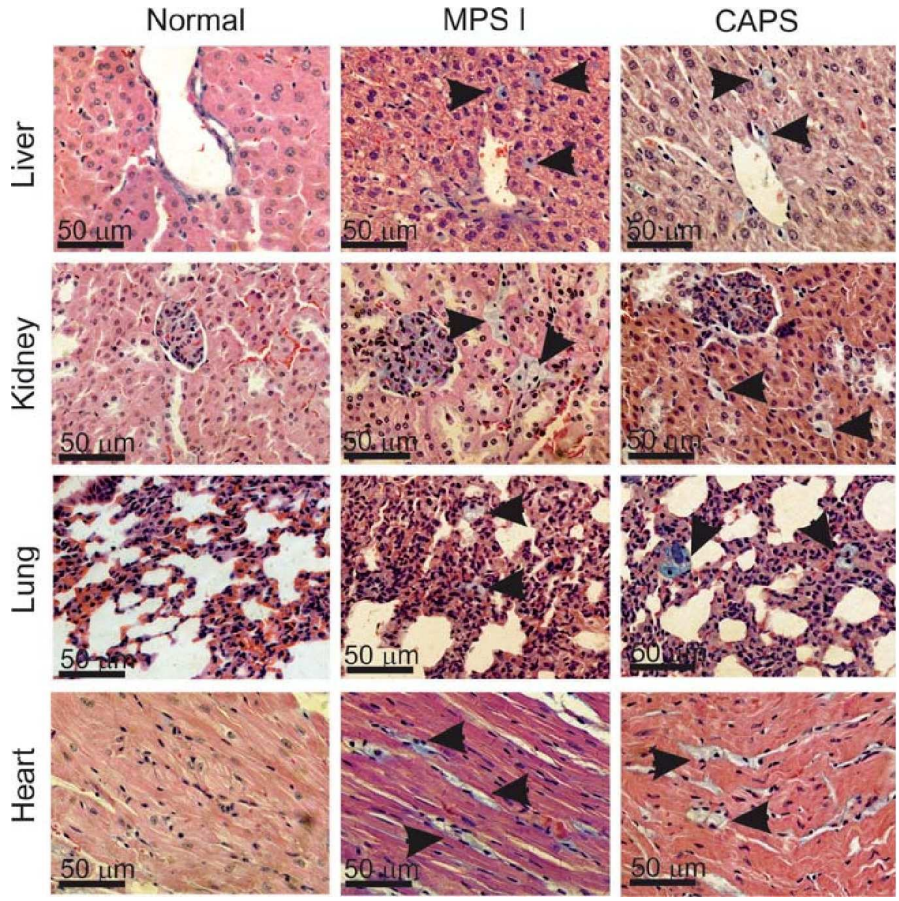

Figure 3. Histologic analysis at 6 months. GAG storage was analyzed in normal, MPS I mice and CAPS treated mice at 6 months using H-E/Alcian blue stain. Normal mice did not present blue cells in tissues, while both MPS I and CAPS mice had cells that accumulated GAG (arrowheads).

with collagen deposition around the capsules, which could prevent enzyme release (Figure 6C). Calcifi-cation of the capsules was not observed using von Kossa staining (data not shown).

We then sought to determine whether treated animals developed IgG antibodies against the enzyme, which could be another reason for the limited response obtained with the treatment. An ELISA was performed and revealed that serum from all four treated animals tested were positive for anti-IDUA antibodies at 6 months. Untreated MPS I and nor-mal mice did not develop any antibody, as expected (*P* § 0.05; Figure 6D).

Table I. Results from echocardiographic analysis in MPS I animals treated with capsules compared with normal and untreated MPS I mice at 6 months of age.

	Normal (n ₃16)	MPS I (n ₃15)	CAPS (n ₃5)
Ejection fraction (%)	60.2 ± 8.6[1]	48.5 ± 11.8	46.6 ± 11.5
Shortening fraction (%)	38.1 ± 6.8[1]	27.6 ± 5.9	27.6 ± 4.3
Fractional area change	51.5 ± 10.4[1]	41.3 ± 10.3	40.1 ± 13.7

[1] *P* § 0.05 compared with untreated MPS I mice, ANOVA and Tukey post-hoc.

Discussion

Although ERT and HSCT are currently available for MPS I, they have proven to be ineffective in correct-ing some organs in MPS I patients, such as the brain and heart valves (2,4). This highlights the need for other therapies, which could be administered alone or in combination with ERT or HSCT. In the pres-ent work, we aimed to verify whether encapsulated cells overexpressing IDUA could correct the disease in the long term when implanted in the peritoneum of MPS I mice.

We have recently reported that these capsules are able to correct MPS I human fibroblasts *in vitro* after co-culture for 45 days, without loss of expression of the enzyme, thus being a potential new approach for the treatment of MPS I (9). Therefore, we implanted

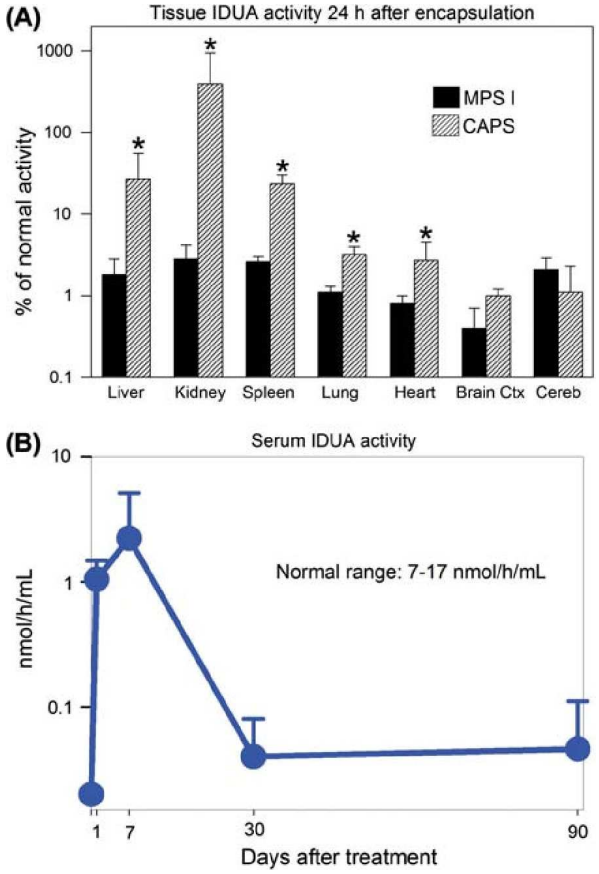

Figure 4. Results from short-term treatment. (A) IDUA levels in tissues 24 h after capsule implantation. $P \leq 0.05$ compared with untreated group, Student's *t*-test. (B) Serum IDUA activity in treated mice at 1, 7, 30 and 90 days after treatment ($n = 3$).

the microcapsules in the peritoneum of MPS I mice, to analyze whether the capsules would maintain the same long-term expression found *in vitro*, and whether the secreted enzyme could be taken up by the tissues. Our initial results indicated that it was possible to reduce GAG levels in the kidney and, although very subtle, there was a significant increase in the heart levels of IDUA, while liver results were statistically borderline. This increase was mild; when analyzing heart function, it was not altered compared with untreated mice.

These initial results led us to investigate fur-ther whether the enzyme was reaching the circula-tion and the tissues after implantation. Short-term results indicated that the enzyme could be produced, secreted from the capsules and reach the circulation and tissues of MPS I mice, preventing the early his-tologic alterations found in the liver at 2 months. However, it was unable to maintain high serum and tissue enzyme levels for prolonged periods of time. In our experience, the liver is the first organ where GAG storage can be visualized histologically, and this happens as early as at 2 months of age. This led us to analyze only this organ at this early time-point. Early correction of the liver can be explained because GAG storage at 2 months is lower than at 6 months (15), so a smaller amount of IDUA can prevent GAG storage in the liver at this time-point.

The partial correction of organs observed in the long term is similar to the findings of other groups when treating MPS II mice with encapsulated myo-blasts (16). Interestingly, the residual activity found in the liver at 6 months correlated with the reduction in GAG levels when analyzing mice individually. This confirms that our approach was indeed able to cor-rect this organ in the long term in some mice, but when analyzing the group as a whole the results were too variable to reach statistical significance. The same variability was found in recent work that used a dif-ferent encapsulated cell line to correct MPS I mice, in which two animals were completely corrected for

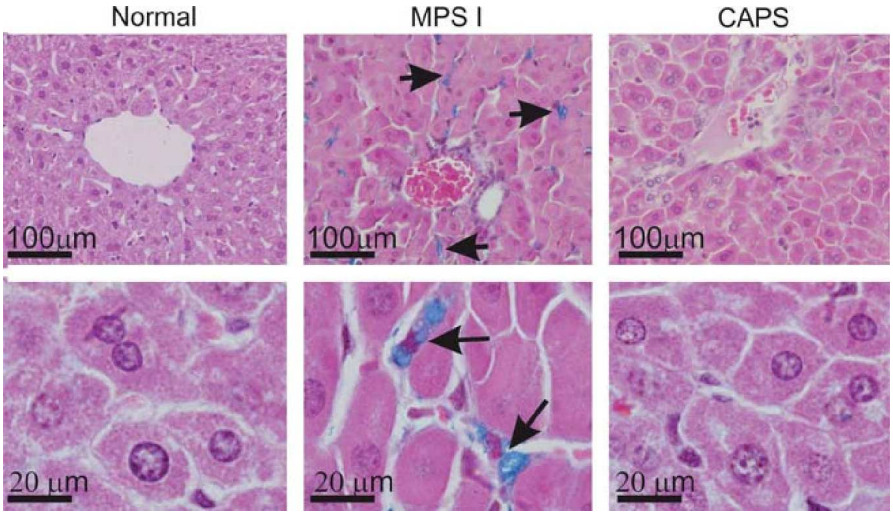

Figure 5. Histologic analysis from livers at 2 months. Liver slides were stained with H-E and Alcian blue, which stains GAG blue (arrows). The treated group did not present blue cells at this time-point.

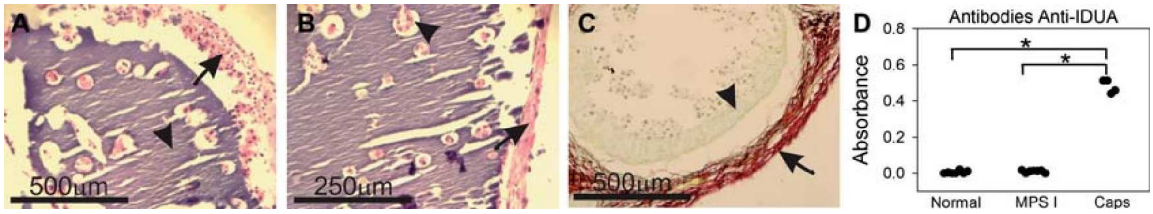

Figure 6. Histologic analysis of capsules and antibody formation. (A) Aspect of a capsule (arrowhead) with macrophages (arrow) around it, H-E stain. (B) Higher magnification of an H-E stain, showing that cells inside the capsule maintained their shape and integrity and even proliferated (arrowheads). (C) Sirius red stain, suggesting that cells around the capsules (arrowheads) are forming a fibrotic layer (red stain, arrow) of collagen. (D) Levels of IgG anti-IDUA antibody in mice serum at 6 months. Each dot represents the results from a single animal. Results are expressed as absorbance. * *P* § 0.05 compared with normal and MPS I mice.

the disease phenotype, while others had only a par-tial correction (17). The transient correction found in both studies led us to investigate possible reasons for the reduction in serum enzyme levels after a few days of treatment.

When animals treated for 5 months were killed, the capsules were recovered and analyzed histo-logically. Immune cells were detected around the capsules, where they formed a foreign body reac-tion. A pericapsular fibrotic process was present, with inflammatory cells surrounding the extracap-sular media. That process was clearly an immune response, triggered by the presence of the alginate beads, which has been described previously and might be the reason why the microcapsules failed in the long-term experiments (18). As IDUA is a rela-tively high molecular weight enzyme (69 kDa), the fibrotic layer could be preventing it from escaping to the extracapsular media. Cells inside the capsules did not present apoptotic or necrotic features. No cell overgrowth was observed, with capsules maintaining their round shape. Those observations do not sug-gest cell death inside the capsules and strengthen the hypothesis that the loss of expression is caused by the fibrotic process against the alginate.

Another possibility for the reduction in serum and tissue IDUA levels observed at 6 months is the devel-opment of neutralizing antibodies against the enzyme. MPS I mice were made by disruption of the Idua gene at exon 6 (10). Therefore these mice are naive for IDUA, and could develop an immune response to the protein. Our ELISA results suggest that MPS I-treated mice do indeed develop antibodies against the enzyme, as shown in other gene-therapy protocols (17,19). Unpublished observations from our group suggest that MPS I mice treated with intravenous ERT develop about the same amount of anti-IDUA antibodies. Interestingly, MPS I patients treated with ERT also develop antibodies against the recombinant IDUA, and the reduction in urinary GAG levels seems to correlate inversely with the level of serum anti-bodies produced (20). However, even patients with high antibody titers respond to treatment to a certain extent, suggesting that the failure in long-term correc-tion observed here is more likely to be caused by the fibrosis around the capsules.

In conclusion, as a proof-of-concept, our results indicate that the implantation of capsules in the peritoneum of MPS I mice leads to secretion of the enzyme into the circulation and uptake by the tissues, allowing short-term correction in MPS I mice.

Acknowledgments

We would like to thank Elisabeth Neufeld (UCLA, USA) for the generous gift of MPS I mice, and Dr Nance Nardi and Dr Melissa Camassola (ULBRA, Brazil) for providing the pR-IDUA vector. This work was supported by grants from Conselho Nacional de Desenvolvimento Cientifico-CNPq and Fundo de Incentivo a Pesquisa do Hospital de Clinicas de Porto Alegre (FIPE-HCPA).

Declaration of interest: The authors report no conflicts of interest. The authors alone are respon-sible for the content and writing of the paper.

References

1. Matte U, Yogalingam G, Brooks D, Leistner S, Schwartz I, Lima L, et al. Identification and characterization of 13 new mutations in mucopolysaccharidosis type I patients. Mol Genet Metab. 2003;78:37–43.
13. Grigull L, Sykora KW, Tenger A, Bertram H, Meyer-Marcotty M, Hartmann H, et al. Variable disease progression after suc-cessful stem cell transplantation: prospective follow-up inves-tigations in eight patients with Hurler syndrome. Pediatr Transplant. 2011;15:861–869.
14. Lange MC, Teive HA, Troiano AR, Bitencourt M, Funke VA, Setúbal DC, et al. Bone marrow transplantation in patients with storage diseases: a developing country experience. Arq Neuropsiquiatr. 2006;64:1–4.
15. Sifuentes M, Doroshow R, Hoft R, Mason G, Walot I, Diament M, et al. A follow-up study of MPS I patients treated with laronidase enzyme replacement therapy for 6 years. Mol Genet Metab. 2007;90:171–80.
16. Souza M, Krug C, Picon P, Schwartz I. High cost drugs for rare diseases in Brazil: the case of lysosomal storage disorders. Ciência Saúde Coletiva (Impresso). 2010;15:3443–554.

Ponder KP, Haskins ME. Gene therapy for mucopolysaccha-ridosis. Expert Opin Biol Ther. 2007;7:1333–45.

Matte U, Lagranha VL, de Carvalho TG, Mayer FQ, Giugliani R. Cell microencapsulation: a potential tool for the treatment of neuronopathic lysosomal storage diseases. J Inherit Metab Dis. 2011;34:983–90.

Mayer FQ, Baldo G, de Carvalho TG, Lagranha VL, Giugliani R, Matte U. Effects of cryopreservation and hypothermic storage on cell viability and enzyme activity in recombinant encapsulated cells overexpressing alpha-L-iduro-nidase. Artif Organs. 2010;34:434–9.

Baldo G, Mayer FQ, Burin M, Carrillo-Farga J, Matte U, Giugliani R. Recombinant encapsulated cells overexpressing alpha-L-iduronidase correct enzyme deficiency in human MPS I cells. Cell Tiss Org. 2012;195:323–9.

10. Ohmi K, Greenberg DS, Rajavel KS, Ryazantsev S, Li HH, Neufeld EF. Activated microglia in cortex of mouse models of mucopolysaccharidoses I and IIIB. Proc Natl Acad Sci USA. 2003;100:1902–7.
11. Bressel T, Paz AH, Baldo G, Cirne-Lima EO, Matte U, Pereira MLS. An effective device for generating alginate microcap-sules. Genet Mol Biol 2008;31:136–40.
12. Lagranha VL, Baldo G, de Carvalho TG, Burin M, Saraiva-Pereira ML, Matte U, Giugliani R. In vitro correction of ARSA deFB01ciency in human skin fibroblasts from metachromatic leukodystrophy patients after treatment with microencapsu-lated recombinant cells. Metab Brain Dis. 2008;23:469–84.
13. Tavares AM, da Rosa Araújo AS, Baldo G, Matte U, Khaper N, Belló-Klein A, et al. Bone marrow derived cells decrease inflam-mation but not oxidative stress in an experimental model of acute myocardial infarction. Life Sci. 2010;87:699–706.
14. Hopwood JJ, Muller V, Smithson A, Baggett N. A fluoromet-ric assay using 4-methylumbelliferyl alpha-L-iduronide for the estimation of alpha-L-iduronidase activity and the detection of Hurler and Scheie syndromes. Clin Chim Acta. 1979; 92:257–65.
15. Wang D, Shukla C, Liu X, Schoeb TR, Clarke LA, Bedwell DM, Keeling KM. Characterization of an MPS I-H knock-in mouse that carries a nonsense mutation analogous to the human IDUA-W402X mutation. Mol Genet Metab. 2010;99:62–71.
16. Friso A, Tomanin R, Alba S, Gasparotto N, Puicher EP, Fusco M, et al. Reduction of GAG storage in MPS II mouse model following implantation of encapsulated recombinant myob-lasts. J Gene Med. 2005;7:1482–91.
17. Piller Puicher E, Tomanin R, Salvalaio M, Friso A, Hortelano G, Marin O, Scarpa M. Encapsulated engineered myoblasts can cure Hurler syndrome: preclinical experiments in the mouse model. Gene Ther, in press.
18. Liu XY, Nothias JM, Scavone A, Garfinkel M, Millis JM. Biocompatibility investigation of polyethylene glycol and alginate-poly-L-lysine for islet encapsulation. Am Soc Art Intern Org J. 2010;56:241–5.
19. Di Domenico C, Villani GR, Di Napoli D, Reyero EG, Lombardo A, Naldini L, Di Natale P. Gene therapy for a mucopolysaccharidosis type I murine model with lentiviral-IDUA vector. Hum Gene Ther. 2005;16:81–90.
20. Wraith JE, Beck M, Lane R, Ploeg A, Shapiro E, Xue Y, et al. Enzyme replacement therapy in patients who have muco-polysaccharidosis I and are younger than 5 years: results of a multinational study of recombinant humanα-l-iduronidase (Laronidase). Pediatrics. 2007;120:e37

Journal of Inherited Metabolic Disease

Retroviral Vector-mediated Gene Therapy to Mucopolysaccharidosis I Mice Improves Sensorimotor Impairments and Other Behavior Deficits

--Manuscript Draft--

Manuscript Number:	
Full Title:	Retroviral Vector-mediated Gene Therapy to Mucopolysaccharidosis I Mice Improves Sensorimotor Impairments and Other Behavior Deficits
Article Type:	Invited Articles
Keywords:	Gene therapy; mucopolysaccharidosis type I; self-inactivating vector; retroviral vector; lysosomal storage disease; behavior tests, vestibular system.
Corresponding Author:	Katherine Ponder, M.D. Washington University School of Medicine St. Louis, MO UNITED STATES
Corresponding Author Secondary Information:	
Corresponding Author's Institution:	Washington University School of Medicine
Corresponding Author's Secondary Institution:	
First Author:	Guilherme Baldo
First Author Secondary Information:	
Order of Authors:	Guilherme Baldo
	David Wozniak
	Kevin K Ohlemiller
	Yanming Zhang
	Roberto Giugliani
	Katherine Ponder, M.D.
Order of Authors Secondary Information:	
Abstract:	Mucopolysaccharidosis I (MPS I) is a lysosomal storage disease due to α-L-iduronidase (IDUA) deficiency that results in the accumulation of glycosaminoglycans (GAG). Systemic gene therapy to MPS I mice can reduce lysosomal storage in the brain, but few data are available regarding the effect upon neurological function. Here, we investigated the effect of gene therapy with a long-terminal repeat (LTR)-intact retroviral vector or a self-inactivating (SIN) vector on neurological function in MPS I mice. The LTR vector was injected intravenously to 6 week-old MPS I mice, while the SIN was given to neonatal or 6 week-old mice. Adult-LTR, Neonatal-SIN, and Adult-SIN-treated mice achieved serum IDUA activity that was 235±20 (84-fold normal), 127±10, and 71±7 units/ml, respectively. All groups had reduction in histochemical evidence of lysosomal storage in the brain, with the Adult-LTR group showing the best response, while Adult-LTR mice had reductions in lysosomal storage in the cristae of the vestibular system. Neurological evaluation was performed at 8 months. Untreated MPS I mice had a markedly reduced ability to hold onto an inverted screen or climb down a pole. LTR vector-treated mice had marked improvements on both of these tests, while Neonatal-SIN mice had improvements in the pole test. We conclude that gene therapy with both vectors can reduce brain disease in MPS I mice, with the LTR vector achieving higher serum IDUA levels and better correction. Vestibular abnormalities may contribute to mobility problems in patients with MPS I.

Dear Editors

Please find submitted online our manuscript entitled “Retroviral Vector-mediated Gene Therapy to Mucopolysaccharidosis I Mice Improves Sensorimotor Impairments and Other Behavior Deficits” which we are respectfully submitting to the Journal of Inherited Metabolic Disease for consideration for publication as an original article. This is an invited submission for the issue on "New strategies for the treatment of metabolic disorders in the brain” which is planned for publication in the January issue of 2013. We have contacted Dr. Mauricio Scarpa who we believe is organizing this special issue, and felt that this manuscript would be appropriate.

In this paper, we demonstrate that intravenous injection of MPS I mice at 1.5 months of age with a retroviral vector that transduces the liver and results in high serum IDUA activity reduces GAG storage in the brain, and improves performance in several behavioral tests. Since we previously demonstrated that expression of the retroviral vector cannot be detected in the brain with a sensitive real-time PCR assay, the implication is that enzyme can diffuse from blood into brain. This result could have profound implications for how to treat patients with neurological disease due to MPS I, as it goes against the dogma that enzyme cannot cross the blood brain barrier. In addition, we describe abnormalities in the vestibular system of MPS I mice, which may contribute to mobility problems. This manuscript has not been published and is not under consideration for publication in any other journal. All authors contributed substantially to the study, and have approved the final version of the manuscript.

We look forward to hearing from you regarding the status of our manuscript. In the meantime, please feel free to contact us if you need any additional information.

Sincerely yours,

Guilherme Baldo

Katherine Ponder, M.D.
Division of Hematology, Box 8125
Department of Internal Medicine
Washington University School of Medicine
660 S. Euclid Avenue, St. Louis, MO
63110
Phone 314-362-5188
FAX 314-362-8813
kponder@dom.wustl.edu

Retroviral Vector-mediated Gene Therapy to Mucopolysaccharidosis I Mice Improves Sensorimotor Impairments and Other Behavior Deficits

Guilherme Baldo[1,5], David F. Wozniak[2], Kevin K. Ohlemiller[3], Yanming Zhang[1]
Roberto Giugliani[5], and Katherine P. Ponder[1,4]

Departments of Internal Medicine,[1] Psychiatry,[2] Otolaryngology,[3] and
Biochemistry and Molecular Biophysics[4]
Washington University School of Medicine, St. Louis MO, USA
Gene Therapy Center,[5] Hospital de Clinicas de Porto Alegre, RS, Brazil

*Corresponding author
Katherine P. Ponder
Department of Internal Medicine
Washington University School of Medicine
660 South Euclid Avenue
St. Louis, MO 63110
(314)-362-5188 (Phone)
(314)-362-8813 (FAX)
kponder@dom.wustl.edu (e-mail)

Word count: 9084
Number of figures: 7 (5 in the main text, 2 in the supplement)
Number of tables: none

Abstract

Mucopolysaccharidosis I (MPS I) is a lysosomal storage disease due to α-L-iduronidase (IDUA) deficiency that results in the accumulation of glycosaminoglycans (GAG). Systemic gene therapy to MPS I mice can reduce lysosomal storage in the brain, but few data are available regarding the effect upon neurological function. Here, we investigated the effect of gene therapy with a long-terminal repeat (LTR)-intact retroviral vector or a self-inactivating (SIN) vector on neurological function in MPS I mice. The LTR vector was injected intravenously to 6 week-old MPS I mice, while the SIN was given to neonatal or 6 week-old mice. Adult-LTR, Neonatal-SIN, and Adult-SIN-treated mice achieved serum IDUA activity that was 235±20 (84-fold normal), 127±10, and 71±7 units/ml, respectively. All groups had reduction in histochemical evidence of lysosomal storage in the brain, with the Adult-LTR group showing the best response, while Adult-LTR mice had reductions in lysosomal storage in the cristae of the vestibular system. Neurological evaluation was performed at 8 months. Untreated MPS I mice had a markedly reduced ability to hold onto an inverted screen or climb down a pole. LTR vector-treated mice had marked improvements on both of these tests, while Neonatal-SIN mice had improvements in the pole test. We conclude that gene therapy with both vectors can reduce brain disease in MPS I mice, with the LTR vector achieving higher serum IDUA levels and better correction. Vestibular abnormalities may contribute to mobility problems in patients with MPS I.

Synopsis: Retroviral vectors can improve neurological and inner ear abnormalities in MPS I mice.

Introduction

Mucopolysaccharidosis I (MPS I) is an autosomal recessive lysosomal storage disease with an incidence of 1:100,000 (Baehner et al 2005). It is due to deficient α-L-iduronidase (IDUA; EC 3.2.1.76) activity and results in the accumulation of the glycosaminoglycans (GAGs) heparan and dermatan sulfate in the lysosome (Neufeld and Muenzer 2001). Clinical manifestations include, but are not limited to, disease of the brain, ear, eye, upper airway, bones and joints, and cardiovascular system. Severe neurological impairment occurs in the severe form of MPS I known as Hurler syndrome (OMIM #607014). Although the attenuated-severity Scheie syndrome is not classically felt to reduce neurological function, 10% of these patients have mild to moderate impairments in cognitive function (Thomas et al 2010). The etiology of neurological dysfunction is unclear. Neurons and microglial cells accumulate GAGs, which can inhibit ganglioside-degradative lysosomal enzymes, causing accumulation of the gangliosides GM2 and GM3 (Walkley 2004), although a causal role for these abnormalities has not been demonstrated. Increased oxidation occurs in the cerebellum (Reolon et al 2009).

Available treatments for patients with MPS I include hematopoietic stem cell transplantation (HSCT) (Staba et al 2004) and enzyme replacement therapy (ERT) (Kakkis et al 2001). All approaches rely at least in part upon uptake of mannose 6-phosphate (M6P)-modified IDUA from the extracellular space by cells via the M6P receptor and translocation of enzyme to the lysosome. For HSCT, blood-derived cells migrate into organs including the brain and secrete enzyme locally, although some enzyme can be secreted into blood. HSCT has improved neurological function in children with Hurler syndrome if performed before 2 years of age (Aldenhoven et al

2008). ERT involves intravenous (IV) injection of M6P-modified IDUA protein, which can be taken up by cells after diffusion from blood. Although it has been assumed that ERT would not improve neurological function due to the blood-brain barrier, early results from a study of Hurler patients that received ERT suggests that they are developing better-than-expected (Wang et al 2009a), while ERT appeared to reduce abnormalities seen on MRI (Wang et al 2009b).

Gene therapy with gamma retroviral vectors (RV), adenovirus-associated (AAV) vectors, adenoviral vectors, lentiviral vectors, and plasmid-based vectors is being evaluated in animal models of MPS and involves transfer of a gene into cells in the body, which can secrete enzyme locally or into the blood (Ponder and Haskins 2007). Gene therapy has resulted in stable expression of IDUA in blood and reduction in lysosomal storage in the brain. However, most studies, including ours with RV, have not evaluated the effect on neurological function. MPS I mice show multiple behavior defects, which include reduced ambulations and rearings in an open-field test, reduced habituation to a new environment, and/or other abnormalities (Pan et al 2008; Hartung et al 2004; Reolon et al 2006; Wang et al 2009a). Neonatal administration of an AAV vector improved habituation in the open field test (Hartung et al 2004), *ex vivo* transduction of hematopoietic stem cells with expression in red blood cells improved habituation to a novel environment (Wang et al 2009a), while direct injection of an AAV8 vector into the brain improved function in a modified Morris water maze test (Wolf et al 2011).

The goal of this study was to determine if RV-mediated gene therapy could improve neurological function in MPS I mice. We have previously injected RV vectors

intravenously (IV) into MPS I mice, and demonstrated reduction in lysosomal storage in the brain for some of the vectors and doses that we were used (Liu et al 2005; Ma et al 2007; Chung et al 2007). However, other vectors and doses (Metcalf et al 2010) have not been evaluated for their effect on storage in the brain, and none of these studies have evaluated the effect on neurological function. In this study, one vector contained a complete long-terminal repeat (LTR; LTR vector), while a second vector contained a deletion in the enhancer region of the 3' LTR that results in self-inactivation upon transduction of a cell by transferring the deletion at the 3' end of the LTR to the 5' end of the LTR to create the self-inactivating (SIN) vector (Metcalf et al 2010). We demonstrate here marked improvement in behavioral dysfunction in MPS I mice after IV injection of the LTR vector to adult MPS I mice, and partial improvements after IV injection of the SIN vector to neonatal or adult MPS I mice.

Materials and Methods

Reagents and Vectors

All reagents were purchased from Sigma-Aldrich Chemical (St. Louis, MO) unless otherwise stated. hAAT-cIDUA-WPRE (designated as the LTR vector here) is a gamma RV with an intact LTR at both the 5' and 3' end, an extended packaging signal, the liver-specific human α_1-antitrypsin (hAAT) promoter, the canine IDUA cDNA, and the Woodchuck hepatitis virus post-transcriptional regulatory element (WPRE) (Liu et al 2005). SIN-hAAT-cIDUA-oPRE (designated as the SIN vector here) is a self-inactivating RV that has a deletion of the retroviral enhancer sequences in the U3 region of the 3`-LTR and lacks promoter or enhancer function at 5`- and 3`- ends of the provirus after

integration; the oPRE is an optimized version of the WPRE (Metcalf et al 2010), as diagramed in Supplementary Fig. 1.

Animal care

All experiments were approved by our ethics committee and National Institutes of Health (NIH) guidelines for the care and use of animals in research were followed. The specific mice evaluated here are identical to those reported previously (Metcalf et al 2010). For the neonatal treatment, MPS I mice on a C57BL/6 background (Ohmi et al 2003) received intravenous (IV) injection of $1x10^{10}$ transducing units (TU)/kg of the SIN vector at 2-3 days of age (designated hereafter as Neonatal-SIN; N=11) as previously described. For adult treatment, 6 week-old MPS I mice were injected intraperitoneally (IP) with hepatocyte growth factor (HGF) as detailed previously, followed by IV injection of the LTR-vector (designated hereafter as Adult-LTR; N=10) or the SIN vector (designated hereafter as Adult-SIN; N=6). The cumulative dose of RV was $1.7x10^{10}$ transducing units (TU)/kg for Adult-LTR-treated mice and $1x10^{10}$ TU/kg for Adult-SIN-treated mice. Adult LTR-treated MPS I mice were also treated transiently with anti-CD40 ligand antibody (blocks the CD40:CD40 ligand co-stimulatory pathway in lymphocytes) and CTLA4-Ig (blocks the CD80/CD86:CD28 co-stimulatory pathway in lymphocytes) to suppress the immune system and prevent mice from developing a cytotoxic T lymphocyte response to IDUA-expressing cells, while Adult-SIN-treated mice did not receive immunosuppression. Heterozygous normal and untreated MPS I mice from the same breeding colony were used as controls. Serum was obtained from the tail vein.

IDUA and GUSB activities

Organs were homogenized in lysis buffer at pH 5.5. as described previously (Baldo et al 2011). GUSB and IDUA assays were performed using the fluorogenic substrates 4-methylumbelliferyl-β-L-glucuronide (Sigma-Aldrich, St Louis, MO) for GUSB and 4-methylumbelliferyl-α-L-iduronide (Toronto Research Chemicals, North York, Canada) for IDUA and a Fluoroskan Ascent microplate fluorometer (Thermo Electron, Milford, MA) as previously described. One unit of enzyme activity converts 1 nmole of substrate to product per hour at 37^0C. Samples were prepared from 5 normal, 6 untreated MPS I, 5 Adult-LTR-, 4 Neonatal-SIN, and 3 Adult-SIN-treated mice; some treated mice were not evaluated due to lack of sample availability.

Histological analysis

Eight-month old mice were perfused with 20 mL of PBS, and brains were removed and fixed in PBS with 4% paraformaldehyde and 2% glutaraldehyde. Pieces of brain were embedded in plastic, and 1 μm-thick sections of cerebellum, cortex, and hippocampus were stained with toluidine blue as described (Ma et al 2007). Purkinje cells in the cerebellum were considered to have storage if they had 2 or more cytoplasmic vacuoles with GAGs when evaluated at 40X magnification. Ten fields were evaluated and the average percentage of positive cells was determined. Neurons and microglial cells of the cortex and hippocampus were considered to have storage if they had at least 3 vacuoles with GAGs. Mouse temporal bones containing the ears were fixed in the same fashion, decalcified, embedded in paraffin, and 4 μm-thick mid-

modiolar sections were stained with toluidine blue. Histology was evaluated for most parts of the brain from 4 normal, 5 untreated MPS I, 4 Adult-LTR-treated, 4 Neonatal-SIN-treated, and 4 Adult-SIN-treated MPS I mice. For the hippocampus, the number evaluated was 3, 3, 4, 2, and 2, respectively, as some sections did not have adequate regions of this somewhat difficult-to-obtain region.

Behavioral tests

Sensorimotor tests were performed to assess balance, strength, and coordination, as previously described (Wozniak et al 2004). For the screen tests, the mouse was placed on a wire mesh grid with 16 squares per 10 cm. For the vertical screen test, the screen was elevated 47 cm above the floor and inclined vertically. Each mouse was placed in the middle of the screen with its head oriented down, and the time to climb to the top of the screen was determined. For the inverted screen test, mice were placed on top of a screen that was oriented 60^{O} from the horizontal plane, and the screen was gently inverted until it was horizontal with the mouse upside-down, and the time to fall off was recorded. A maximum score of 60 seconds was given if the mouse did not fall. For the screen tests, two trials were performed, and values for the second trial are reported. For the pole test, a mouse was placed head upward on top of a vertical rod (8 mm diameter and 55 cm tall) that had a finely textured surface, and was timed for how long it took to climb down the pole. If a mouse fell from the pole before reaching the floor, it was given the maximum score of 120 seconds. Two trials were performed, and the values for the second trial were averaged. Forelimb grip strength was evaluated with a grip strength meter (Stoelting Co., Wooddale, IL) as described

(Wozniak et al 2007). The mouse was placed over a Perspex plate in front of a "grasping trapeze", which functions as the arm of a force transducer connected to a peak amplifier. The mouse was taught to grab the trapeze when pulled by the tail until the pulling force overcame its grip strength, and the peak pull force was measured. Each mouse received 3 days of habituation in which several trials were performed until it performed 5 good pulls. Testing involved two 5-trial sessions, with each session being conducted on consecutive days. The mean of the pull force of the 5 trials performed on the second day are shown here.

Motor coordination and balance were evaluated using the rotorod test (Rotamex-5, Columbus Instruments, Columbus, OH) when it was stationary, rotating at 5 revolutions per minute (rpm) for up to 60 seconds, and accelerating where the speed increased from 5 rpm to 20 rpm over 180 seconds, and the time to fall off the rod was determined (Wozniak et al 2007). The Morris water maze test was performed as described (Wozniak et al 2004). During cued trials, mice were trained to swim to a submerged platform marked with visual cues, and mice received four trials per day for two consecutive days. Place trials, which are not shown here, were also performed to test the ability of a mouse to learn the position of a platform. General locomotor activity was quantified using a computerized, photobeam system (MotorMonitor, Hamilton-Kinder, LLC, Poway, CA), according to previously published methods (Wozniak et al 2004). The number of ambulations (whole body movements) and vertical rearings made over 12 separate 5 minute blocks or for the entire hour were recorded. In addition, walking initiation, ledge, and platform tests were performed as described previously, but are not shown here.

Statistics

ANOVA with Tukey post-hoc analysis or the Student's t test compared values in different groups using Sigma Stat software version 3.1 (Systat Software, Inc., Point Richmond, CA). Fisher's exact test determined if the frequency of an event differed between two groups.

Results

Gene transfer and brain enzyme activity

The goal of this study was to evaluate the effect of gene transfer to neonatal or adult (1.5 month-old) MPS I mice on neurological function at 8 months of age. All mice evaluated here were previously described in terms of their transduction, but the effect on lysosomal storage in the brain and neurological function was not reported. Adult-LTR mice were treated at 6 weeks of age with transient administration of HGF to induce the hepatocyte replication needed for transduction with this vector in adults, followed by a cumulative dose of $1.7x10^{10}$ TU/kg of the LTR vector (Metcalf et al 2010), which was 1.7 fold the dose given in our initial study with this vector in adult mice (Ma et al 2007). All mice achieved stable expression of IDUA activity in serum, as shown in Fig. 1A, with a mean activity of 235±20 U/ml, which was substantially higher than the value of 2.8±0.1 U/ml in homozygous normal mice, and the value of 0.2±0.01 U/ml in untreated MPS I mice. A different cohort of MPS I mice were treated with the SIN vector (Metcalf et al 2010). Some received neonatal IV injection of $1x10^{10}$ TU/kg (Neonatal-SIN), while others received IV injection of HGF at 6 weeks of age to induce hepatocyte replication

followed by $1x10^{10}$ TU/kg (Adult-SIN). Neonatal-SIN and Adult-SIN mice achieved serum IDUA activity of 127±10 U/mL and 71±7 U/mL, respectively, as shown in Fig. 1A.

Brain IDUA activity is shown in Fig. 1B, which was performed on samples that were collected after perfusion of mice with saline to remove enzyme from blood. Adult-LTR mice achieved 5±6 U/mg of IDUA activity in the front half of the brain, which was 73% normal (7±2 U/mg) and 96-fold the level in untreated MPS I mice, although these differences between Adult-LTR and untreated MPS I mice did not quite achieve significance ($p=0.052$ versus MPS I mice) due to marked variation in individual mice. It is possible that some treated animals had poor perfusion prior to the collective of tissues and were contaminated with IDUA from blood. Average IDUA levels in the forebrain from Neonatal-SIN and Adult-SIN were 0.3±0.2 U/mg and 1.4±1.1 U/mg, respectively, which were 5-fold and 19-fold, respectively, the values for untreated mice (0.05±0.03 U/mg), although none of these differences were significant. Cerebellum IDUA activity in Neonatal-SIN and Adult-SIN-treated mice were 1.8 and 3.1-fold the values in untreated MPS I mice, respectively, and did not reach significance. IDUA levels were not analyzed in cerebellum of Adult-LTR mice due to the failure to collect samples.

Activity of the lysosomal enzyme, β-glucuronidase (GUSB), was also evaluated, as other lysosomal enzymes are usually elevated in MPS I, and normalization of activity is a good biochemical indicator of correction of disease (Baldo et al 2011). Adult-LTR-treated mice had a significant reduction in forebrain GUSB activity compared with untreated MPS I mice, while Neonatal-SIN- and Adult-SIN-treated MPS I mice had a significant reduction in cerebellar but not forebrain GUSB activity. GAG levels were not evaluated in treated mice, as our prior studies failed to identify elevations in untreated

MPS I mice.

Histopathological analysis of brain

Histopathological analysis was performed to determine if neurons and microglial cells had a reduction in accumulation of lysosomal storage material, as shown for representative examples in Supplemental Fig. 2, and as quantified in Fig. 2. In untreated MPS I mice, 44±13% of Purkinje cells had 2 or more vacuoles with the appearance of lysosomal storage, which was higher than the value of 4±3% of cells in normal mice ($p<0.01$). Adult-LTR-treated mice had storage in 7±7% of cells ($p<0.01$ *vs*. MPS I), while Neonatal-SIN and adult-SIN mice were partially corrected with storage in 23±12% and 18±6% of cells, respectively ($p<0.01$ *vs*. MPS I mice; $p=0.02$ for Neonatal SIN *vs*. normal).

In the cortex, MPS I mice had storage in 25±5% of neurons and 45±8% of glial cells, which were higher than the values of 2±1% and 2±2% of cells in normal mice, respectively ($p<0.01$ in both cases). Adult-LTR treated mice had marked reductions in storage in both cell types ($p<0.01$ *vs*. MPS I), while Neonatal-SIN and Adult-SIN-treated mice had partial reductions ($p<0.01$ *vs*. MPS I). A similar pattern was seen in the hippocampus, where the percentage of cells with lysosomal storage material was elevated in untreated MPS I mice, and treated mice had statistically significant reductions.

Effect of MPS I on neurological function

A battery of tests were performed at 8 months of age to evaluate MPS I mice for

neurological abnormalities. Since Adult-LTR-treated MPS I mice were evaluated at a different time from the Neonatal-SIN- and the Adult-SIN-treated mice, behavioral tests are shown separately for these cohorts of mice. MPS I mice performed similarly to normal controls in the time that it took to climb to the top of a vertically-oriented screen, suggesting that their general coordination and strength were relatively intact (Fig. 3A). However, MPS I mice could not hold onto an inverted screen for the entire 60-second trial, as 100% fell off the screen when it was inverted so that the mouse was hanging upside-down, although only 13% of normal mice fell off ($p<0.001$ with Fisher exact test). For Adult-LTR-treated MPS I mice, only 20% of the mice fell off the inverted screen, which was significantly lower than the value in MPS I mice ($p<0.001$), but was not different from the value in normal mice (Fig. 3B). In addition, the average time that MPS I mice held onto the inverted screen was very short at 23±17 seconds (Fig. 3C). In contrast, normal mice held onto the screen for 57±7 seconds ($p<0.01$ *vs.* MPS I), which was very close to 60 seconds, the maximum duration of the trial. Adult-LTR-treated mice stayed on the screen for 56±9 seconds, which was significantly longer ($p<0.01$) than for untreated MPS I mice, but was not different from the value in normal mice.

Mice were also evaluated for their ability to climb down a pole (Fig. 3D and 3E), which is a task that requires strength, coordination, and vestibular function. For MPS I mice, 70% fell off the pole, and the average time to climb down was long at 96±41 seconds, where any animal that fell was considered to take 120 seconds to climb down. For heterozygous normal mice, 13% fell off ($p=0.004$ *vs*. MPS I), and they took only 33±36 seconds to climb down the pole ($p=0.005$ *vs*. MPS I). For Adult-LTR-treated mice, only 10% fell off ($p=0.02$ *vs*. MPS I; not significant *vs*. normal), and they took 38±37

seconds to climb down (p=0.006 *vs*. MPS I, not significant *vs*. normal). It is unlikely that the MPS I mice were weak, as their forelimb grip strength was normal (Fig. 3F). MPS I mice did have slightly reduced swimming speeds in the Morris water maze test (Fig. 3G), although spatial learning and memory capabilities were not found to be impaired (data not shown). The swim speed improved with Adult-LTR treatment.

Evaluation of Activity

During the 1 hour-locomotion test, untreated MPS I mice exhibited 168±81 rearings, which represented a 51% reduction relative to normal mice (341±106; p=0.007), as shown in Fig. 3H. The number of rearings in Adult-LTR-treated MPS I mice was at an intermediate level (232±134; 68% normal), although values were not significantly different from those in either normal or untreated MPS I mice. The MPS I mice also showed a greatly attenuated ambulatory response to initially being placed in a novel environment. Specifically, untreated MPS I mice showed reduced activity during the first 5 minutes (126±64 ambulations), which was 56% of normal (p=0.005). In contrast, RV-treated MPS I mice exhibited normal levels of ambulatory activity during the first 5 minutes of the session (232±112; 102% normal; p=0.002 *vs*. MPS I, not significant *vs*. normal). In addition, the number of ambulations did not change much over the 1-hour test session in untreated MPS I mice, as the value in the last 5 minute block was 81% of that found in the first 5 minute block (not significant for comparison of the initial and late values with the Students t test), while ambulations at the end of the hour in normal mice fell to 51% of the initial value (p=0.001), and those in RV-treated mice fell to 50% of the initial value (p<0.001). Thus, the MPS I mice showed a blunted ambulatory

response to novelty and did not show the typical decrease in activity across the test session indicative of habituation, and Adult-LTR-treated mice were normalized in both of these parameters. Values did not differ between normal, untreated MPS I, and Adult-LTR-treated MPS I mice for the time to initiate walking, the time spent on a ledge, and the time spent on a platform (data not shown).

Histopathological evaluation of the middle and inner ear

Since the reduced ability of MPS I mice to climb down a pole and to hold onto an inverted screen could reflect reduced vestibular function, ears were evaluated for histopathological abnormalities of the vestibular system. Another reason for evaluating the ear is that we previously demonstrated that hearing was abnormal in MPS I mice and was partially improved with Adult-LTR therapy (Metcalf et al 2010), and we wanted to determine the histopathological explanation for this improvement. The stapes is one of the three ossicles of the middle ear, and its footplate attaches to the wall of the vestibule via the annular ligament to form the oval window which separates the middle from the inner ear. Sound waves cause the footplate of the stapes to move, which results in a fluid wave in the inner ear that is detected by sensory cells in the cochlea. Fig. 4 shows histopathology of the stapes where it attaches via the annular ligament to the bony wall of the vestibule of the inner ear. In the MPS I mouse, the ligament shows a great deal of lysosomal storage material that appears as white vacuoles (Fig. 4F) that may be a factor in the reduced hearing. The ligaments of two Adult-LTR-treated mice looked normal. All animals had some degree of exudate surrounding the stapes, which is abnormal and is consistent with a middle ear infection. The results shown are representative for 6 normal

mice, 4 untreated MPS I mice, and 4 Adult-LTR treated mice.

The round window membrane is the second region where the boundary between the inner and the middle ear is not solid bone. Proper compliance of the round window membrane is necessary for the stapes to generate a fluid wave within the inner ear. Fig. 5A, 5E, and 5I show that the round window membrane is thin in a normal mouse, and that the surrounding space (the antrum) is clear. In contrast, the round window membrane of an MPS I mouse is markedly thickened and contains white vacuoles with lysosomal storage material (Fig. 5J), while the round window antrum appears full of exudative material (Fig. 5B and 5F). Both the thickness of the round window membrane and the exudate in the adjacent antrum may reduce the compliance of the round window membrane and contribute to hearing loss. The round window of two Adult-LTR-treated mice was less thickened than for the MPS I mouse, but the middle ear still contained substantial exudate, as shown in Fig. 5C-5D and Fig. 5G-5K.

The semicircular canals contain ampular cristae with hair cells, which are mechanoreceptor cells that sense rotation. The cristae appear as cone-shaped structures identified with arrows in the low and middle power views in Fig. 5A-4D, and Fig. 5E-5H, respectively. In the high power image shown in Fig. 5J of the MPS I mouse, both hair cells and surrounding support cells contain large amounts of lysosomal storage material that is absent in the normal mouse in Fig. 5K. These defects are consistent with the hypothesis that abnormal vestibular function could contribute to sensorimotor abnormalities. The Adult-LTR-treated mouse with the lowest expression of the group had a marked, but not complete, reduction in lysosomal storage material in the cristae, while an Adult-LTR-treated mouse with higher expression had complete resolution of

lysosomal storage.

Behavior studies in Neonatal-SIN- and Adult-SIN-treated MPS I mice

Behavioral studies were also performed in Neonatal-SIN and Adult-SIN-treated MPS I mice along with a separate cohort of heterozygous normal and untreated MPS I mice, as shown in Fig. 6. For this cohort of untreated MPS I mice, reduced ability to hold onto an inverted screen, reduced ability to climb down a pole, reduced swim speed, reduced rearing, reduced initial activity in a novel environment, and reduced habituation to the novel environment were similar to that depicted in Fig. 3. The only test where performance differed from that shown in Fig. 3 was the grip strength test, where the MPS I mice had a grip strength of 34±6 grams, which was lower than the value of 42±6 grams in normal mice (71% of normal, $p<0.001$ for MPS I *vs*. normal). The reason for the latter discrepancy is unclear, as the age and gender composition of the normal and untreated MPS I mice in the two studies were similar. Ambulatory activity during the first 5 minutes of the 1-hour locomotor activity test in MPS I mice was 50% of normal levels ($p=0.007$ for MPS I *vs*. normal), which resembles the result found in the MPS I mice in Fig. 3. MPS I mice did not exhibit habituation of ambulatory activity, since levels during the last 5-minute block were not significantly different from those observed in the first 5-minute block [105 *vs*. 73 for a 30% reduction with time ($p=0.10$)]. In contrast, the normal mice exhibited robust habituation of ambulatory activity across the test session (209 *vs*. 121 ambulations during the first and last 5 minute blocks), for a 42% reduction ($p=0.002$).

The Neonatal-SIN-treated mice demonstrated a significant reduction in the percent that fell off the vertical pole ($p=0.003$ *vs*. MPS I), a reduction in the time to crawl

down the vertical pole (p=0.002 *vs*. MPS I), increase in forelimb grip strength (p<0.001 *vs*. MPS I), and increased numbers of ambulations in the first 5-minute block in the 1 hour-locomotor activity test (p=0.05) relative to untreated MPS I mice, but did not show improvements in their ability to hold onto an inverted pole, swim speeds, or the number of rearings relative to MPS I mice. In addition, the number of ambulations in the last 5-minute time block of the 1 hour-locomotion test were only reduced by 37%, which was not a significant difference from the number of ambulations in the first 5-minute block (p=0.15). Adult-SIN-treated mice had greater numbers of ambulations in the first 5-minute block of the activity test compared to untreated MPS I mice (p=0.007 vs. MPS I) and showed habituation, with a 48% reduction in movement from the first to the last 5-minute blocks (p=0.009), but did not show improvements in other tests. Histopathological evaluation of the ears was not performed in the SIN vector-treated mice due to the time involved in sectioning and evaluating the ear.

Discussion

Neurological impairment is an important feature of MPS I in human patients. We had previously demonstrated that Neonatal-LTR-treated (Chung et al 2007) and Adult-LTR-treated (Ma et al 2007) MPS I mice that received $1x10^{10}$ TU/kg of vector had reduced lysosomal storage in neurons and microglial cells of the brain, but had not previously evaluated brains for storage in Adult-LTR mice that received a higher dose of $1.7x10^{10}$ TU/kg of the LTR vector, or in Neonatal-SIN or Adult-SIN mice that received $1x10^{10}$ TU/kg of the SIN vector. In addition, although hearing and visual tests were performed previously for all of these groups of mice, we had not previously performed

other neurological function tests. These studies evaluated the latter 3 groups of treated mice mentioned above, but did not evaluate the former 2 groups, as the behavioral tests were not set up when they were sacrificed.

Adult-LTR-, Neonatal-SIN, and Adult-SIN-treated MPS I mice achieved an average lifetime serum IDUA activity of 235±20, 127±10, and 71±7 U/mL, respectively. The Adult-LTR-treated mice had the highest forebrain IDUA activity at 73% of normal, although the marked variability in values for individual mice led to the failure to observe statistical significance, and we cannot eliminate the possibility that some brain samples from treated mice were contaminated with IDUA activity present in blood due to an imperfect perfusion. The Neonatal-SIN and the Adult-SIN-treated mice had forebrain and cerebellar IDUA activity that was 2% to 20% of normal, although the variability in the values for individual samples led to a lack of significance when compared with samples from untreated MPS I mice, and concerns about our ability to consistently removed all blood from the brain with perfusion apply here as well. The Adult-LTR-treated mice had statistically significant reductions in forebrain GUSB activity compared with untreated MPS I mice, which should not be confounded by contamination of samples with serum, and suggests that indeed, IDUA enzyme activity in brain is sufficient to improve this biochemical marker of disease. Neonatal-SIN- and Adult-SIN-treated MPS I mice had partial reductions in cerebellar GUSB activity that were statistically significant, although apparent partial reductions in forebrain GUSB activity did not quite achieve significance, possibly due to the small number of samples. All groups had reductions in the number of neurons and microglial cells with lysosomal storage in the cerebellum, cortex, and hippocampus, with the Adult-LTR-treated mice demonstrating the most complete

reductions in storage, and the Neonatal-SIN and Adult-SIN mice exhibiting partial improvements.

Vestibular function

In this study, MPS I mice had many behavioral abnormalities. This is the first report that MPS I mice have a profoundly reduced ability to hold onto an inverted screen and to climb down a pole. Since these mice behaved normally in both the constant speed and accelerating rotorod test (data not shown), could readily climb to the top of a vertical screen (Fig. 3A and 6A), and had a normal grip strength in one of the two studies that were performed (Fig. 3F), we infer that their cerebellar and motor functions were relatively well-maintained. Nevertheless, since the grip strength was abnormal in the second study (Fig. 6F), the swim speed was consistently reduced, the rearings were consistently reduced, and MPS I mice have abnormal joint histology (GB and RG, unpublished data), we cannot rule out the possibility that musculoskeletal abnormalities contributed to reduced function in these tests. We favor the hypothesis that abnormal vestibular function contributes to the reduced ability to hold onto an inverted screen and climb down a pole, as we demonstrate here that MPS I mice have enormous amounts of lysosomal storage material in the hair cells and accessory cells of the cristae ampullaris of the semicircular canals, which are critical for sensing the position in space. Similar histochemical abnormalities were observed in the cristae of MPS VII mice (Ohlemiller et al 2002), although no functional abnormality was associated with this finding. It is unclear if humans have abnormalities in tests that might correlate with those observed here in mice.

Adult-LTR-treated mice showed an improved ability to hold onto an inverted screen and climb down a pole compared with untreated MPS I mice. The reduction in lysosomal storage in the cristae of the semicircular canals of the inner ear in Adult-LTR-treated compared with untreated MPS I mice may have contributed to their improved function on these tests, although improvements in bone and joint disease or in muscle strength could play a role. The Neonatal-SIN and Adult-SIN-treated mice did not have statistically significant improvements in their performance on the inverted screen, although the Neonatal-SIN-treated mice (but not Adult-SIN-treated mice) had improvements in their ability to climb down a pole and in their grip strength compared with untreated MPS I mice. The failure to correct the inverted screen performance may reflect the lower serum IDUA activity achieved for both SIN groups compared with the Adult-LTR-treated mice. Ears were not evaluated histopathologically in either of the SIN groups due to the time involved in sectioning through an entire ear.

Locomotor activity

This paper confirms the consistent report of others that the number of rearings is reduced, the initial activity in a novel environment is lower, and activity fails to decline with habituation to an environment in MPS I compared with normal mice (Reolon et al 2006; Pan et al 2008). We did document abnormalities in the acoustic startle response (data not shown), but felt that the interpretation of these tests was complicated by the known hearing defect in MPS I mice. This study failed to identify significant differences in the time and path length to reach a platform in both cued and place trials between normal and MPS I mice in the Morris water maze test for the first cohort of mice that

were evaluated (data not shown), although the swimming speed was reduced to ~80% of that in normal mice. Some (Wolf et al. 2011) but not others (Pan et al. 2008) have reported differences at older ages in the Morris water maze test, although in these studies, the time to reach the platform was reported and the swim speed was not commented upon, raising the possibility that slow swimming was a factor.

In this study, the Adult-LTR-treated mice did not have statistically significant improvement in the number of rearings, although there appeared to be partial improvement. Adult-LTR-treated mice did have significant improvements in their initial activity in a novel environment and their habituation over time, suggesting that treatment normalized their ambulatory response to a novel environment and subsequent habituation in activity. Neonatal-SIN and Adult-SIN-treated mice did not have improvements in the number of rearings, although both had increased activity in the first 5-minute block in a novel environment compared with untreated MPS I mice. The Adult-SIN-treated mice showed habituation over time, while the Neonatal-SIN mice did not show significant habituation, although the activity for this latter group in the last 5 minute block of an hour-long test session was reduced by 37% relative to the activity in the first 5 minutes, which was marginally non-significant ($p=0.15$). Altogether, these data suggest that Neonatal-SIN and Adult-SIN gene therapy was less effective than Adult-LTR gene therapy, which likely reflects the lower serum IDUA activity achieved with the SIN vector compared with the LTR vector. However, the SIN vector did result in some neurological improvements.

Histochemical evaluation of the ear

Schachern et al (2007) previously reported that reduced hearing in MPS I mice was associated with a middle ear exudate at 2 months or older and that modest amounts of lysosomal storage were present in the fibrocytes of the spiral ligament and mesothelial cells of the basilar and Reissner's membranes. It was also reported that there was a reduction in the number of hair cells of the cochlea at 1 year or older. We previously demonstrated that hearing was improved, but not normalized, in the same Adult-LTR-treated MPS I mice that were evaluated here relative to untreated MPS I mice, as MPS I mice require 89±2 decibels (db) of sound at 10 kHz to evoke a brainstem response, and the same Adult-LTR-treated mice whose ears were evaluated here only required 59±2 db, although this remained higher than the value in normal mice of 39±6 db (Metcalf et al 2010). However, histochemical evaluation of the inner and middle ear was not performed previously. Here we report that lysosomal storage was markedly reduced in the annular ligament, and was reduced, but not eliminated, in the round window membrane, which could contribute to improved hearing. However, a middle ear exudate was still consistently present in Adult-LTR-treated mice, and we hypothesize that the failure to prevent an exudate with gene therapy may be a factor in the hearing deficit that persists in the Adult-LTR-treated MPS I mice.

Mechanism of improvement in neurological function

These data suggest a beneficial effect of Adult-LTR gene therapy on biochemical, histopathological, and functional abnormalities in the brain of MPS I mice, and partial improvement in some parameters in Neonatal-SIN and Adult-SIN-treated mice. Since we were previously unable to detect RNA in the brain (Metcalf et al 2010) of the same

mice that were evaluated here, we believe that improvements in neurological function likely reflect diffusion of enzyme from blood into the brain. This contradicts the dogma that enzyme cannot cross the blood:brain barrier, although the barrier is not absolute (Banks 2004), and there are some data that it is disrupted in MPS IIIB (Garbuzova-Davis et al 2011) plus other data that GUSB in serum can traverse the barrier and reach the brain (Vogler et al 2005, Grubb et al 2008).

The SIN vector was less effective in this study than the LTR vector, which likely reflects the lower transduction efficiency and lower expression observed *in vivo*, as discussed previously (Metcalf et al 2010). Thus, although SIN vectors are generally safer *in vivo* than LTR-intact vectors due to their inability to enhance expression of a nearby oncogene (Trobridge 2011), their reduced efficacy in our hands poses a problem, and a more detailed risk:benefit analysis will need to be done in the future to decide which vector to use. It remains possible that a better effect could be observed with the SIN vector if higher doses were used.

Implications for future gene therapy studies

One of the major concerns of any therapy for MPS I or related diseases is the question of whether or not it will improve neurological function. Although it has been presumed that enzyme in blood will not cross the blood brain barrier, a variety of data suggest that some enzyme can reach the brain from blood, albeit the process is somewhat inefficient. This study demonstrating that a gene therapy approach that does not result in expression in the brain can indeed improve neurological function is encouraging that either ERT or systemic gene therapy can improve this important

parameter, although the caveat is that very high levels of enzyme in blood, over 200 U/ml, are required to achieve an optimal effect.

Acknowledgments

We thank Elizabeth Neufeld for sending us the MPS I mice, and Sara Conyers for performing behavioral tests. This work was supported by the Ryan Foundation, the National MPS Society, and the National Institutes of Health (DK66448 awarded to KPP). Histology was supported by P30 DC004665 to awarded to R. Chole, and behavioral studies were supported by NIH Neuroscience Blueprint Interdisciplinary Center Core Grant P30 NS057105 awarded to Washington University (DFW). GB received a scholarship from the Conselho Nacional de Desenvolvimento Cientifico (CNPq) of Brazil (200584/2010-3).

References

Aldenhoven M, Boelens JJ, de Koning TJ (2008) The Clinical Outcome of Hurler Syndrome after Stem Cell Transplantation. Biology of Blood and Marrow Transplantation 14:485-498

Baehner F, Schmiedeskamp C, Krummenauer F et al (2005) Cumulative incidence rates of the mucopolysaccharidoses in Germany. J Inherit Metab Dis 28:1011-1017

Baldo G, Wu S, Howe R et al (2011) Pathogenesis of aortic dilatation in MPS VII mice may involve complement activation. Mol Genet Metab 104:608-19

Banks WA (2004) Are the extracellular pathways a conduit for the delivery of therapeutics to the brain. Curr Pharm Des.10:1365-70

Chung S, Ma X, Liu Y, Lee D, Tittiger M, Ponder KP (2007) Effect of neonatal administration of a retroviral vector expressing alpha-L-iduronidase upon lysosomal storage in brain and other organs in mucopolysaccharidosis I mice. Mol Genet Metab. 90:181-92

Garbuzova-Davis S, Louis MK, Haller EM, Derasari HM, Rawls AE, Sanberg PR. Blood-brain barrier impairment in an animal model of MPS III B. PLoS One. 2011 Mar 7;6(3):e16601

Grubb JH, Vogler C, Levy B, Galvin N, Tan Y, Sly WS (2008). Chemically modified beta-glucuronidase crosses blood-brain barrier and clears neuronal storage in murine mucopolysaccharidosis VII. Proc Natl Acad Sci USA 105:2616-21

Hartung SD, Frandsen JL, Pan D et al (2004) Correction of metabolic, craniofacial, and neurologic abnormalities in MPS I mice treated at birth with adeno-associated virus vector transducing the human alpha-L-iduronidase gene. Mol Ther 9:866–

875

Kakkis ED, Muenzer J, Tiller GE, et al (2001) Enzyme-replacement therapy in mucopolysaccharidosis I. N Engl J Med 344:182-8

Liu Y, Xu L, Hennig AK, et al (2005) Liver-directed neonatal gene therapy prevents cardiac, bone, ear, and eye disease in mucopolysaccharidosis I mice. Mol Ther 11:35-47

Ma X, Liu Y, Tittiger M et al. (2007) Improvements in mucopolysaccharidosis I mice after adult retroviral vector-mediated gene therapy with immunomodulation. Mol Ther.15:889-902

Metcalf J, Ma X, Linders B, Wu S et al. (2010) A self-inactivating gamma-retroviral vector reduces manifestations of mucopolysaccharidosis I in mice. Molecular Therapy 18:334-42

Neufeld EF, Muenzer J (2001) The Mucopolysaccharidoses. *In Metabolic and Molecular Basis of Inherited Disease*, ed. Scriver CR, Beaudet AL, Sly WS, Valle D, New York: McGraw Hill, 3421-3452

Ohlemiller KK, Hennig AK, Lett JM, Heidbreder AF, Sands MS (2002) Inner ear pathology in the mucopolysaccharidosis VII mouse. Hear Res 16:969–84

Ohmi K, Greenberg DS, Rajavel KS, Ryazantsev S, Li HH, and Neufeld EF (2003) Activated microglia in cortex of mouse models of mucopolysaccharidoses I and IIIB. Proc Natl Acad Sci USA. 100:1902-1907

Pan D, Sciascia A, Vorhees C and Williams MT (2008) Progression of multiple behavior deficits with various age of onsets in a murine model of Hurler syndrome. Brain Research 1188:241-253

Ponder KP, Haskins ME (2007) Gene therapy for mucopolysaccharidosis. Expert Opin Biol Ther 7:1333-45

Reolon GK, Braga LM, Camassola M, Luft T, Henriques JAP, Nardi NB, Roesler R (2006). Long-term memory for aversive training is impaired in IDUA$^{-/-}$ mice, a genetic model of mucopolysaccharidosis type I. Brain Research 1076:225-230

Reolon GK, Reinke A, de Oliveira MR et al. (2009) Alterations in oxidative markers in the cerebellum and peripheral organs in MPS I mice. Cell Mol Neurobiol 29:443-8

Schachern PA, Cureoglu S, Tsuprun V, Paparella MM, Whitley CB (2007) Age-related functional and histopathological changes of the ear in the MPS I mouse. Int J Pediatr Otorhinolaryngol. 71:197-203

Staba SL, Escolar ML, Poe M, et al. (2004) Cord-blood transplants from unrelated donors in patients with Hurler's syndrome. N Engl J Med 350:1960-9

Thomas JA, Beck M, Clarke JT, Cox GF (2010) Childhood onset of Scheie syndrome, the attenuated form of mucopolysaccharidosis I. J Inherit Metab Dis. 33:421-7

Trobridge GD (2011) Genotoxicity of retroviral hematopoietic stem cell gene therapy. Expert Opin Biol Ther. 11:581-93

Vogler C, Levy B, Grubb JH, Galvin N, Tan Y, Kakkis E, Pavloff N, Sly WS (2005). Overcoming the blood-brain barrier with high-dose enzyme replacement therapy in murine mucopolysaccharidosis VII. Proc Natl Acad Sci USA 102: 14777-82.

Walkley SU (2004). Secondary accumulation of gangliosides in lysosomal storage disorders. Semin Cell Dev Biol. 15:433-444

Wang D, Zhang W, Kalfa TA, Grabowski G, Davies S, Malik P, Pan D (2009a). Reprogramming erythroid cells for lysosomal enzyme production leads to visceral

and CNS cross-correction in mice with Hurler syndrome. Proc Natl Acad Sci U S A. 106:19958-63

Wang RY, Cambray-Forker EJ, Ohanian K, Karlin DS, Covault KK, Schwartz PH, Abdenur JE (2009b). Treatment reduces or stabilizes brain imaging abnormalities in patients with MPS I and II. Mol Genet Metab. 98:406-11

Wolf DA, Lenander AW, Nan Z, et al. (2011). Direct gene transfer to the CNS prevents emergence of neurologic disease in a murine model of mucopolysaccharidosis type I. Neurobiol Dis. 43:123-33

Wozniak DF, Xiao M, Xu L, Yamada KA, Ornitz DM (2007) Impaired spatial learning and defective theta burst induced LTP in mice lacking fibroblast growth factor 14. Neurobiol Dis. 26:4-26

Wozniak DF, Hartman RE, Boyle MP (2004) Apoptotic neurodegeneration induced by ethanol in neonatal mice is associated with profound learning/memory deficits in juveniles followed by progressive functional recovery in adults. Neurobiol. Dis 17: 403-414

Wraith JE, Beck M, Lane R (2007) Enzyme replacement therapy in patients who have mucopolysaccharidosis I and are younger than 5 years: results of a multinational study of recombinant human alpha-L-iduronidase (laronidase). Pediatrics; 120: e37-46

Figure Legends

Fig. 1. Serum α-L-iduronidase (IDUA) activity. A. Serum IDUA activity after treatment in MPS I mice. Mice were injected with $1.7x10^{10}$ TU/kg of the RV designated hAAT-cIDUA-WPRE at 1.5 months of age (Adult-LTR), with $1x10^{10}$ TU/kg of the self-inactivating version of the RV designated SIN-hAAT-cIDUA-oPRE at 2 to 3 days after birth (Neonatal-SIN), or with $1x10^{10}$ TU/kg of the SIN vector at 1.5 months of age (Adult-SIN) and serum IDUA ± the standard deviation (SD) was measured using a fluorogenic substrate as described in the methods section every 2 months until 8 months of age. Results represent the average of the lifetime average for the indicated number of mice in each group. **B. Forebrain and cerebellar IDUA activity.** Animals were sacrificed at 8 months and IDUA levels were measured in the forebrain and cerebellum for normal mice, untreated MPS I mice, and both groups treated with the SIN-vector, and in the forebrain only of the Adult-LTR-treated mice. **C. β-glururonidase (GUSB) activity.** * represents a p value of 0.01 to 0.05 and ** indicates a p value <0.01 for the indicated groups compared with MPS I mice using ANOVA with Tukey post hoc analysis.

Fig 2. Histochemical analysis for lysosomal storage in the brain. Normal mice, untreated MPS I mice, or MPS I mice that were treated as detailed in Fig. 1 were sacrificed at 8 months of age. Brains were fixed, embedded in plastic, and 1-μm thick sections were stained with toluidine blue, as shown for representative samples in Supplementary Figure 2. The percentage of Purkinje cells in the cerebellum with 2 or more vacuoles thought to be lysosamal storage was determined as detailed in the methods. For the neurons and microglial cells of the cortex and the hippocampus, the

percentage of the cells with 3 or more granules thought to represent lysosomal storage was determined. ** indicates that values were statistically significant for a particular group compared with those in untreated MPS I mice with a $p<0.01$ using ANOVA and Tukey post hoc analysis.

Fig. 3. Neurological tests in Adult-LTR mice. Some MPS I mice with treated with IV injection of the LTR-intact RV at 1.5 months of age as described in Fig. 1, while other MPS I and heterozygous normal littermates were not treated. Behavioral tests were performed as detailed in the methods section at 8 months of age. **A. Vertical screen**. The average time in seconds ± SD to climb to the top of a vertical screen was determined**. B-C. Inverted screen test**. The percentage of mice that fell off an inverted screen (panel B) and the average time that mice held onto the inverted screen (panel C) was determined. For the latter panel, the trial was terminated after 60 seconds. Analysis for the significance of the frequency of events between two groups was determined with Fisher's exact test, while ANOVA with Tukey post-hoc analysis was performed to compare values in panel C. **D-E. Vertical pole test.** The percentage of mice that fell of a vertical pole and the time to climb down the vertical pole were determined as described for panels B-C except the maximum time for the trial was 120 seconds. **F. Forelimb grip strength** The mean of the pull force at which mice in each group released a trapeze was determined. **G. Swim speed.** The average swim speed in the cued trials of the Morris water maze test was determined for 8 trials over 2 days. **H. Rearing.** The number of rearings per hour when placed into a novel environment was determined. * and ** indicate that there were significant differences between the

indicated group and untreated MPS I mice with p=0.01 to 0.05 and p<0.01, respectively, using ANOVA with Tukey post-hoc analysis.**I. Ambulations.** The number of ambulations over 5-minute blocks was determined for 12 consecutive intervals over an hour. Statistical comparisons for this panel are discussed in the main text.

Fig. 4. Histopathology of the stapes of the middle ear. Ears were collected at 8 months of age from normal, untreated MPS I, or MPS I mice that were treated with the LTR vector at 1.5 months of age (Adult-LTR), and processed as detailed in the methods. Sections from mice of the indicated groups were stained with toluidine blue. For the Adult-LTR mice, the average serum IDUA activity for the specific animals shown is indicated. **A-D. Stapes.** Low power view of the stapes where it articulates with the cochlear capsule via the annular ligament at the oval window. Arrows indicate the margins of the stapes footplate, while the arrowhead indicates exudative material. **E-H. Annular ligament.** The annular ligament has large amounts of lysosomal storage that appear as white bubbles (white arrow) in untreated MPS I mice. No storage is visible in normal or treated mice. The size markers are indicated in the panels.

Fig. 5. Histopathological analysis of the cochlea, round window, and cristae. Mice were treated as detailed in Fig. 4, and ears were collected at 8 months of age, processed, sectioned, and stained with toluidine blue. **A-D. Low power cochlear images.** The asterisk indicates the inner ear and the arrows indicates a crista of one semicircular canal. The box indicates the region shown at higher power with some

rotation in panels E-H. **E-H. Intermediate power views of the inner ear, round window membrane, and round window antrum.** The asterisk indicates the inner ear, and the box indicates the region with the round window membrane shown at higher power in panels I-L. The middle ear is located to the right of the round window membrane in all panels. The antrum is clear in the normal mouse (panel E) but is filled with exudate in the other panels. The arrow indicates crista of one semicircular canal. **I-L. Round window membrane.** The asterisk indicates the inner ear, and the arrow indicates lysosomal storage material in the round window membrane in the untreated MPS I mouse. **M-P. High power views of crista.** The black arrow in the untreated MPS I mouse shown in panel N identifies lysosomal storage material, which is present in hair and accessory cells of the crista. The Adult-LTR-treated mouse shown in panel O also has lysosomal storage, although the normal mouse in panel M and the Adult-LTR-treated mouse with higher expression of IDUA in serum in panel P does not have detectable storage. Size markers are indicated in the panels.

Figure 6. Behavior tests in Neonatal-SIN and Adult-SIN mice. MPS I mice were injected with the SIN vector as newborns (Neo-SIN) or as adults (Adult-SIN) as detailed in Fig. 1, while heterozygous normal and untreated MPS I littermates served as controls. Behavioral tests were performed as detailed in Fig. 3.

Supplementary materials

Supplementary Figure 1. Vectors. **A. SIN-hAAT-cIDUA-oPRE.** The diagram shows the SIN-hAAT-cIDUA-oPRE vector, which is referred to here as the SIN vector. The 5' end contains the simian virus 40 enhancer (SV40) and the respiratory syncytial virus promoter (RSV) instead of the U3 (unique to the 3' end of the RNA). Most of the U3 region of the 3' LTR has been deleted to form a ΔU3 lacking enhancer and promoter elements, with only 22 bp from the 5' end and 14 bp from the 3' end of the original 449 bp U3. The U5 (unique to the 5' end of the RNA) and the R (redundant; present at both the 5' and the 3' end of the RNA) are also shown. Upon integration, the 3' ΔLTR is copied to the 5' LTR position, and both are transcriptionally inactive. The human α1-antitrypsin (hAAT) promoter drives expression of the canine α-L-iduronidase gene (cIDUA) after transduction, as indicated by the black arrow. The optimized post-transcriptional regulatory element (oPRE) lacks open reading frames and the sequence and promoter of the potentially oncogenic X protein. **B. hAAT-cIDUA-WPRE**. The diagram shows the LTR-intact hAAT-cIDUA-WPRE vector, which is referred to here as the LTR vector. The LTR is complete at both ends, and upon integration can drive expression of the cIDUA in non-hepatic cells. This vector also contains the Woodchuck hepatitis virus post-transcriptional regulatory element (WPRE), which is similar to the oPRE but is longer and does not have the modifications noted above. The construction of these vectors was reported previously (Metcalf et al 2010).

Supplementary Fig. 2. Histological analysis of GAG storage in the brains. Sections of 8 month-old mice were stained with toluidine blue, after which GAGs appear as white vacuoles in the cytoplasm. The top row shows Purkinje cells from the cerebellum, the

middle row shows neurons from the cortex, and the bottom rows shows microglial cells from the cortex. Representative examples of normal, untreated MPS I mice, MPS I mice treated at 1.5 months with the LTR-intact vector (Adult-LTR) and MPS I mice treated with the SIN vector at 2-3 days of age (Neonatal-SIN) or at 1.5 months of age (Adult-SIN) are shown. Black arrows indicate cells with no storage, while white arrows indicate cells with storage. Similar analysis was performed for the hippocampus (data not shown).

Figure 1
Click here to download high resolution image

Figure 1

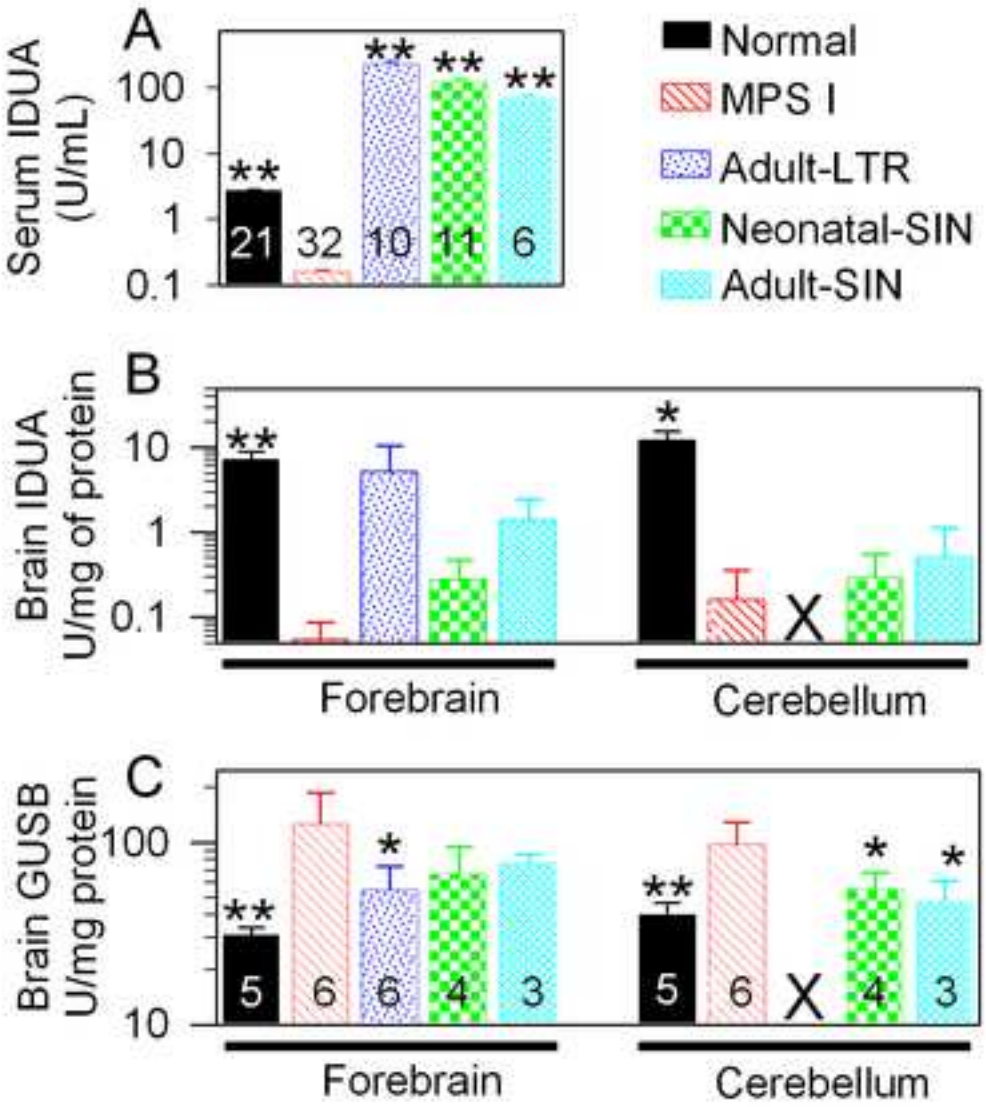

Figure 2
Click here to download high resolution image

Figure 2

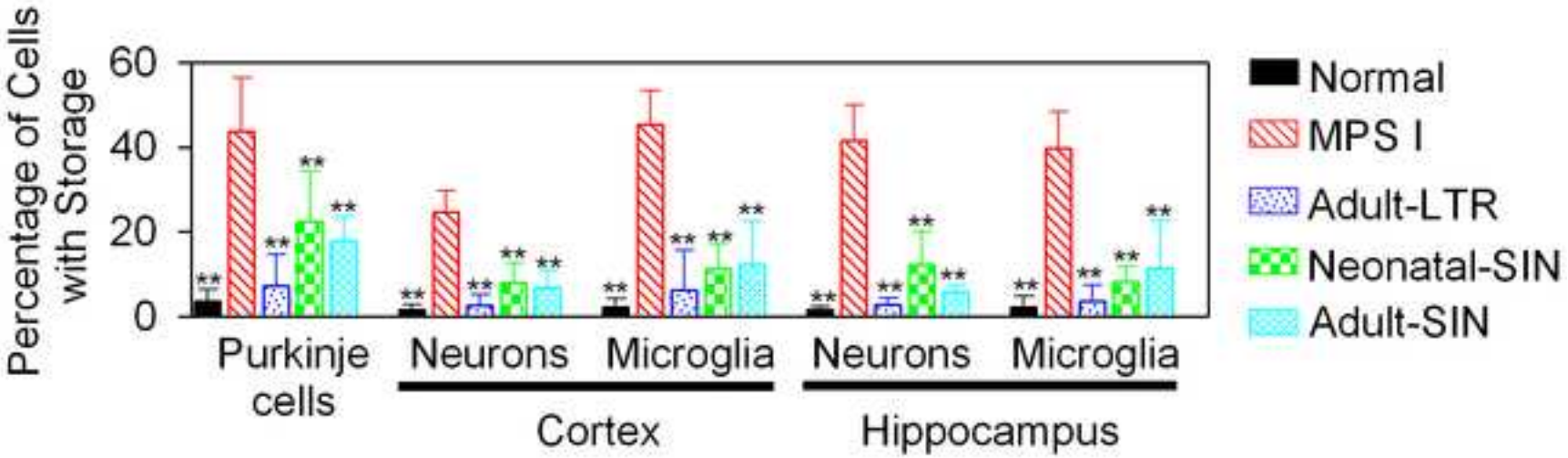

Figure 3
Click here to download high resolution image

Figure 3

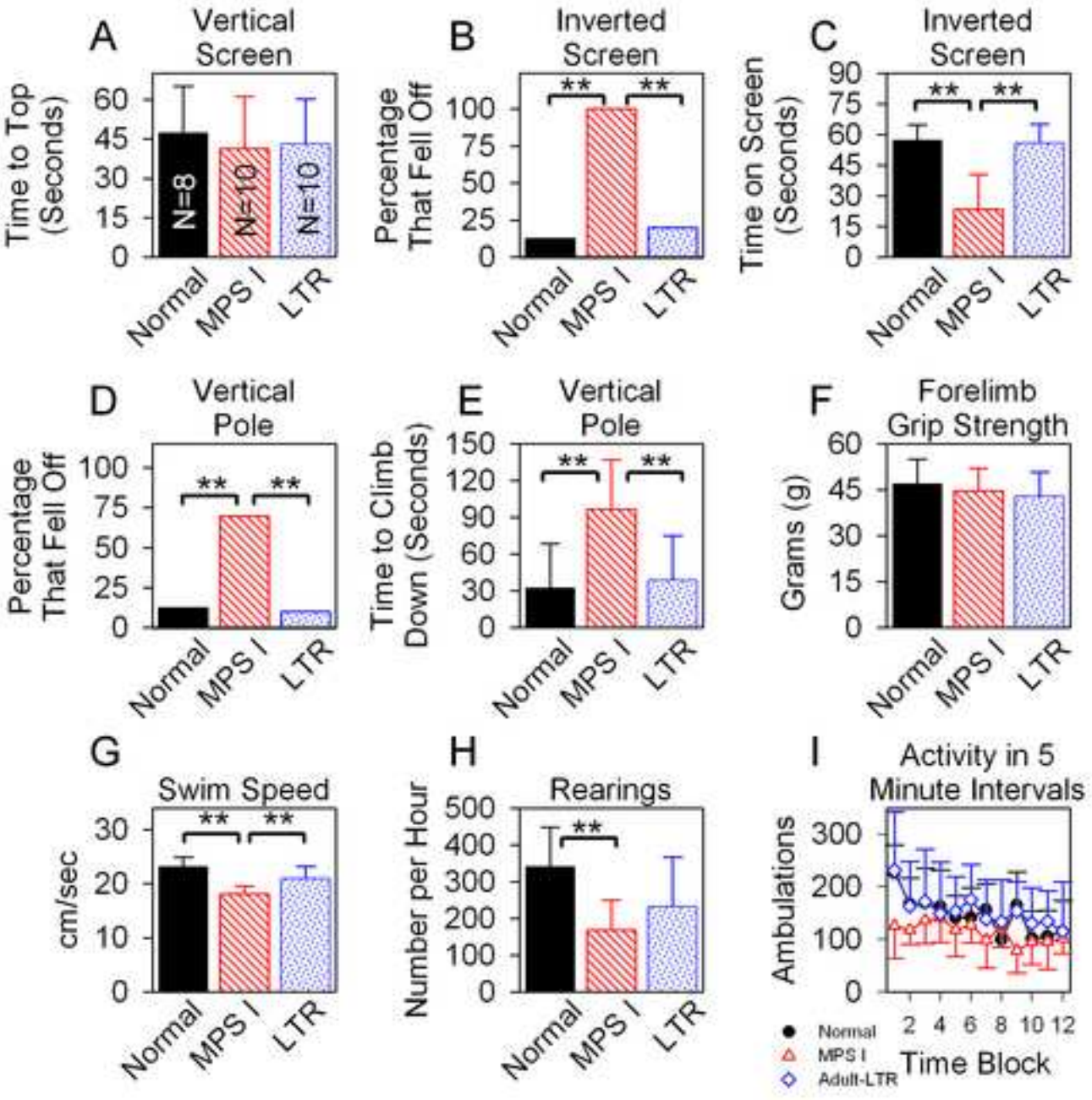

Figure 4
Click here to download high resolution image

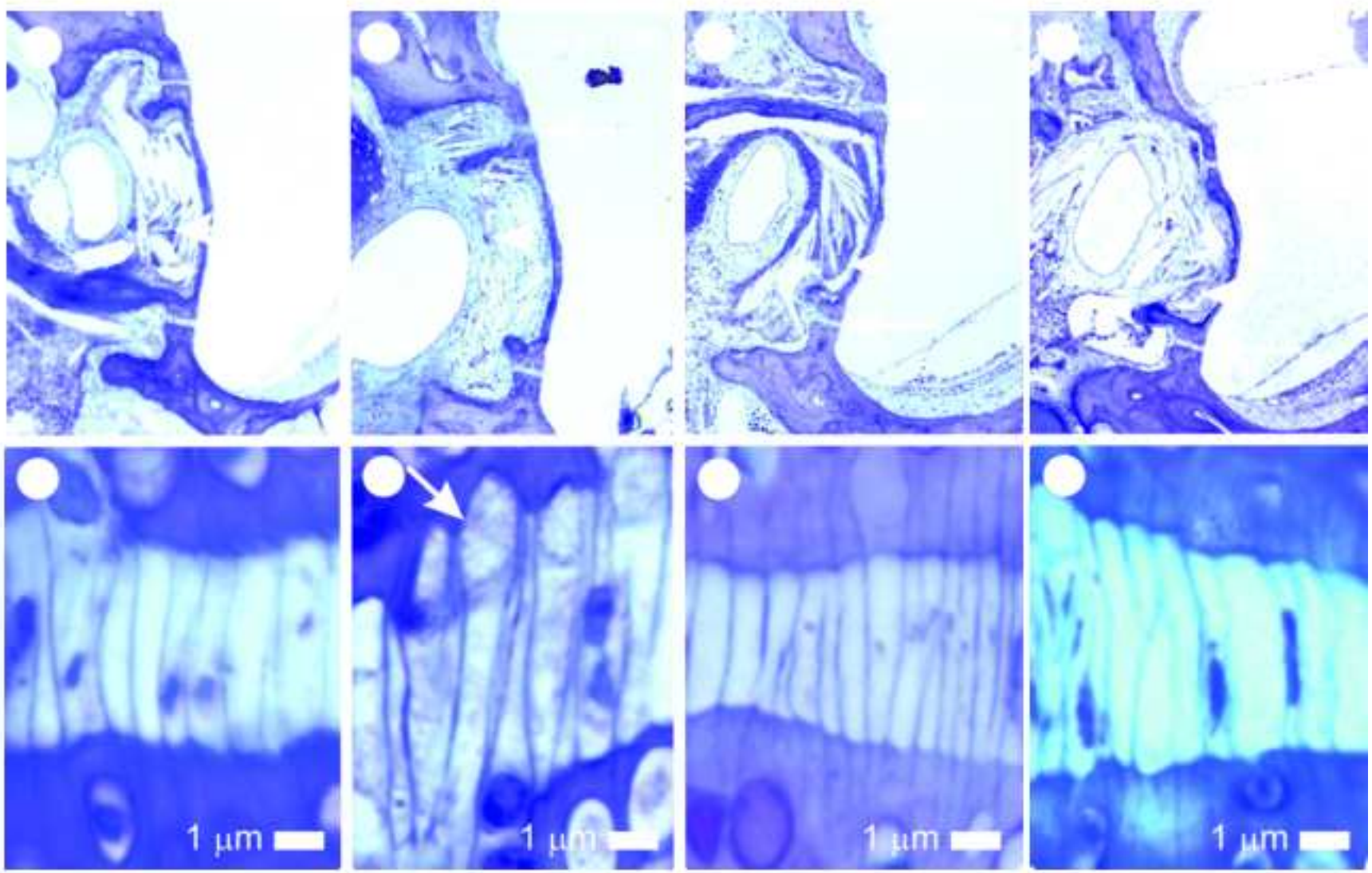

Figure 5
Click here to download high resolution image

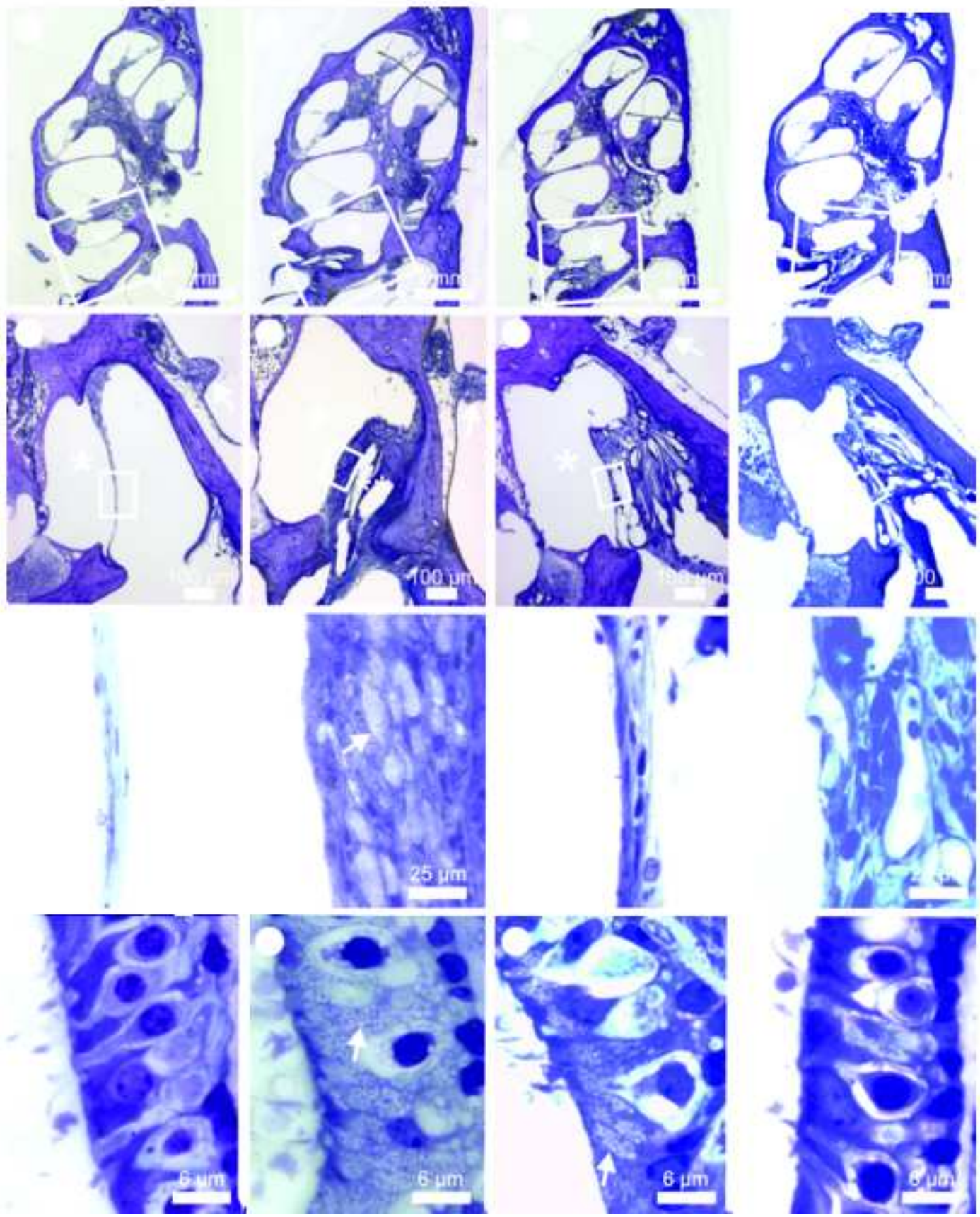

Figure 6
Click here to download high resolution image

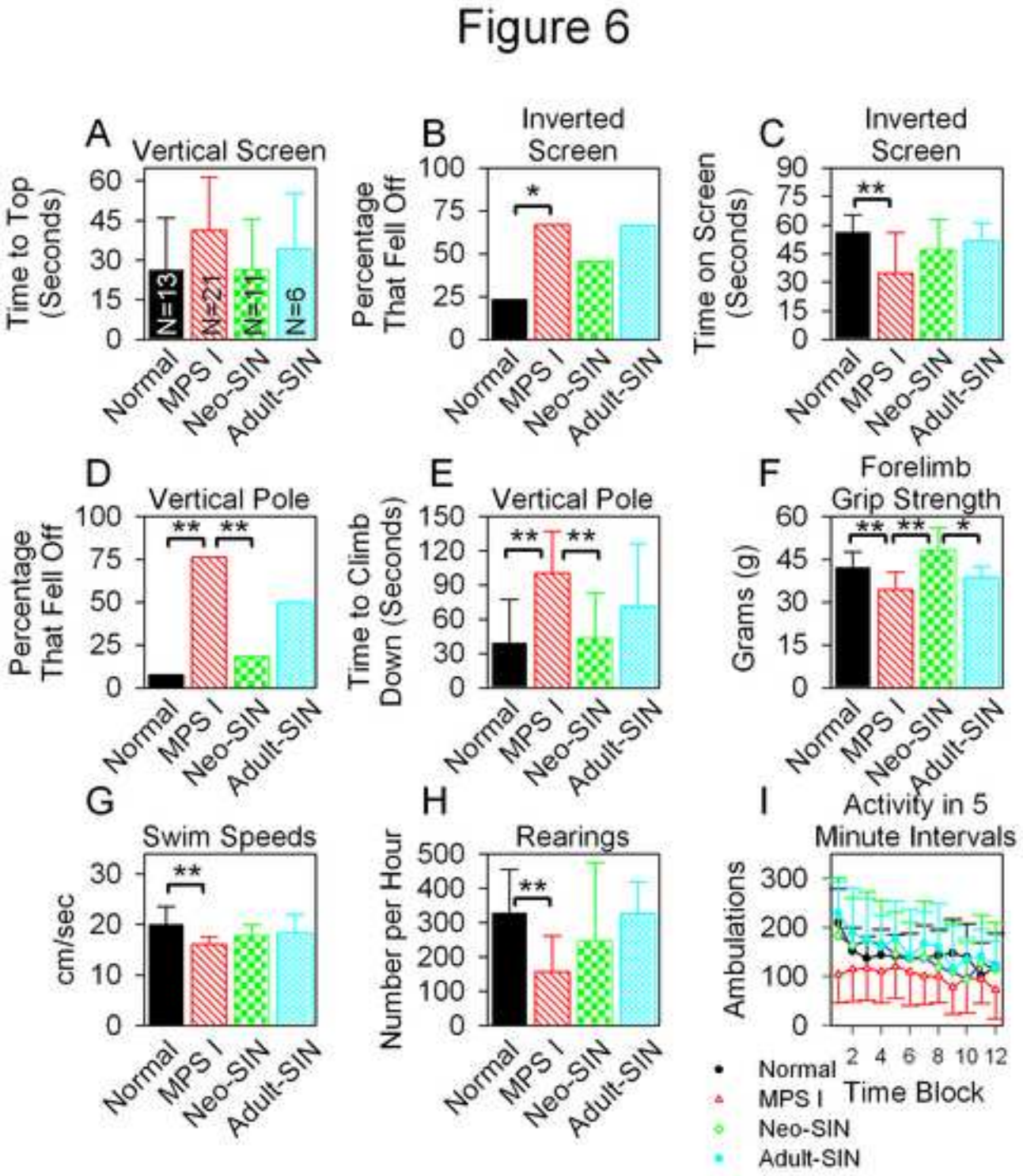

Supplementary Figure 1

Click here to download Other material: Vectors Supplement Fig. 1.tif

Supplementary Figure 2
Click here to download Other material: Supplementary Figure 2.tif

A comparison of enzyme replacement therapy started at birth or at adult age in mucopolissacharidosis type I mice

Baldo G[1,2], Mayer F[1], Martinelli BZ[1,2], de Carvalho TG[1,3], Meyer F[4], de Oliveira P[5], Meurer L[6], Tavares A[7], Matte U[1,3], Giugliani R[1,2,3].

[1]Centro de Terapia Gênica- Hospital de Clinicas de Porto Alegre, RS, Brazil.
[2]Programa de Pós-graduação em Ciências Biológicas: Bioquímica, UFRGS, RS, Brazil.
[3]Programa de Pós-graduação em Genética e Biologia Molecular, UFRGS, RS, Brazil.
[4]Unidade de Experimentação Animal, Hospital de Clinicas de Porto Alegre, RS, Brazil.
[5]Laboratório de Doenças Auto-imunes, HCPA, RS, Brazil.
[6]Unidade de Patologia Experimental, Hospital de Clinicas de Porto Alegre, RS, Brazil
[7]Programa de Pós-graduação em Fisiologia, UFRGS, RS, Brazil.

Abstract

Since we previously observed that in patients with mucopolysaccharidosis (MPS) the storage of undegraded glycosaminoglycans (GAG) occurs from birth, in the present study we aimed to compare normal, untreated MPS I mice, and MPS I mice treated with Laronidase (1.2 mg/kg every 2 weeks) started from birth (ERT-neo) or from 2 months of age (ERT-ad). Both treatments were equally effective in normalizing GAG levels in the liver, kidney, lung, testis and heart. Heart function analyzed by echocardiography was also improved with both treatments. On the other hand, mice treated from birth presented better outcomes in the difficult-to-treat aortas and heart valves. Knee joints were evaluated and we did not observe improvements in treated groups. Surprisingly, both groups showed improvements in behavior tests, and reduced GAG levels in the brain. Therefore we treated some three-month old animals with a single dose of Laronidase. IDUA injection resulted in detectable levels in the brain tissue 1 hour after administration, suggesting that the enzyme crossed the BBB. ERT-ad mice developed significantly more anti-IDUA-IgG antibodies, and mice that didn't develop antibodies had better performances in behavior tests. Our results suggest that ERT started from birth leads to better outcomes in the aorta and heart valves, as well as a reduction in antibody levels. Some poor vascularized organs, such as the joints, aorta and heart valves show partial or no benefit and ancillary therapies might be needed for patients. Treatment from birth should be considered whenever possible.

1. Introduction

Mucopolysaccharidosys type I (MPS I) is a disorder characterized by deficiency of the lysosomal hydrolase alpha-L-iduronidase (IDUA) and storage of undegraded glycosaminoglycans (GAG) heparan sulphate and dermatan sulphate. The disease spectrum varies from the severe Hurler syndrome (OMIM #67014) to the attenuated Scheie syndrome (OMIM # 67016). The Hurler form presents severe mental retardation in addition to other systemic manifestations (organomegaly, heart enlargement, joint stiffness) which are also found in the attenuated forms of the disease (Martins et al, 2010).

Enzyme replacement therapy (ERT) is available for MPS I patients since early 2000`s, and it is currently the most used treatment for this disorder (Giugliani et al, 2010). It relies on the ability of deficient cells to internalize a systemic delivered enzyme using the mannose-6-phosphate receptor (Matte et al, 2011), which reaches the lysosome and degrades the GAG.

In the later years, reports in large animal models (Dierenfeld et al, 2010) and human subjects (Wraith et al, 2007) suggest that early introduction of ERT leads to better outcomes. For example, a multicentric clinical study with early treatment (started before 5 years of age) reported improvement in heart function, decrease in urinary GAG and normal mental development (Wraith et al, 2007). However, a systematic comparison of ERT started at birth or at young adult age was never performed.

We have recently described that in human patients with different types of MPS, GAG storage can be detected already in the placental tissue, suggesting that in those patients GAG accumulation starts in the fetal life (Baldo et al, 2011). Therefore, we decided to systematically investigate the benefits from ERT started at birth comparing to the adult period in MPS I mice.

2. Material and Methods

2.1 Experimental Groups

The study was approved by the authors' institutional ethics review board and mice on a C57BL/6 background (kindly donated by Dr Elizabeth Neufeld, UCLA, USA) were used. MPS I and normal mice were genotyped by PCR as previously described (Baldo et al, submitted).

We compared four groups of male mice: in the first group, MPS I mice (knockout for the IDUA gene) received ERT (Laronidase®, Genzyme) from birth (ERT-neo, n=10) at 1.2 mg/kg intravenously every two weeks. The second group received the same treatment but it was started at 60 days of age (ERT-ad, n=8). We compared those groups to untreated MPS I mice (MPS I, n=13) and to wild-type mice (Normal, n=10). All animals were weighted and sacrificed at 6 months of age. In treated mice, the sacrifice was performed two weeks after the last injection.

In addition, some 3-4 month-old MPS I mice were injected with a single dose of laronidase (0, 1.2 or 2.4 mg enzyme/kg weight) through the tail vein. Animals were anesthetized, serum was collected and animals were perfused with 20mL of PBS 1 hour after the injection to measure enzyme activity in the brain.

2.2 IDUA activity

Tissues were homogeneized with a dismembrator in distilled water. Alpha-L-iduronidase activity assay was performed incubating the protein extracts with the fluorescent substrate 4-methylumbelliferyl-alpha-L-iduronide (Glycosynth, UK) at 37^{o}C for 1h in pH 3.5 formate buffer (Baldo et al, 2012). Results were expressed as fold-change, compared to MPS I untreated mice. Protein content was measured using the method described by Lowry.

2.3 Cathepsin D activity

Tissues were homogeneized in 100 mM sodium acetate pH 5.5 containing 2.5 mM ethylenediaminetetraacetic acid, 0.1% Triton X-100, and 2.5 mM dithiothreitol. The cathepsin D (CtsD) assay was performed at pH 4 with 5 μM of the substrate 7-methoxycoumarin-4-acetyl (Mca)-Gly-Lys- Pro-Ile-Leu-Phe-Phe-Arg-Leu-Lys-2,4 nitrophenyl (Dnp)-D-Arg-NH2, which can also be cleaved by CtsE, with Mca-Pro-Leu-OH (Enzo Life Sciences, USA) as the standard, as previously described (Baldo et al, 2011).

2.4 GAG measurement

Tissues were homogeneized in phosphate buffer and GAGs were measured using the dymethyl blue technique. In this technique, 25 uL of supernatant was mixed with freshly prepared dymethyl blue solution (Dymethyl blue 0.3 mol/L with 2 mol/L Tris) and absorbance was read at 530 nm. Results were expressed as percentage of normal

mice. Urine samples were centrifuged and 25 µL were used for measuring GAG levels, and results were calculated as µg GAG/mg creatinine and expressed as % from normal values. Creatinine was measured using the Picric acid method (Baldo et al, in press).

2.5 Echocardiographic analysis

Six-month old mice were anesthetized with isofluorane and positioned on a controlled temperature bed. Animals were placed in left lateral decubitus position (45° angle) to obtain cardiac images. An EnVisor HD System, Philips Medical (Andover, MA, USA), with a 12-4 MHz transducer was used, at 2 cm depth with fundamental and harmonic imaging. Images were captured by a trained operator with experience in small animal echocardiography.

Left ventricular ejection fraction (LVEF) was calculated as: (end diastolic volume− end-systolic volume/ end-diastolic volume) × 100; end-diastolic and end-systolic cavity volumes were calculated using Simpson's rule (Tavares et al, 2010). LV fraction shortening (LVFS) values were obtained using the following equation: LVFS = DD − SD / DD × 100 (diastolic diameter — DD; systolic diameter — SD). Fractional area change (FAC) was calculated as follows: FAC = diastolic area – systolic area / diastolic area.

In the pulmonary valve the measures of the ejection and acceleration times were obtained using Doppler echocardiography, and their ratio was used as an index of pulmonary vascular resistance (PVR) (Jones et al, 2002).

2.6 Behavioral tests

2.6.1 Open field test

Locomotor and exploratory activities were accessed using an open field test. The test consisted of a square arena (52 × 52 cm^2) with 60 cm high walls. The floor was divided into 16 squares by parallel and intersecting lines, obtaining four centered squares and 12 periphery squares. Mice were placed in one of the corners of the open field and (a) ambulation (number of times a mouse crossed with 4 paws one of the lines in the floor), and (b) exploratory behavior (rearings) were observed during 5 min for both control and MPS I animals.

2.6.2 Repeated Open field

This test is used as a measure of habituation memory. In this test, mice are put in the open field apparatus for 5 min and activity (number of crossings and rearings) is measured. The test is repeated 30 and 60 minutes after the first trial to evaluate habituation to the new environment (a reduction in the activity should be observed in mice after each trial), and the results from the third trial are compared to the first one.

2.7 Histological analysis

At the time of sacrifice, mice were anesthetized, serum was collected by retro-orbital puncture and mice were sacrificed by cervical dislocation. Liver, lungs, kidneys, heart, testicles, aorta, and brain (cerebellum, cortex and hippocampus) were isolated and systematically divided in two pieces. One was flash frozen in liquid nitrogen for biochemical analysis and the other portion was fixed in buffered formalin. Thin cross sections were submitted to routine histological processing, stained with hematoxylin-eosin/alcian blue and analyzed.

Heart valves were obtained by sectioning the basal part of the heart, and valve thickness was measured in at least 5 different points using a software (CellF, Olympus, Hamburg, Germany) and the average was used as a measure of the valve thickness.

Knee joints were collected and placed in buffered formalin for 2-7 days following decalcification with EDTA 14% for an additional week. Paraffin processing was performed according to routine techniques. A score was created to evaluate histological abnormalities, according to our previous study (supplementary table 1). The higher the score, the worse are the joints (de Oliveira et al, submitted).

2.8 Antibody formation

We measured the formation of antibodies against the recombinant enzyme in serum collected at time of sacrifice. For the assay, 96-well ELISA plates were coated with 4 μg/mL of Laronidase in acid PBS overnight and blocked with 3% BSA. Diluted serum was added (1:50) and incubated for 2h. A secondary antibody (Goat anti-mouse IgG, Sigma, USA) conjugated to peroxidase was diluted 1:1000, incubated for 3h and revealed with TMB for 6 minutes. The reaction was stopped with H_2SO_4 1M and the absorbance read at 450 nm (Baldo et al, in press).

2.9 Ethics and Statistics

All experiments were approved by the ethics committee of our institution with all experiments monitored by our veterinary. For statistical analysis SigmaStat version 3.0 was used. Results were compared using ANOVA and Tukey or student t test, as indicated. A $p<0.05$ was considered as statistically significant.

3. Results

3.1 Body weight and urinary GAG

No obvious adverse reactions were observed in ERT-neo or ERT-ad. MPS I mice were significantly heavier than normal mice (31.6 g vs 26 g, $p<0.01$). Mice treated from birth presented a significant reduction in their weight, compared to MPS I untreated mice (27.2 g, $p<0.01$) while mice treated from 2 months presented intermediate weight (30.1 g), which was not different from untreated mice (figure 1A). Urinary GAG presented a 56% reduction in ERT-neo mice and a 48% reduction in ERT-ad, both being significant compared to untreated MPS I ($p<0.05$) and not different from normal mice (figure 1B).

3.2 GAG storage in visceral organs

Tissue GAG were extracted and quantified. GAG levels were elevated in liver (5.5-fold the normal values, $p < 0.05$ vs normal), kidney (4.1-fold, $p<0.05$), heart (2.5-fold, $p < 0.05$) and lungs (2-fold, $p<0.05$). Both ERT-neo and ERT-ad were equally effective in restoring normal GAG levels (figure 2A). Furthermore, histological analysis confirmed the reduction in tissue GAG in these organs and also in the testis (figure 2B).

3.3 Heart function

Echocardiography analysis was performed in 6-month old mice to analyze heart function. MPS I animals presented abnormalities in the left ventricle, with reduced ejection fraction, shortening fraction and fractional area change ($p<0.05$ vs normal). Untreated mice also had a reduced AT/ET ratio in the pulmonary valve, which might indicate a pulmonary hypertension. Both treatments were able to restore normal heart function, with Neo-ERT performing slightly better (figure 3).

3.4 Aorta and heart valves

MPS I mice present aorta dilatation and heart valves thickening. Those structures have been proving to be hard to correct by existing therapies, therefore we measured thickening of heart valves and aorta in these mice. MPS I mice aortas were distended (2.2-fold normal, $p< 0.01$ vs normal) and had high amounts of storage, as evidenced by white vacuoles that can be visualized in H-E staining (figure 4 A). ERT-neo aortas were 1.5-fold the normal values (not significant versus normal, $p<0.05$ versus MPS I) while ERT-ad were 1.8-fold the normal values ($p<0.05$ versus normal, not significant vs MPS I). Both treated groups still had some degree of storage in the aortas.

The width of heart valves from the left ventricle was also measured at 6 months (figure 4B). Untreated MPS I mice presented thickened heart valves, which were 3.5-fold the normal values ($p<0.01$). ERT-neo group showed a significant reduction (1.4-fold normal, $p<0.01$ compared to MPS I, not significant versus normal), while ERT-ad presented intermediate values (2.1-fold normal) which were not different from either normal ($p=0.088$) or MPS I ($p=0.052$) values. These results suggest that the heart valve is hard to correct, but ERT-neo seem to better prevent the thickening of these structures.

3.5 Brain function

Brain function was assessed using the open field test. MPS I mice have reduced crossings and rearings at the open field test, as previously reported (Baldo et al, *in press*). Surprisingly, both ERT-neo and ERT-ad had marked improvements in their locomotor activity and exploratory behavior (figure 5A).

The open field can be used as a test of non-aversive memory if done repeated times. MPS I mice fail to habituate to the new environment, evidenced by a very small reduction in their activity comparing the first and the third trials. On the other hand, ERT-neo and ERT-ad mice habituate similarly to normal mice, and their activity in the third trial was about 50-60% of the first trial (figure 5B).

Based on these results, we measured GAG in the cortex of these mice. GAG levels were in MPS I mice were 1.8-fold the normal values ($p< 0.01$ vs normal), and both treatment reduced GAG to normal levels (figure 5C). Since GAG levels were not markedly elevated, we measured activity of cathepsin D, which we have found to be consistently elevated in the brains of MPS I mice and could be used as a biomarker (unpublished data). The CtsD activity in MPS I mice was 5-fold normal ($p<0.01$ vs normal), and was reduced in ERT-neo (2.3-fold, not significant vs normal, $p<0.05$ vs

MPS I) and ERT-ad (1.8-fold, not significant versus normal, $p<0.05$ vs MPS I) as can be visualized in figure 5D.

3.6 IDUA crosses the blood-brain barrier

As our results from behavior and biochemical tests suggest that a fraction of the enzyme can cross the blood-brain-barrier, we decided to do an additional group of adult mice that were injected with 1.2 mg/kg of enzyme and sacrificed 1h later. IDUA activity was 1.7-fold higher than in the untreated mice in the hippocampus (not significant), 1.1-fold in the cerebellum (not significant) and 3-fold in the cortex ($p< 0.05$ vs untreated). When the dose was increased twice (2.4 mg/kg of body weight) enzyme levels were markedly elevated, reaching almost normal levels in some areas, as can be seen in figure 5E.

3.7 Joint analysis

We have created a score to better describe the abnormalities found in MPS I knee joints using H-E stain. These abnormalities included presence of a mild inflammatory infiltrate and loss of articular architecture, among other features. The average score of MPS I mice was significantly worse than Normal mice. In addition, both treatments were not able to improve joint aspect (figure 6).

3.8 Antibody formation and correlation with behavior test

We next sought to determine if treatment when started at earlier times could lead to a reduced antibody response against the enzyme. Using an ELISA assay, we could demonstrate that anti-IDUA antibodies could be detected in only 1 animal out of seven ERT-neo tested mice. On the other hand, in Ad-ERT mice, we detected antibodies in 5 out of 7 animals tested ($p<0.05$, compared to other groups). No antibodies were detected in normal or untreated MPS I mice (figure 7A).

We then hypothesized that, since only a small fraction of IDUA was able to cross the BBB, the development of antibodies against IDUA could reduce serum enzyme availability and less enzyme would be reaching the brain. When we separated mice who developed antibodies from those who didn't (regardless when treatment was started), the mice who developed antibodies were the ones who failed to habituate to a new environment in the repeated open field test ($p<0.05$, figure 7B).

4. Discussion

Several clinical studies have demonstrated improvement in biochemical and functional measures of MPS I disease after treatment with laronidase (Kakkis et al, 2001; Wraith et al, 2004). Also, a clinical study performed in children younger than 5 years have shown reduction liver and heart dimensions and normal mental development (Wraith et al, 2007). In addition, a study performed in MPS I dogs has shown that a higher dose of the enzyme (1.6 mg/kg) led to normalization of GAG storage in visceral organs, synovium and the mitral valve, as well as the brain (Dierenfeld et al, 2010). All these studies as well as our previous observation that GAG storage occurs from birth in MPS patients (Baldo et al, 2011) led us to systematically investigate the benefits from neonatal treatment comparing to treatment started at adult age in MPS I mice.

The abnormal heavier weight observed in MPS I mice may be attributed to abnormalities in liver and spleen sizes, to metabolic alterations, as well as bone disease (Pan et al, 2008; Woloszynek et al, 2007). Our results suggest that, when weight is evaluated, ll the ERT-neo mice have a better outcome than ERT-ad, although results might not be significant for ERT-ad due to a smaller number of animals analyzed. The urinary GAG levels are used as a biomarker of treatment effectiveness, and results suggest that both treatments lead to improvements.

GAG levels were elevated in visceral organs, and both treatments were equally effective in reducing them. However, results from previous studies have shown contradictory results regarding improvement of heart function after ERT (Braulin et al, 2006; Sifuentes et al, 2007; Wraith et al, 2007). Therefore, we evaluated several parameters using echocardiography. Both treatments were able to restore left ventricular function, as well as pulmonary hypertension parameters in mice, suggesting that ERT can prevent heart disease in MPS I.

The aorta and the heart valves in mucopolysaccharidosis have been shown to be difficult to treat by ERT, HSCT or even gene therapy (Baldo et al, 2011; Braulin et al, 2006; Sifuentes et al, 2007; Watanabe et al, 2011) and therefore they are structures that need a careful evaluation. In the present work, we measured thickness of the heart valves and ascending aorta, as well as the storage in these structures. Both treatments were only partially effective in treating these aspects of the disease, however we could observe that ERT-neo had results that approached the normal group. The aortas in MPS I mice show loss of elastin and increased distension as early as 1.5 months, which is

progressive (Ma et al, 2008). We suggest that the benefit from early treatment comes from the fact that once established, the structural changes in these organs cannot be reverted, and therefore treatment should be started before the onset of symptoms. Also, these organs seem to be only partially corrected, since GAG storage was still present even in treated mice, possibly because these structures are poorly vascularized.

One of the most unexpected findings of this study is certainly the improvement in brain function. It is believed that the recombinant enzyme is not able to cross the blood-brain-barrier (BBB) and reach the brain (Kakkis et al, 2001), although some studies suggest improvements in cognitive function in treated MPS I children (Wraith et al, 2007; Wang et al, 2009). Here, we have shown that both ERT-neo and ERT-ad groups improved in behavioral tests and reduced GAG levels in the cortex. Furthermore, we evaluated the activity of cathepsin D, which was found to be markedly elevated in MPS I mice and reduced in both treated groups. Cathepsin D activity was measures since we have previously shown that other lysosomal enzymes are usually elevated in MPS I, and normalization of their activities is a good biochemical indicator of correction of disease (Baldo et al 2011). It is interesting to notice that mice treated from 2 months also showed improvements, since at this time point abnormalities such as hypoactivity (Pan et al, 2008) as well as increase neuroinflammation (Baldo et al, submitted) could already be detectable in these mice. Our results raise the question if the brain disease is complete irreversible in MPS I as initially thought.

Based on those findings, we tested if the enzyme was able to cross the BBB in the dose that we have administered (1.2 mg/kg) as well as at a higher dose (2.4 mg/kg). We found a small increase in IDUA activity in the brain cortex with the 1.2 mg/kg dose, and a major increase in all brain regions with the higher dose. A recent study (Dierenfeld et al, 2010) in dogs have also found a reduction in GAG levels in the brain even with a smaller dose (0.6mg/kg), confirming that some enzyme can cross the BBB in animal models. We have also shown that gene therapy with a retroviral vector reaches high serum activity and some enzyme can be detected in the brain and reduce tissue GAG levels (Baldo et al, submitted). However, in the gene therapy study, we cannot exclude the possibility that the enzyme was being taken to the brain by immune cells that migrated through the BB. This seems not to be the case in the present work, since mice were sacrificed 1 hour after the injection, not giving enough time for a significant amount of cells to get the enzyme and cross the BBB.

Despite marked improvements in the brain, some organs did not show any improvement. We have recently developed a score to evaluate the histological disease of MPS I mice and we demonstrated that ERT started at 2 months was not effective in correcting the disease (de Oliveira et al, submitted). In the present work we extend those findings to the ERT-neo group, confirming that the poor vascularized joint is also difficult to correct, despite early treatment. The results in patients suggest that ERT is only able to slow the progression of the symptoms (Tylki-Szymanska et al, 2010), and suggest that improvement in bone and joint disease might pass through ancillary therapies.

Finally, antibody levels were measured as we have previously described (Baldo et al, in press). ERT-ad mice developed higher antibody levels than ERT-neo mice, consistent with the induction of immune tolerance in neonates, which have been described before in MPS I dogs (Dierenfeld et al, 2010). Interestingly, mice who developed antibodies performed significantly worse in the open field habituation test, suggesting that the presence of serum antibodies might be neutralizing part of the serum IDUA, and reducing the fraction of the enzyme that crosses the BBB. Since most of MPS I patients also develop neutralizing antibodies (Kakavanos et al, 2003; Ponder, 2008), the early treatment could lead to a better efficacy of the therapy.

In conclusion, our results suggest that early introduction of ERT is more effective in preventing abnormalities in the aorta and the heart valves, as well as in reducing anti-Laronidase antibodies, while other parameters do not show marked differences from late treatment. Neonatal treatment should be considered whenever possible.

5. Acknowledgements

The authors would like to thank Elizabeth Neufeld (UCLA, USA) for providing the MPS I mice. Grant support was provided by Conselho Nacional de Desenvolvimento Cientifico (CNPq) and Fundo de Incentivo a Pesquisa do HCPA (FIPE-HCPA).

6. References

Baldo G, Metcalf J, Wozniak D, Ohlemiller KO, Ma X, Zhang Y, Giugliani R, Ponder KP. Retroviral Vector-mediated Gene Therapy to Mucopolysaccharidosis I Mice Improves Behavior and Sensorimotor Abnormalities. Journal Of Inherited Metabolic disease, submitted.

Baldo G, Mayer FQ, Martinelli B , Dilda A, Meyer F, Ponder KP, Giugliani R, Matte U. Evidence of a progressive motor dysfunction in Mucopolysaccharidosis type I mice. Behav Brain Res, *in press*.

Baldo G, Mayer FQ, Martinelli B, Meyer FS, Burin M, Meurer L, Tavares AMV, Giugliani R, Matte U. Intraperitoneal implant of recombinant encapsulated cells overexpressing alpha-L-iduronidase partially corrects visceral pathology in Mucopolysaccharidosis type I mice. Cytotherapy, *in press*.

Baldo G, Matte U, Artigalas O, Schwartz IV, Burin MG, Ribeiro E, Horovitz D, Magalhaes TP, Elleder M, Giugliani R. Placenta analysis of prenatally diagnosed patients reveals early GAG storage in mucopolysaccharidoses II and VI. Mol Genet Metab. 2011 Jun;103(2):197-8.

Baldo G, Wu S, Howe RA, Ramamoothy M, Knutsen RH, Fang J, Mecham RP, Liu Y, Wu X, Atkinson JP, Ponder KP. Pathogenesis of aortic dilatation in mucopolysaccharidosis VII mice may involve complement activation. Mol Genet Metab. 2011; 104(4):608-19.

Baldo G, Quoos Mayer F, Burin M, Carrillo-Farga J, Matte U, Giugliani R. Recombinant encapsulated cells overexpressing alpha-L-iduronidase correct enzyme deficiency in human mucopolysaccharidosis type I cells. Cells Tissues Organs. 2012; 195(4):323-9.

Braunlin EA, Berry JM, Whitley CB. Cardiac findings after enzyme replacement therapy for mucopolysaccharidosis type I. Am J Cardiol. 2006; 98(3):416-8.

de Oliveira PG, Baldo G, Mayer FQ, Martinelli B, Meurer L, Giugliani R, Matte U, Xavier RM. Characterization of joint disease in mucopolysaccharidosis type I mice and the effects of enzyme replacement therapy. Osteoarthritis and cartilage, submitted.

Dierenfeld AD, McEntee MF, Vogler CA, Vite CH, Chen AH, Passage M, Le S, Shah S, Jens JK, Snella EM, Kline KL, Parkes JD, Ware WA, Moran LE, Fales-Williams AJ, Wengert JA, Whitley RD, Betts DM, Boal AM, Riedesel EA, Gross W, Ellinwood NM, Dickson PI. Replacing the enzyme alpha-L-iduronidase at birth ameliorates symptoms in the brain and periphery of dogs with mucopolysaccharidosis type I. Sci Transl Med. 2010; 2(60):60ra89.

Giugliani R, Federhen A, Rojas MV, Vieira T, Artigalás O, Pinto LL, Azevedo AC, Acosta A, Bonfim C, Lourenço CM, Kim CA, Horovitz D, Bonfim D, Norato D, Marinho D, Palhares D, Santos ES, Ribeiro E, Valadares E, Guarany F, de Lucca GR, Pimentel H, de Souza IN, Correa J Neto, Fraga JC, Goes JE, Cabral JM, Simionato J, Llerena J Jr, Jardim L, Giuliani L, da Silva LC, Santos ML, Moreira MA, Kerstenetzky M, Ribeiro M, Ruas N, Barrios P, Aranda P, Honjo R, Boy R, Costa R, Souza C, Alcantara FF, Avilla SG, Fagondes S, Martins AM. Mucopolysaccharidosis I, II, and VI: Brief review and guidelines for treatment. Genet Mol Biol. 2010; 33(4):589-604.

Jones JE, Mendes L, Rudd MA, Russo G, Loscalzo J, Zhang YY. Serial noninvasive assessment of progressive pulmonary hypertension in a rat model. Am J Physiol Heart Circ Physiol 2002; 283: 364-371.

Kakavanos R, Turner CT, Hopwood JJ, Kakkis ED, Brooks DA. Immune tolerance after long-term enzyme-replacement therapy among patients who have mucopolysaccharidosis I. Lancet. 2003; 361(9369):1608-13.

Kakkis ED, Muenzer J, Tiller GE, et al. Enzyme replacement therapy in mucopolysaccharidosis I. N Engl J Med. 2001; 344: 182–188.

Kakkis ED, Schuchman E, He X, Wan Q, Kania S, Wiemelt S, Hasson CW, O'Malley T, Weil MA, Aguirre GA, Brown DE, Haskins ME. Enzyme replacement therapy in feline mucopolysaccharidosis I. Mol Genet Metab. 2001; 72(3):199-208.

Ma X, Tittiger M, Knutsen RH, Kovacs A, Schaller L, Mecham RP, Ponder KP. Upregulation of elastase proteins results in aortic dilatation in mucopolysaccharidosis I mice. Mol Genet Metab. 2008; 94(3):298-304.

Martins AM, Dualibi AP, Norato D, Takata ET, Santos ES, Valadares ER, Porta G, de Luca G, Moreira G, Pimentel H, Coelho J, Brum JM, Semionato Filho J, Kerstenetzky MS, Guimarães MR, Rojas MV, Aranda PC, Pires RF, Faria RG, Mota RM, Matte U, Guedes ZC. Guidelines for the management of mucopolysaccharidosis type I. J Pediatr. 2009; 155(4 Suppl):S32-46.

Matte U, Lagranha VL, de Carvalho TG, Mayer FQ, Giugliani R. Cell microencapsulation: a potential tool for the treatment of neuronopathic lysosomal storage diseases. J Inherit Metab Dis. 2011 Oct;34(5):983-90.

Pan D, Sciascia A 2nd, Vorhees CV, Williams MT. Progression of multiple behavioral deficits with various ages of onset in a murine model of Hurler syndrome. Brain Res. 2008; 1188:241-53.

Ponder KP. Immune response hinders therapy for lysosomal storage diseases. J Clin Invest. 2008; 118(8):2686-9.

Wraith JE, Clarke LA, Beck M, et al. Enzyme replacement therapy for mucopolysaccharidosis I: a randomized, doubleblinded, placebo-controlled, multinational study of recombinant human alpha-L-iduronidase (laronidase). J Pediatr. 2004; 144:581–588

Wraith JE, Beck M, Lane R, van der Ploeg A, Shapiro E, Xue Y, Kakkis ED, Guffon N. Enzyme replacement therapy in patients who have mucopolysaccharidosis I and are younger than 5 years: results of a multinational study of recombinant human alpha-L-iduronidase (laronidase). Pediatrics. 2007; 120(1):e37-46.

Sifuentes M, Doroshow R, Hoft R, Mason G, Walot I, Diament M, Okazaki S, Huff K, Cox GF, Swiedler SJ, Kakkis ED. A follow-up study of MPS I patients treated with laronidase enzyme replacement therapy for 6 years. Mol Genet Metab. 2007; 90(2):171-80.

Tavares AM, da Rosa Araújo AS, Baldo G, Matte U, Khaper N, Belló-Klein A, Rohde LE, Clausell N. Bone marrow derived cells decrease inflammation but not oxidative stress in an experimental model of acute myocardial infarction. Life Sci. 2010; 87(23-26):699-706.

Tylki-Szymanska A, Marucha J, Jurecka A, Syczewska M, Czartoryska B. Efficacy of recombinant human alpha-L-iduronidase (laronidase) on restricted range of motion of upper extremities in mucopolysaccharidosis type I patients. J Inherit Metab Dis. 2010; 33:151-7.

Wang RY, Cambray-Forker EJ, Ohanian K, Karlin DS, Covault KK, Schwartz PH, Abdenur JE. Treatment reduces or stabilizes brain imaging abnormalities in patients with MPS I and II. Mol Genet Metab. 2009 Dec;98(4):406-11.

Watanabe N, Anagnostopoulos PV, Azakie A. Aortic stenosis in a patient with Hurler's syndrome after bone marrow transplantation. Cardiol Young. 2011 Jun;21(3):349-50.

Woloszynek JC, Coleman T, Semenkovich CF, Sands MS. Lysosomal dysfunction results in altered energy balance. J Biol Chem. 2007; 282(49):35765-71

Figures

Figure 1: Body weight and urinary GAG levels at 6 months. a) Body weight. Mice were weighed at 6 months. **p<0.01 and * p<0.05, compared to normal. ANOVA and Tukey *post hoc* b) Urinary GAG. Urine was collected from 6-month old mice, 2 weeks after the last Laronidase injection. *P<0.05 compared to normal, ANOVA and Tukey *post hoc*.

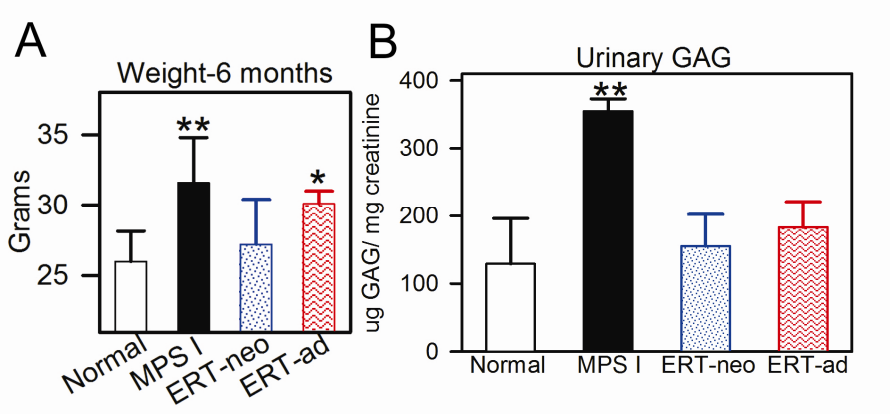

Figure 2: Tissue GAG levels. A) Tissue GAG were measured using the dymethil blue technique in visceral organs, and results are presented as percentage of normal levels. *P<0.05 compared to normal levels, ANOVA and Tukey post hoc. N=5-6/ group. B) Representative histological sections stained with H-E/ alcian blue (which show GAG storage in blue, indicated by black arrows) in visceral organs.

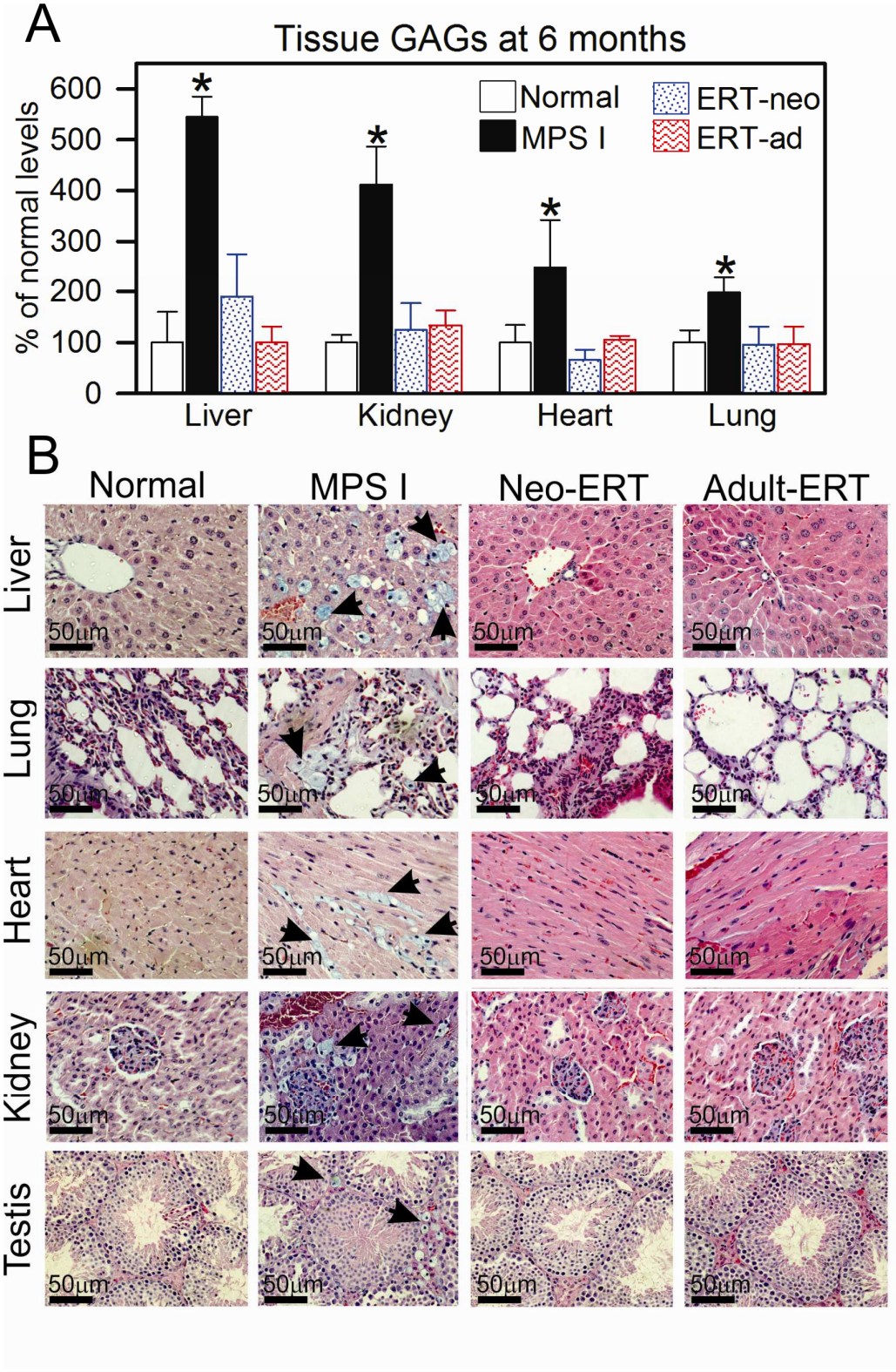

Figure 3: Results from echocardiography. Analyses were performed in 6-month old mice as described in methods section. A) Ejection fraction. B) Shortening fraction. C) Fractional area change and D) The ratio between ejection and acceleration times measured at the pulmonary valve. The 3 first parameters suggest left ventricular dysfunction, while the AT/ET ratio suggests pulmonary hypertension in MPS I mice. *P<0.05 compared to normal, ANOVA and Tukey. N= 6-13 animals/group.

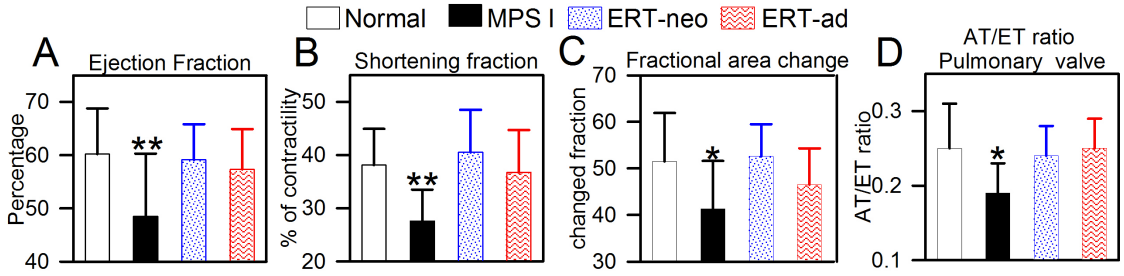

Figure 4: Aorta and heart valves. A) Example of ascending aortas and heart valves from normal, MPS I and ERT-treated groups stained with H-E/alcian blue. Note aortic distension, valve thickening and storage (arrows) in MPS I mice and GAG storage (white vacuoles, arrow). B) Quantification of aortic distension in the 4 groups N=3-8 animals/group. C) Quantification of heart valve thickness. N=3-4/group. * P<0.05; ** P<0.01, ANOVA and Tukey *post hoc*.

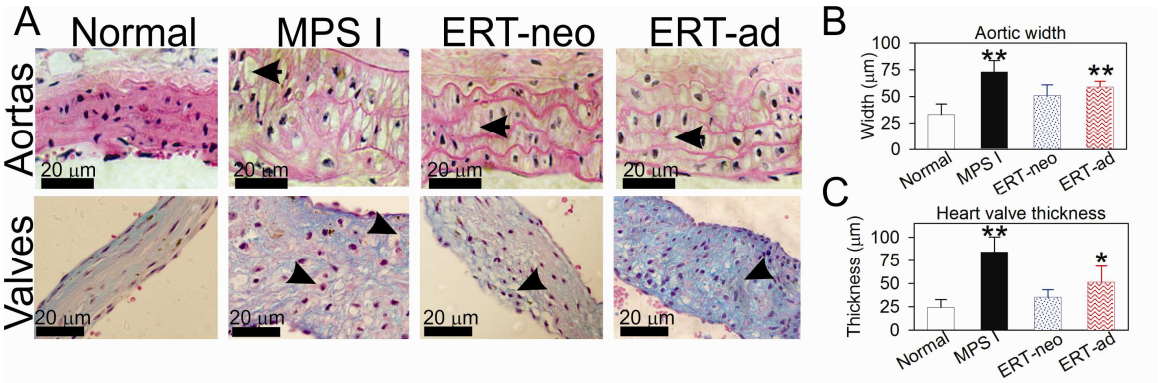

Figure 5: Improvements in brain disease at 6 months. A) Open field test was used as a measure of locomotor (crossings) and exploratory (rearings) activities. N=6-9/group B) The repeated open field test is a measure of habituation (non-aversive memory). The activity in the 3rd trial was compared to the 1st trial, as results are expressed as percentage of activity from 1st trial. N=6-9/group C) GAG levels measured in the brain cortex. N=5-6/group D) Cathepsin D (CtsD) activity was measured at pH 4 using a fluorescent substrate. N=5/group. E) IDUA activity in 3-month old treated mice. For this experiment, mice received a single injection of 1.2 mg/kg (n=4) or 2.4 mg/kg (n=2) of Laronidase, and 1 hour later, brain was perfused and collected for IDUA assay, and results were compared to untreated mice. Enzyme activity could be detected in the brain areas, suggesting that the enzyme could cross the blood-brain-barrier.*p<0.05; **p<0.01, ANOVA and Tukey.

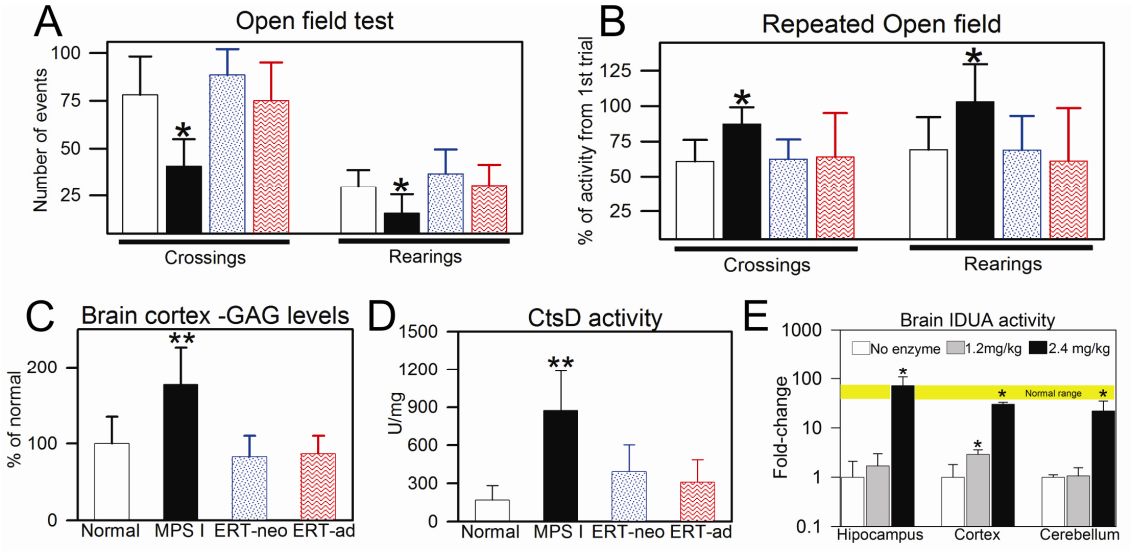

Figure 6: Joint disease. A) A score was created based on the abnormalities found in untreated MPS I mice, and no benefit was found from either ERT-neo or ERT-ad treatments. *p<0.05, ANOVA and Tukey post hoc versus normal. N=7-10/group.

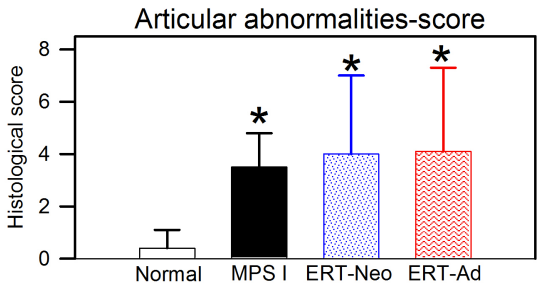

Figure 7: Antibody formation. A) Serum IgG-anti-Laronidase antibodies in mice at 6-months. Each dot represents results from individual mice. ERT-ad developed significantly higher levels of antibodies ($p<0.05$ compared to other groups, ANOVA and Tukey *post hoc*). B) Analysis of performance in repeated open field test in mice who develop antibodies and those who did not. Treated mice that developed antibodies (n=4) were separated from those who didn't (n=8), regardless when treatment was started, and analysis of repeated open field test suggests that the ones who develop antibodies perform worse in the test. $P<0.05$ compared to animals who didn't develop antibodies, Student`s t test.

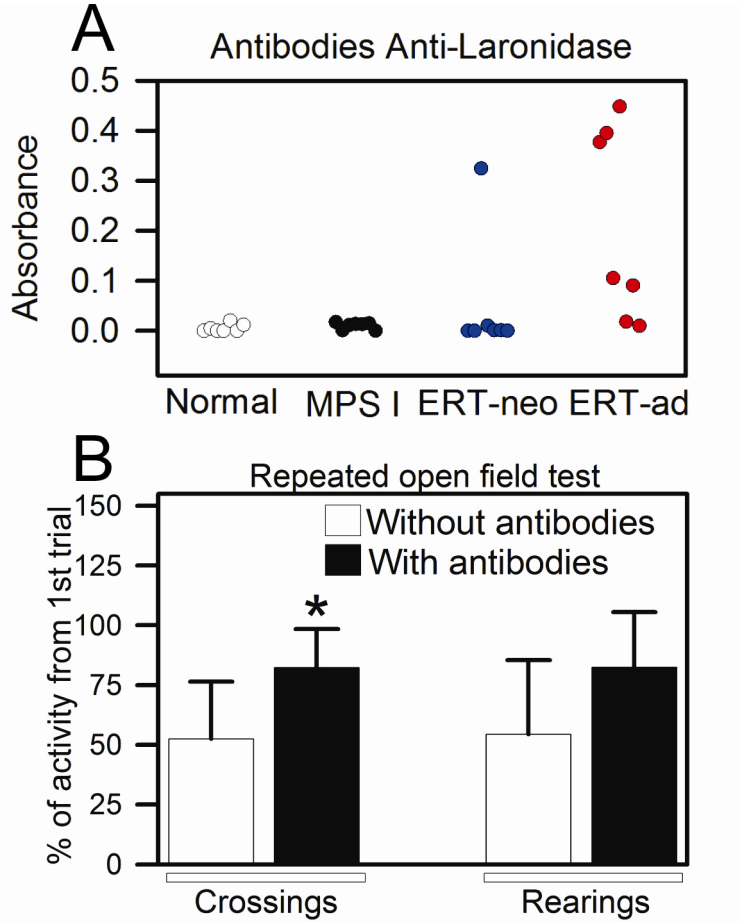

Suppl. table 1: Histological score used to evaluate MPS I joints and effect of treatments with ERT in H-E slides.

Abnormality	**Score**
Presence of inflammatory infiltrate	0- absent 1-present
Fibrocartilaginous proliferation	0-absent; 1- mild; 2 moderate; 3-severe
Bone resorption	0-absent; 1- mild; 2 moderate; 3-severe
Damage of articular surface	0- absent 1-present
Fibrocartilaganous bridge	0- absent 1-present
Cartilage resorption	0-absent; 1- mild; 2 moderate; 3-severe
Maximum score	12

PARTE III

DISCUSSÃO

Os mecanismos bioquímicos causadores das MPS já são conhecidos há várias décadas: a deficiência de uma enzima que participa na degradação de GAG leva ao acúmulo dos seus substratos nos diferentes tecidos e órgãos do corpo. No entanto, os mecanismos patogênicos das MPS ainda não estão elucidados. Muitos aspectos destas enfermidades têm uma origem desconhecida, e o estudo dos mesmos pode auxiliar no desenvolvimento de novas terapias. O presente estudo focou-se principalmente na MPS I, que, pelo seu curso progressivo e multisistêmico, é considerada o modelo prototípico destas doenças. Por outro lado, o modelo animal de MPS VII apresenta, assim como em pacientes, uma forma mais grave de MPS, com uma manifestação mais precoce. Isso faz da MPS VII o modelo ideal para a realização mais rápida de experimentos que tomariam muito tempo caso fossem realizados com o modelo de MPS I, o que nos motivou a realizar alguns estudos nos modelos murino e canino de MPS VII.

Um dos objetivos deste estudo foi buscar possíveis mecanismos responsáveis pela doença em órgãos que demonstram pouca ou nenhuma melhora pelas terapias atuais disponíveis (TRE e TCTH). Para tanto, uma coorte de animais normais e MPS I foi acompanhada durante 1 ano, tendo sido avaliado parâmetros ecocardiográficos, comportamentais, bioquímicos, histológicos e de sobrevida. Além disso, o acompanhamento minucioso destes animais nos permitiu conhecer de forma muito detalhada os momentos em que cada manifestação da doença pode ser detectada, o que auxiliou na escolha dos tempos de início de tratamento nos estudos posteriores.

Patogênese da doença no sistema cardiovascular

O aspecto cardíaco das MPS merece destaque, uma vez que é uma causa freqüente de morbidade e mortalidade nesses pacientes (Braulin et al, 2011). Um estudo inicial acompanhando 5 pacientes com MPS I em TRE por 5 anos demonstrou que um dos pacientes desenvolveu cardiomegalia após o tratamento, enquanto 2 permaneceram estáveis e outros 2 apresentaram melhora no mesmo parâmetro (Sifuentes et al, 2007). Outros estudos sugerem que a TRE (Braulin et al, 2006) e o TCTH (Braulin et al, 2003) melhoram a função do músculo cardíaco. Baseado nestes dados inconclusivos, nós

resolvemos investigar as características da doença cardíaca na MPS, sua progressão e possíveis mecanismos envolvidos na dilatação do miocárdio.

Nos camundongos MPS I o miocárdio se mostrou dilatado a partir dos 6 meses de idade. Nesse mesmo tempo, foi possível observar uma significativa redução da função do ventrículo esquerdo, com redução da fração de ejeção, fração de encurtamento e mudança de área fracional. Estas alterações se mostraram progressivas, com piora aos 8 meses. Outra anormalidade detectada no tempo mais tardio foi o aumento do diâmetro da raiz da aorta, sugerindo dilatação da mesma. A redução na contratilidade do músculo cardíaco na MPS I já havia sido descrita previamente como acontecendo a partir dos 6 meses de idade, no entanto a diminuição na fração de ejeção havia sido detectada apenas aos 10 meses (Jordan et al, 2005). O presente trabalho sugere que a doença cardíaca na MPS I pode ser detectada já aos 6 meses de idade, o que é especialmente importante para a avaliação de terapias.

Tentando buscar possíveis explicações para a dilatação cardíaca nas MPS, a medida da atividade de catepsina B (CtsB) foi realizada em animais de 2 e 8 meses. Esta enzima foi escolhida porque trabalhos prévios demonstraram seu aumento na aorta de camundongos MPS I (Ma et al, 2008) e também porque o seu aumento já foi relacionado ao desenvolvimento de cardiopatia dilatada em seres humanos (Ge et al, 2006). De forma surpreendente, o aumento de CtsB foi detectado já aos 2 meses de idade, mesmo antes de um aumento no nível de GAG no tecido ser detectado de forma significativa. As alterações na matriz extracelular necessárias para o aparecimento da dilatação cardíaca na MPS I podem ser mediadas pela superexpressão crônica de CtsB, embora outras proteases não tenham sido testadas, e também poderiam estar contribuindo para a dilatação do miocárdio.

Embora as alterações no miocárdio encontrem resultados conflitantes na literatura com relação a sua reversibilidade após tratamentos, já é consenso que, no caso das válvulas cardíacas, existe pouco ou nenhum beneficio tanto da TRE quanto do TCTH (Braulin et al, 2006; Braulin et al, 2011; Watanabe et al, 2011). Portanto, o estudo dos mecanismos que levam à regurgitação e ao espessamento das válvulas é de especial interesse, uma vez que terapias auxiliares certamente serão necessárias para os pacientes. Embora as medidas ecocardiográficas de fluxo tenham mostrado apenas pequenas alterações nas válvulas cardíacas, é provável que estas sejam muito mais pronunciadas e que não tenham sido detectadas por limitações do equipamento ecocardiográfico utilizado. Nesse sentido, a análise histológica nos pareceu mais

informativa, sendo possível visualizar o espessamento destas estruturas já aos 6 meses de idade, como descrito em estudos anteriores (Jordan et al, 2005; Braulin et al, 2006).

A coloração de picrosírius demonstrou de forma muito clara uma redução no conteúdo de colágeno nas válvulas dos animais MPS I. Como o colágeno é responsável por cerca de 55% do peso seco da válvula (Balguid et al, 2007), a perda de colágeno observada pode ter implicações muito importantes na patogênese da doença valvular nas MPS. Devido ao seu tamanho reduzido e à dificuldade de obtenção, o número de experimentos que podem ser conduzidos nessas estruturas em camundongos é muito pequena. No entanto, estudos desenvolvidos durante o período de doutorado sanduíche no laboratório da Dra Kathy Ponder tentaram exatamente suprir esta limitação. Foram estudadas válvulas mitral e aórtica de cachorros com MPS VII, e através da realização de *microarray* para expressão gênica, ensaios enzimáticos e dosagem do conteúdo de colágeno, concluiu-se que existe um aumento na expressão de catepsinas, incluindo as catepsinas B e K, e uma redução no nível de colágeno tecidual (Baldo G, dados não-publicados). De forma especulativa, pode-se sugerir que o aumento da espessura e a regurgitação das válvulas observadas nos cachorros e em camundongos MPS I possam ser devido ao aumento na atividade de proteases, como a catepsina B, embora mais estudos estejam sendo conduzidos para comprovar esta hipótese.

Outro órgão que parece responder de forma pouco efetiva a terapias nas MPS é a aorta. No modelo murino de MPS I, a aorta ascendente se mostra bastante dilatada, com quebras na estrutura da elastina, aumento no nível de catepsinas e MMPs e fosforilação de proteínas como STAT-1, STAT-3 e MAPK (Ma et al, 2008). Nesse mesmo estudo (Ma et al, 2008), foi observado um aumento na expressão de catepsina S (CtsS) e na metaloproteinase de matriz tipo 12 (MMP-12), as quais nos pareceram ser bons candidatos para explicar as alterações observadas, por um conjunto de fatores: primeiramente, a CtsS é apontada por diversos estudos como sendo a única catepsina ativa e estável em pH neutro (Vasiljeva et al, 2005; Jordans et al, 2009), que é o pH da matrix extracelular. Além disso, ela tem conhecida capacidade de elastase (Ma et al, 2008). Por outro lado, o nocaute de MMP-12 provou ser capaz de reduzir a dilatação da aorta em um modelo animal de aneurisma (Longo et al, 2005). Tendo como base estes estudos, nos pareceu interessante realizar o nocaute destes dois genes sozinhos ou de forma combinada nos animais com MPS VII (já que a doença acontece de forma mais rápida que na MPS I).

A primeira preocupação foi comprovar que a doença ocorre de forma similar nas MPS I e VII. Para tanto, foram realizados ensaios de medida de diâmetro da aorta nos camundongos MPS VII após aplicação de pressão externa, ativação de STAT-3, níveis de mRNA e atividade enzimática, conforme realizado para a MPS I. Os resultados confirmaram que o perfil de expressão gênica, atividade de enzimas e alterações funcionais na aorta eram similares nas duas doenças, apenas acontecendo de forma mais precoce na MPS VII.

O passo seguinte foi a medida dos diâmetros da aorta nos animais normais (*Gusb*$^{+/?}$), animais MPS VII (*Gusb*$^{-/-}$), duplos (G*usb*$^{-/-}$*Ctss*$^{-/-}$ e G*usb*$^{-/-}$*Mmp12*$^{-/-}$) e triplos nocaute (G*usb*$^{-/-}$*Ctss*$^{-/-}$*Mmp12*$^{-/-}$). Para nossa surpresa, dentro do grupo de animais MPS VII, pela primeira vez pode-se distinguir 2 subgrupos distintos, um com uma dilatação da aorta bastante expressiva, como a que havia sido previamente encontrada, e um segundo subgrupo com uma dilatação muito mais discreta ou inexistente. Após reconfirmar o genótipo dos animais, um estudo mais detalhado do processo de *inbreeding* nos levou a conclusão que o segundo subgrupo era proveniente de animais da colônia de MPS VII que haviam sido cruzados em algum momento com animais da colônia deficiente em CtsS, e que provavelmente um segundo gene, até o momento desconhecido, estava causando essa disparidade. Para tentar descobrir qual era o gene responsável por essa disparidade nos resultados, ou que outros genes este controlava, foi realizado um ensaio de microarray em 3 animais normais, 3 animais com MPS VII com a aorta dilatada, e 2 animais MPS VII com a aorta pouco dilatada. O resultado do *microarray* pode ser vizualizado na figura 6 e demonstra um perfil de expressão bastante diferente entre os animais normais e MPS VII, enquanto os animais MPS VII com pouca dilatação da aorta apresentam um perfil intermediário entre os outros dois fenótipos. Diversos genes pertencentes a vias inflamatórias (C1qa, C4a, Tlr7, Trem2) e proteases (Ctsa, Ctsb) estavam diminuídos nos animais MPS VII sem dilatação, comparado aos MPS VII dilatados.

A segunda conclusão desta fase do estudo foi que, mesmo com o nocaute de ambos genes (CtsS e MMP-12), os animais MPS VII continuavam com dilatação na aorta, demonstrando que a nossa hipótese inicial não estava correta, e que não são estes 2 genes sozinhos ou em combinação os responsáveis pela dilatação. Tentando verificar o porquê de a estratégia ter falhado, foi medida (em pH neutro) a atividade de catepsinas nas aortas destes animais, e surpreendentemente mesmo os animais que tinham o gene da CtS deletada continuavam com altos níveis de catepsinas no tecido, dosado pelo

substrato inespecífico Phe-Arg-AMC. Então, realizando testes com enzimas purificadas e inibidores específicos, concluímos que, ao contrário do que a maioria dos trabalhos sugere, outras catepsinas como a catepsina K e a catepsina B também têm atividade em pH neutro e são estáveis por pelo menos 2 horas, tempo do ensaio enzimático. Através da análise de atividade enzimática nas aortas, mais uma vez observamos um aumento expressivo na atividade de CtsB, assim como um aumento mais discreto, porém significativo, na CtsK.

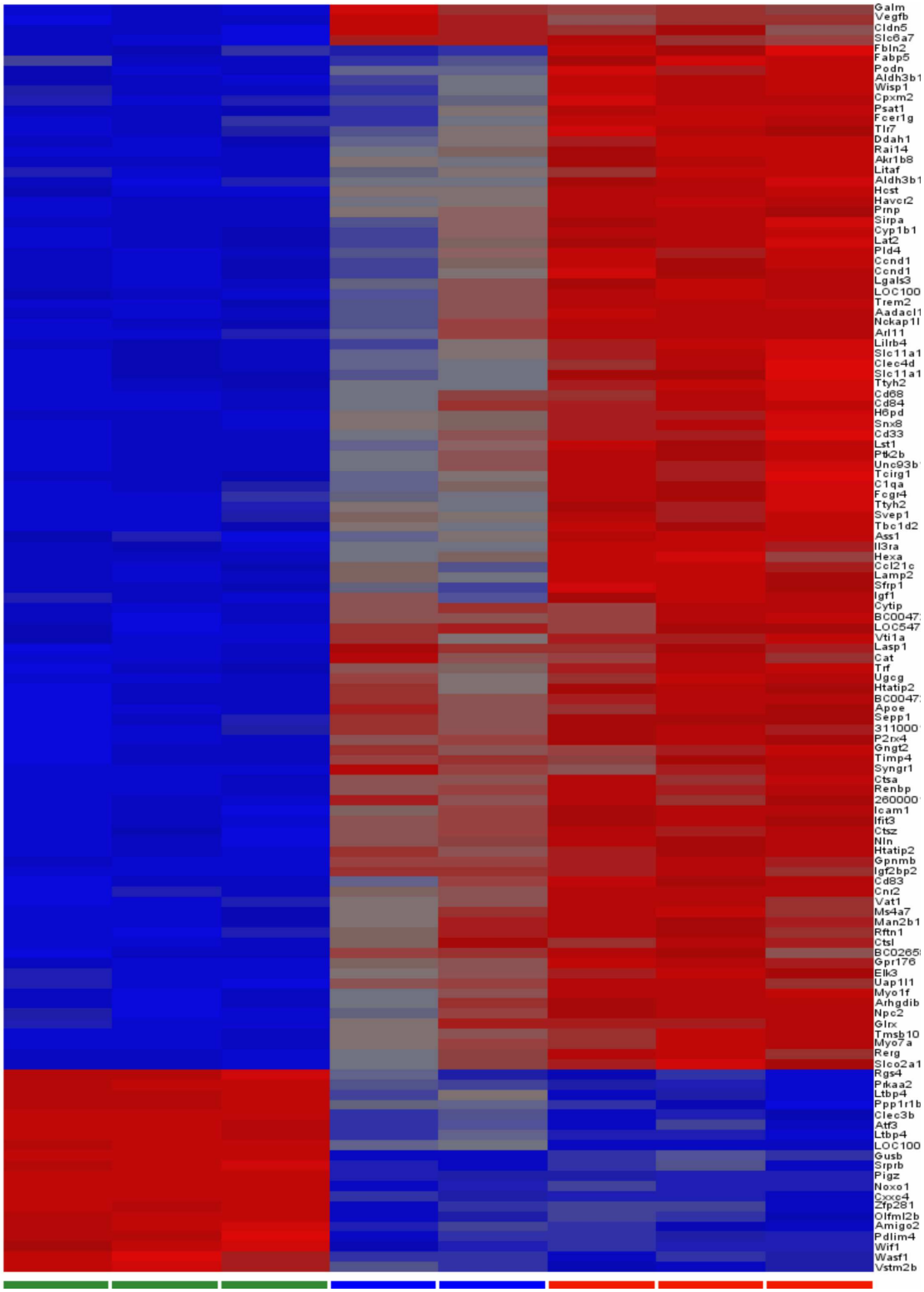

Figura 6: Perfil de expressão gênica em animais normais (n=3, colunas com símbolos inferiores verdes) animais MPS VII com aorta não-dilatada (n=2, símbolos inferiores azuis) e animais MPS VII com aorta dilatada (n=3, símbolos inferiores vermelhos) analisado por microarray. Cada linha corresponde a um gene (identificado pelo símbolo à direita). A cor azul indica que o gene esta subexpresso, enquanto a cor vermelha indica superexpressão, com cinza como valor intermediário.

Por fim, na tentativa de buscar outros possíveis mecanismos para a dilatação aórtica, foi analisado o perfil de expressão gênica dos 3 animais normais e dos 3 MPS VII por microarray. Diversos genes se mostraram diferencialmente expressos nos animais MPS VII, incluindo proteases, citocinas e proteínas de matriz extracelular. De forma muito interessante, um expressivo número de genes relacionados ao sistema complemento estavam superexpressos nos animais MPS VII, pertencentes a via clássica, alternativa e das lectinas. Uma análise por imunohistoquímica (IHQ) confirmou o aumento nos níveis da proteína C3 na aorta dos animais MPS VII, sugerindo ativação do sistema complemento. A técnica de PCR em tempo real também foi utilizada para tentar descobrir que via estaria participando dessa ativação, porém genes das 3 vias apareceram aumentados, o que não nos permitiu chegar a uma conclusão. Estes dados nos permitiram formular uma nova hipótese de trabalho: a de que os GAG parcialmente degradados que se acumulam na MPS VII possam estar ativando o sistema complemento, e levando a dilatação da aorta por pelo menos duas maneiras: uma delas é diretamente pela ativação do fator D do sistema complemento, que é uma conhecida elastase (Zhu et al, 1994). A segunda forma seria pela liberação das anafilotoxinas C3a e C5a, que poderiam gerar uma resposta inflamatória no tecido e uma superexpressão de colagenases e elastases, como as catepsinas e as MMPs. No presente momento camundongos duplos nocaute (G*usb*$^{-/-}$C3$^{-/-}$ e G*usb*$^{-/-}$FatorD$^{-/-}$) estão sendo produzidos nos Estados Unidos para responder a esta questão.

A hipótese de que os GAG parcialmente degradados possam ativar vias de sinalização não é totalmente nova. Dois trabalhos prévios sugerem que os GAG possam ativar a via dos receptores tipo *toll* (TLR) e o nocaute do gene TLR-4 provou melhorar a doença óssea em animais com MPS VII (Simonaro et al, 2010) e reduzir marcadores inflamatórios em cérebro de animais com MPS IIIB (Ausseil et al, 2008). Na aorta, vários genes da via do TLR-4 aparecem superexpressos, e o nocaute deste gene também está sendo realizado. É possível que os GAG parcialmente degradados estejam ativando múltiplas vias de sinalização, e o somatório destas seja responsável pela doença.

Por fim, este estudo confirmou que o tratamento da dilatação aórtica na MPS VII ainda é um desafio. O uso de um vetor retroviral, mesmo atingindo níveis séricos de GUSB 100X superiores aos níveis normais, e sendo capaz de corrigir as mais distintas manifestações da doença (Xu et al, 2002; Mango et al, 2004), demonstrou apenas ser parcialmente eficaz na correção da aorta. Um possível mecanismo para este sucesso

apenas parcial pode ser atribuído a pouca vascularização da aorta, de forma que pouca enzima consegue penetrar no tecido a partir do soro.

Mecanismos patogênicos no sistema esquelético e articular

Os pacientes com MPS apresentam graves problemas articulares e esqueléticos, que contribuem para a morbidade e mortalidade dessas síndromes. As principais manifestações clinicas são enrijecimento articular, baixa estatura, disostose multiplex, degeneração de discos vertebrais e compressão medular (Cimaz et al, 2009; Munoz-Rojas et al, 2008; Smith et al, 2010). O tratamento com TRE ou TCTH parece surtir pouco efeito sobre o sistema esquelético nas MPS (Malm et al, 2008; Tylki-Szymanska et al, 2010b), e pouco se sabe sobre a patogênese dessa doença.

No presente trabalho um escore histológico para avaliar o dano articular no joelho foi desenvolvido, baseado nos achados de animais com MPS I aos 12 meses de idade. As alterações encontradas na análise histológica por hematoxilina e eosina incluíram a presença de um discreto infiltrado inflamatório, proliferação fibrocartilaginosa e irregularidades na superfície articular, que se mostraram progressivas com a idade.

Uma vez que os pacientes com MPS I possuem tamanho normal ao nascer, mas desenvolvem baixa estatura após os primeiros anos de vida, uma das nossas hipóteses era de que alterações na composição ou organização da placa de crescimento pudessem estar alteradas em momentos mais tardios. No entanto, não foram observadas alterações na mesma. Previamente, Metcalf e colaboradores (2010) descreveram uma diminuição na zona proliferativa da placa de crescimento de camundongos MPS VII com 3 semanas, mas não de camundongos MPS I. Nossos achados confirmam o que foi encontrado neste estudo prévio, e os mecanismos que levam à baixa estatura na MPS I ainda são desconhecidos. Uma possível explicação para não haver sido encontrada diferença seria a de que, ao contrário dos pacientes, os camundognos MPS I tem tamanho muito próximo ao normal (Metcalf et al, 2010), sugerindo que talvez o modelo murino não reproduza todas as caracteristicas da doença.

Através de colorações como safranina (Schmitz et al, 2010) e picrosírius (dados não-mostrados), pode-se detectar uma perda no conteúdo de colágeno nas articulações de animais com MPS I. Uma vez que a articulação possui principalmente colágeno tipo II (Zhen et al, 2008), decidiu-se estudar a expressão de duas proteases (MMP-2 e MMP-

9) que tem a capacidade de clivar este tipo de colágeno (Shapiro, 1998). Um aumento foi encontrado na expressão destas duas colagenases, e isso pode auxiliar a explicar o mecanismo pelo qual as articulações dos animais com MPS apresentam-se com sua arquitetura alterada. Não se pode descartar que outras proteases, como as próprias catepsinas, também tenham sua expressão alterada nas articulações, e estudos posteriores irão investigar este aspecto mais a fundo.

Outros grupos já demonstraram aumento na expressão de MMP-2 e MMP-9 na articulação de ratos com MPS VI (Simonaro et al, 2005), enquanto que, contraditoriamente, a expressão de catepsina K foi encontrada diminuída (Wilson et al, 2009) nos animais com MPS I. Um aumento nas proteases foi também encontrado na coluna vertebral de cachorros com MPS VII, sendo novamente encontrado aumento nas CtsB e K, além do aumento no nível de mRNA do TLR-4 (Smith et al, in press- anexo 2). Estes resultados em conjunto sugerem que os mecanismos envolvendo a doença articular e óssea nas mucopolissacaridoses também possam ser explicados pela ativação de vias inflamatórias e superexpressão de proteases, assim como na aorta. Outra hipótese recentemente sugerida seria a de que as células-tronco de pacientes com MPS I possuem mais propensão à diferenciação em osteoclastos, o que pode contribuir para a degeneração óssea observada (Gatto et al, 2012). Ainda, combinando estas duas hipóteses, não se pode descartar que estes osteoclastos seriam os responsáveis pelo aumento de catepsinas e MMPs observados nos nossos estudos, já que são as células responsáveis pelo remodelamento ósseo. De qualquer forma, a inibição de vias inflamatórias e de proteases parece ser uma possível alternativa terapêutica para a doença óssea e articular nas MPS, já que recentemente foi descrito que, mesmo atingindo níveis séricos muito superiores aos normais, a injeção de um vetor retroviral não consegue reverter a degeneração na coluna vertebral de cachorros MPS VII (Smith et al, in press).

Patogênese no sistema nervoso central

A doença no sistema nervoso ainda permanece como um dos aspectos mais intrigantes das MPS. Além do acúmulo de GAG no cérebro, outras substâncias, como gangliosídeos e colesterol, também acumulam neste órgão (Walkley, 2004). Os pacientes com MPS I apresentam desenvolvimento normal ao nascimento e nos primeiros meses de vida, no entanto aproximadamente ao final do primeiro ano os

pacientes com a forma grave (síndrome de Hurler) começam a apresentar um déficit cognitivo (Neufeld and Muenzer, 2001). Este déficit é provavelmente um dos aspectos mais devastadores da doença e acredita-se que seja irreversível, de forma que o tratamento com o TCTH somente é indicado para pacientes com menos de 2 anos de idade, sem um grave comprometimento neurológico (Giugliani et al, 2010).

Para avaliar a função neurológica dos camudongos, uma bateria de testes comportamentais foi aplicada, tentando principalmente esclarecer aspectos com resultados contraditórios na literatura e também com o intuito de avaliar eficácia de terapias. Dois testes de ansiedade (teste da cruz elevada e porcentagem de tempo no centro do aparato de campo aberto) foram realizados, sem diferença entre animais normais e MPS em qualquer dos tempos testados. Estes resultados estão de acordo com os encontrados por Reolon e colaboradores (2006), que, utilizando a permanência no centro do campo aberto como parâmetro, também não observaram alterações. Ao contrário, Pan e colaboradores (2008) utilizaram dois testes distintos para avaliação de ansiedade (*elevated zero maze e marble buring*), encontrando diferenças discretas porém significativas apenas neste último, em animais com 8 meses de idade. Nós utilizamos o teste de cruz elevada para avaliação de ansiedade porque este se constitui num teste similar ao *zero maze* previamente testado por Pan e colaboradores (2008). O *marble buring* não foi realizado porque o grupo não tinha experiência com este teste, o qual recentemente têm tido a sua validade como teste de ansiedade questionada (Corina et al, 2011). Os nossos dados sugerem que os animais com MPS I não apresentam alterações de ansiedade, em nenhum tempo analisado.

Outros testes, incluindo o campo aberto, o teste de *hang wire* e a avaliação de marcha foram utilizados para avaliação de atividade locomotora e função cerebelar. Os animais MPS I se mostraram hipoativos no campo aberto a partir dos 4 meses de idade, com redução no número de cruzamentos e na atividade exploratória. Estes resultados novamente se mostravam discrepantes na literatura, com um estudo (Pan et al, 2008) corroborando nossos achados, enquanto o outro (Reolon et al, 2006) encontrava alterações apenas no número de *rearings.* Uma coorte diferente de animais com 8 meses de idade foi avaliada no mesmo teste por um grupo de pesquisadores na Washington University em St. Louis para verificação dos efeitos da terapia gênica nestes animais. Os resultados encontrados também corroboram nossos achados, pelo qual concluímos que os animais MPS I possuem uma reduzida atividade locomotora e exploratória.

Os testes de *hang wire* e de análise de marcha são utilizados para avaliar função cerebelar (Alonso et al, 2008; Takahashi et al, 2009) e se mostraram alterados na MPS I, fato que nos motivou a buscar alterações histológicas no cerebelo. Embora não tenhamos encontrado sinais de morte celular, o acúmulo de GAG pode ser detectado em células de Purkinje. Além disso, alterações na expressão de GFAP evidenciaram um processo neuroinflamatório no cerebelo. Este processo já havia sido descrito no córtex de animais MPS I (Ohmi et al, 2003), o que foi confirmado no presente estudo. No entanto, até o presente momento não existiam relatos de que o mesmo estaria ocorrendo em outras regiões do cérebro. A ativação de células da glia já foi descrita em diversas doenças neurodegenerativas e está relacionada a uma perda da função neuronal (Li et al, 2011). Estas células podem prejudicar a atividade e plasticidade sináptica por diversos mecanismos, incluindo secreção de citocinas inflamatórias, ativação do sistema complemento e alteração do metabolismo de neurotransmissores, como o glutamato (Kawashita et al, 2009).

Outros dois testes (habituação no campo aberto e esquiva inibitória) foram realizados em animais de 6 a 8 meses, para avaliação da memória. Conforme previamente descrito (Reolon et al, 2006), os animais MPS I apresentaram um tempo de latência menor que os animais normais no teste de esquiva inibitória, evidenciando não lembrar do estimulo aversivo (choque) que havia sido dado 24 horas antes no treino. Da mesma forma, os camundongos MPS I demonstraram não se habituar ao ambiente de campo aberto com o passar do tempo, enquanto que os animais normais tendem a reduzir sua atividade (Hartung et al, 2004; Pan et al, 2008). Nós optamos por não fazer outros testes que avaliassem memória, como o labirinto aquático de Morris, pois os resultados na literatura eram conflitantes e os dados obtidos na avaliação da terapia gênica com o retrovirus sugeriam diferenças na velocidade de natação entre animais normais e MPS, o que poderia ser um fator de confusão na interpretação dos dados. Este aspecto é de especial importância na interpretação dos resultados de testes comportamentais em animais com MPS: se tratando de uma doença multisistêmica, outras alterações (anormalidades nas articulações, ossos, orelhas, capacidade respiratória...) podem levar a interpretações errôneas. A nossa sugestão é que mais de um teste seja utilizado para avaliar cada aspecto, e que outras informações, como alterações histológicas, também sejam consideradas.

As observações dos testes de esquiva inibitória e memória de habituação, que sugerem perda de memória, juntamente a estudos prévios que sugeriam alterações no

hipocampo destes animais (Reolon et al, 2006; Pan et al, 2008) nos levaram a buscar proteínas que estivessem diferencialmente expressas nesta região do cérebro, e que pudessem ser responsáveis pela perda da cognição observada. Optou-se por uma análise em que as proteínas são extraídas, clivadas com tripsina, e diretamente colocadas num Nano-HPLC acoplado a um espectrômetro de massas em *tanden*, sem precisar da realização de géis de 2 dimensões para separar as proteínas previamente, o que torna o trabalho mais rápido.

Amostras de 5 animais normais e de 5 camundongos com MPS machos aos 8 meses foram avaliadas em duplicata, e 296 proteínas foram identificadas, das quais aproximadamente 30 estavam diferencialmente expressas. De forma interessante, 3 proteínas lisossômicas apareceram como as mais superexpressas em animais MPS I, sendo elas as catepsinas D e B e a prosaposina. A nossa primeira hipótese para explicar o mecanismo da doença cerebral na MPS I foi então que o aumento nas catepsinas D e B poderia levar à morte de neurônios por apoptose (Ceccariglia et al, 2011) ou por morte mediada por lisossomo (Kreuzaler et al, 2011). No entanto, assim como observado no hipocampo e córtex no estudo prévio, não foi possível detectar morte celular nestes animais aos 8 meses. Outros grupos que trabalham com MPS I e MPS IIIB (Vitry S, comunicação pessoal) também relatam achados similares. Embora não tenha sido testado no presente trabalho, o aumento nas enzimas lisossômicas pode ser explicado devido à ativação do fator de transcrição EB (TFEB) que se encontra super expresso e ativado em situações de acúmulo de moléculas no lisossomo, e controla a expressão de diversas outras enzimas lisossômicas (Sardiello et al, 2009). O aumento das catepsinas observado parece não ativar morte celular, mas o seu papel na patogênese da doença cerebral na MPS I não pode ser totalmente descartado, já que estas participam da clivagem de diversos substratos (Turk et al, 2012).

O aumento de outras proteínas também nos chamou a atenção. Primariamente, a superexpressão de GFAP confirmada por IHQ evidenciou que, similar ao encontrado no cerebelo e córtex, há um processo neuroinflamatório ocorrendo também no hipocampo, de modo que é razoável assumir que isso aconteça por todo o cérebro. A proteína MAPK também se mostrou superexpressa, e o estudo do seu grau de fosforilação no hipocampo está em andamento, assim como o estudo de outras cinases de estresse, como a STAT-3, que está ativada na aorta dos animais com MPS VII (Ma et al, 2008).

Outra proteína encontrada aumentada no perfil proteômico de animais MPS I foi a proteína associada ao crescimento 43 (GAP-43), que esta envolvida no crescimento de

neuritos. A superexpressão de GAP-43 já foi demonstrada no cérebro de animais com MPS IIIB, e que a mesma mediava o crescimento de neuritos não-funcionais (Hocquemiller et al, 2010). Embora resultados do nosso grupo tenham evidenciado aumento discreto no nível de mRNA para GAP-43 no hipocampo de animais com 6 meses (Martinelli B, comunicação pessoal), a análise por western blot não atingiu significância, sugerindo que, mesmo que exista a expressão aumentada de GAP-43, ela é bastante discreta e não deve ser determinante para a patogênese da doença.

Recentemente, estudos têm sugerido que nas MPS poderia haver um acúmulo de proteínas dobradas incorretamente ou não-dobradas, devido ao aumento da oxidação de proteínas encontrado em certos tipos de MPS (Villani et al, 2009). A calnexina é uma chaperona cuja principal função é garantir o dobramento correto das proteínas no retículo endoplasmático (Ren et al, 2010), e se mostrou aumentada no estudo proteômico. Portanto, a expressão da mesma foi avaliada por western blot, sem nenhuma diferença encontrada. Nossos resultados confirmam o que recentemente foi descrito por Villani et al (2012), que demonstrou não haver mal-dobramento de proteínas em fibroblastos de pacientes com diferentes tipos de MPS. Outra proteína que não demonstrou diferença foi a ubiquitina, sugerindo que, ao contrário de outras doenças lisossômicas (Bifsha et al, 2007), não existe poliubiquitinação de proteínas neste modelo animal.

Por fim, proteínas relacionadas à função e plasticidade sináptica apareceram diminuídas no perfil proteômico de animais com MPS I. Entre estas proteínas, pode ser observada uma diminuição na sinaptofisina, que é a proteína mais abundante na membrana da vesícula sináptica (Evans e Cousin, 2005), e já foi demonstrada estar diminuída na MPS IIIB devido a um aumento da degradação da mesma pelo proteossomo (Vitry et al, 2009). No entanto, a análise por western blot novamente não confirmou sua redução. Outras proteínas relacionadas à plasticidade sináptica também se mostraram diferencialmente expressas, o que nos levou a verificar a expressão da proteína PSD-95, que possui um papel-chave para este processo (Xu, 2011; Zheng et al, 2011). Foi possível verificar um aumento de cerca de 60% nos níveis da PSD-95 nos animais MPS I, através de análise por western blot. O aumento de PSD-95 está relacionado a uma desorganização dos microtúbulos e diminuição da dendritogênese (Sweet et al, 2011). De maneira interessante, outras duas proteinas relacionadas à dendritogênese (Mta1a e Mta1b) estão drasticamente diminuídas nos animais com MPS

I, sendo possível que o somatório destas alterações possa contribuir de forma significativa para o déficit cognitivo na MPS I.

Avaliação de tratamentos

As limitações encontradas nas terapias atuais para as MPS nos fizeram estudar outras possíveis abordagens terapêuticas para estas doenças. Em especial, a avaliação do uso de células encapsuladas, da terapia gênica com retrovírus, e da TRE neonatal foram o segundo grande objetivo deste estudo. Tendo como base as alterações encontradas nos estudos anteriores abordando patogênese das MPS, uma série de testes pode ser realizada neste estágio do trabalho para avaliação das terapias.

A primeira forma de terapia avaliada foi a utilização de células encapsuladas como tratamento da MPS I. Para tanto, a linhagem celular *baby hamster kidney* (BHK) foi transfectada com um plasmideo pREP-9 contendo o gene da IDUA, chamado de pR-IDUA (Camassola et al, 2005). Após seleção de clones que superexpressam a enzima, estes foram encapsulados em microcapsulas de alginato. Duas concentrações de alginato foram testadas (1% e 1,5%) e, embora a secreção da enzima para o meio extracapsular tenha sido maior na concentração de 1%, também se observou aumento no número de cápsulas mal-formadas com esta concentração. Estudos prévios (King et al, 2001) sugerem que cápsulas com formatos irregulares podem levar a um crescimento celular exacerbado e rompimento das cápsulas, motivo pelo qual todos os experimentos subseqüentes foram testados com a concentração de 1,5%.

Foi possível constatar que, embora houvesse uma perda de cerca de 30-40% na viabilidade celular após 30 dias de criopreservação, as cápsulas conseguiam manter esses mesmos valores de viabilidade após 90 dias, possivelmente porque no processo de congelamento/descongelamento o alginato consiga promover alguma forma de proteção aos estresses sofridos pelas células livres, tais como pipetagens e centrifugação, o que também pode explicar o porquê da atividade enzimática de IDUA ter sido maior após os 90 dias, já que estas células estariam metabolicamente menos estressadas, podendo produzir mais enzima. Outros estudos também sugerem um efeito benéfico da encapsulação na viabilidade celular após a criopreservação, embora os mecanismos para este achado ainda não serem conhecidos (Aoki et al, 2005).

O estudo de preservação hipotérmica em 24h sugere que as células dentro das cápsulas não sofram morte celular de forma significativa quando colocadas por 24 horas

a 4°C, o que em um país de dimensões continentais como o Brasil e bastante importante, já que estas poderiam ser produzidas num único centro, e transportadas a outros lugares nessas condições, sem perda significativa da atividade enzimática e viabilidade celular.

O próximo passo foi verificar se estas cápsulas secretavam a enzima na sua forma madura, que poderia ser então captada por células deficientes. Para tanto, as cápsulas foram colocadas em cultura para avaliação da viabilidade e crescimento celular, bem como secreção da IDUA ao longo do tempo. Nossos resultados sugerem que o tempo de duplicação das células BHK dentro das cápsulas *in vitro* é de aproximadamente 30 dias, o que é muito maior comparado às células livres, que geralmente dobram seu número em menos de 24 horas (Charp et al, 1983). Além disso, a viabilidade celular durante os primeiros 30 dias sempre foi maior que 90%, e a secreção da enzima se manteve constante após as 24h iniciais, sugerindo que não existe um silenciamento ou perda do vetor *in vitro*.

O co-cultivo das cápsulas com fibroblastos de pacientes com MPS I restabeleceu a atividade enzimática por até 45 dias. Além disso, houve redução no acumulo de GAG, sugerindo que a enzima estava sendo produzida e processada corretamente, chegando ao lisossomo. Ainda, o mecanismo de entrada nas células parece ser via receptor de manose-6-fosfato, embora não se tenha testado se toda a enzima produzida estava sendo corretamente fosforilada. Outros grupos já demonstraram que uma superexpressão de IDUA pode saturar os mecanismos de fosforilação, de modo que nem toda enzima é fosforilada corretamente (Metcalf et al, 2010) e este ainda é um ponto a ser averiguado. Por fim, corroborando com nossos dados prévios, cápsulas criopreservadas por 1 ano, quando descongeladas, ainda foram capazes de corrigir a atividade de IDUA em fibroblastos MPS I.

Tendo obtido resultados promissores *in vitro* decidiu-se implantar as cápsulas no peritôneo de camundongos para verificar se havia correção da doença *in vivo*. Embora esta metodologia possa ser utilizada em sítios específicos como o cérebro, o peritôneo foi escolhido como prova de conceito, já que estudos prévios haviam sido feitos em camundongos MPS II com implante no mesmo local (Friso et al, 2005). A dose inicial de células implantadas foi de 1×10^5 cel/g de peso, mas após não ser possível observar melhora nos animais (dados não-mostrados), uma dose 10 vezes superior foi escolhida. Ainda, decidiu-se começar o tratamento aos 30 dias de vida devido ao pequeno tamanho dos animais antes desse período, e a troca das cápsulas foi realizada a cada dois meses

para corrigir a dose baseada no peso do animal e já que os estudos *in vitro* tinham se limitado há poucos meses.

Os animais MPS I apresentaram melhoras no aspecto geral, redução de GAG no rim, além de um aumento pequeno, porém significativo, de atividade de IDUA no coração, e um aumento próximo da significância no fígado. Estes resultados parcialmente satisfatórios nos fizeram investigar se a enzima estava atingindo a circulação. Foi observado um aumento na atividade de IDUA sérica em até sete dias, com posterior queda ao nível inicial. Estes resultados nos fizeram acreditar que estavamos conseguindo dar "pulsos" de terapia a cada troca de capsulas, porém por algum motivo a liberação da enzima não estava sendo eficaz em longo prazo.

A nossa primeira hipótese foi a de que as cápsulas estavam sofrendo um processo de fibrose e/ou calcificação ao seu redor, evidenciado pelo aspecto fosco e esbranquiçado das mesmas ao serem retiradas do animal, 60 dias após o tratamento. Além disso, uma resposta imune com formação de fibrose ao redor do biomaterial *in vivo* já havia sido descrita previamente em outros estudos utilizando microcápsulas de alginato (Li et al, 2006; Liu et al, 2010). Esta resposta adquire forma completa poucas semanas após o implante, culminando com a formação de uma camada densa de colágeno que recobre a cápsulas (Ratner et al, 2004). Através de uma coloração com picrosirius, pode-se observar a formação de colágeno ao redor das microcapsulas, o que poderia dificultar a passagem de uma proteína grande como a IDUA para o meio extra-capsular.

A segunda hipótese era a de que os animais MPS I estivessem desenvolvendo anticorpos anti-IDUA, e para tanto, um ensaio de ELISA foi realizado. Embora os animais tratados tenham realmente desenvolvido anticorpos contra a enzima, o nível de anticorpos foi parecido com o encontrado nos animais tratados com TRE, para os quais a terapia continuou mostrando eficácia. Isso nos sugere que o principal motivo pela perda na atividade sérica e tecidual de IDUA seria a formação da fibrose pericapsular. Além disso, outros trabalhos utilizando as mesmas cápsulas, ou terapia gênica, já demonstraram que os animais MPS I desenvolvem anticorpos contra a enzima, porém, a sua neutralização total não ocorre e as terapias perdem apenas parte da sua eficácia (Piller Puicher et al, 2012).

Embora os resultados *in vivo* não tenham se mostrado tão animadores como o esperado, os nossos dados concordam com dados previamente publicados na literatura. Num estudo em camundongos MPS II, no qual uma linhagem de mioblastos

superexpressando iduronato sulfatase (IDS) foi encapsulada, observou-se um aumento dos níveis enzimáticos da IDS nos órgãos ate 21 dias, com subseqüente diminuição na atividade (Friso et al, 2005). De forma similar, houve uma redução transitória nos GAG urinários, que após 56 dias já haviam se elevado novamente aos níveis de animais não-tratados. Um segundo estudo (Piller Puicher et al, 2012), desta vez em animais com MPS I, utilizando a mesma linhagem celular de mioblastos, porém transfectados com o gene da IDUA, também demonstrou aumento da enzima após algumas semanas, com posterior queda. No entanto, em nenhum destes trabalhos foi avaliada e formação de fibrose ao redor das cápsulas, embora no segundo tenha sido comprovada a formação de anticorpos anti-IDUA. A nossa expectativa é que, em se comprovando o papel da formação da fibrose como fator determinante para a perda de eficácia da terapia, possa-se aperfeiçoar a técnica de encapsulação, caminhando rumo a ensaios clínicos futuros. No momento outros estudos estão sendo realizados pelo grupo para comprovar este aspecto e propor soluções para esta questão.

A segunda forma de tratamento testada neste trabalho foi a terapia gênica com um vetor retroviral. Mais especificamente, avaliou-se o efeito da injeção sistêmica de um vetor com a porção LTR intacta ou sua versão auto-inativante (SIN) sobre aspectos cerebrais da MPS I. Previamente estes mesmos vetores já haviam sido testados em camundongos MPS I (Ma et al, 2007; Metcalf et al, 2010). O vetor LTR havia sido capaz de corrigir os aspectos da doença estudados, incluindo alterações ósseas, oculares, viscerais, valvulares e cerebrais, enquanto que comparativamente a versão SIN demonstrou uma eficácia menor, corrigindo parcialmente órgãos como o olho e a aorta, o que foi atribuído a uma menor eficiência de transdução por este último.

O objetivo deste estudo foi verificar se estes vetores conseguiam corrigir a doença no sistema nervoso central de camundongos MPS I, avaliando aspectos bioquímicos, histológicos e comportamentais. Como previamente descrito, os níveis séricos de IDUA após a transdução se mantiveram constantes, e muito acima dos níveis normais, com o vetor com a LTR intacta atingindo os níveis mais altos. A análise histológica revelou uma diminuição nos GAG teciduais dos animais tratados com os três vetores, com os animais tratados com o vetor SIN ainda possuindo células com acúmulo de GAG não-degradado.

Os testes de comportamento utilizados neste estudo diferiram dos previamente testados pelo nosso grupo no trabalho anterior, uma vez este trabalho foi concebido nos EUA por um grupo com *expertise* em outros testes (Wozniak et al, 2004; Wozniak et al,

2007). Em linhas gerais, os animais MPS I demonstraram um desempenho pior nos testes sensorimotores, que tinham por objetivo verificar equilíbrio, força e coordenação. Ainda, realizando testes similares aos que havíamos previamente utilizado, os animais MPS I se mostraram hipoativos no campo aberto, além de um déficit na memória de habituação, corroborando nossos dados. O tratamento com o vetor LTR demonstrou melhoras em todos os aspectos estudados, embora o número de *rearings* não tenha atingido significância. Por outro lado, os animais tratados com o vetor SIN ao nascimento ou aos 2 meses demonstraram apenas melhoras parciais em alguns aspectos.

Embora a atividade de IDUA no cérebro não tenha atingido diferenças significativas devido a grande variabilidade nos resultados e ao pequeno número de animais testados, nossos resultados de atividade de GUSB, aliados aos dados histológicos e comportamentais, sugerem que parte da enzima esteja passando a barreira hemato-encefálica (BHE), o que se acreditava não ocorrer no caso das enzimas lisossômicas. O fato de um vetor retroviral somente se integrar em células em divisão, aliado ao promotor tecido-especifico (alfa-1-antitripsina) utilizado, sugerem que a maior parte da enzima esteja sendo produzida no fígado, sendo lançada para a circulação e corrigindo outros órgãos, inclusive o cérebro. No trabalho prévio do grupo, não houve expressão do vetor no cérebro (Metcalf et al, 2010), e quase a totalidade da expressão foi encontrada no fígado, o que confirma este dado.

Existem duas possíveis explicações para a enzima estar atingindo o tecido cerebral e diminuindo os GAG nessa situação: a primeira é que células do sistema imune estejam captando a enzima, e, ao atravessar a BHE, secretem a enzima para neurônios, num mecanismo similar ao que acontece no TCTH, ou ainda sendo transportadas por transporte axono-dendrítico (Chen et al, 2006). A segunda hipótese é de que, em altas concentrações séricas, uma pequena fração da enzima consiga cruzar a barreira através de um mecanismo desconhecido e pouco eficiente, o que já foi demonstrado acontecer para outras enzimas lisossômicas, como a GUSB (Vogler et al, 2005). De qualquer modo, a partir destes dados, o uso destes dois vetores passa a ser uma opção interessante para a terapia gênica em estudos clínicos. No momento, estudos em animais maiores estão sendo conduzidos para verificar a segurança e eficácia desta abordagem. Embora o vetor com a LTR intacta tenha se mostrado melhor na eficiência de transdução e níveis de IDUA séricos atingidos, um dos cachorros tratados com este vetor desenvolveu um tumor benigno que expressava cópias do retrovírus (Ponder, comunicação pessoal), o que levanta uma série de questionamentos quanto a sua

segurança. Espera-se que os estudos em animais maiores possam ajudar na escolha do melhor vetor para o tratamento de pacientes.

Uma vez que as cápsulas não demonstraram sucesso em longo prazo e a terapia gênica, apesar dos bons resultados, ainda não se encontrar em ensaios clínicos, a terceira forma de tratamento avaliada nesse estudo foi a TRE, mais especificamente os benefícios que o tratamento começado no inicio da vida trariam, comparado ao tratamento iniciado na idade adulta. Estudos clínicos sugerem que, quanto antes o tratamento for iniciado, melhor é a resposta por parte do paciente (Wraith et al, 2007; Gabrielli et al, 2010). No entanto, não havendo nenhum estudo comparativo, decidiu-se investigar que órgãos/sistemas teriam mais beneficio com a TRE neonatal em comparação a iniciada na idade adulta.

Para tanto, decidiu-se pela injeção de 1,2 mg Laronidase /kg de peso a cada duas semanas, numa dose e regime similares aos utilizados em humanos (Giugliani et al, 2009). Devido ao tamanho muito pequeno do animal ao nascimento, a primeira injeção nos neonatos foi realizada através da veia temporal (figura 7), baseado na técnica inicialmente descrita por Sands e Barker (2000). As injeções subseqüentes foram realizadas pela veia da cauda. Não houve sinais evidentes de efeitos adversos nas injeções nos neonatos ou nos adultos. Um animal do grupo injetado desde o nascimento morreu no terceiro mês de vida, sete dias após a última administração, de causas desconhecidas.

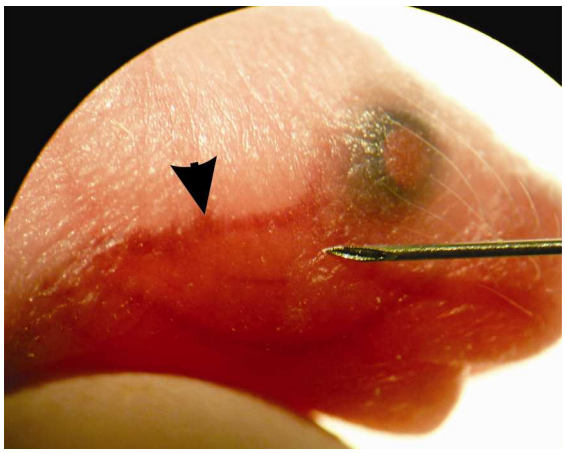

Figura 7: Exemplo de injeção em animal neonato. A seta indica a veia pela qual a enzima foi injetada.

Ambos tratamentos foram igualmente eficazes na correção de órgãos como fígado, pulmão, coração, testículo e rim. Estes órgãos são os que melhor demonstram correção pela TRE. Os pacientes tratados com TRE diminuem a organomegalia nestas

estruturas e melhoram os níveis de GAG urinários (Giugliani et al, 2010), de modo que estes resultados estão de acordo com o observado em pacientes. Ainda, mesmo que relatos de reversibilidade da doença cardíaca sejam ainda de certa forma inconclusivos, nossos achados sugerem que este aspecto da doença também foi revertido nos dois grupos tratados, com melhora de importantes parâmetros como as frações de ejeção e de encurtamento. No entanto, ainda fica em aberto a questão de quão reversível seria o tratamento em animais mais velhos, que já possuem uma dilatação cardíaca estabelecida.

Ao contrário dos órgãos viscerais já citados, a aorta e as válvulas cardíacas demonstraram um aspecto mais próximo ao normal nos animais tratados desde o nascimento, com redução do espessamento e acúmulo de GAG. Por serem órgãos de difícil correção na clínica, esse aspecto torna-se ainda mais relevante. Uma possível explicação é a ocorrência de modificações na matriz extracelular destes órgãos (conforme discutido anteriormente), o que leva ao processo de dilatação (na aorta) ou espessamento (das válvulas), os quais, uma vez estabelecidos, não podem ser revertidos. Embora não tenha sido possível avaliar válvulas de dois meses de idade neste projeto, nossos dados sugerem que aos seis meses a dilatação já é evidente, sendo razoável supor que as alterações sejam encontradas em alguma escala mesmo aos dois meses. Assim, no momento do início do tratamento no grupo adulto, algumas alterações já estariam presentes. Ainda, estudos prévios nos animais com MPS I sugerem que as primeiras alterações na elasticidade da aorta já podem ser detectadas antes dos dois meses de idade (Ma et al, 2008), o que reforça esta hipótese. Cabe também ressaltar que o fato destas duas estruturas serem pouco vascularizadas contribui para o insucesso ou sucesso parcial da TRE, de forma que, mesmo os animais tratados desde o nascimento, não são capazes de manter uma estrutura igual a normal, como acontece com as demais vísceras. Estes dados da TRE também reforçam nossa observação anterior nos animais com MPS VII tratados por terapia gênica, que, embora melhorem, não conseguem reverter totalmente as anormalidades na aorta em longo prazo.

Outras estruturas pouco vascularizadas também foram de difícil correção, como as articulações. O escore desenvolvido no nosso trabalho descrevendo a patogênese da doença se mostrou bastante adequado para avaliação da terapia, que não demonstrou efeito, independente de quando o tratamento foi iniciado. Cabe ressaltar aqui um ponto fraco do nosso trabalho: a avaliação realizada se baseia em achados histológicos nas articulações e ossos do joelho, que, embora comprovem que a enzima não consiga ser

distribuída até essas regiões, não necessariamente significa que não exista nenhuma melhora funcional. Em pacientes, a função articular medida geralmente é a mobilidade da articulação (Tylki-Szymanska et al, 2010a), o que não foi medido no presente trabalho. Em trabalhos futuros será necessário associar essas alterações a possíveis restrições de movimento que elas possam causar nos camundongos.

Um dos aspectos mais surpreendentes do presente trabalho foi a melhora no aspecto cerebral da doença. Ambos os grupos demonstraram melhorar a sua performance em testes comportamentais, bem como reduzir níveis de GAG no tecido. Uma vez que os testes classicamente usados para medir os GAG no cérebro nem sempre detectam seu aumento nessa estrutura (Ma et al, 2007), a atividade de catepsina D foi utilizada como um marcador secundário, já que esta havia se mostrado muito elevada no estudo de proteômica. A atividade desta protease também se mostrou diminuída nos animais tratados, confirmando os dados de GAG e dos testes comportamentais.

Baseado nestes dados e nos de terapia gênica, um experimento adicional no qual animais eram tratados com uma dose única de TRE (1,2 ou 2,4 mg/kg) foi planejado. Os animais foram sacrificados 1 hora após a injeção, e após perfusão dos animais com 20 mL de solução salina, as estruturas cerebrais foram retiradas e a atividade de IDUA foi medida. Estudos prévios indicam que os receptores de M6P existem na BHE de camundongos nas primeiras 2 semanas de vida (Urayama et al, 2008), motivo pelo qual este teste foi realizado em animais de 3 meses. O tempo de 1 hora foi escolhido para permitir a difusão da enzima, caso ela ocorresse, e ainda descartar a hipótese de que células do sistema imune estariam levando a enzima através da BHE, já que é um tempo muito curto para que isso ocorra. Os resultados confirmaram que uma pequena fração da enzima foi capaz de ultrapassar a barreira na dose de 1,2 mg/kg, o que já havia sido sugerido em um trabalho recente realizado em cachorros (Dierenfeld et al, 2010) enquanto que um aumento bastante pronunciado na captação da enzima pelo cérebro foi encontrado na dose de 2,4 mg/kg. Esse fato nos abre duas hipóteses de trabalho: a primeira é que este mecanismo de entrada da enzima para o cérebro seja um processo real, que se torna eficiente apenas em concentrações mais altas da enzima na circulação. A segunda hipótese é que, especialmente nos animais com 2,4 mg/kg, a perfusão dos animais não foi corretamente executada, e havia alguma contaminação com enzima do sangue, o que também pode ter havido nos experimentos de terapia gênica. Experimentos em mais animais serão realizados para confirmar estes achados. Cabe ressaltar que mesmo na concentração de 2,4 mg/kg, o volume injetado no animal é de

cerca de 100 μL (≈5% da volemia do animal), e, portanto não deve causar alterações na permeabilidade da BHE.

É paradoxal que, apesar de não existirem relatos na literatura de pacientes com síndrome de Hurler mais velhos tratados por TRE que tivessem sua cognição avaliada, é senso comum que a TRE não melhora os sintomas cerebrais da doença (Giugliani et al, 2010). Inclusive, pacientes com Hurler não possuem indicação de tratamento por TRE, exatamente por acreditar-se que não existe benefício neste aspecto da doença (de Ru et al, 2011). De forma interessante, pacientes Hurler tratados com TRE desde os primeiros anos de vida mostraram desenvolvimento mental normal (Wraith et al, 2007), o que sugere que na verdade a presunção de que a enzima não atravessa a BHE e nenhum beneficio cerebral viria da TRE pode estar incorreto.

De qualquer maneira, nossos resultados somados aos resultados bioquímicos e dos testes comportamentais sugerem que uma fração da enzima realmente atravessa a BHE, por mecanismos ainda desconhecidos. Ainda, estes dados levantam outra hipótese interessante, a de que a doença cerebral nas MPS talvez não seja irreversível, como até hoje se supunha. Os animais com MPS I já demonstram alterações na expressão de GFAP aos dois meses de idade, conforme demonstrado no nosso estudo. Além disso, estudos comportamentais (Pan et al, 2008) sugerem que as primeiras alterações também já possam ser detectadas aos dois meses, o que sugere que, em alguma extensão, já existiam anormalidades no sistema nervoso dos animais adultos no momento em que a TRE foi iniciada, e estas puderam ser revertidas.

Obviamente outros fatores, como o desenvolvimento cerebral de seres humanos e camundongos ocorrer de forma diferente, devem ser considerados na interpretação destes dados e tradução dos mesmos para os pacientes. Estudos subseqüentes do nosso grupo tentarão avaliar a eficácia da TRE em camundongos quando iniciada após o estabelecimento da doença cerebral, aos 6 meses de idade.

Por fim, a formação de anticorpos contra a enzima já foi demonstrada em pacientes e animais, e está relacionada a uma diminuição da eficácia da mesma (Dickson et al, 2012), sugerindo que a neutralização da enzima pelos anticorpos pode ser um fator importante na eficácia da terapia. O tratamento neonatal foi capaz de prevenir de forma mais efetiva a formação de anticorpos. Isso sugere a indução de uma tolerância imune nos neonatos, o que já havia sido descrito em cachorros tratados desde o nascimento (Dierenfeld et al, 2010). Mais importante, ao separar os animais que desenvolveram anticorpos daqueles que não desenvolveram, pode-se perceber que os

animais que tinham anticorpos contra a enzima apresentaram um desempenho pior no teste de habituação de campo aberto. A nossa hipótese é a de que, como apenas uma pequena fração da enzima atravessa a BHE, a formação de anticorpos reduz sua biodisponibilidade no soro, e prejudica sua entrada para o tecido cerebral, tornando o processo ainda mais inefetivo.

Na prática, a TRE iniciada ao nascimento apenas poderia acontecer em casos com histórico familiar, ou se fosse realizada a triagem neonatal para a MPS I. Um estudo de eficácia de terapias mais minucioso, bem como estudos de prevalência e de relação custo/beneficio deverão ser realizados para que se possa avaliar a viabilidade da triagem neonatal para MPS I ou outras doenças lisossômicas. No entanto, estudos recentes no Brasil propõem que se faça triagem neonatal para essas doenças em cidades ou regiões com alta prevalência, como no caso da MPS VI no interior da Bahia (Giugliani et al, *in press*).

Em conjunto, os nossos dados sugerem que múltiplos mecanismos estão envolvidos na patogênese das MPS, incluindo o aumento de proteases e ativação de processos inflamatórios. Ainda, o tratamento com cápsulas foi parcialmente efetivo na MPS I, e alguns ajustes na técnica ainda necessitam ser implementados antes de que se possa sugerir um ensaio clinico com as mesmas. Por outro lado, a terapia gênica se mostrou uma opção muito interessante para o tratamento da MPS I, e os trabalhos subseqüentes deverão avaliar a eficácia e segurança em animais maiores. Por fim, a TRE iniciada no período neonatal trouxe benefícios em órgãos de difícil correção, como aorta e válvulas, alem de prevenir a formação de anticorpos, e deve ser considerada quando possível para pacientes com MPS I.

CONCLUSÕES

Camundongos com MPS I apresentam dilatação cardíaca associada à perda da contratilidade do miocárdio. Por outro lado, as válvulas cardíacas se apresentam espessas e com redução no conteúdo de colágeno. A superexpressão de proteases como a catepsina B podem estar envolvidas nestes processos.

Os animais com MPS VII possuem dilatação na aorta, com quebras na elastina. No entanto, o nocaute de duas conhecidas elastases (MMP-12 e CtsS) provou não ser suficiente para a reversão do fenótipo. Outras vias, incluindo o sistema complemento e a via do TLR-4 podem estar levando a dilatação da aorta.

A doença articular nos camundongos MPS I se caracteriza por um processo destrutivo que inclui anormalidades como infiltrado inflamatório, reabsorção da cartilagem e perda da integridade da superfície articular e aumento na expressão de MMP-2 e MMP-9, o que pode se constituir em uma possível explicação para as alterações histológicas observadas.

Os camundongos MPS I desenvolvem progressivas alterações motoras, detectáveis a partir dos 4 meses, que podem ser mediadas por um processo neuroinflamatório, sem ocorrer, no entanto, morte neuronal.

Múltiplos mecanismos devem contribuir para as alterações cognitivas observadas na MPS I, incluindo processos neuroinflamatórios e alterações no nível de proteínas importantes para a plasticidade sináptica, como a PSD-95.

A produção e criopreservação de cápsulas de alginato contendo clones que superexpressam IDUA parece ser viável, com a encapsulação conseguindo manter a atividade enzimática e a viabilidade celular após períodos de criopreservação mais longos de forma eficiente.

O co-cultivo das cápsulas com fibroblastos de pacientes com MPS I foi capaz de corrigir estes últimos por até 45 dias, reestabelecendo a atividade enzimática e diminuindo o acúmulo de GAG.

O implante das cápsulas no peritôneo dos animais com MPS I permitiu uma correção em curto prazo, porém a formação de uma fibrose ao redor das mesmas e a formação de anticorpos contra a enzima podem ter sido fatores decisivos para a correção incompleta observada em longo prazo.

O tratamento de camundongos MPS I com os vetores retrovirais permitiu correção da doença no sistema nervoso, com o vetor com a LTR intacta se mostrando

mais eficaz. A terapia gênica iniciada no período neonatal em camundongos MPS VII atingiu níveis séricos muito superiores aos normais, porém a eficácia no tratamento da aorta se mostrou limitada.

O tratamento com TRE iniciado desde o nascimento parece surtir melhores efeitos em órgãos de difícil correção como a aorta e as válvulas cardíacas, além de prevenir a formação de anticorpos contra a enzima. Ainda, embora alguns órgãos como as articulações demonstrem pouca melhora com a TRE, uma fração da enzima parece cruzar a BHE e corrigir a doença no sistema nervoso dos animais.

REFERENCIAS

Aldenhoven M, Boelens JJ, de Koning TJ. The clinical outcome of Hurler syndrome after stem cell transplantation. Biol Blood Marrow Transplant 2008;14:485-98.

Alonso I, Marques JM, Souza N, Sequeiros J, Olsson IAS, Silveira I. Motor and cognitive deficits in the heterozygous leaner mouse, a Cav2.1 voltage-gated Ca2+ channel mutant. Neurobiology of Aging 2008; 29: 1733–1743.

Aoki T, Koizumi T, Kobayashi Y, et al. A novel method of cryopreservation of rat and human hepatocytes by using encapsulation technique and possible use for cell transplantation. Cell Transplant 2005; 14:609–20.

Ausseil J, Desmaris N, Bigou S, Attali R, Corbineau S, Vitry S, Parent M, Cheillan D, Fuller M, Maire I, Vanier MT, Heard JM. Early neurodegeneration progresses independently of microglial activation by heparan sulfate in the brain of mucopolysaccharidosis IIIB mice. PLoS One. 2008; 3(5):e2296

Balguid A, Rubbens MP, Mol A, Bank RA, Bogers AJ, van Kats JP, de Mol BA, Baaijens FP, Bouten CV. The role of collagen cross-links in biomechanical behavior of human aortic heart valve leaflets relevance for tissue engineering. Tissue Eng. 2007; 13(7):1501-11.

Beck M,.; Mucopolysaccharidosis type I (MPSI). Orphanet encyclopedia, September 2003: http://www.orpha.net/data/patho/GB/uk-MPS1.pdf

Bhaumik M, Muller VJ, Rozaklis T, Johnson L, Dobrenis K, Bhattacharyya R, Wurzelmann S, Finamore P, Hopwood JJ, Walkley SU, Stanley P. A mouse model for mucopolysaccharidosis type III A (Sanfilippo syndrome). Glycobiology. 1999; 9(12):1389-96.

Bifsha P, Landry K, Ashmarina L, Durand S, Seyrantepe V, Trudel S, Quiniou C, Chemtob S, Xu Y, Gravel RA, Sladek R, Pshezhetsky AV. Altered gene expression in cells from patients with lysosomal storage disorders suggests impairment of the ubiquitin pathway. Cell Death Differ. 2007; 14(3):511-23

Boado RJ, Hui EK, Lu JZ, Zhou QH, Pardridge WM. Reversal of lysosomal storage in brain of adult MPS-I mice with intravenous Trojan horse-iduronidase fusion protein. Mol Pharm. 2011; 8(4):1342-50

Boelens JJ, Rocha V, Aldenhoven M et al. Risk factor analysis of outcomes after unrelated cord blood transplantation in patients with hurler syndrome. Biol Blood Marrow Transplant 2009;15:618-25.

Boya P, Kroemer G. Lysosomal membrane permeabilization in cell death. Oncogene 2008; 27: 6434-6451.

Braunlin E, Mackey-Bojack S, Panoskaltsis-Mortari A, Berry JM, McElmurry RT, Riddle M, Sun LY, Clarke LA, Tolar J, Blazar BR. Cardiac functional and histopathologic findings in humans and mice with mucopolysaccharidosis type I: implications for assessment of therapeutic interventions in hurler syndrome. Pediatr Res. 2006; 59(1):27-32.

Braunlin EA, Stauffer NR, Peters CH, Bass JL, Berry JM, Hopwood JJ, Krivit W. Usefulness of bone marrow transplantation in the Hurler syndrome. Am J Cardiol. 2003 Oct 1;92(7):882-6.

Braunlin EA, Harmatz PR, Scarpa M, Furlanetto B, Kampmann C, Loehr JP, Ponder KP, Roberts WC, Rosenfeld HM, Giugliani R. Cardiac disease in patients with mucopolysaccharidosis: presentation, diagnosis and management. J Inherit Metab Dis. 2011; 34(6):1183-97.

Brooks DA, Kakavanos R, Hopwood JJ. Significance of immune response to enzyme-replacement therapy for patients with a lysosomal storage disorder. Trends Mol Med. 2003; 9(10):450-3.

Camassola M, Braga LM, Delgado-Cañedo A, Dalberto TP, Matte U, Burin M, Giugliani R, Nardi NB. Nonviral in vivo gene transfer in the mucopolysaccharidosis I murine model. J Inherit Metab Dis. 2005; 28(6):1035-43

Ceccariglia S, D'Altocolle A, Del Fa' A, Pizzolante F, Caccia E, Michetti F, Gangitano C. Cathepsin D plays a crucial role in the trimethyltin-induced hippocampal neurodegeneration process. Neuroscience. 2011; 174:160-70.

Cervantes-García D, Ortiz-López R, Mayek-Pérez N, Rojas-Martínez A. Oncolytic virotherapy. Ann Hepatol. 2008; 7(1):34-45.

Charp, P.A., R.J. Kinders, T.C. Johnson (1983) G2 cell cycle arrest induced by glycopeptides isolated from the bovine cerebral cortex. J Cell Biol 97: 311–316

Chen F, Vitry S, Hocquemiller M, Desmaris N, Ausseil J, Heard JM. alpha-L-Iduronidase transport in neurites. Mol Genet Metab. 2006; 87(4):349-58.

Cimaz R, Coppa GV, Koné-Paut I, Link B, Pastores GM, Elorduy MR, Spencer C, Thorne C, Wulffraat N, Manger B. Joint contractures in the absence of inflammation may indicate mucopolysaccharidosis. Pediatr Rheumatol Online J. 2009;7:18.

Clarke LA, Russell CS, Pownall S, Warrington CL, Borowski A, Dimmick JE, Toone J, Jirik FR. Murine mucopolysaccharidosis type I: targeted disruption of the murine alpha-L-iduronidase gene. Hum Mol Genet. 1997; 6(4):503-11.

Clarke L, Wraith JE, Beck M et al. Long-term efficacy and safety of laronidase in the treatment of mucopolysaccharidosis I. Pediatrics 2009;123:229_40.

Cox TM, Cachón-González MB. The cellular pathology of lysosomal diseases. J Pathol. 2012; 226(2):241-54.

Cox-Brinkman J, Smeulders MJ, Hollak CE, Wijburg FA. Restricted upper extremity range of motion in mucopolysaccharidosis type I: no response to one year of enzyme replacement therapy. J Inherit Metab Dis 2007; 30:47–50

de Ru MH, Boelens JJ, Das AM, Jones SA, van der Lee JH, Mahlaoui N, Mengel E, Offringa M, O'Meara A, Parini R, Rovelli A, Sykora KW, Valayannopoulos V, Vellodi A, Wynn RF, Wijburg FA. Enzyme replacement therapy and/or hematopoietic stem cell transplantation at diagnosis in patients with mucopolysaccharidosis type I: results of a European consensus procedure. Orphanet J Rare Dis. 2011; 6:55.

Degn SE, Jensenius JC, Thiel S. Disease-causing mutations in genes of the complement system. Am J Hum Genet. 2011; 88(6):689-705.

Dickson PI, Ellinwood NM, Brown JR, Witt RG, Le SQ, Passage MB, Vera MU, Crawford BE. Specific antibody titer alters the effectiveness of intrathecal enzyme replacement therapy in canine mucopolysaccharidosis I. Mol Genet Metab. 2012, *in press*.

Dierenfeld AD, McEntee MF, Vogler CA, Vite CH, Chen AH, Passage M, Le S, Shah S, Jens JK, Snella EM, Kline KL, Parkes JD, Ware WA, Moran LE, Fales-Williams AJ, Wengert JA, Whitley RD, Betts DM, Boal AM, Riedesel EA, Gross W, Ellinwood NM, Dickson PI. Replacing the enzyme alpha-L-iduronidase at birth ameliorates symptoms in the brain and periphery of dogs with mucopolysaccharidosis type I. Sci Transl Med. 2010; 2(60):60ra89

DiRosario J, Divers E, Wang C, Etter J, Charrier A, Jukkola P, Auer H, Best V, Newsom DL, McCarty DM, Fu H. Innate and adaptive immune activation in the brain of MPS IIIB mouse model. J Neurosci Res. 2009; 87(4):978-90.

Donsante A, Miller DG, Li Y, Vogler C, Brunt EM, Russell DW, Sands MS. AAV vector integration sites in mouse hepatocellular carcinoma. Science. 2007; 317(5837):477.

Ellinwood NM, Ausseil J, Desmaris N, Bigou S, Liu S, Jens JK, Snella EM, Mohammed EE, Thomson CB, Raoul S, Joussemet B, Roux F, Chérel Y, Lajat Y, Piraud M, Benchaouir R, Hermening S, Petry H, Froissart R, Tardieu M, Ciron C, Moullier P, Parkes J, Kline KL, Maire I, Vanier MT, Heard JM, Colle MA. Safe, efficient, and reproducible gene therapy of the brain in the dog models of Sanfilippo and Hurler syndromes. Mol Ther. 2011; 19(2): 251-9.

Evans GJ, Cousin MA. Tyrosine phosphorylation of synaptophysin in synaptic vesicle recycling. Biochem Soc Trans. 2005; 33(Pt 6):1350-3.

Evers M, Saftig P, Schmidt P, Hafner A, McLoghlin DB, Schmahl W, Hess B, von Figura K, Peters C. Targeted disruption of the arylsulfatase B gene results in mice

resembling the phenotype of mucopolysaccharidosis VI. Proc Natl Acad Sci U S A. 1996; 93(16):8214-9.

Fischer TA, Lehr HA, Nixdorff U, Meyer J. Combined aortic and mitral stenosis in mucopolysaccharidosis type I-S (Ullrich-Scheie syndrome). Heart. 1999; 81(1):97-9.

Friso A, Tomanin R, Alba S, Gasparotto N, Puicher EP, Fusco M, Hortelano G, Muenzer J, Marin O, Zacchello F, Scarpa M. Reduction of GAG storage in MPS II mouse model following implantation of encapsulated recombinant myoblasts. J Gene Med. 2005; 7(11):1482-91.

Fuller M, Meikle PJ, Hopwood JJ. Epidemiology of lysosomal storage diseases: an overview. In: Mehta A, Beck M, Sunder-Plassmann G, editors. Fabry Disease: Perspectives from 5 Years of FOS. Oxford: Oxford PharmaGenesis; 2006. Chapter 2.

Gabrielli O, Clarke LA, Bruni S, Coppa GV. Enzyme-replacement therapy in a 5-month-old boy with attenuated presymptomatic MPS I: 5-year follow-up. Pediatrics. 2010; 125(1):e183-7.

Gatto F, Redaelli D, Salvadè A, Marzorati S, Sacchetti B, Ferina C, Roobrouck VD, Bertola F, Romano M, Villani G, Antolini L, Rovelli A, Verfaillie CM, Biondi A, Riminucci M, Bianco P, Serafini M. Hurler Disease Bone Marrow Stromal Cells Exhibit Altered Ability to Support Osteoclast Formation. Stem Cells Dev. 2012 Mar 2. [Epub ahead of print]

Ge J, Zhao G, Chen R, Li S, Wang S, Zhang X, Zhuang Y, Du J, Yu X, Li G, Yang Y. Enhanced myocardial cathepsin B expression in patients with dilated cardiomyopathy. Eur J Heart Fail. 2006; 8(3): 284-9.

Giugliani R. Newborn screening for lysosomal diseases: current status and potential interface with population medical genetics in Latin America. J Inherit Metab Dis., no prelo.

Giugliani R, Rojas VM, Martins AM, Valadares ER, Clarke JT, Góes JE, Kakkis ED, Worden MA, Sidman M, Cox GF. A dose-optimization trial of laronidase (Aldurazyme) in patients with mucopolysaccharidosis I. Mol Genet Metab. 2009; 96(1):13-19

Giugliani R, Federhen A, Rojas MV, Vieira T, Artigalás O, Pinto LL, Azevedo AC, Acosta A, Bonfim C, Lourenço CM, Kim CA, Horovitz D, Bonfim D, Norato D, Marinho D, Palhares D, Santos ES, Ribeiro E, Valadares E, Guarany F, de Lucca GR, Pimentel H, de Souza IN, Correa J Neto, Fraga JC, Goes JE, Cabral JM, Simionato J, Llerena J Jr, Jardim L, Giuliani L, da Silva LC, Santos ML, Moreira MA, Kerstenetzky M, Ribeiro M, Ruas N, Barrios P, Aranda P, Honjo R, Boy R, Costa R, Souza C, Alcantara FF, Avilla SG, Fagondes S, Martins AM. Mucopolysaccharidosis I, II, and VI: Brief review and guidelines for treatment. Genet Mol Biol. 2010; 33(4): 589-604.

Grigull L, Sykora KW, Tenger A, Bertram H, Meyer-Marcotty M, Hartmann H, Bültmann E, Beilken A, Zivicnjak M, Mynarek M, Osthaus AW, Schilke R, Kollewe K, Lücke T. Variable disease progression after successful stem cell transplantation: prospective follow-up investigations in eight patients with Hurler syndrome. Pediatr Transplant. 2011; 15(8):861-9.

Hacein-Bey-Abina S, Garrigue A, Wang GP, Soulier J, Lim A, Morillon E, Clappier E, Caccavelli L, Delabesse E, Beldjord K, Asnafi V, MacIntyre E, Dal Cortivo L, Radford I, Brousse N, Sigaux F, Moshous D, Hauer J, Borkhardt A, Belohradsky BH, Wintergerst U, Velez MC, Leiva L, Sorensen R, Wulffraat N, Blanche S, Bushman FD, Fischer A, Cavazzana-Calvo M. Insertional oncogenesis in 4 patients after retrovirus-mediated gene therapy of SCID-X1. J Clin Invest. 2008; 118(9):3132-42

Harada H, Uchiwa H, Nakamura M, Ohno S, Morita H, Katoh A, Yoshino M, Ikeda H. Laronidase replacement therapy improves myocardial function in mucopolysaccharidosis I. Mol Genet Metab. 2011; 103(3):215-9.

Hartung SD, Frandsen JL, Pan D, Koniar BL, Graupman P, Gunther R, Low WC, Whitley CB, McIvor RS. Correction of metabolic, craniofacial, and neurologic abnormalities in MPS I mice treated at birth with adeno-associated virus vector transducing the human alpha-L-iduronidase gene. Mol Ther. 2004; 9(6):866-75.

Haskins ME, Otis EJ, Hayden JE, Jezyk PF, Stramm L. Hepatic storage of glycosaminoglycans in feline and canine models of mucopolysaccharidoses I, VI, and VII. Vet Pathol. 1992; 29(2):112-9.

Haskins ME. Animal models for mucopolysaccharidosis disorders and their clinical relevance. Acta Paediatr Suppl. 2007; 96(455):56-62.

Herati RS, Ma X, Tittiger M, Ohlemiller KK, Kovacs A, Ponder KP. Improved retroviral vector design results in sustained expression after adult gene therapy in mucopolysaccharidosis I mice. J Gene Med. 2008; 10(9):972-82.

Hobbs JR, Hugh-Jones K, Barrett AJ et al. Reversal of clinical features of Hurler's disease and biochemical improvement after treatment by bone-marrow transplantation. Lancet 1981; 2: 709-12.

Hocquemiller M, Vitry S, Bigou S, Bruyère J, Ausseil J, Heard JM. GAP43 overexpression and enhanced neurite outgrowth in mucopolysaccharidosis type IIIB cortical neuron cultures. J Neurosci Res. 2010; 88(1):202-13.

Holst B, Raby AC, Hall JE, Labéta MO. Complement takes its Toll: an inflammatory crosstalk between Toll-like receptors and the receptors for the complement anaphylatoxin C5a. Anaesthesia. 2012; 67(1):60-4.

Hopwood JJ, Morris CP. The mucopolysaccharidosis. Diagnosis, molecular genetics and treatment. Mol Biol med 1990; 7:381-404.

Horstman LL, Jy W, Ahn YS, Maghzi AH, Etemadifar M, Alexander JS, McGee JC, Minagar A. Complement in neurobiology. Front Biosci. 2011; 17:2921-60.

Imundo L, Leduc CA, Guha S, Brown M, Perino G, Gushulak L, Triggs-Raine B, Chung WK. A complete deficiency of Hyaluronoglucosaminidase 1 (HYAL1) presenting as familial juvenile idiopathic arthritis. J Inherit Metab Dis. 2011; 34: 1013-22.

Jimenez-Gomez C, Osentoski A, Woods JH. Pharmacological evaluation of the adequacy of marble burying as an animal model of compulsion and/or anxiety. Behav Pharmacol. 2011; 22(7):711-3.

Jordan MC, Zheng Y, Ryazantsev S, Rozengurt N, Roos KP, Neufeld EF. Cardiac manifestations in the mouse model of mucopolysaccharidosis I. Mol Genet Metab. 2005; 86(1-2):233-43.

Jordans S, Jenko-Kokalj S, Kühl NM, Tedelind S, Sendt W, Brömme D, Turk D, Brix K. Monitoring compartment-specific substrate cleavage by cathepsins B, K, L, and S at physiological pH and redox conditions. BMC Biochem. 2009; 10:23.

Jung SC, Park ES, Choi EN, Kim CH, Kim SJ, Jin DK. Characterization of a novel mucopolysaccharidosis type II mouse model and recombinant AAV2/8 vector-mediated gene therapy. Mol Cells. 2010; 30(1):13-8.

Khan SA, Nelson MS, Pan C, Gaffney PM, Gupta P. Endogenous heparan sulfate and heparin modulate bone morphogenetic protein-4 signaling and activity. Am J Physiol Cell Physiol. 2008; 294(6):C1387-97

Killedar S, Dirosario J, Divers E, Popovich PG, McCarty DM, Fu H. Mucopolysaccharidosis IIIB, a lysosomal storage disease, triggers a pathogenic CNS autoimmune response. J Neuroinflammation. 2010; 7:39.

King A, Sandler S, Andersson A. The effect of host factors and beads composition on the cellular overgrowth on implanted alginate beads. J Biomed Mater Res 2001; 57:374–83.

Kreuzaler PA, Staniszewska AD, Li W, Omidvar N, Kedjouar B, Turkson J, Poli V, Flavell RA, Clarkson RW, Watson CJ. Stat3 controls lysosomal-mediated cell death in vivo. Nat Cell Biol. 2011; 13: 303-9

Kuester D, Lippert H, Roessner A, Krueger S. The cathepsin family and their role in colorectal cancer. Pathol Res Pract. 2008; 204(7):491-500.

Lachman R, Martin KW, Castro S, Basto MA, Adams A, Teles EL. Radiologic and neuroradiologic findings in the mucopolysaccharidoses. J Pediatr Rehabil Med. 2010;3(2):109-18.

Li HH, Yu WH, Rozengurt N, Zhao HZ, Lyons KM, Anagnostaras S, Fanselow MS, Suzuki K, Vanier MT, Neufeld EF. Mouse model of Sanfilippo syndrome type B produced by targeted disruption of the gene encoding alpha-N-acetylglucosaminidase. Proc Natl Acad Sci U S A. 1999; 96(25):14505-10.

Li HB, Jiang H, Wang CY, Duan CM, Ye Y, Su XP, Kong QX, Wu JF, Guo XM. Comparison of two types of alginate microcapsules on stability and biocompatibility in vitro and in vivo. Biomed Mater. 2006; 1(1):42-7.

Liu XY, Nothias JM, Scavone A, Garfinkel M, Millis JM. Biocompatibility investigation of polyethylene glycol and alginate-poly-L-lysine for islet encapsulation. ASAIO J. 2010; 56(3):241-5.

Lloyd-Evans E, Morgan AJ, He X, Smith DA, Elliot-Smith E, Sillence DJ, Churchill GC, Schuchman EH, Galione A, Platt FM. Niemann-Pick disease type C1 is a sphingosine storage disease that causes deregulation of lysosomal calcium. Nat Med. 2008; 14(11):1247-55.

Longo GM, Buda SJ, Fiotta N, Xiong W, Griener T, Shapiro S, Baxter BT. MMP-12 has a role in abdominal aortic aneurysms in mice. Surgery. 2005; 137(4):457-62.

Ma X, Liu Y, Tittiger M, Hennig A, Kovacs A, Popelka S, Wang B, Herati R, Bigg M, Ponder KP. Improvements in mucopolysaccharidosis I mice after adult retroviral vector-mediated gene therapy with immunomodulation. Mol Ther. 2007; 15(5):889-902.

Ma X, Tittiger M, Knutsen RH, Kovacs A, Schaller L, Mecham RP, Ponder KP. Upregulation of elastase proteins results in aortic dilatation in mucopolysaccharidosis I mice. Mol Genet Metab. 2008; 94(3):298-304.

Maetzig T, Galla M, Baum C, Schambach A. Gammaretroviral vectors: biology, technology and application. Viruses. 2011; 3(6):677-713.

Malm G, Gustafsson B, Berglund G, Lindström M, Naess K, Borgström B, von Döbeln U, Ringdén O. Outcome in six children with mucopolysaccharidosis type IH, Hurler

syndrome, after haematopoietic stem cell transplantation (HSCT). Acta Paediatr. 2008; 97(8):1108-12.

Mango RL, Xu L, Sands MS, Vogler C, Seiler G, Schwarz T, Haskins ME, Ponder KP. Neonatal retroviral vector-mediated hepatic gene therapy reduces bone, joint, and cartilage disease in mucopolysaccharidosis VII mice and dogs. Mol Genet Metab. 2004; 82(1):4-19.

Martin DC, Atmuri V, Hemming RJ, Farley J, Mort JS, Byers S, Hombach-Klonisch S, Csoka AB, Stern R, Triggs-Raine BL. A mouse model of human mucopolysaccharidosis IX exhibits osteoarthritis. Hum Mol Genet. 2008; 17(13):1904-15.

Matte U, Yogalingam G, Brooks D, Leistner S, Schwartz I, Lima L, Norato DY, Brum JM, Beesley C, Winchester B, Giugliani R, Hopwood JJ. Identification and characterization of 13 new mutations in mucopolysaccharidosis type I patients. Mol Genet Metab. 2003; 78(1):37-43.

Matte U, Lagranha VL, de Carvalho TG, Mayer FQ, Giugliani R. Cell microencapsulation: a potential tool for the treatment of neuronopathic lysosomal storage diseases. J Inherit Metab Dis. 2011; 34(5):983-90

McGlynn R, Dobrenis K, Walkley S. Differential subcellular localization of cholesterol, gangliosides, and glycosaminoglycans in murine models of mucopolysaccharide storage disorders. J Comp Neurol 2004; 480:415-426.

Metcalf JA, Ma X, Linders B, Wu S, Schambach A, Ohlemiller KK, Kovacs A, Bigg M, He L, Tollefsen DM, Ponder KP. A self-inactivating gamma-retroviral vector reduces manifestations of mucopolysaccharidosis I in mice. Mol Ther. 2010; 18(2):334-42.

Metcalf JA, Linders B, Wu S, Bigg P, O'Donnell P, Sleeper MM, Whyte MP, Haskins M, Ponder KP. Upregulation of elastase activity in aorta in mucopolysaccharidosis I and VII dogs may be due to increased cytokine expression. Mol Genet Metab. 2010; 99: 396-407.

Meikle PJ, Hopwood JJ, Clague AE, Carey WF. Prevalence of lysosomal storage disorders. JAMA. 1999; 281(3):249-54.

Meikle, P.J., Fietz, M.J., Hopwood, J.J. Diagnosis of lysosomal storage disorders: current techniques and future directions. Expert Rev Mol Diagn. 2004; 4: 677–691.

Morgenstern PF, Marongiu R, Musatov SA, Kaplitt MG. Adeno-associated viral gene delivery in neurodegenerative disease. Methods Mol Biol. 2011;793:443-55.

Mu TW, Fowler DM, Kelly JW. Partial restoration of mutant enzyme homeostasis in three distinct lysosomal storage disease cell lines by altering calcium homeostasis. PLoS Biol. 2008; 6(2):e26.

Munoz-Rojas MV, Vieira T, Costa R, Fagondes S, John A, Jardim LB, Vedolin LM, Raymundo M, Dickson PI, Kakkis E, Giugliani R. Intrathecal enzyme replacement therapy in a patient with mucopolysaccharidosis type I and symptomatic spinal cord compression. Am J Med Genet A. 2008; 146A(19):2538-44.

Nayak JV, Hokey DA, Larregina A, He Y, Salter RD, Watkins SC, Falo LD Jr. Phagocytosis induces lysosome remodeling and regulated presentation of particulate antigens by activated dendritic cells. J Immunol 2006; 177:8493-503.

Nathwani AC, Tuddenham EG, Rangarajan S, Rosales C, McIntosh J, Linch DC, Chowdary P, Riddell A, Pie AJ, Harrington C, O'Beirne J, Smith K, Pasi J, Glader B, Rustagi P, Ng CY, Kay MA, Zhou J, Spence Y, Morton CL, Allay J, Coleman J, Sleep S, Cunningham JM, Srivastava D, Basner-Tschakarjan E, Mingozzi F, High KA, Gray JT, Reiss UM, Nienhuis AW, Davidoff AM. Adenovirus-associated virus vector-mediated gene transfer in hemophilia B. N Engl J Med. 2011; 365(25): 2357-65.

Neufeld E.F., Muenzer J. The Mucopolysaccharidoses. In Scriver CR, et al., eds. The Metabolic and Molecular Bases of Inherited Disease 2001; Eighth edition: 3421-3452.

Ohmi K, Zhao HZ, Neufeld EF. Defects in the medial entorhinal cortex and dentate gyrus in the mouse model of Sanfilippo syndrome type B. PLoS One. 2011;6(11):e27461.

Osborn MJ, McElmurry RT, Lees CJ, DeFeo AP, Chen ZY, Kay MA, Naldini L, Freeman G, Tolar J, Blazar BR. Minicircle DNA-based gene therapy coupled with immune modulation permits long-term expression of α-L-iduronidase in mice with mucopolysaccharidosis type I. Mol Ther. 2011; 19(3):450-60.

Otomo T, Higaki K, Nanba E, Ozono K, Sakai, N. Lysosomal storage causes cellular dysfunction in mucolipidosis II skin fibroblasts. J Biol Chem 2011; 286; 35283-90.

Pan C, Nelson MS, Reyes M, Koodie L, Brazil JJ, Stephenson EJ, Zhao RC, Peters C, Selleck SB, Stringer SE, Gupta P. Functional abnormalities of heparan sulfate in mucopolysaccharidosis-I are associated with defective biologic activity of FGF-2 on human multipotent progenitor cells. Blood. 2005; 106(6):1956-64.

Pan D, Sciascia A 2nd, Vorhees CV, Williams MT. Progression of multiple behavioral deficits with various ages of onset in a murine model of Hurler syndrome. Brain Res. 2008; 1188:241-53.

Petrey AC, Flanagan-Steet H, Johnson S, Fan X, De la Rosa M, Haskins ME, Nairn AV, Moremen KW, Steet R. Excessive activity of cathepsin K is associated with cartilage defects in a zebrafish model of mucolipidosis II. Dis Model Mech. no prelo.

Piller Puicher E, Tomanin R, Salvalaio M, Friso A, Hortelano G, Marin O, Scarpa M. Encapsulated engineered myoblasts can cure Hurler syndrome: preclinical experiments in the mouse model. Gene Ther. 2012; 19(4):355-64.

Polyakova O, Dear D, Stern I, Martin S, Hirst E, Bawumia S, Nash A, Dodson G, Bronstein I, Bayley PM. Proteolysis of prion protein by cathepsin S generates a soluble beta-structured intermediate oligomeric form, with potential implications for neurotoxic mechanisms. Eur Biophys J. 2009; 38:209-18.

Ratner BD, Bryant SJ. Biomaterials: where we have been and where we are going. Annu Rev Biomed Eng. 2004;6:41-75.

Reiser J, Adair B, Reinheckel T. Specialized roles for cysteine cathepsins in health and disease. J Clin Invest. 2010; 120(10):3421-31

Reolon GK, Braga LM, Camassola M, Luft T, Henriques JA, Nardi NB, Roesler R. Long-term memory for aversive training is impaired in Idua(-/-) mice, a genetic model of mucopolysaccharidosis type I. Brain Res. 2006; 1076(1):225-30.

Ren G, Takano T, Papillon J, Cybulsky AV. Cytosolic phospholipase A(2)-alpha enhances induction of endoplasmic reticulum stress. Biochim Biophys Acta. 2010 Apr;1803(4):468-81.

Reptik U, Stoka V, Turk V, Turk B. Lysosomes and lysosomal cathepsins in cell death. Biochim Biophys Acta 2012; 1824; 22-33

Ryazantsev S, Yu WH, Zhao HZ, Neufeld EF, Ohmi K. Lysosomal accumulation of SCMAS (subunit c of mitochondrial ATP synthase) in neurons of the mouse model of mucopolysaccharidosis III B. Mol Genet Metab. 2007; 90(4): 393-401.

Saftig P, Hunziker E, Wehmeyer O, Jones S, Boyde A, Rommerskirch W, Moritz JD, Schu P, von Figura K. Impaired osteoclastic bone resorption leads to osteopetrosis in cathepsin-K-deficient mice, Proc. Natl. Acad. Sci. USA 1998; 95; 13453–13458.

Saftig P. Physiology of the lysosome. In: Mehta A, Beck M, Sunder-Plassmann G, editors. Fabry Disease: Perspectives from 5 Years of FOS. Oxford: Oxford PharmaGenesis; 2006. Chapter 3.

Saftig P, Klumperman J. Lysosome biogenesis and lysosomal membrane proteins: trafficking meets function. Nat Rev Mol Cell Biol. 2009; 10(9):623-35

Sands MS, Barker JE. Percutaneous intravenous injection in neonatal mice. Lab Anim Sci. 1999; 49(3):328-30.

Sands MS, Birkenmeier EH. A single-base-pair deletion in the beta-glucuronidase gene accounts for the phenotype of murine mucopolysaccharidosis type VII. Proc Natl Acad Sci U S A. 1993; 90(14):6567-71.

Schroder BA, Wrocklage C, Hasilik A, Saftig P. The proeome of lysosomes. Proteomics 2010; 12: 4053-76.

Sardiello M, Palmieri M, di Ronza A, Medina DL, Valenza M, Gennarino VA, Di Malta C, Donaudy F, Embrione V, Polishchuk RS, Banfi S, Parenti G, Cattaneo E, Ballabio A. A gene network regulating lysosomal biogenesis and function. Science. 2009; 325(5939):473-7.

Scott HS, Anson DS., Orsborn AM, Nelson PV, Clements PR, Morris CP, Hopwood JJ. Human alpha-L-iduronidase: cDNA isolation and expression. Proc. Natl. Acad. Sci. U.S.A. 1991; 88, 9695-9699

Settembre C, Fraldi A, Rubinztein DC, Ballabio A. Lysosomal storage disorders as disorders of authophagy. Autophagy 2008; 4: 113-4.

Shapiro SD. Matrix metalloproteinase degradation of extracellular matrix: biological consequences. Current opinion in cell biology 1998; 10:602-8

Sifuentes M, Doroshow R, Hoft R, Mason G, Walot I, Diament M, Okazaki S, Huff K, Cox GF, Swiedler SJ, Kakkis ED. A follow-up study of MPS I patients treated with laronidase enzyme replacement therapy for 6 years. Mol Genet Metab. 2007; 90(2):171-80.

Simonaro CM, D'Angelo M, Haskins ME, Schuchman EH. Joint and bone disease in mucopolysaccharidoses VI and VII: identification of new therapeutic targets and biomarkers using animal models. Pediatr Res. 2005; 57(5 Pt 1):701-7.

Simonaro CM, D'Angelo M, He X, Eliyahu E, Shtraizent N, Haskins ME, Schuchman EH. Mechanism of glycosaminoglycan-mediated bone and joint disease: implications for the mucopolysaccharidoses and other connective tissue diseases. Am J Pathol. 2008; 172: 112-22.

Simonaro CM, Ge Y, Eliyahu E, He X, Jepsen KJ, Schuchman EH. Involvement of the Toll-like receptor 4 pathway and use of TNF-alpha antagonists for treatment of the mucopolysaccharidoses. Proc Natl Acad Sci U S A. 2010; 107:222-7.

Shi GP, Villadangos JA, Dranoff G, Small C, Gu L, Haley KJ, Riese R, Ploegh HL, Chapman HA. Cathepsin S required for normal MHC class II peptide loading and germinal center development. Immunity 1999; 10: 197–206.

Schmitz N, Laverty S, Kraus VB, Aigner T. Basic methods in histopathology of joint tissues. Osteoarthritis and Cartilage 2010; 18: S113-S116.

Smith LJ, Martin JT, Szczesny SE, Ponder KP, Haskins ME, Elliott DM. Altered lumbar spine structure, biochemistry, and biomechanical properties in a canine model of mucopolysaccharidosis type VII. J Orthop Res. 2010; 28(5):616-22.

Smith LJ, Martin JT, O'Donnell P, Wang P, Elliott DM, Haskins ME, Ponder KP. Effect of neonatal gene therapy on lumbar spine disease in mucopolysaccharidosis VII dogs. Molecular Genetics and Metabolsim, in press.

Smith LJ, Baldo G, Wu S, Liu Y, Whyte MP, Giugliani R, Elliott DM, Haskins ME, Ponder KP. Pathogenesis of lumbar spine disease in mucopolysaccharidosis VII. Molecular Genetics and Metabolsim, in press.

Sohn H, Kim YS, Kim HT, Kim CH, Cho EW, Kang HY, Kim NS, Kim CH, Ryu SE, Lee JH, Ko JH. Ganglioside GM3 is involved in neuronal cell death. FASEB J. 2006; 20(8):1248-50.

Sweet ES, Tseng CY, Firestein BL. To branch or not to branch: How PSD-95 regulates dendrites and spines. Bioarchitecture. 2011; 1(2):69-73.

Takahashi E, Niimi K, Itakura C. Motor coordination impairment in aged heterozygous rolling Nagoya, Cav2.1 mutant mice. Brain Research 2009; 1279: 50-57.

Tomatsu S, Gutierrez M, Nishioka T, Yamada M, Yamada M, Tosaka Y, Grubb JH, Montaño AM, Vieira MB, Trandafirescu GG, Peña OM, Yamaguchi S, Orii KO, Orii T, Noguchi A, Laybauer L. Development of MPS IVA mouse (Galnstm(hC79S.mC76S)slu) tolerant to human N-acetylgalactosamine-6-sulfate sulfatase. Hum Mol Genet. 2005; 14(22):3321-35.

Traas AM, Wang P, Ma X, Tittiger M, Schaller L, O'donnell P, Sleeper MM, Vite C, Herati R, Aguirre GD, Haskins M, Ponder KP. Correction of clinical manifestations of canine mucopolysaccharidosis I with neonatal retroviral vector gene therapy. Mol Ther. 2007; 15(8):1423-31.

Trask TW, Trask RP, Aguilar-Cordova E, Shine HD, Wyde PR, Goodman JC, Hamilton WJ, Rojas-Martinez A, Chen SH, Woo SL, Grossman RG. Phase I study of adenoviral delivery of the HSV-tk gene and ganciclovir administration in patients with current malignant brain tumors. Mol Ther. 2000; 1(2):195-203.

Turk V, Stoka V, Vasiljeva O, Renko M, Sun T, Turk B, Turk D. Cysteine cathepsins: from structure, function and regulation to new frontiers. Biochim Biophys Acta. 2012; 1824(1):68-88.

Tylki-Szymanska A, Marucha J, Jurecka A, Syczewska M, Czartoryska B. Efficacy of recombinant human alpha-L-iduronidase (laronidase) on restricted range of motion of upper extremities in mucopolysaccharidosis type I patients. J Inherit Metab Dis. 2010a;33(2):151-7.

Tylki-Szymanska A, Rozdzynska A, Jurecka A, Marucha J, Czartoryska B. Anthropometric data of 14 patients with mucopolysaccharidosis I: retrospective analysis and efficacy of recombinant human alpha-L-iduronidase (laronidase). Mol Genet Metab. 2010b; 99(1):10-7.

Urayama A, Grubb JH, Sly WS, Banks WA. Mannose 6-phosphate receptor-mediated transport of sulfamidase across the blood-brain barrier in the newborn mouse. Mol Ther. 2008; 16(7):1261-6.

Vasiljeva O, Dolinar M, Pungercar JR, Turk V, Turk B. Recombinant human procathepsin S is capable of autocatalytic processing at neutral pH in the presence of glycosaminoglycans. FEBS Lett. 2005; 579(5):1285-90.

Valayannopoulos V, Wijburg FA. Therapy for the mucopolysaccharidoses. Rheumatology (Oxford). 2011; 50 Suppl 5:v49-v59.

Venkat-Raman N, Sebire NJ, Murphy KW. Recurrent fetal hydrops due to mucopolysaccharidoses type VII. Fetal Diagn Ther. 2006; 21(3):250-4.

Vieira T, Schwartz I, Muñoz V, Pinto L, Steiner C, Ribeiro M, Boy R, Ferraz V, de Paula A, Kim C, Acosta A, Giugliani R. Mucopolysaccharidoses in Brazil: what happens from birth to biochemical diagnosis? Am J Med Genet A. 2008; 146A(13):1741-7.

Villani GR, Di Domenico C, Musella A, Cecere F, Di Napoli D, Di Natale P. Mucopolysaccharidosis IIIB: oxidative damage and cytotoxic cell involvement in the neuronal pathogenesis. Brain Res 2009; 1279: 99–108.

Villani GR, Chierchia A, Di Napoli D, Di Natale P. Unfolded protein response is not activated in the mucopolysaccharidoses but protein disulfide isomerase 5 is deregulated. J Inherit Metab Dis. 2012; 35(3):479-93.

Visigalli I, Delai S, Politi LS, Di Domenico C, Cerri F, Mrak E, D'Isa R, Ungaro D, Stok M, Sanvito F, Mariani E, Staszewsky L, Godi C, Russo I, Cecere F, Del Carro U, Rubinacci A, Brambilla R, Quattrini A, Di Natale P, Ponder K, Naldini L, Biffi A. Gene therapy augments the efficacy of hematopoietic cell transplantation and fully corrects mucopolysaccharidosis type I phenotype in the mouse model. Blood. 2010; 116(24):5130-9.

Vitry S, Ausseil J, Hocquemiller M, Bigou S, Dos Santos Coura R, Heard JM. Enhanced degradation of synaptophysin by the proteasome in mucopolysaccharidosis type IIIB. Mol Cell Neurosci. 2009; 41(1):8-18.

Vogler C, Levy B, Grubb JH, Galvin N, Tan Y, Kakkis E, Pavloff N, Sly WS. Overcoming the blood-brain barrier with high-dose enzyme replacement therapy in murine mucopolysaccharidosis VII. Proc Natl Acad Sci U S A. 2005; 102: 14777-82.

Walkley SU. Secondary accumulation of gangliosides in lysosomal storage disorders. Semin Cell Dev Biol. 2004 Aug;15(4):433-44.

Walther W, Stein U. Viral vectors for gene transfer. Drugs 2000; 60; 249-271.

Wang D, Shukla C, Liu X, Schoeb TR, Clarke LA, Bedwell DM, Keeling KM. Characterization of an MPS I-H knock-in mouse that carries a nonsense mutation analogous to the human IDUA-W402X mutation. Mol Genet Metab. 2010; 99(1):62-71.

Watanabe N, Anagnostopoulos PV, Azakie A. Aortic stenosis in a patient with Hurler's syndrome after bone marrow transplantation. Cardiol Young. 2011; 21(3):349-50.

Wayengera M. Proviral HIV-genome-wide and pol-gene specific Zinc Finger Nucleases: usability for targeted HIV gene therapy. Theor Biol Med Model. 2011 22; 8:26.

Wilson JM. Lessons learned from the gene therapy trial for ornithine transcarbamylase deficiency. Mol Genet Metab. 2009; 96(4):151-7

Wilson S, Hashamiyan S, Clarke L, Saftig P, Mort J, Dejica VM, Brömme D. Glycosaminoglycan-mediated loss of cathepsin K collagenolytic activity in MPS I contributes to osteoclast and growth plate abnormalities. Am J Pathol. 2009; 175(5):2053-62.

Wolf DA, Lenander AW, Nan Z, Braunlin EA, Podetz-Pedersen KM, Whitley CB, Gupta P, Low WC, McIvor RS, Increased longevity and metabolic correction following syngeneic BMT in a murine model of mucopolysaccharidosis type I. Bone Marrow Transplant, no prelo.

Wolf DA, Lenander AW, Nan Z, Belur LR, Whitley CB, Gupta P, Low WC, McIvor RS. Direct gene transfer to the CNS prevents emergence of neurologic disease in a murine model of mucopolysaccharidosis type I. Neurobiol Dis. 2011; 43(1):123-33.

Woloszynek JC, Coleman T, Semenkovich CF, Sands MS. Lysosomal dysfunction results in altered energy balance. J Biol Chem. 2007; 282(49):35765-71.

Woloszynek JC, Kovacs A, Ohlemiller KK, Roberts M, Sands MS. Metabolic adaptations to interrupted glycosaminoglycan recycling. J Biol Chem. 2009; 284(43):29684-91.

Wozniak DF, Hartman RE, Boyle MP. Apoptotic neurodegeneration induced by ethanol in neonatal mice is associated with profound learning/memory deficits in juveniles followed by progressive functional recovery in adults. Neurobiol. Dis 2004; 17, 403–414.

Wozniak DF, Xiao M, Xu L, Yamada KA, Ornitz DM. Impaired spatial learning and defective theta burst induced LTP in mice lacking fibroblast growth factor 14. Neurobiol Dis. 2007; 26: 14-26.

Wraith JE, Beck M, Lane R, van der Ploeg A, Shapiro E, Xue Y, Kakkis ED, Guffon N. Enzyme replacement therapy in patients who have mucopolysaccharidosis I and are younger than 5 years: results of a multinational study of recombinant human alpha-L-iduronidase (laronidase). Pediatrics. 2007; 120(1):e37-46.

Xu W. PSD-95-like membrane associated guanylate kinases (PSD-MAGUKs) and synaptic plasticity. Curr Opin Neurobiol. 2011; 21(2):306-12

Xu L, Mango RL, Sands MS, Haskins ME, Ellinwood NM, Ponder KP. Evaluation of pathological manifestations of disease in mucopolysaccharidosis VII mice after neonatal hepatic gene therapy. Mol Ther. 2002; 6(6):745-58.

Zaferani A, Vivès RR, van der Pol P, Hakvoort JJ, Navis GJ, van Goor H, Daha MR, Lortat-Jacob H, Seelen MA, van den Born J. Identification of tubular heparan sulfate as a docking platform for the alternative complement component properdin in proteinuric renal disease. J Biol Chem. 2011; 286(7):5359-67

Zhen EY, Brittain IJ, Laska DA, Mitchell PG, Sumer EU, Karsdal MA, Duffin KL. Characterization of metalloprotease cleavage products of human articular cartilage. Arthritis Rheum. 2008; 58:2420-31.

Zheng Y, Rozengurt N, Ryazantsev S, Kohn DB, Satake N, Neufeld EF. Treatment of the mouse model of mucopolysaccharidosis I with retrovirally transduced bone marrow. Mol Genet Metab. 2003; 79(4):233-44.

Zheng CY, Seabold GK, Horak M, Petralia RS. MAGUKs, synaptic development, and synaptic plasticity. Neuroscientist. 2011 Oct;17(5):493-512.

Zhu L, Wigle D, Hinek A, Kobayashi J, Ye C, Zuker M, Dodo H, Keeley FW, Rabinovitch M. The endogenous vascular elastase that governs development and progression of monocrotaline-induced pulmonary hypertension in rats is a novel enzyme related to the serine proteinase adipsin. J Clin Invest. 1994; 94(3):1163-71.

ANEXOS

PRODUÇÃO CIENTIFICA RELACIONADA

Neste item constam dois artigos publicados durante o período do doutorado em temas relacionados ao da tese, bem como um capítulo de livro sobre terapia gênica não viral para doenças lisossômicas.

Molecular Genetics and Metabolism 103 (2011) 197–198

Contents lists available at ScienceDirect

Molecular Genetics and Metabolism

journal homepage: www.elsevier.com/locate/ymgme

Brief Communication

Placenta analysis of prenatally diagnosed patients reveals early GAG storage in mucopolysaccharidoses II and VI

Guilherme Baldo [a,b], Ursula Matte [a], Osvaldo Artigalas [a], Ida Vanessa Schwartz [c,d], Maira Graeff Burin [c], Erlane Ribeiro [e], Dafne Horovitz [f], Tatiana Pacheco Magalhaes [f], Milan Elleder [g], Roberto Giugliani [a,b,c,d,*]

[a] Gene Therapy Center, Hospital de Clinicas, Porto Alegre, Brazil
[b] Postgraduate Program in Biological Sciences: Biochemistry, UFRGS, Porto Alegre, Brazil
[c] Medical Genetics Service, Hospital de Clinicas, Porto Alegre, Brazil
[d] Department of Genetics, UFRGS, Porto Alegre, Brazil
[e] Hospital Geral Cesar Cals, Fortaleza, Brazil
[f] Instituto Fernandes Figueira-FIOCRUZ, Rio de Janeiro, Brazil
[g] Institute of Inherited Metabolic Disorders, Prague, Czech Republic

ARTICLE INFO

Article history:
Received 22 January 2011
Received in revised form 2 March 2011
Accepted 2 March 2011
Available online 8 March 2011

Keywords:
Mucopolysaccharidoses
Hunter syndrome
Maroteaux–lamy syndrome
Prenatal diagnosis
Glycosaminoglycans
Lysosomal storage diseases

ABSTRACT

We analyzed placental tissue in one fetus with MPS II (iduronate sulphatase deficiency) and another with MPS VI (arylsulfatase B deficiency). Both were diagnosed prenatally, but families decided to continue pregnancies and placentas were collected at birth. We were able to demonstrate early storage of GAGs in both diseases by GAG measurement and microscopy analysis. Our results suggest that some alterations related to MPS storage, although not pronounced, may be observed in placental tissue of patients affected by MPS II and MPS VI.

1. Introduction

Some lysosomal storage disorders (LSDs) may present prenatal storage of large molecules, observed as membrane bound vacuoles in endothelial cells, trophoblasts and fibroblasts [1]. Among these LSDs there have been reports of vacuolated cells in some mucopolysaccharidoses (MPS), including MPS I and MPS VII [2]. We report — for the first time, to the best of our knowledge — analyses of placental tissue in fetuses with MPS II (iduronate sulphatase deficiency) and MPS VI (arylsulfatase B deficiency). The cases were diagnosed prenatally and in both situations the families decided to continue the pregnancy (abortion is, in most cases, illegal in Brazil), and placentas were collected at birth for analysis.

2. Clinical and laboratory report

In the first case, the mother (who had a brother with the severe form of MPS II) had 2 previous pregnancies (1 severe MPS II child, 1 spontaneous abortion). Prenatal diagnosis in amniocytes was performed (enzyme activity measurement and DNA analysis for the family mutation p.R88H) and confirmed MPS II. The parents decided to continue the pregnancy and planned to attempt all possible therapeutic alternatives. The baby was born at term (37 weeks 2 days), birth weight of 3320 g, height of 51 cm and OFC of 34 cm. Clinical examination at birth revealed subtle lumbar gibbus, with corresponding radiological abnormality (L3–L5); neurological examination disclosed hyper-reactivity, compatible with a more premature baby. Abdominal and cerebral ultrasound, echocardiogram, ophthalmologic and auditory evaluations and pulmonary function tests (oxymetry, pulmonary expansion and pulmonary resistance) were normal. Activity of iduronate sulphatase on the newborn was low both in plasma (1.2 nmol/4 h/ml — normal range: 122–463) and leukocytes (4.3 nmol/4 h/ml — normal range: 31–110). Placenta was collected and processed for electron microscopy (EM) analysis and glycosaminoglycan (GAG) measurement. Analysis of GAG content was performed using the dimethyl blue assay after GAG extraction [3]. Levels were about 4-fold higher than normal range (1265 μg GAG/g

Abbreviations: MPS II, mucopolysaccharidoses type II; MPS VI, mucopolysaccharidoses type VI; GAGs, glycosaminoglycans; LSD, lysosomal storage disorder; EM, electron microscopy.

* Corresponding author at: Serviço de Genética Médica, Hospital de Clínicas de Porto Alegre, Rua Ramiro Barcelos 2350, 90035-903 Porto Alegre, RS, Brazil. Fax: +55 51 3359 8010.
E-mail address: rgiugliani@hcpa.ufrgs.br (R. Giugliani).

1096-7192/$ – see front matter © 2011 Elsevier Inc. All rights reserved.
doi:10.1016/j.ymgme.2011.03.002

tissue, normal range 286–318 μg/g). Extensive EM examination disclosed discrete storage in lysosomes with ultrastructure compatible with the group of MPS disorders (Fig. 1). They were localized in occasional endothelial cells and in pericytes. Fibroblasts were free of storage. Hofbauer cells contained normal lysosomal apparatus which has been described to be physiologically distended [4]. There were no signs of storage in the trophoblast layer.

In the second case, there was a recurrence risk of MPS VI, because the couple already had two children affected with the severe form of MPS VI (confirmed by biochemical diagnosis). The previous sibs had the rapid progressing form of the disease (early diagnosis, hepatosplenomegaly, dysostosis multiplex, severe joint restrictions, significant heart disease and pulmonary disease). Despite these occurrences, the family looked for medical advice regarding genetic risks only on the third trimester of the new pregnancy. Cordocentesis was performed at 34 weeks, being the measurement of arylsulphatase B activity performed in dried fetal blood spots [5]. No clinical abnormalities were observed at birth: clinical examination, skeletal radiographs and echocardiogram were normal. Placenta was collected at birth, placed in buffered formalin, embedded in paraffin and analyzed using both H–E and Alcian Blue staining. A discrete storage in pericytes was observed, with no other convincing sign of storage at cytological level. As in the MPS II case, GAG levels were increased (490 μg/g tissue). Unfortunately we were not able to perform EM studies on this sample.

3. Conclusion

Our results suggest that some abnormalities related to MPS storage, although not pronounced, may be already observed in placental tissue of patients affected by MPS II and MPS VI. These results are especially important as they reinforce the prenatal onset of storage. Since treatment with enzyme replacement therapy for these two conditions is available, the presence of early storage may indicate that earlier introduction of therapy could probably lead to better results, as highlighted by the case described by McGill et al. [6]. Long-term results on a reasonable number of patients should be obtained to verify the efficacy of this approach, but the present study highlights the evidence for an early GAG accumulation and provides a rationale for a prenatal and/or newborn diagnosis (potentially with newborn screening) to enable earlier introduction of therapy, which could contribute to improve clinical outcomes on these conditions.

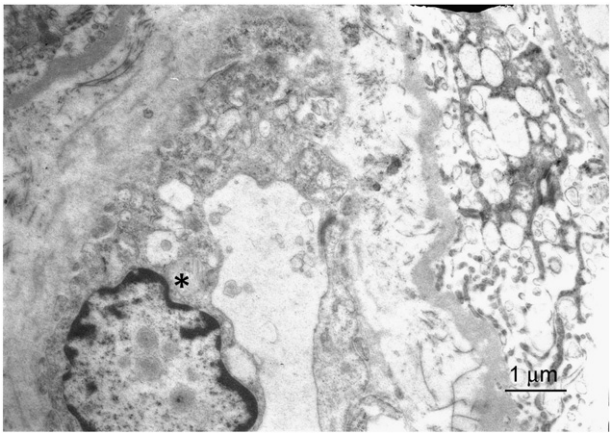

Fig. 1. Electron microscopy of the MPS II placenta, showing discrete storage of GAGs in the lysosome in the perinuclear region (asterisk). Magnification 8000×.

Acknowledgments

This work was supported by CNPq, the MPS Brazil Network and INAGEMP — Brazilian Institute of Population Medical Genetics.

References

[1] D.J. Fowler, G. Anderson, A. Vellodi, M. Malone, N.J. Sebire, Electron microscopy of chorionic villus samples for prenatal diagnosis of lysosomal storage disorders, Ultrastruct. Pathol. 31 (2007) 15–21.
[2] J. Nelson, B. Kenny, B. O'Hara, A. Harper, D. Broadhead, Foamy changes of placental cells in probable beta-glucuronidase deficiency associated with hydrops fetalis, J. Clin. Pathol. 46 (1993) 370–371.
[3] M. Camassola, L.M. Braga, A. Delgado-Cañedo, T.P. Dalberto, U. Matte, M. Burin, R. Giugliani, N.B. Nardi, Nonviral in vivo gene transfer in the mucopolysaccharidosis I murine model, J. Inherit. Metab. Dis. 28 (2005) 1035–1043.
[4] B.D. Lake, E.P. Young, B.G. Winchester, Prenatal diagnosis of lysosomal storage diseases, Brain Pathol. 8 (1998) 133–149.
[5] M.G. Burin, E. Ribeiro, J. Mari, I.V. Schwartz, M. Martins, R. Giugliani, Prenatal diagnosis of mucopolysaccharidosis VI by enzyme assay in a dried spot of fetal blood: a pioneering case report, Prenat. Diagn. 30 (2010) 89–90.
[6] J.J. McGill, A.C. Inwood, D.J. Coman, M.L. Lipke, D. de Lore, S.J. Swiedler, J.J. Hopwood, Enzyme replacement therapy for mucopolysaccharidosis VI from 8 weeks of age — a sibling control study, Clin. Genet. 77 (2009) 492–498.

Molecular Genetics and Metabolism xxx (2012) xxx–xxx

Contents lists available at SciVerse ScienceDirect

Molecular Genetics and Metabolism

journal homepage: www.elsevier.com/locate/ymgme

Pathogenesis of lumbar spine disease in mucopolysaccharidosis VII

Lachlan J. Smith [a,*], Guilherme Baldo [b,d], Susan Wu [b], Yuli Liu [b], Michael P. Whyte [b,c], Roberto Giugliani [d], Dawn M. Elliott [a,e], Mark E. Haskins [f], Katherine P. Ponder [b]

[a] Department of Orthopaedic Surgery, Perelman School of Medicine, University of Pennsylvania, Philadelphia, PA, USA
[b] Department of Internal Medicine, School of Medicine, Washington University, St. Louis, MO, USA
[c] Center for Metabolic Bone Disease and Molecular Research, Shriners Hospital for Children, St. Louis, MO, USA
[d] Biochemistry, UFRGS, Porto Alegre, RS, Brazil
[e] Department of Biomedical Engineering, College of Engineering, University of Delaware, Newark, DE, USA
[f] Department of Pathobiology, School of Veterinary Medicine, University of Pennsylvania, Philadelphia, PA, USA

ARTICLE INFO

Article history:
Received 19 March 2012
Accepted 19 March 2012
Available online xxxx

Keywords:
Lumbar spine
Mucopolysaccharidosis VII
Bone
Intervertebral disk
Cathepsin
Inflammation

ABSTRACT

Mucopolysaccharidosis type VII (MPS VII) is characterized by deficient β-glucuronidase (GUSB) activity, which leads to accumulation of chondroitin, heparan and dermatan sulfate glycosaminoglycans (GAGs), and multisystemic disease. MPS VII patients can develop kypho-scoliotic deformity and spinal cord compression due to disease of intervertebral disks, vertebral bodies, and associated tissues. We have previously demonstrated in MPS VII dogs that intervertebral disks degenerate, vertebral bodies have irregular surfaces, and vertebral body epiphyses have reduced calcification, but the pathophysiological mechanisms underlying these changes are unclear. We hypothesized that some of these manifestations could be due to upregulation of destructive proteases, possibly via the binding of GAGs to Toll-like receptor 4 (TLR4), as has been proposed for other tissues in MPS models. In this study, the annulus fibrosus of the intervertebral disk of 6-month-old MPS VII dogs had cathepsin B and K activities that were 117- and 2-fold normal, respectively, which were associated with elevations in mRNA levels for these cathepsins as well as TLR4. The epiphyses of MPS VII dogs had a marked elevation in mRNA for the cartilage-associated gene collagen II, consistent with a developmental delay in the conversion of the cartilage to bone in this region. The spine obtained at autopsy from a young man with MPS VII exhibited similar increased cartilage in the vertebral bodies adjacent to the end plates, disorganization of the intervertebral disks, and irregular vertebral end plate morphology. These data suggest that the pathogenesis of destructive changes in the spine in MPS VII may involve upregulation of cathepsins. Inhibition of destructive proteases, such as cathepsins, might reduce spine disease in patients with MPS VII or related disorders.

1. Introduction

The mucopolyaccharidoses (MPS) are a subset of lysosomal storage disorders characterized by deficiencies in enzymes that contribute to degradation of glycosaminoglycans (GAGs), and which exhibit multisystemic disease manifestations [1]. Spine abnormalities are prevalent, can require surgery, and significantly impact patients' quality of life [2,3]. MPS VII (Sly Syndrome) is characterized by deficient β-glucuronidase (GUSB) activity, which leads to accumulation of chondroitin, heparan and dermatan sulfate GAGs [4,5]. The impact of MPS VII on the spine can include odontoid hypoplasia, vertebral body collapse, thoracolumbar kyphosis and scoliosis, intervertebral disk degeneration, and spinal cord compression [4–9]. The naturally occurring MPS VII dog has a missense mutation (R166H) in the GUSB gene [10] and exhibits many of the musculoskeletal manifestations of the disorder observed in humans [11–13]. In recent studies, we demonstrated that the lumbar spines of 6-month-old MPS VII dogs had radiolucent, cartilaginous lesions in the ventral and dorsal regions of the vertebral epiphyses, suggestive of a failure to convert cartilage to bone during development [14], and which was consistent with a reduction in calcium in those regions. In addition, the vertebral endplates and intervertebral disk annulus fibrosus (AF) of MPS VII dogs contained elevated levels of GAG compared to those from normal animals [14]. Functionally, lumbar spine segments from MPS VII dogs exhibit reduced stiffness (increased laxity) and increased range of motion, which are likely due to a combination of the abnormalities in structure and composition [14].

The molecular bases of these abnormalities in MPS VII lumbar spines have not been described, limiting the development of new therapeutic strategies. In other tissues, such as joints and the aorta, upregulation of destructive enzymes such as matrix metalloproteinases (MMPs) and

* Corresponding author at: Department of Orthopaedic Surgery, Perelman School of Medicine, University of Pennsylvania, 424 Stemmler Hall, 36th and Hamilton Walk, Philadelphia, PA 19104, USA. Fax: +1 215 573 2133.
E-mail address: lachlans@mail.med.upenn.edu (L.J. Smith).

1096-7192/$ – see front matter © 2012 Elsevier Inc. All rights reserved.
doi:10.1016/j.ymgme.2012.03.014

cathepsins (Cts) is believed to play an important role in the pathogenesis of MPS [15,16]. These enzymes degrade key components of the extracellular matrix including elastin, collagens and proteoglycans [17]. Elevation of destructive enzymes in MPS may be due to induction of inflammatory pathways, such as those induced by Toll-like receptor 4 (TLR4) [18–20]. While liposaccharide (LPS) is the classical ligand of TLR4, heparan sulfate, one of the GAGs that accumulates in MPS VII, acts as an endogenous ligand of TLR4 and activates an inflammatory response via the NFκB signaling pathway [21,22]. TLR4/MPSVII double knockout mice have improved cranial and long bone morphology and growth plate organization compared to MPS VII mice [23]. TLR4 expression is significantly elevated in the aorta of MPS VII dogs [15] and in cells of the articular cartilage and synovium of MPS VI rats [20]. The first goal of this study was to determine if upregulation of proteolytic enzymes, inflammatory cytokines, and/or TLR4 contributes to extracellular matrix breakdown and altered biomechanical function in the lumbar spines of MPS VII dogs.

Humans with MPS VII are known to have hypoplastic anterior vertebrae [4], which can result in wedging of the vertebral body and contribute to a gibbus deformity. The spine also exhibits broad destructive changes in the vertebral bodies and intervertebral disks that can result in pain and contribute to joint instability. However, histopathological evaluation of a spine from a patient with MPS VII has never been reported. The second objective of this study, therefore, was to perform this analysis on a spine that was obtained from a 19-year old man with MPS VII.

2. Methods

2.1. Animals

The dogs used in this study were raised at the School of Veterinary Medicine at the University of Pennsylvania, under NIH and USDA guidelines for the care and use of animals in research. Females that were heterozygous for MPS VII ($GUSB^{+/-}$) were bred with retroviral vector-treated $GUSB^{-/-}$ males to generate heterozygous $GUSB^{+/-}$ or homozygous $GUSB^{-/-}$ dogs, which were identified by PCR of blood cell DNA at birth and confirmed with GUSB enzyme assay of serum. Most normal controls were littermates of MPS VII dogs or had at least one parent in common. Radiographs of the lumbar spines were obtained while under anesthesia with an intramuscular injection of 0.02 mg/kg of atropine (Phoenix Pharmaceutical, St. Joseph, MO) and 0.1 mg/kg of hydromorphone (Elkins-Sinn, Cherry Hill, NJ), and an IV injection of 2 mg/kg of propofol (Abbott, Chicago, IL). Euthanasia was performed for animals with substantial clinical manifestations, or for collection of tissues, using 80 mg/kg of sodium pentobarbital (Veterinary Laboratories, Lenexa, KS) in accordance with the American Veterinary Medical Association guidelines.

Lumbar spines (T12-sacrum) were dissected out immediately following euthanasia. For enzyme activity and mRNA analyses, the entire nucleus pulposus (NP) and the ventral AF were removed via sharp dissection from the T12–L1 disk. Samples from the ventral epiphysis of the L1 vertebral body that contained both cortical and trabecular bone were removed using bone shears.

2.2. Enzyme activity assays

For cathepsin activity assays, samples from the NP, AF and ventral vertebral epiphysis from 4 normal and 4 MPS VII dogs were homogenized with a hand-held homogenizer in 100 mM sodium acetate pH 5.5 containing 2.5 mM ethylenediaminetetraacetic acid (EDTA), 0.01% Triton X-100, and 2.5 mM dithiothreitol (DTT), and centrifuged at 10,000 *g* for 5 min at 4 °C as described previously [16]. For the total cathepsin assay, approximately 0.3 μg of the supernatant was incubated with 100 μM benzyloxycarbonyl-L-phenylalanyl-L-arginine-7-amido-4-methylcoumarin (Z-Phe-Arg-AMC) from Anaspec (San Jose, CA) at pH 7.5 in 100 mM sodium acetate with 2.5 mM EDTA, 0.01% Triton X-100, and 2.5 mM DTT in a microtiter plate at 37 °C. The amount of product was determined by excitation at 355 nm and emission at 460 nm using kinetic readings and comparison with 7-amino-4-methylcoumarin (AMC) standards from Anaspec. One unit (U) of enzyme produced 1 nmol of the product per hour at 37 °C. The protein concentration was determined with the Bradford assay (BioRad Laboratories; Hercules CA). The cathepsin B assay was performed using the same extracts and the substrate Z-Arg-Arg-AMC (Bachem; Torrance, CA) at pH 7.5. CtsK activity was measured at pH 7.5 with 10 μM of the substrate 2-aminobenzoic acid-HPGGPQ-N-(2,4-dinitrophenyl)-ethylenediamine (Abz-HPGGPQ-EDDnp) (Anaspec), which is cleaved by CtsK but not other cathepsins, and 2-aminobenzoic acid was the standard. The CtsD assay was performed at pH 4.0 with 10 μM of the substrate 7-methoxycoumarin-4-acetyl (Mca)-Gly-Lys-Pro-Ile-Leu-Phe-Phe-Arg-Leu-Lys-2,4 nitrophenyl (Dnp)-D-Arg-NH2, which can also be cleaved by CtsE, with Mca-Pro-Leu-OH (Enzo Life Sciences) as the standard. CtsK and CtsD assays were read at 320 nm for excitation and 420 nm for emission. Inhibition assays were performed as described previously [16] using cathepsin inhibitors obtained from Calbiochem (San Diego, CA) and included the CtsK inhibitor I [1,3-Bis(N-carbobenzoyloxy-L-leucyl) amino acetone; #219377] and the CtsB inhibitor Ac-Leu-Val-Lysinal (#219385). Samples were incubated with the inhibitor for 10 min prior to starting the assay. An MMP-12 enzyme activity assay was performed using a kit from Anaspec as detailed previously [16].

2.3. Messenger RNA levels

Frozen tissue samples from the NP, AF and ventral vertebral epiphysis from 5 normal and 5 MPS VII dogs were were homogenized for 30 s in a Mikro-Dismembrator (Braun Biotech International, Melsungen, Germany), then 1 ml of Trizol was added, and RNA was isolated using a Qiagen column as described previously [16]. Reverse transcription was performed on 1 μg of DNase I-treated RNA with an oligo (dT) 20 primer using a Superscript III kit (Invitrogen Corp; Carlsbad, CA) in a 20 μl volume, followed by real-time PCR on 0.4 μl of each cDNA sample per well using SYBR green reagents (Applied Biosystems; Foster City, CA). Primers are listed in Supplementary Table 1. The percent of a test RNA to that of β-actin was calculated by subtracting the cycle to reach the threshold (C_T) for a gene from the C_T for a separate real-time assay using β-actin primers to determine the ΔC_T, and the formula: Percent β-actin $= (100) \times 2^{\Delta CT}$. PCR reaction efficiency was determined for each primer by running serial dilutions of two control samples, and the slope demonstrated to be similar to that of β-actin. In addition, data were only accepted if the dissociation curve observed at the end of 40 PCR cycles was sharp and consistent for all the samples.

2.4. Statistical analysis

Values for samples from normal and MPS VII dogs were first compared using unpaired Student's *t*-tests and Sigma Plot 12 software (Systat Software, Inc.; Chicago, USA). If normality or equal variance tests failed, values were compared using the Mann–Whitney U test. Significance was defined as $p < 0.05$. All results are expressed as mean ± standard deviation.

2.5. Radiological and histological analysis of human MPS VII spinal tissue

Lumbar spine tissue comprising the intervertebral disk and vertebral bone was obtained at post-mortem at age 19 and fixed with formalin, decalcified, and embedded in paraffin. Four μm-thick sections were either stained with Masson's trichrome, double stained with alcian blue and picrosirius red [14], or stained with picrosirius red alone and viewed under polarized light [15]. Thoracolumbar radiographs had been obtained prior to death at age 18.

Please cite this article as: L.J. Smith, et al., Pathogenesis of lumbar spine disease in mucopolysaccharidosis VII, Mol. Genet. Metab. (2012), doi:10.1016/j.ymgme.2012.03.014

3. Results

3.1. Enzyme activity

We demonstrated previously that the endplate surface is markedly irregular at age 6 months [14], and demonstrate in the accompanying article [Smith et al., "Effect of neonatal gene therapy on lumbar spine disease in mucopolysaccharidosis VII dogs"] that several intervertebral disks had degenerated at 8 to 11 years-of-age in MPS VII dogs that were treated with neonatal gene therapy with a retroviral vector. To test the hypothesis that these abnormalities were due to upregulation of destructive enzymes, cathepsin activities in extracts of AF, NP and epiphyseal bone in normal and untreated MPS VII samples were evaluated using the fluorogenic substrate Z-Phe-Arg-AMC (Fig. 1A), which releases the fluorescent product AMC upon cleavage by a cathepsin. This particular substrate is cleaved by most cysteine cathepsins, and, thus, this represents a general cathepsin assay, although some cathepsins have reduced activity at neutral pH. Here we found that general cathepsin activity in MPS VII dogs was significantly elevated in the AF at $11{,}663 \pm 3922$ U/mg (110-fold normal; $p = 0.001$). General cathepsin activity was readily detectable in the NP at 88 ± 65 U/mg in MPS VII dogs, which was 440-fold normal ($p < 0.001$), although the absolute level was not as high as in the AF. General cathepsin activity was also high in the epiphysis of MPS VII dogs at 9166 ± 269 U/mg, or 9-fold normal ($p < 0.001$).

The promiscuity of the general cathepsin assay made it difficult to determine which of the 11 cysteine cathepsins contributed to activity. Therefore, assays were performed with inhibitors known to be relatively specific for distinct cathepsins, as shown in Figs. 1B and C. For samples from the AF and the epiphysis, the majority of the enzyme activity was inhibited with 10 nM of a CtsB inhibitor, suggesting that most of the original activity was due to CtsB. The CtsK inhibitor had slight inhibition of the CtsK activity at 100 to 1000 nM, but this is a concentration where the inhibitor has some activity against CtsB [16]. The inhibitor assay was not performed for the NP samples, as the amount of material was more limited and the enzyme activity was lower. The specificity of the cathepsin present in the extracts was also assessed using the substrate Z-Arg-Arg-AMC, which is relatively specific for CtsB, as shown in Fig. 1D. The enzyme activity was very similar to that observed for the general cathepsin assay, further confirming the hypothesis that the majority of the activity was due to CtsB.

CtsK is a very important enzyme for this study, as it is a potent collagenase. Although the majority of the cathepsin activity was clearly due to CtsB, it remained possible that some CtsK activity was present and was masked by the CtsB activity. Therefore, we performed a CtsK specific assay using a substrate that is reported to be specific for CtsK, which we verified experimentally [16]. Fig. 1E demonstrates that CtsK activity in the AF was 48 ± 2 U/mg, which was elevated at 2-fold normal ($p < 0.001$ vs. normal), but was only 0.5% of the activity of CtsB. CtsK activity was not elevated in the epiphysis. Finally, cathepsin D (CtsD) is an aspartyl protease that can cleave and activate CtsB. CtsD activity (Fig. 1F) was elevated to 1683 ± 783 U/mg (26-fold normal, $p < 0.001$) in the AF of MPS VII dogs. MMP-12 activity was also tested using a fluorogenic substrate, and was not elevated in either the AF or the epiphysis (data not shown).

3.2. Messenger RNA levels

3.2.1. Annulus fibrosus

Messenger RNA from the AF of the lumbar spine was evaluated to determine if changes in enzyme activity were due to changes in mRNA levels of those enzymes, and to determine if expression of other genes was affected (Fig. 2). Neither collagen Iα1 nor collagen IIα1 was altered at the mRNA level in the AF of MPS VII dogs compared with normal dogs. Small leucine-rich proteoglycans (SLRP) are proteoglycans that associate with collagens and contribute to their assembly. In MPS VII dogs, the SLRP decorin was reduced to 7% of the level in normal dogs ($p = 0.01$) although it remained abundant at 1.9-fold that of β-actin in the MPS VII dogs. Messenger RNA levels of lumican and biglycan were not significantly affected in MPS VII dogs. Levels of the large aggregating proteoglycan, aggrecan, were reduced to 24% of normal ($p = 0.04$). Levels of elastin in the AF were low and were not affected by MPS VII.

Levels of mRNA for several cathepsins were evaluated in the AF. CtsB is the cysteine cathepsin whose enzyme activity was noted to be elevated (see Section 3.1). CtsB mRNA was abundant in normal dogs at 70% of β-actin, and was 7-fold normal in MPS VII dogs ($p = 0.002$). Other

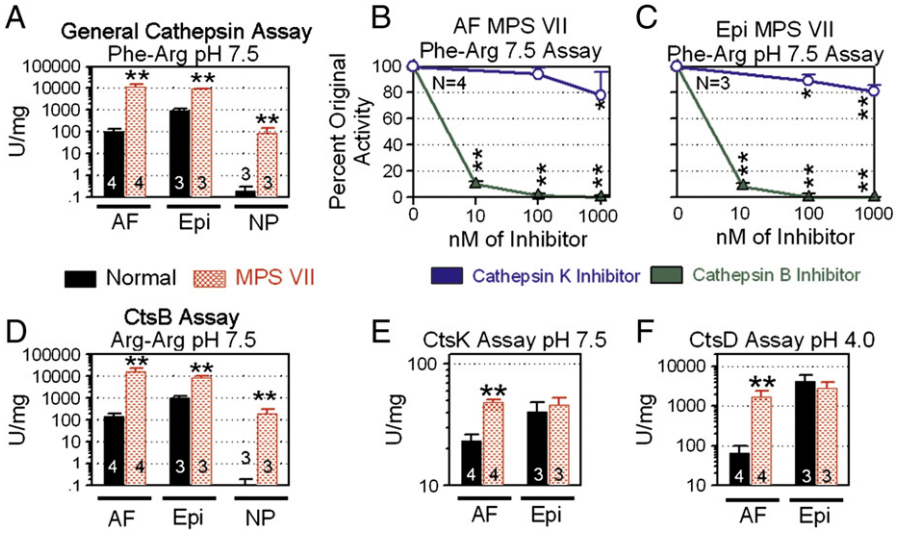

Fig. 1. Cathepsin enzyme activity. Samples from the indicated number of normal and untreated MPS VII dogs that were collected at 6 months of age were homogenized and enzyme assays performed using a fluorogenic substrate. Activity was normalized to the amount of protein in the sample. A. General cathepsin assay. B. General cathepsin assay of Annulus Fibrosus (AF) samples using cathepsin inhibitors. Samples from the AF of 4 MPS VII dogs were incubated with Z-Phe-Arg-AMC without or with the indicated concentrations of a CtsB or CtsK inhibitor, and the activity relative to that in the absence of an inhibitor determined and average percent remaining activity ± SD was determined. C. General cathepsin assay of epiphysis samples with inhibitors of specific cathepsins. D. CtsB assay. E. CtsK assay. F. CtsD assay. Student's t test was used to compare values between normal and MPS VII samples in panels A, D, E, and F; Student's *t*-test was used to compare values in samples that were incubated with an inhibitor with those in the same samples without an inhibitor in panels B and C. *$p < 0.05$, **$p < 0.005$.

Please cite this article as: L.J. Smith, et al., Pathogenesis of lumbar spine disease in mucopolysaccharidosis VII, Mol. Genet. Metab. (2012), doi:10.1016/j.ymgme.2012.03.014

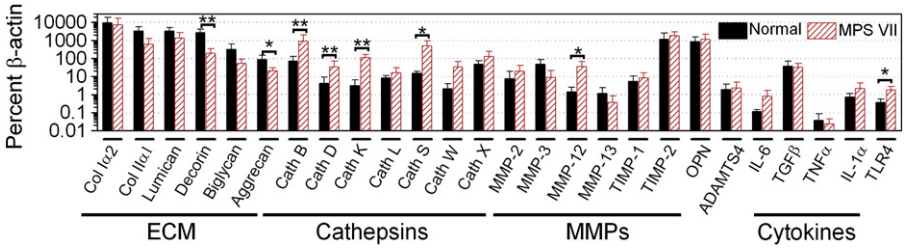

Fig. 2. Annulus fibrosus (AF) mRNA. Messenger RNA was isolated from the AF at the T12/L1 level for samples obtained from 6 month-old dogs. Reverse transcription was followed by real-time PCR, and levels of specific genes relative to that of β-actin in individual animals were determined as detailed in the Methods section, and the mean ± SD was determined. Genes for extracellular matrix molecules, catabolic enzymes, cytokines and receptors were assessed. Samples from 5 normal and 5 MPS VII dogs were analyzed. Values that were statistically different between the groups are indicated, where *$p<0.05$, and **$p<0.005$.

cysteine cathepsin mRNAs that were elevated in MPS VII dogs included CtsK (37-fold normal; $p=0.001$ vs. normal), CtsS (5-fold normal, $p=0.002$), and CtsW (2-fold normal, $p=0.002$). In addition, mRNA for an aspartyl cathepsin, CtsD, was elevated to 5-fold normal in untreated MPS VII dogs ($p=0.002$), consistent with the enzyme data shown above.

Levels of mRNA for several MMPs were examined in the AF. In MPS VII dogs, MMP12 mRNA was elevated to 25-fold normal ($p=0.03$) and was reasonably abundant at 33% of the level of β-actin. However, tissue inhibitor of metalloproteinase 2 (TIMP-2) was even higher at 18-fold that of β-actin in MPS VII dogs, which may explain why the MMP-12 activity was not elevated. Osteopontin (OPN) is a protein that has been reported to activate MMPs in a non-proteolytic fashion, although it can also play a role in signal transduction. Levels of mRNA for OPN were not affected in MPS VII dogs. Levels of mRNA for ADAMTS4, a protease that cleaves aggrecan, were also not different between normal and MPS VII dogs.

Various cytokines have been proposed to play a role in the pathogenesis of MPS in the aorta and synovium [15,19]. Interleukin-6 (IL-6) mRNA was 8-fold normal in MPS VII dogs, although this did not reach significance, which may relate to the small sample size. Levels of mRNA for TGF-β, TNF-α, and IL-1α were not elevated. The only signal transduction pathway gene that was tested by mRNA analysis that was significantly elevated in MPS VII dogs was TLR4, which was present at 2% of the level of β-actin in MPS VII dogs, and was 5-fold normal ($p=0.05$). Thus, TLR4 is present and should be capable of responding to GAG accumulation with expression of cytokines. Levels of mRNA for a number of other genes such as ADAMTS5, IL-6-like cytokines, receptors for IL-6 and related cytokines, and TLR5 did not exhibit differences in expression levels between normal and MPS VII samples in the AF, as shown in Supplementary Table 1.

3.2.2. Nucleus pulposus

The NP was also tested for mRNA levels, as shown in Supplementary Fig. 1. There were no apparent differences between MPS VII and normal dogs for any of the genes that were tested, although relatively low yields of mRNA made it difficult to test many genes. Cathepsin B, with enzyme activity that was elevated in NP in MPS VII compared with normal dogs, was not elevated at the mRNA level, raising the possibility that enzyme may diffuse from the AF to the NP.

3.2.3. Vertebral epiphysis

For the epiphysis (Fig. 3), values in samples from each group were more variable than for the AF or the NP, which likely reflected technical difficulties in obtaining and homogenizing samples from a calcified structure. Collagen IIα1, which is abundant in cartilage but not in bone, was elevated to 52-fold normal in MPS VII dogs ($p=0.03$). This is consistent with previously published histological data showing that the epiphysis contained cartilaginous lesions in place of bone, and with biochemical data demonstrating a reduction in calcium in these regions [14]. Messenger RNA levels for CtsK and CtsS were significantly elevated in MPS VII dogs, while mRNA levels for CtsB and CtsD appeared somewhat elevated in MPS VII samples, although differences were not significant. Messenger RNA levels for MMP12 were also significantly ($p=0.001$) elevated in the epiphyses of MPS VII dogs.

3.3. Analysis of radiographic abnormalities in MPS VII dogs during growth

We previously demonstrated that the ventral and to a lesser extent the dorsal epiphyses had cartilaginous lesions with reduced calcium content compared with normal dogs at 6 months of age, which correlated with the reduced calcification on radiographs [14]. Radiographs were used to evaluate the time course of abnormalities in calcification of the epiphysis in the lumbar spine (Fig. 4). Three normal and 3 MPS VII dogs were examined at each age. At 1 week after birth, lateral radiographs of the lumbar spine appeared similar for normal and untreated MPS VII dogs. However, reduced calcification of the epiphysis was apparent in the untreated MPS VII dogs at 1 and 2 months compared with normal controls. These data illustrate that abnormal calcification of the epiphysis is apparent as early as 1 month after birth in MPS VII dogs, and that shortening of the lumbar vertebral body lengths is apparent by 2 months.

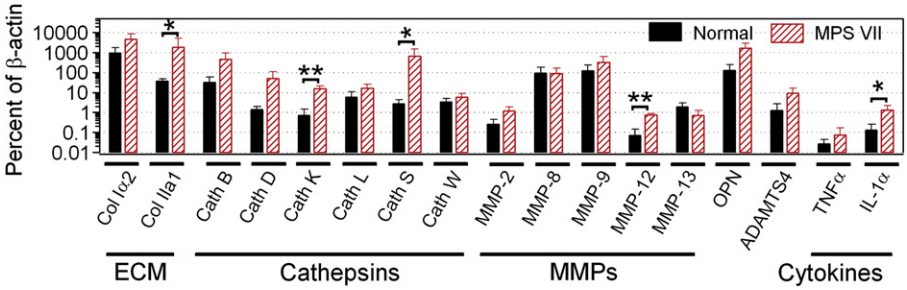

Fig. 3. Vertebral epiphysis mRNA. Messenger RNA from the anterior T12 vertebral epiphysis was analyzed for samples obtained from 6-month-old dogs. Reverse transcription was followed by real-time reverse transcriptase PCR as detailed in the legend of Fig. 3. Samples from 5 normal and 5 MPS VII dogs were analyzed.

Please cite this article as: L.J. Smith, et al., Pathogenesis of lumbar spine disease in mucopolysaccharidosis VII, Mol. Genet. Metab. (2012), doi:10.1016/j.ymgme.2012.03.014

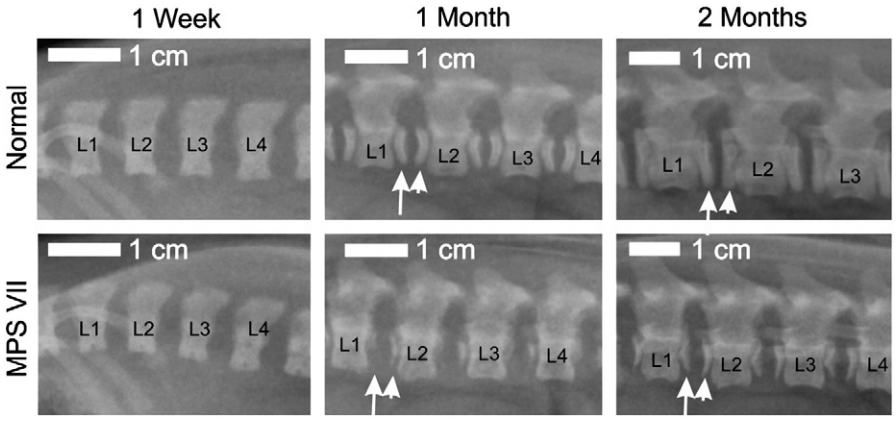

Fig. 4. Analysis of calcification of the lumbar spine in normal and MPS VII dogs during postnatal growth. Lateral radiographs of the lumbar spine from L1 to more caudal regions were obtained at the indicated age after birth from normal or untreated MPS VII dogs. The ventral aspect is at the bottom and the dorsal aspect at the top. At one week after birth, the length of the vertebrae was similar for the two groups, and epiphyses were not present in either group. For normal dogs, the caudal epiphysis of L1 (long arrow) and the cranial epiphysis of L2 (short arrow) were readily seen at 1 month after birth, and by age 2 months calcification of the ventral endplates extended as far as edge of the vertebral body. For MPS VII dogs, the size of the epiphyses was markedly reduced at age 1 month, and the epiphyses remained hypoplastic at age 2 months, which was most marked in the ventral region. At 2 months, the vertebral body lengths were clearly shorter in the MPS VII compared to the normal dogs. The radiographs shown are representative of those seen for 3 dogs for each age per group.

3.4. Radiographic and histological assessment of lumbar spine disease in human MPS VII

We undertook radiographic and histological analyses to determine if the lumbar spine in a human patient with MPS VII had morphological abnormalities that resembled those reported previously for MPS VII dogs. The patient examined was the first reported patient with MPS VII. He was diagnosed at 7 weeks of age when he presented with feet that turned inward and was noted to have other abnormalities including kyphosis that were consistent with MPS. Leukocyte GUSB enzyme activity was 2% of normal [4]. As shown in the previous publication, at 1 year-of-age he had a gibbus abnormality at T12, and underdevelopment of the anterior-superior portions of T10, T11, and L1 to L4. Lateral radiographs of the spine of the same patient when he was 18 years old (Fig. 5A) demonstrated a sharp angle at the position of T12 consistent with a gibbus deformity, although T12 itself could not be identified. The anterior-superior aspect of L1 was still hypoplastic, although other vertebrae appeared to have more complete anterior calcification than was present at 1 year of age. There were also increased lumbar intervertebral spaces and irregular endplates, similar to those reported in MPS VII dogs [24]. The posterior–anterior radiograph shown in Fig. 5B demonstrates marked scoliosis in the thoracic spine and degenerative changes.

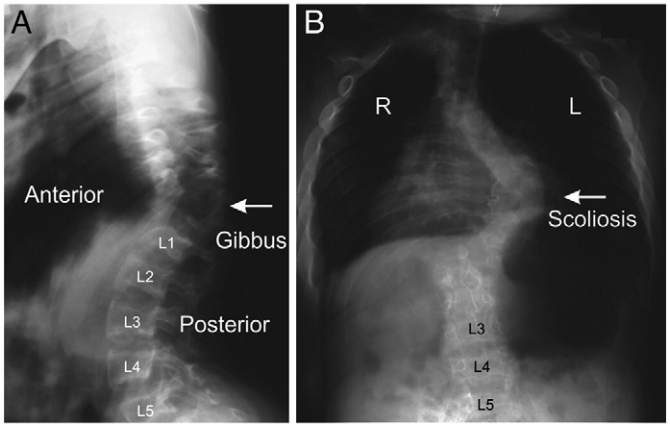

Fig. 5. Radiographs of the thoracolumbar spine of an 18 year-old man with MPS VII. A. Lateral radiograph. The positions of the lumbar vertebrae (L1 to L5) are indicated. There is a gibbus deformity of the spine at the position of T12 as indicated by the arrow, although a vertebral body cannot be identified at that position. The lumbar intervertebral space is increased relative to that found in a normal spine, and the surfaces of the endplates are irregular. The superior anterior aspect of L1 is hypoplastic. B. Posterior–anterior radiograph. The positions of the L3 to L5 vertebrae are indicated. Severe scoliosis of the thoracic spine is indicated with an arrow.

The patient died suddenly at age 19 years, possibly due to aspiration. A post mortem examination was performed. Grossly, the spine had a very irregular bone–cartilage interface, as previously reported [5]. The paraffin block of the lumbar spine that was prepared at the time of autopsy was retrieved from the pathology department for this study, and histochemical stains were performed, as shown in Fig. 6. Low magnification images of the entire section in Figs. 6A, D, and G are stained with alcian blue and picrosirius red, picrosirius red only (polarized light) and Masson's trichrome, respectively. With the alcian blue–picrosirius red stain (Fig. 6A), cartilage appears blue due to its GAG content, as indicated with asterisks, while bone and disk appear red due to collagen content. The cartilage was 1 to 2 mm thick for most of the interface between the vertebral body and the intervertebral disk, which is markedly abnormal. The region at the bone:cartilage interface indicated with the red arrow in Fig. 6A is shown at higher power in Fig. 6B, and illustrates cells with a characteristic morphology of chondrocytes. This region had a relatively low yellow/red signal when a picrosirius red-stained slide was evaluated with polarized light (Fig. 6E), which indicates that the collagen was not highly aligned. This region did, however, stain blue with Masson's trichrome (Fig. 6H), demonstrating that it contained collagen. In contrast, the red-staining region of the intervertebral disk indicated with the green arrow in Fig. 6D was highly birefringent in Fig. 6F, as would be expected for AF. These data indicated that there are large cartilaginous regions at the bone:intervertebral disk interface in a human with MPS VII, which resembles what occurs in MPS VII dogs, and would likely result in structural abnormalities similar to those found the dog model.

4. Discussion

4.1. Role of proteolytic enzymes and extracellular matrix in the pathogenesis of lumbar spine disease in MPS VII

The principal extracellular matrix (ECM) molecules responsible for maintaining tissue integrity in the AF include collagen types I and II, the large aggregating proteoglycan, aggrecan, and elastin [25,26]. In the NP, aggrecan is critical for maintaining tissue hydration which

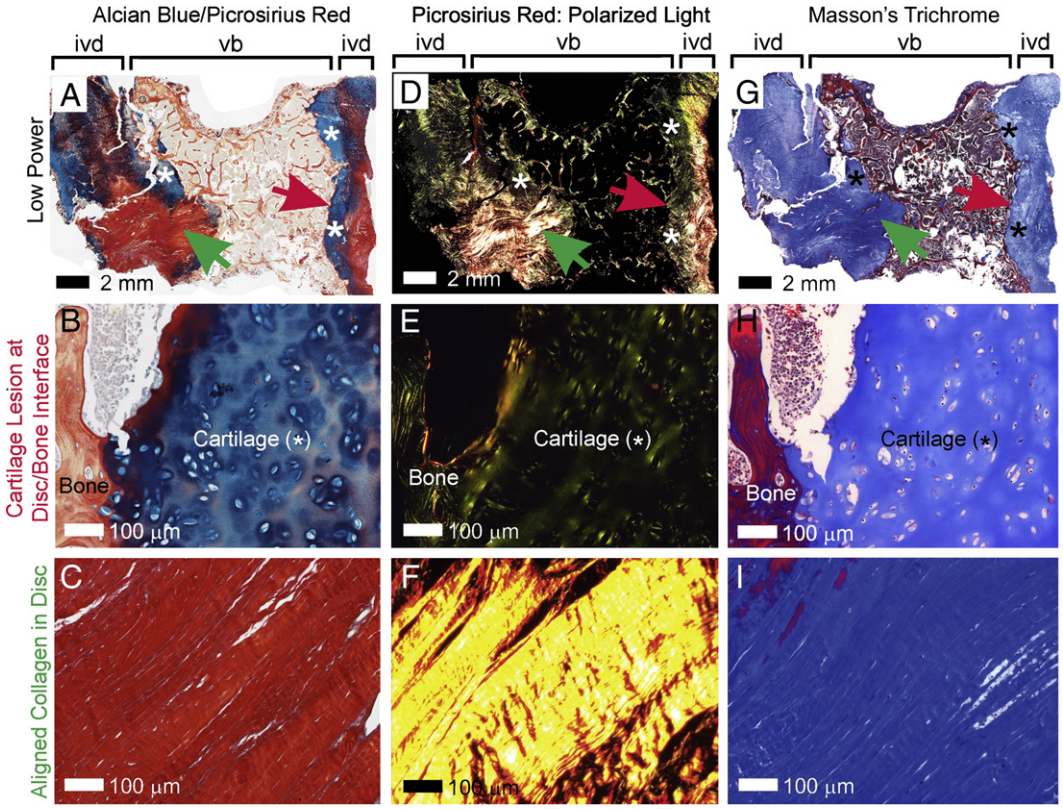

Fig. 6. Histological evaluation of the lumbar spine of a 19 year-old man with MPS VII. Sections containing a vertebral body and adjacent intervertebral disks were stained with alcian blue and picrosirius red (panels A–C; GAGs are blue and collagen is red), picrosirius red viewed under polarized light (panels D–F; triple-helical collagen is red to yellow), and Masson's trichrome stain (panels G–I; collagen is blue). The regions identified with the red arrow for the low power images contain an area of bone:cartilage interface, and are shown at higher power in panels B, E, and H. The region identified with the green arrow for the low power images contains an area with intervertebral disk, most likely AF, and is shown at higher power in panels C, F, and I.

enables the NP to evenly transfer and distribute loads between the vertebrae, while in the bone, collagen I is the major ECM protein. These tissues also contain SLRPs such as biglycan, decorin and lumican [27,28], which perform important structural and biological functions by interacting with collagens, elastin and various cytokines.

In this study, we hypothesized that abnormal structure and function in the lumbar spines of MPS VII dogs were due in part to upregulation of proteolytic enzymes in the vertebral bone and substructures of the intervertebral disk. The lysosomal cysteine cathepsins B, K, L, S and W can degrade one or more of these matrix molecules [17,29–32] and are associated with a number of degenerative musculoskeletal conditions, including osteoarthritis [31] and rheumatoid arthritis [33]. In addition, previous studies have suggested that they play an active role in the destructive changes in the aorta of mice and dogs with MPS [15,16,34]. In the AF, NP, and epiphysis, enzyme activity for CtsB was very high at 110-fold, 440-fold, and 9-fold normal, respectively, while CtsB mRNA was elevated in the AF at 7-fold normal. CtsB is a potent aggrecanase [30] and we propose that CtsB is an excellent candidate for an enzyme that contributes to desiccation of the NP. CtsB also has some activity against collagens I and II, although it is a less potent collagenase than CtsK [35]. Thus, CtsB could contribute to degradation of collagen I in bone and AF, collagen II in AF and endplate cartilage, and aggrecan in the endplate and AF. Of note was that the increase in enzyme activity was far greater than the increase in mRNA levels for CtsB. CtsD is an enzyme that cleaves and activates CtsB, and both mRNA and enzyme activity for CtsD were elevated in the MPS VII dog AF.

CtsK is able to cleave aggrecan, collagen II, and collagen I, key constituents of the NP, AF, and bone [29–31]. CtsK is upregulated in AF during the course of age-associated disk degeneration, and likely contributes to progressive loss of aggrecan [36,37]. Collagenolytic activity of cathepsin K is enhanced by chondroitin and keratan sulfates, whereas heparan and dermatan sulfates inhibit it [35,38]. Since MPS VII results in accumulation of the CtsK-activating chondroitin sulfate and the CtsK-inhibiting heparan and dermatan sulfates, the effect of these GAGS on CtsK activity requires further study. In the AF, CtsK activity was shown to be 2-fold normal in MPS VII dogs, while the mRNA was 37-fold normal. Thus, CtsK could contribute to degenerative changes, although the absolute level of CtsK activity appeared rather low and was <1% of the activity of CtsB.

Elastinolytic activity of MMP-12 and cathepsin S have previously been suggested to be associated with aortic disease in MPS I mice, and in MPS I and MPS VII dogs [15,34], although a more recent study demonstrated that deficiency of these enzymes did not protect against aortic dilatation, and further characterization of the cathepsin activity suggested that CtsB was actually responsible for what was initially thought to represent CtsS [16]. In this study, there were also some increases in mRNA for other cathepsins, but the absence of a specific assay and limited information regarding their specificity made it difficult to predict if they might contribute to degenerative changes. Although mRNA for MMP12 was elevated in MPS VII dogs, enzyme activity was not elevated. This could reflect the high levels of the MMP-inhibitor TIMP2.

Abnormal synthesis or assembly could contribute to ECM protein abnormalities. The inner AF normally contains significant quantities of aggrecan [26]. Aggrecan mRNA was 24% of normal in AF of MPS VII animals, pointing to potentially abnormal proteoglycan biosynthesis. Similarly, mRNA levels of the SLRP, decorin, were only 7% of normal in MPS VII animals. Although not significant, biglycan was 17% of normal. These proteoglycans perform important roles in collagen fibrillogenesis and fibril organization [39], and their dysregulation could disrupt AF structural development and mechanical function.

Please cite this article as: L.J. Smith, et al., Pathogenesis of lumbar spine disease in mucopolysaccharidosis VII, Mol. Genet. Metab. (2012), doi:10.1016/j.ymgme.2012.03.014

4.2. Role of inflammation in the pathogenesis of lumbar spine disease in MPS VII

Understanding the mechanism by which proteases are upregulated in spinal tissues in MPS VII is very important, as the failure to prevent spine disease with hematopoietic stem cell transplantation, ERT, or gene therapy leads us to predict that a new approach will be required to treat this particular manifestation. Upregulation of destructive proteases in synovium and aorta of MPS animals has been proposed to be due to induction of an inflammatory cascade via TLR4. In addition to its classical ligand, lipopolysaccharide, TLR4 also recognizes extracellular matrix breakdown products, such as hyaluronan fragments, heparan sulfate, fibrinogen, fibronectin extra domain A, lung surfactant protein A, and high-mobility group box 1 (HMGB1) proteins [40–43]. In this study we found that mRNA for TLR4 was significantly upregulated in the AF of MPS VII affected animals, while our previous study demonstrated that GAGs were 2-fold normal in the AF [14]. Upregulation of TLR4 has been demonstrated in articular chondrocytes and synoviocytes from MPS VI cats [20], and TLR4/MPSVII double knockout mice had improved cranial and long bone morphology, and growth plate organization compared to MPS VII mice [23]. It is possible that the TLR4 receptor on AF cells recognizes accumulated GAG fragments, initiating and sustaining an inflammatory response that drives increased activity of catabolic enzymes. It is also likely that TLR4 is upregulated as part of a feedback loop in which damage-associated molecular pathogens are generated as a consequence of increased matrix catabolism within the pre-existing local inflammatory environment. TLR4 may, therefore, present an attractive upstream therapeutic target for combating disk degeneration in MPS VII [44].

In this study, mRNA for cytokines such as IL-6, TNF-α, and TGF-β that have been elevated in other tissues in MPS was not significantly elevated in the AF in MPS VII dogs. It is possible that the relatively small number of samples analyzed here contributed to our failure to identify significant differences, as some genes such as IL-6 were 8-fold normal in MPS VII dogs. Alternatively, this may indicate that a different set of cytokines is expressed in the AF compared with the synovium or aorta. Further studies will attempt to test additional candidates for cytokines that may be playing an important role in the upregulation of destructive enzymes. For this study, the limited amount of RNA obtained per sample precluded testing additional genes.

4.3. Pathogenesis of poorly-calcified vertebral epiphyses in the spines of MPS VII dogs

Previously, we demonstrated that the ventral and dorsal epiphyses were poorly calcified at age 6 months, but the developmental progression of this abnormality was not clear. We now have demonstrated that the epiphysis of normal dogs exhibits calcification at 1 month-of-age and that calcification is already reduced at this age in the MPS VII dogs. mRNA analysis at 6 months demonstrated that collagen 2 (Col2α1) expression was 52-fold normal in the epiphyses of MPS VII dogs (collagen II is abundant in cartilage and low in bone), which is consistent with previous radiological and histological reports at age 6 months. This abnormality may be a major cause of the reduced stiffness of spine motion segments at age 6 months, and may also contribute to the vertebral body collapse that can occur in the thoracolumbar spine in MPS VII patients [9]. Ongoing work will seek to further address why the conversion from cartilage to bone is abnormal using samples from 1 month-old normal and MPS VII dogs, as differences between calcification in these groups appear to be most profound at that age. Abnormal cartilage to bone conversion may reflect delayed endochondral ossification during development, perhaps due to dysregulation of growth factor signaling by accumulating GAGs, altered vascular supply, or other factors.

4.4. Radiographic and histological presentation of lumbar spine disease in human MPS VII

This is the first report of histochemical evaluation of the spine in an adult human patient with MPS VII. Radiographs at 18 years demonstrated severe degenerative abnormalities of the vertebral bodies and kyphoscoliosis that were substantially more severe than was observed at 1 year-of-age from the same patient [4]. At age 19 years, histology demonstrated that there were residual cartilage remnants adjacent to the vertebral end plates, which likely relate to a failure to convert cartilage to bone during development, as occurred in the MPS VII dog model, although the possibility that this represents a thickening of the articular cartilage of the endplate cannot be ruled out. The marked irregularities of the vertebral body surface were also similar to what occurs in the MPS VII dog model, and may be due to upregulation of destructive proteases. These findings suggest that abnormalities in the spine are similar in humans and dogs with MPS VII, and strongly support the continued use of the canine model for studying spine disease pathogenesis and outcomes of therapeutic interventions in MPS VII.

4.5. Summary and implications

Upregulation of destructive enzymes in MPS VII likely contributes to intervertebral disk and vertebral bone degeneration, which may be induced by the TLR4 pathway. Possible treatments for this manifestation of disease could include the inhibition of proteases such as CtsB and CtsK that are responsible for the destructive changes, or inhibition of the TLR4 pathway or downstream cytokines. The failure to fully convert cartilage to bone in the epiphysis is likely due to a different mechanism and results in regions in the vertebral bodies that are not calcified and are less resistant to forces, contributing to spine instability. Developing treatments for this aspect of disease will require a better understanding of the underlying biological processes that are abnormal.

Supplementary materials related to this article can be found online at doi:10.1016/j.ymgme.2012.03.014.

Acknowledgments

This study was funded by grants from the NIH (DK054481, HD061879, RR002512 and OD012095), a Research Grant from the University of Pennsylvania, and the Penn Center for Musculoskeletal Disorders. We thank Dr William H. McAlister for help in evaluating radiographs.

References

[1] E.F. Neufeld, J. Muenzer, The mucopolysaccharidoses, in: C.R. Scriver, A.L. Beaudet, W.S. Sly, D. Valle (Eds.), The Metabolic and Molecular Bases of Inherited Disease, McGraw-Hill, New York, 2001, pp. 3421–3452.
[2] J.E. Wraith, The mucopolysaccharidoses: a clinical review and guide to management, Arch. Dis. Child. 72 (1995) 263–267.
[3] K.K. White, P. Harmatz, Orthopedic management of mucopolysaccharide disease, J. Pediatr. Rehabil. Med. 3 (2010) 47–56.
[4] W.S. Sly, B.A. Quinton, W.H. McAlister, D.L. Rimoin, Beta glucuronidase deficiency: report of clinical, radiologic, and biochemical features of a new mucopolysaccharidosis, J. Pediatr. 82 (1973) 249–257.
[5] C. Vogler, B. Levy, J.W. Kyle, W.S. Sly, J. Williamson, M.P. Whyte, Mucopolysaccharidosis VII: postmortem biochemical and pathological findings in a young adult with beta-glucuronidase deficiency, Mod. Pathol. 7 (1994) 132–137.
[6] P.D. Pizzutillo, J.A. Osterkamp, C.I. Scott Jr., M.S. Lee, Atlantoaxial instability in mucopolysaccharidosis type VII, J. Pediatr. Orthop. 9 (1989) 76–78.
[7] A.L. Beaudet, N.M. DiFerrante, G.D. Ferry, B.L. Nichols Jr., C.E. Mullins, Variation in the phenotypic expression of beta-glucuronidase deficiency, J. Pediatr. 86 (1975) 388–394.
[8] R.D. Dickerman, K.O. Colle, C.A. Bruno Jr., S.J. Schneider, Craniovertebral instability with spinal cord compression in a 17-month-old boy with Sly syndrome (mucopolysaccharidosis type VII): a surgical dilemma, Spine 29 (2004) E92–E94.
[9] R.D. de Kremer, I. Givogri, C.E. Argarana, E. Hliba, R. Conci, C.D. Boldini, A.P. Capra, Mucopolysaccharidosis type VII (beta-glucuronidase deficiency): a chronic variant

with an oligosymptomatic severe skeletal dysplasia, Am. J. Med. Genet. 44 (1992) 145–152.
[10] J. Ray, A. Bouvet, C. DeSanto, J.C. Fyfe, D. Xu, J.H. Wolfe, G.D. Aguirre, D.F. Patterson, M.E. Haskins, P.S. Henthorn, Cloning of the canine beta-glucuronidase cDNA, mutation identification in canine MPS VII, and retroviral vector-mediated correction of MPS VII cells, Genomics 48 (1998) 248–253.
[11] M. Haskins, M. Casal, N.M. Ellinwood, J. Melniczek, H. Mazrier, U. Giger, Animal models for mucopolysaccharidoses and their clinical relevance, Acta Paediatr. Suppl. 91 (2002) 88–97.
[12] M.E. Haskins, R.J. Desnick, N. DiFerrante, P.F. Jezyk, D.F. Patterson, Beta-glucuronidase deficiency in a dog: a model of human mucopolysaccharidosis VII, Pediatr. Res. 18 (1984) 980–984.
[13] D.C. Silverstein Dombrowski, K.P. Carmichael, P. Wang, T.M. O'Malley, M.E. Haskins, U. Giger, Mucopolysaccharidosis type VII in a German Shepherd Dog, J. Am. Vet. Med. Assoc. 224 (2004) 553–557.
[14] L.J. Smith, J.T. Martin, S.E. Szczesny, K.P. Ponder, M.E. Haskins, D.M. Elliott, Altered lumbar spine structure, biochemistry, and biomechanical properties in a canine model of mucopolysaccharidosis type VII, J. Orthop. Res. 28 (2010) 616–622.
[15] J.A. Metcalf, B. Linders, S. Wu, P. Bigg, P. O'Donnell, M.M. Sleeper, M.P. Whyte, M. Haskins, K.P. Ponder, Upregulation of elastase activity in aorta in mucopolysaccharidosis I and VII dogs may be due to increased cytokine expression, Mol. Genet. Metab. 99 (2010) 396–407.
[16] G. Baldo, S. Wu, R.A. Howe, M. Ramamoothy, R.H. Knutsen, J. Fang, R.P. Mecham, Y. Liu, X. Wu, J.P. Atkinson, K.P. Ponder, Pathogenesis of aortic dilatation in mucopolysaccharidosis VII mice may involve complement activation, Mol. Genet. Metab. 104 (2011) 608–619.
[17] M.E. McGrath, The lysosomal cysteine proteases, Annu. Rev. Biophys. Biomol. Struct. 28 (1999) 181–204.
[18] C.M. Simonaro, Cartilage and chondrocyte pathology in the mucopolysaccharidoses: the role of glycosaminoglycan-mediated inflammation, J. Pediatr. Rehabil. Med. 3 (2010) 85–88.
[19] C.M. Simonaro, M. D'Angelo, M.E. Haskins, E.H. Schuchman, Joint and bone disease in mucopolysaccharidoses VI and VII: identification of new therapeutic targets and biomarkers using animal models, Pediatr. Res. 57 (2005) 701–707.
[20] C.M. Simonaro, M. D'Angelo, X. He, E. Eliyahu, N. Shtraizent, M.E. Haskins, E.H. Schuchman, Mechanism of glycosaminoglycan-mediated bone and joint disease: implications for the mucopolysaccharidoses and other connective tissue diseases, Am. J. Pathol. 172 (2008) 112–122.
[21] G.B. Johnson, G.J. Brunn, Y. Kodaira, J.L. Platt, Receptor-mediated monitoring of tissue well-being via detection of soluble heparan sulfate by Toll-like receptor 4, J. Immunol. 168 (2002) 5233–5239.
[22] J. Ausseil, N. Desmaris, S. Bigou, R. Attali, S. Corbineau, S. Vitry, M. Parent, D. Cheillan, M. Fuller, I. Maire, M.T. Vanier, J.M. Heard, Early neurodegeneration progresses independently of microglial activation by heparan sulfate in the brain of mucopolysaccharidosis IIIB mice, PLoS One 3 (2008) e2296.
[23] C.M. Simonaro, Y. Ge, E. Eliyahu, X. He, K.J. Jepsen, E.H. Schuchman, Involvement of the Toll-like receptor 4 pathway and use of TNF-alpha antagonists for treatment of the mucopolysaccharidoses, Proc. Natl. Acad. Sci. U. S. A. 107 (2010) 222–227.
[24] R.S. Herati, V.W. Knox, P. O'Donnell, M. D'Angelo, M.E. Haskins, K.P. Ponder, Radiographic evaluation of bones and joints in mucopolysaccharidosis I and VII dogs after neonatal gene therapy, Mol. Genet. Metab. 95 (2008) 142–151.
[25] L.J. Smith, N.L. Fazzalari, The elastic fibre network of the human lumbar anulus fibrosus: architecture, mechanical function and potential role in the progression of intervertebral disc degeneration, Eur. Spine J. 18 (2009) 439–448.
[26] J. Urban, Disc biochemistry in relation to function, in: S.W. Wiesel, J.N. Weinstein, H.N. Herkowitz, J. Dvorak, G. Bell (Eds.), The Lumbar Spine, Saunders, Philadelphia, 1996, pp. 271–280.
[27] K. Singh, K. Masuda, E.J. Thonar, H.S. An, G. Cs-Szabo, Age-related changes in the extracellular matrix of nucleus pulposus and anulus fibrosus of human intervertebral disc, Spine (Phila Pa 1976) 34 (2009) 10–16.
[28] S. Brown, J. Melrose, B. Caterson, P. Roughley, S.M. Eisenstein, S. Roberts, A comparative evaluation of the small leucine-rich proteoglycans of pathological human intervertebral discs, Eur. Spine J. (2012), doi:10.1007/s00586-012-2179-1.
[29] W.S. Hou, Z. Li, F.H. Buttner, E. Bartnik, D. Bromme, Cleavage site specificity of cathepsin K toward cartilage proteoglycans and protease complex formation, Biol. Chem. 384 (2003) 891–897.
[30] J.S. Mort, M.C. Magny, E.R. Lee, Cathepsin B: an alternative protease for the generation of an aggrecan 'metalloproteinase' cleavage neoepitope, Biochem. J. 335 (Pt. 3) (1998) 491–494.
[31] V.M. Dejica, J.S. Mort, S. Laverty, M.D. Percival, J. Antoniou, D.J. Zukor, A.R. Poole, Cleavage of type II collagen by cathepsin K in human osteoarthritic cartilage, Am. J. Pathol. 173 (2008) 161–169.
[32] M. Novinec, R.N. Grass, W.J. Stark, V. Turk, A. Baici, B. Lenarcic, Interaction between human cathepsins K, L, and S and elastins: mechanism of elastinolysis and inhibition by macromolecular inhibitors, J. Biol. Chem. 282 (2007) 7893–7902.
[33] E. Solau-Gervais, F. Zerimech, R. Lemaire, C. Fontaine, G. Huet, R.M. Flipo, Cysteine and serine proteases of synovial tissue in rheumatoid arthritis and osteoarthritis, Scand. J. Rheumatol. 36 (2007) 373–377.
[34] X. Ma, M. Tittiger, R.H. Knutsen, A. Kovacs, L. Schaller, R.P. Mecham, K.P. Ponder, Upregulation of elastase proteins results in aortic dilatation in mucopolysaccharidosis I mice, Mol. Genet. Metab. 94 (2008) 298–304.
[35] Z. Li, Y. Yasuda, W. Li, M. Bogyo, N. Katz, R.E. Gordon, G.B. Fields, D. Bromme, Regulation of collagenase activities of human cathepsins by glycosaminoglycans, J. Biol. Chem. 279 (2004) 5470–5479.
[36] H.E. Gruber, J.A. Ingram, G.L. Hoelscher, N. Zinchenko, H.J. Norton, E.N. Hanley Jr., Constitutive expression of cathepsin K in the human intervertebral disc: new insight into disc extracellular matrix remodeling via cathepsin K and receptor activator of nuclear factor-kappaB ligand, Arthritis Res. Ther. 13 (2011) R140.
[37] K. Ariga, K. Yonenobu, T. Nakase, M. Kaneko, S. Okuda, Y. Uchiyama, H. Yoshikawa, Localization of cathepsins D, K, and L in degenerated human intervertebral discs, Spine (Phila Pa 1976) 26 (2001) 2666–2672.
[38] S. Wilson, S. Hashamiyan, L. Clarke, P. Saftig, J. Mort, V.M. Dejica, D. Bromme, Glycosaminoglycan-mediated loss of cathepsin K collagenolytic activity in MPS I contributes to osteoclast and growth plate abnormalities, Am. J. Pathol. 175 (2009) 2053–2062.
[39] S. Kalamajski, A. Oldberg, The role of small leucine-rich proteoglycans in collagen fibrillogenesis, Matrix Biol. 29 (2010) 248–253.
[40] P.A. Hopkins, S. Sriskandan, Mammalian Toll-like receptors: to immunity and beyond, Clin. Exp. Immunol. 140 (2005) 395–407.
[41] J.A. Sloane, D. Blitz, Z. Margolin, T. Vartanian, A clear and present danger: endogenous ligands of Toll-like receptors, Neuromolecular Med. 12 (2010) 149–163.
[42] Z. Zhang, H.J. Schluesener, Mammalian Toll-like receptors: from endogenous ligands to tissue regeneration, Cell. Mol. Life Sci. 63 (2006) 2901–2907.
[43] M.F. Tsan, B. Gao, Endogenous ligands of Toll-like receptors, J. Leukoc. Biol. 76 (2004) 514–519.
[44] F. Peri, M. Piazza, Therapeutic targeting of innate immunity with Toll-like receptor 4 (TLR4) antagonists, Biotechnol. Adv. 30 (1) (2011) 251–260.

Please cite this article as: L.J. Smith, et al., Pathogenesis of lumbar spine disease in mucopolysaccharidosis VII, Mol. Genet. Metab. (2012), doi:10.1016/j.ymgme.2012.03.014

7

Non Viral Gene Transfer Approaches for Lysosomal Storage Disorders

Ursula Matte, Guilherme Baldo and Roberto Giugliani
Hospital de Clinicas de Porto Alegre
Brazil

1. Introduction

The lysosomal storage disorders (LSDs) are a group of almost 50 genetic diseases, characterized by mutations and loss of activity of lysosomal enzymes or, less frequently, non-lysosomal proteins that are involved in protein maturation or lysosomal biogenesis (Meikle et al, 2004). Most LSDs have an autosomal recessive inheritance, with some exceptions as Hunter syndrome (X-linked recessive), Danon disease (X-linked dominant) and Fabry disease (X-linked with a high proportion of heterozygous affected females).

Storage of distinct undegraded or partially degraded material, usually the substrate of the defective enzyme, occurs in the lysosome. The substrate type is used to group the LSDs into general categories (table 1), including mucopolysaccharidoses (characterized by the storage of mucopolysaccharides, also called glycosaminoglycans), lipidoses (storage of lipids), glycogenoses (storage of glycogen) and oligosaccharidoses (storage of small sugar chains). Despite this categorization, many clinical similarities are observed between groups as well as within each group. Generally these diseases are multisystemic, and clinical features of many LSDs include organomegaly, central nervous system dysfunction and coarse hair and faces. Most LSDs are characterized by their progressive course with high morbidity and increased mortality, although there are significant variations between different diseases, and even among patients with the same disease (Walkley 2009). Lysosomal enzymes are ubiquitously distributed, but substrate storage is usually restricted to cells, tissues and organs with higher substrate turnover.

Recently, it has been suggested that the primary gene defect and substrate storage are triggers of a complex cascade of events that lead to many of the disease manifestations (Bellettato & Scarpa, 2010). In this context, secondary substrate storage, perturbations of Calcium homeostasis and lipid trafficking would contribute to disease pathogenesis. Other manifestations, related to the lysosome's role in vescicle trafficking, including antigen presentation, innate immunity, and signal transduction would cause inflammatory and auto-immune disturbances observed in the LSD (Parkinson-Lawrence et al., 2010). In addition, general mechanisms such as unfolded protein response, reticulum stress, oxidative stress and autophagy blockade would also play a role in the pathogenesis (Vitner et al., 2010).

The incidence and prevalence of these diseases varies from different countries and regions. For example, the overall incidence of GM1 Gangliosidosis is considered to be 1:100,000-

1:200,000, however in some countries as Malta (1:3,700) and the South of Brazil (1:13,317) it is considerably higher (Baiotto et al, 2011). Large population studies suggest that the overall incidence of the LSDs vary from 1:5,000- 1:7,700 (Fuller et al, 2006).

The treatment options available for the LSDs were restricted to support measures until a few decades ago. Nowadays, specific treatments are available for a certain number of LSDs, even though some of them are still in the experimental phase or have limited effects. Treatment options listed in table 1 consider those already approved or under clinical trial, including compassionate use. Support measures and palliative care are not considered treatment options in this context.

Disease	OMIM	Gene	Enzyme	Available Treatments
Aspartylglucosaminuria	208400	*AGA*	N-aspartyl-beta-glucosaminidase	HSCT
Canavan disease	271900	*ASPA*	Aspartocylase	None
Cystinosis	219800	*CTNS*	Cystinosin	Cysteamine (drug)
Danon disease	300257	*LAMP2*	Lysosomal-associated membrane protein 2	None
Fabry disease	301500	*GLA*	A-galactosidase A	ERT
Farber disease	228000	*ASAH1*	Ceramidase	HSCT
Fucosidosis	230000	*FUCA1*	α-L-fucosidase	HSCT
Galactosialidosis	256540	*CTSA*	Cathepsin A	None
Gaucher disease	230800	*GBA*	acid β-glucosidase	ERT, GT, HSCT, PCT, SSI
GM1 gangliosidosis	230600	*GLB1*	β-Galactosidase	HSCT
Krabbe disease	245200	*GALC*	galactocerebrosidase	HSCT
Lysosomal Acid Lipase Deficiency	278000	*LIPA*	Lysosomal acid lipase	HSCT
α- mannosidosis	248500	*MAN2B1*	α -D -mannosidase	HSCT
β- mannosidosis	248510	*MANBA*	β -D-mannosidase	None
Metachromatic leucodystrophy	250100	*ARSA*	Arylsulphatase-A	HSCT
Metachromatic leucodystrophy	249900	*ARSA*	Saposin-B	HSCT
Mucolipidosis type I	256550	*NEU1*	Sialidase	None
Mucolipidosis types II/III	252500	*GNPTAB*	N-acetylglucosamine-1-phosphotransferase	None
Mucolipidosis type IIIC	252605	*GNPTG*	N-acetylglucosamine-1-phosphotransferase γ-subunit	None
Mucolipidosis type IV	252650	*MCOLN1*	Mucolipin 1	None
Mucopolysaccharidosis type I	607014	*IDUA*	α-L-iduronidase	ERT, HSCT
Mucopolysaccharidosis type II	309900	*IDS*	Iduronate sulfatase	ERT, GT, HSCT
Mucopolysaccharidosis type IIIA	252900	*SGSH*	Heparan-N-sulfatase	None
Mucopolysaccharidosis type IIIB	252920	*NAGLU*	α- N-acetylglucosaminidase	None
Mucopolysaccharidosis	252930	*HGSNAT*	AcetylCoa-glucosamine-N-	None

type IIIC			acetyltransferase	
Mucopolysaccharidosis type IIID	252940	*GNS*	N-acetylglucosamine-6-sulfatase	None
Mucopolysaccharidosis type IVA	253000	*GALNS*	N-acetylgalactosamine-6-sulphatase	ERT
Mucopolysaccharidosis type IVB	253010	*GLB1*	β-Galactosidase	None
Mucopolysaccharidosis type VI	253200	*ARSB*	N-acetylgalactosamine-4-sulphatase	ERT
Mucopolysaccharidosis type VII	253220	*GUSB*	β-Glucuronidase	None
Mucopolysaccharidosis type IX	601492	*HYAL1*	Hyaluronidase	None
Multiple sulphatase deficiency	272200	*SUMF1*	Formylglicine-generating-enzyme	None
Neuronal ceroid lipofuscinosis 1	256730	*PPT1*	Palmitoyl protein thioesterase-1	HCST
Neuronal ceroid lipofuscinosis 2	204500	*TPP1*	Tripeptydil-peptidase I	GT
Neuronal ceroid lipofuscinosis 3	204200	*CLN3*	CLN3 protein	None
Neuronal ceroid lipofuscinosis 5	256731	*CLN5*	CLN5 protein	None
Neuronal ceroid lipofuscinosis 6	601780	*CLN6*	CLN6 protein	None
Neuronal ceroid lipofuscinosis 8	600143	*CLN8*	CLN8 protein	None
Niemann-Pick disease A/B	257200	*SMPD1*	Acid sphingomyelinidase	None
Niemann-Pick disease C1	257220	*NPC1*	NPC1 protein	SSI
Niemann-Pick disease C2	607625	*NPC2*	NPC2 protein	SSI
Pompe disease	232300	*GAA*	Alpha-glucosidase	ERT, GT
Prosaposin deficiency	176801	*PSAP*	Prosaposin	None
Pycnodysostosis	265800	*CTSK*	Cathepsin K	Hormone therapy
Sandhoff disease	268800	*HEXB*	Hexosaminidase B	PCT
Schindler disease	609241	*NAGA*	Alpha-N-acetylgalactosaminidase	None
Sialic acid storage disease	269920	*SLC17A5*	Sialin	None
Sialuria	269921	*GNE*	UDP-N-acetylglucosamine-2-epimerase	None
Tay-Sachs disease	272800	*HEXA*	Hexosaminidase A	PCT, SSI

Abbreviations: GT – Gene Therapy; HSCT – Hematopoetic Stem Cell Transplantation; PCT – Pharmacological Chaperone Therapy; OMIM – Online Mendelian Inheritance in Man; SSI – Specific Substrate Inhibition; ERT – Enzyme Replacement Therapy

Table 1. List of lysosomal storage diseases with their respective OMIM accession number, gene and enzyme deficiency and treatment options (including experimental ones).

The two most widely used treatment options are Hematopoietic Stem Cell Transplantation (HSCT) and Enzyme Replacement Therapy (ERT). HSCT has proven to be

efficient to some of these diseases, especially if performed early enough to prevent irreversible lesions. Nevertheless, limitations such as the need of an early diagnosis, the difficulties to find a compatible donor in short time, and the high rates of morbidity and mortality associated with the procedure still limit this type of treatment (Malatack et al, 2003). Therefore, despite the many advances in this treatment over the last 30 years (Boelens et al 2010), its use has been deferred in favor of ERT whenever it is available. Enzyme replacement therapy is approved for a growing number of LSD, especially those without CNS involvement. It has proven to reduce some visceral symptoms as hepatosplenomegaly and improve respiratory function (Sifuentes et al, 2007), however difficult-to-reach organs such as the brain and the bones are still a major challenge. Innovative routes of enzyme delivery have been tested to achieve the CNS, such as intrathecal ERT (Munoz-Rojas et al, 2008; Munoz-Rojas et al, 2010).

Other treatment approaches already under clinical use or experimentation are Specific Substrate Inhibition (SSI) and Pharmacological Chaperone Therapy (PCT). SSI aims to decrease the storage by reducing substrate synthesis through an inhibitor. PCT uses small molecules able to stabilize the mutant enzyme and help it escape proteasomal degradation, thus restoring some residual enzyme activity. All such treatments have limitations (table 2), that justify the development of gene therapy approaches for these diseases.

Approach	Brief Description	Pros	Limitations
Intravenous enzyme replacement therapy	Intravenous injection of a recombinant version of the missing enzyme	Ameliorates several visceral symptoms	High cost Does not correct difficult-to-reach sites Need of repeated injections
Intrathecal enzyme replacememnt therapy	Intrathecal injection of a recombinant version of the missing enzyme	Reaches the CNS	High Cost Need of repeated injections Efficacy uncertain
Hematopoietic stem cell tranplantation	Non-autologous transplantation of CD 34+ cells	Able to correct visceral and CNS symptoms if performed early	Limited efficacy Relatively high morbidity and mortality rates
Specific substrate inhibition	Use of drugs that can inhibit the synthesis of the undegraded material	Orally administered Reaches the CNS	Limited efficacy High cost
Pharmacological chaperone therapy	Drugs that can stabilize the mutated protein, allowing some enzyme activity	Orally administered Reaches the CNS	Works only in patients with specific mutations
Stop-codon read-through therapy	Use of molecules that can suppress stop-codon mutations	Orally administered Reaches the CNS Low cost	Works only in stop-codon mutations Clinical trials yet to be performed
Gene Therapy	Administration of a normal copy of the mutated gene	Potentially effective with single injection	Safety concerns Efficacy uncertain

Abbreviations: CNS – Central Nervous System

Table 2. Pros and limitations of different therapeutic approaches for lysosomal storage diseases.

2. Rationale for gene therapy in LSDs

The rationale for gene therapy and other enzyme-based approaches for treatment of LSDs was first introduced almost five decades ago by Christian de Duve, and can be summarized in the following sentence from his original work "In our pathogenic speculations and in our therapeutic attempts, it may be well to keep in mind that any substance which is taken up intracellularly in an endocytic process is likely to end up within lysosomes." (de Duve, 1964). His work and other pioneer studies showing cross-correction between fibroblasts from patients with Mucopolysaccharidosis type I and type II (deficient in alpha-L-iduronidase and iduronate-sulphatase, respectively) established that the enzyme produced in one cell could be uptaken by a deficient cell, thus restoring its phenotype (Fratantoni et al, 1968). Later studies identified that this uptake was a saturable, receptor-mediated process, and the main actor of this process was the mannose-6-phosphate (M6P) receptor localized in the plasmatic membrane. The post-translational modification of addition of the M6P to the protein was discovered to be a signal not only to endocytosis but also for targeting nascent hydrolases to lysosomes (Fisher et al, 1980; Sly et al., 1981).

These pivotal discoveries in the field of endocytosis and targeting of lysosomal enzymes provided the basis for treatments like HSCT and ERT. In the same way, LSDs may be considered good targets for gene therapy, despite their multisystemic involvement. The correction of a few cells could lead to the enzyme being secreted into the circulation and uptaken by the deficient cells, resulting in widespread correction of the biochemical defect (figure 1).

Since long term gene expression is desirable, most clinical and preclinical trials used viral based vectors. Initial studies on fibroblasts showed promising data using retroviruses (Anson et al, 1992). However, when tests in animal models started, it became clear that some organs as the brain would not be easily corrected, as the enzyme could not cross the blood-brain-barrier (Elinwood et al, 2004). This is a major hurdle as most LSD shows some degree of CNS involvement. Nevertheless, CNS targeted approaches could be envisaged to overcome this obstacle. For instance, Worgall et al. (2008) showed a slowing of progression of Neuronal Ceroid Lipofuscinosis 2 in ten children treated with serotype 2 adeno-associated virus expressing *CLN2* cDNA. Another clinical trial, for Pompe disease, also used adeno-associated-based vector, but in this case serotype 1 (NCT00976352-www.clinicaltrials.gov). Other two trials performed in the late 1990s used retroviral vectors for Gaucher (Dunbar et al., 1998) and Mucopolysaccharidosis type II (NCT00004454 - www.clinicaltrials.gov).

Safety issues related to immune response of the adenoviral vectors (Wilson, 2009) and the possibility of insertional mutagenesis of the retroviral vectors (Hacein-Bey-Abina S et al., 2008) led researchers to develop a series of studies in parallel using non-viral approaches to treat lysosomal storage disorders.

3. Non-viral approaches

Non-viral vectors have important safety advantages over viral approaches, including their reduced pathogenicity and capacity for insertional mutagenesis, as well as their low cost and ease of production (Fraga et al., 2008). The application of non-viral vectors to humans has, however, been held back by the poor efficiency of their delivery to cells and the transient expression of the transgenes. As new strategies are being developed for the

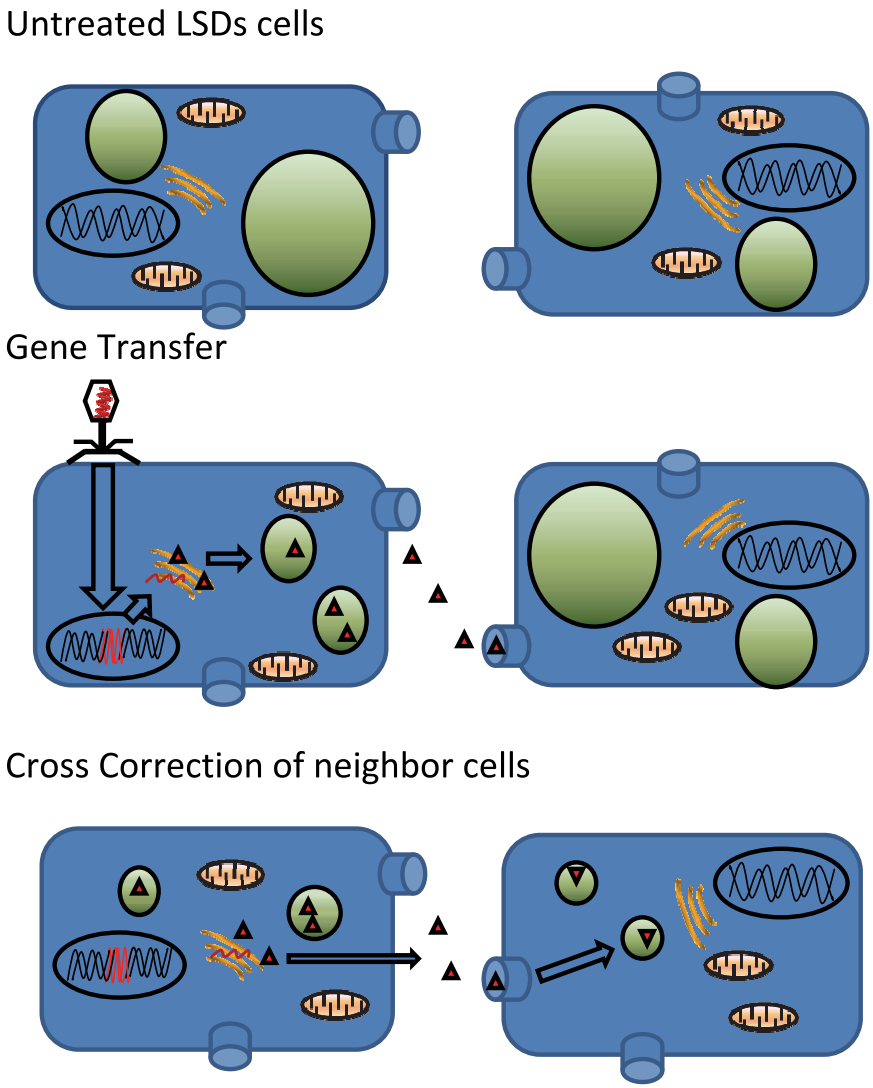

Fig. 1. Rationale for Gene Therapy in Lysosomal Storage Disorders: Cross-correction. The upper part of the figure shows two cells from a patient with LSD, with large lysosomes (green) due to accumulation of undegraded material. The gene transfer of a normal copy of the missing enzyme (red structure in the nucleus), allows the enzyme (red triangles) to be produced, and degrade the material accumulated in the lysosomes. Part of the enzyme is secreted from the recombinant cell and is captured by neighbouring cells via the mannose-6-phosphate receptors (light blue structures located on the cell membrane), reaching the lysosomes and being able to correct their phenotype, in a process called cross-correction. Note that the cell on the right was never transduced, but is able to capture the enzyme from the circulation or from the neighbouring cell.

application of non-viral vectors as nucleic acid delivery systems (Resina et al., 2009; Wasungu and Hoekstra, 2006), progress is being made in the application of this kind of therapy to LSDs.

3.1 Naked plasmid transfection

The direct injection of a plasmid containing the gene of interest and the regulatory mechanisms to ensure its expression is the simplest form of gene therapy. It has some advantages over the virus mediated gene transfer systems. First, DNA preparation is simple and can be performed at relatively low cost. In addition, the safety concerns are much lower and large amounts of DNA can be transferred. However, the major limitation of this method is that it requires a local administration and the level of transgene expression is relatively low and restricted to the injection site (Glover et al., 2005).

Hydrodynamic injection (Liu et al, 1999) is an experimental method capable to achieve efficient gene transfer and high level of transgene expression by systemic administration. In this procedure, a large volume of saline containing plasmid DNA is injected in a short period of time. The large volume and high injection rate forces the DNA solution into the liver, probably due to the permeability of liver fenestrae. A small hepatotoxicity, probably due to the large volume of saline, is observed and resolves within a few days. Even though this procedure is widely used in mice by tail vein injection, its feasibility has been demonstrated in larger animal models using a balloon occlusion catheter-based method to mimic hydrodynamic injection (Brunetti-Pierri et al, 2007; Kamimura et al, 2009).

This approach has been used in a proof-of-concept study to show the importance of coexpression of the formylglycine-generating enzyme for synthesis and secretion of functional Arylsulfatase A in a mouse model of Metachromatic Leukodystrophy (Takakusaki et al., 2005). This enzyme is a posttranslational modifying enzyme essential for activating multiple forms of sulfatases including Arylsulfatase A and therefore limits the amount of functional enzyme that can be secreted from transduced cells.

It has also been used in Mucopolysaccharidosis (MPS) type I (Camassola et al, 2005) and type VII (Richard et al, 2009). In the MPS I animals, storage content was reduced and enzyme activity was elevated in the liver and spleen. For the MPS VII model, a beneficial effect on the pathology was also observed, as liver-directed gene transfer led to the correction of secondary enzymatic elevations and to the reduction of GAGs storage in peripheral tissues and brain, as well as to histological correction in many tissues.

3.2 Liposomes and nanotechnology

Liposomes are lipid particles that resemble the cell membrane. Liposome-based gene delivery was first reported by Felgner in 1987, and is still one of the major techniques for non viral gene delivery into cells (Niidome & Huang, 2002). Lipoplexes are formed by the interaction of anionic nucleic acids binding to the surface of cationic lipids, forming multilamellar lipid–nucleic acid complexes where the negatively charged nucleic acid remains trapped inside the lipid bilayer (Dass, 2004). Since its discovery, different lipid formulations have been tested and modified. For example, stealth liposomes sterically stabilized with methoxypoly(ethylene glycol)distearoylphosphatidylethanolamine conjugates (PEG-DSPE) have long circulation half-lives following intravenous injection (Moreira et al., 2001). In addition, linear polycations such as linear, branched and dendritic vectors based on poly(ethylenimine) (PEI), poly(L-lysine) (PLL) and a range of

poly(ethylene glycol) (PEG) were also developed (Hunter, 2006). Although linear PEI shows greater *in vivo* efficiency because of a dynamic structure change of the complex under high salt concentrations as found in blood (Niidome & Huang, 2002), it also possesses greater toxicity (Morille et al., 2008).

Cationic nanoemulsions have been more recently considered as potential systems for nucleic acid delivery. The interest in these systems is justified by the fact that they are biocompatible and able to form complexes with DNA protecting it from enzymatic degradation (Nam et al., 2009). Other practical advantages include ease of production and the potential for repeated administration (Al-Dorsari and Gao, 2009). We have investigated the influence of phospholipids on the properties of cationic nanoemulsions/pDNA complexes. Complexes containing the phospholipids DSPC (1,2-distearoyl-sn-glycero-3-phosphocholine) and DSPE (1,2- distearoyl-sn-glycero-3- phosphoethanolamine) were less toxic in comparison with the formulations obtained with lecithin, DOPC (1,2-dioleoyl-sn-glycero-3-phosphocholine) and DOPE (1,2-dioleoyl-sn-glycero-3-phosphoethanolamine). In addition, higher amounts of reporter DNA were detected for the formulation obtained with the DSPC phospholipid (Fraga et al., in press).

These cationic macromolecules can readily condense DNA or RNA into stable nanostructures for use in gene delivery (Hunter, 2006) but also for other nanotechnology-based approaches useful for the treatment of LSDs (Muro, 2010). Nanomaterials, as a result of their small size and their large surface area offer great promise for neuro-therapeutics (Ragnail et al., 2011) and thus may be a valid option for a large number of LSDs that affect the CNS.

Liposome-mediated gene transfer for LSD has been performed *in vitro* using patient's fibroblasts as target cells. Estruch et al. (2001) delivered therapeutic genes by integrin-mediated uptake into fibroblasts from patients with Fucosidosis and Fabry disease. The vectors consisted of a complex of lipofectin and a peptide containing an integrin-targeting domain and a poly-lysine domain to which plasmid DNA was bound. Transfected cells produced the corresponding enzyme at levels which were 10-40% of the total activity in cultures of normal fibroblasts. Although 95-98% of this activity was secreted, it did not appear to affect the viability of the cells. Our group used Lipofectamine to transduce fibroblasts from GM1 Gangliosidosis patients with the beta-galactosidase gene. Treated cells showed 33 to 100- fold increases in enzyme activity compared to untreated fibroblasts. However, after seven days enzyme activity was back to uncorrected values (Balestrin et al., 2008). When Geneticin was added to the medium (figure 2), stable expression at therapeutic levels was observed (mean 300 nmoles/h/mg prot) for 30 days, although at values lower than the normal range (mean 1,300 nmoles/h/mg prot).

In vivo, PEG-coated liposomes have been modified with monoclonal antibodies in order to reach the CNS. A liposome is coated with peptidomimetic monoclonal antibodies that undergo receptor-mediated transcytosis across the blood-brain barrier on the endogenous peptide receptor transporters (Pardridge, 2007). These Trojan horses (figure 3) may use the insulin or transferrin receptor, and since the MAb binding site is different from the binding site of the endogenous ligand, there is no interference of endogenous ligand transport (Skarlatos et al, 1995).

This approach has been used to deliver a non-viral plasmid DNA to the brain across the blood-brain-barrier after intravenous administration of liposomes coated with monoclonal antibody to the mouse transferrin receptor in a mouse model of Mucopolysaccharidosis type VII (Zhang et al, 2008). The enzyme activity was increased greater than ten-fold in brain, liver, spleen, lung, and kidney, but not in heart. A similar strategy has been used by Osborn

et al (2008) for Mucopolysaccharidosis type I, although they used a plasmid bearing a fusion gene consisting of Transferrin (Tf) and α-L-iduronidase. The fusion product consisted of an enzymatically active protein that was transported into the CNS by TfR-mediated endocytosis. Short-term treatment resulted in a decrease in GAGs in the cerebellum of Mucopolysaccharidosis type I mice.

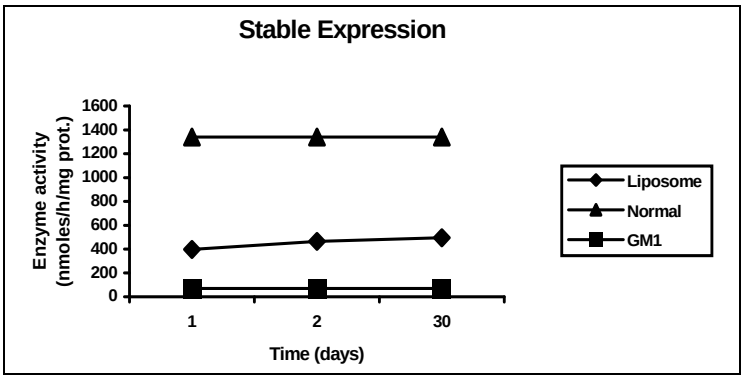

Fig. 2. Stable expression of β-Galactosidase in fibroblasts from G1 Gangliosidosis patients after *in vitro* liposome-based gene transfer. Mean values of liposome-treated cells: 300 nmoles/h/mg prot.; mean values of normal fibroblasts: 1,300 nmoles/h/mg prot.; mean values of affected fibroblasts: 68 nmoles/h/mg prot. (Balestrin et al., 2008).

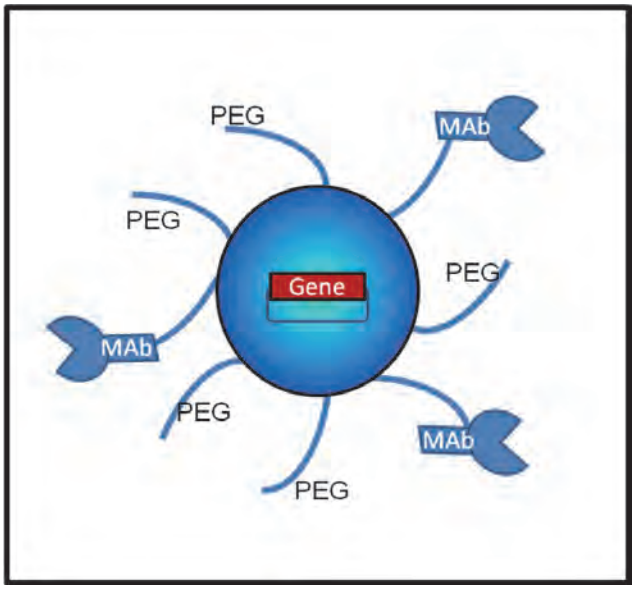

Fig. 3. Schematic view of a Trojan horse liposome. A stealth PEGylated liposome is complexed with monoclonal antibodies (MAb) that undergo receptor-mediated transcytosis across the blood-brain barrier.

3.3 Cell microencapsulation

Cell microencapsulation is an approach in which cells are trapped in a semipermeable membrane, allowing the exchange of metabolites and nutrients between them and the external environment. The membrane prevents the access of the immune system to the cells, without the need for continued immunosuppression of the host (Uludag et al., 2000). Furthermore, this technique allows the localized and controlled release, and long term duration of therapeutic products derived from the microencapsulated cells (Orive et al., 2002). Microencapsulation has become an important system for cellular preservation (Mayer et al., 2010) and a potential strategy for the controlled delivery of therapeutic products (Orive et al., 2003). Alginate has been the most important encapsulation polymer due to its abundance, easy gelling properties and biocompatibility. Agarose, chitosan, and hyaluronic acid are other polymers used for microencapsulation (Orive et al., 2003).

Cell microencapsulation presents the potential to deliver the therapeutic product of interest directly to the Central Nervous System (CNS). This has been achieved by different groups for brain tumors (Kuijlen et al 2007) and neurodegenerative diseases (Spuch et al 2010). A phase I clinical trial was conducted in Huntington's patients without signs of toxicity (Bloch et al 2004). This approach delivers the gene of interest in the spinal fluid, similar to the intrathecal enzyme replacement therapy. Thus, cell encapsulation can be suitable for the treatment of LSD, once the deficient enzyme could be released for long term directly in the CNS (Matte et al., 2011).

In order to obtain larger amounts of secreted enzyme, the encapsulated cells should be genetically modified to over-express the enzyme of interest. This enzyme would then be released to the extracapsular space (Bressel et al 2008) and uptaken by adjacent deficient cells (figure 4). This strategy has been used experimentally for different LSD, especially the Mucopolysaccharidosis (MPS).

Three *in vitro* studies were performed in LSDs other than the MPS, one in Fabry disease and the other two in Metachromatic Leukodystrophy (MLD). Naganawa et al (2002) co-cultured fibroblasts from patients with Fabry disease with microencapsulated recombinant Chinese Hamster Ovary cells (CHO) over-expressing alpha-galactosidase. The deficient cells were able to uptake the enzyme decreasing their levels of globotriaosylceramide storage. A similar approach was used by our group to test the ability of Baby Hamster Kidney (BHK) cells over-expressing ARSA to correct the deficiency of this enzyme in human skin fibroblasts from MLD patients. Fibroblasts co-cultured with the encapsulated cells for four weeks showed levels of enzyme activity higher than normal. Transmission electron microscopy showed evidence of normalization of the lysosomal ultra structure, suggesting that the secreted enzyme was able to degrade the substrate (Lagranha et al., 2008). Consiglio et al (2007) collected the conditioned media of C2C12 cells over-expressing ARSA encapsulated in polyether-sulfone polymer and used it to treat oligodendrocytes from MLD mice. The deficient cells internalized the enzyme and it was normally sorted to the lysosomal compartment, reaching 80% of physiological levels and restoring sulfatide metabolism.

Both *in vitro* and *in vivo* studies have been performed in the MPS types I, II and VII. For MPS II two studies were performed. The first was a proof of principle in which Hunter primary fibroblasts were co-cultured with alginate microcapsules containing C2C12 cell clones over-expressing IDS. After 5 days of co-culture this strategy was able to increase IDS activity inside the deficient fibroblasts to levels similar to normal (Tomanin et al 2002). The second study was a pre-clinical experiment in which APA (alginate-poli-L-lysine-alginate) microcapsules containing 1.5 x 10^6 allogeneic C2C12 myoblasts over-expressing IDS were

implanted in the peritoneum of the MPS II mouse model. An increase in IDS activity in plasma was observed, along with a reduction on urinary GAG between the fourth and the sixth week of treatment. After 8 weeks, a reduction of 30% in the amount of GAG accumulated in the liver and 38% in the kidney were shown (Friso et al 2005).

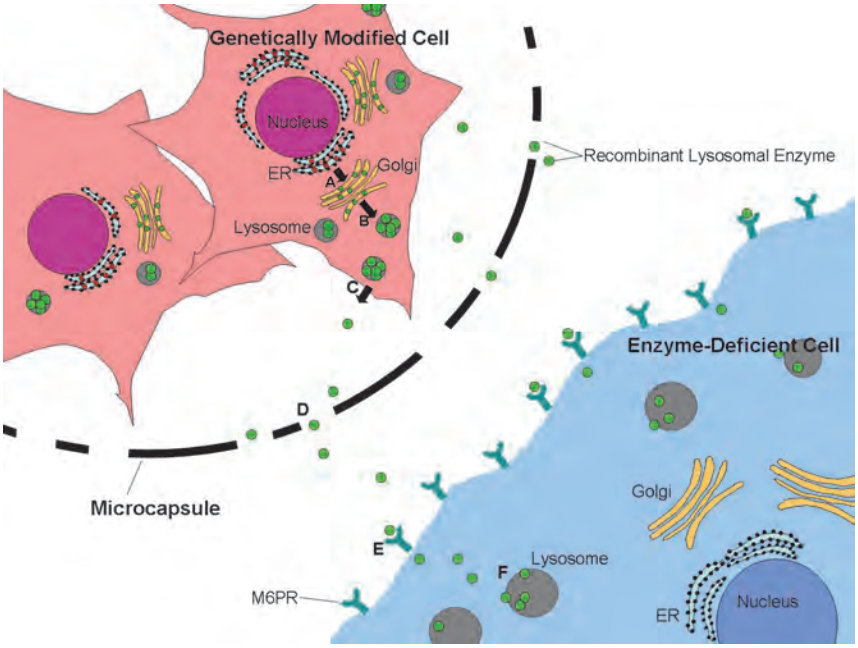

Fig. 4. Traffic of lysosomal enzymes throughout the encapsulated cells. The nascent lysosomal enzymes are glycosylated in the endoplasmic reticulum (ER) of the genetically modified cells. (A) The enzymes are phosphorylated at the residue of mannose-6 in the Golgi apparatus. (B) Most enzymes are transported to mature lysosomes. (C) Some, however, are secreted to the extracellular environment and (D) to outside of the microcapsules. (E) Phosphorylated enzymes bind to mannose-6-phosphate receptors (M6PR) of the enzyme-deficient cells (F) where they are endocyted and subsequently targeted to the lysosomes (Matte et al., 2011).

To evaluate the usefulness of this technique to treat MPS VII, Ross et al (2000a) injected APA encapsulated non-autologous cells overexpressing Gusb in the peritoneum of MPS VII mice. The results showed the presence of Gusb in the plasma 24 hours after implantation, reaching 66% of physiological levels by 2 weeks post implantation. Activity of Gusb was also detected in liver and spleen for the duration of the 8-week experiment. Accumulation of GAG was significantly reduced in liver and spleen sections and urinary GAG content reached normal levels. In another study, enzyme released by APA encapsulated 2A50 fibroblasts implanted directly into the lateral ventricles of the brain of MPS VII mice was delivered throughout most of the CNS, reversing the histological pathology (Ross et al., 2000b). *In vitro* studies were performed by Nakama et al (2006) who encapsulated immortalized recombinant human amniotic epithelial cells with MPS VII human and mouse fibroblasts and high GUSB

activity was detected in the medium. Addition of mannose-6-phosphate led to decreased enzyme activity, suggesting that enzyme uptake was mediated by mannose-6-phosphate receptor.

Our group has shown that the correction of MPS I fibroblasts by recombinant encapsulated BHK cells is also mediated by mannose-6-phosphate receptor. The effect of the ratio fibroblasts:encapsulated cells was also analysed (figure 5). The amount of enzyme uptaken by the fibroblasts is essentially the same under the different ratios (5:1; 1:1; 1:5) although the enzyme activity in the medium increases, as more enzyme is released.

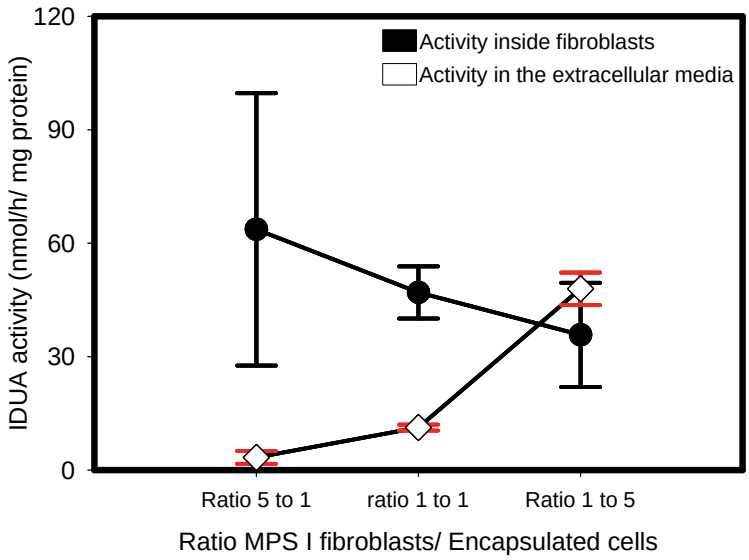

Fig. 5. IDUA enzyme activity in MPS I fibroblasts co-cultured with recombinant BHK cells overexpressing IDUA at different ratios.

Our results also showed an increase in IDUA activity in MPS I fibroblasts after 15, 30 and 45 days of co-culture with the capsules. Cytological analysis showed a marked reduction in GAG storage within MPS I cells (Baldo et al., 2011). Ongoing experiments are under way in the MPS I mouse model. The capsules were implanted in the peritoneum (figure 6) and animals were sacrificed at 4 months later. Histological analysis showed a reduction on GAG storage although plasma and tissue enzyme activity levels were not increased.

These results are quite different from those of Barsoum et al (2003) who implanted genetically modified Madin-Darby canine kidney cells (MDCK) over-expressing canine Idua in the brain parenchyma of one MPS I dog. Enzyme in plasma and cerebrospinal fluid was low but detectable for 21 days. Immunohistochemistry with anti-IDUA antibody showed the presence of the enzyme in various brain regions, however an extensive inflammatory reaction was noted, both at the sites of implantation and in the immediate vicinity. This may be the reason why histological correction of lysosomal inclusions has not been observed.

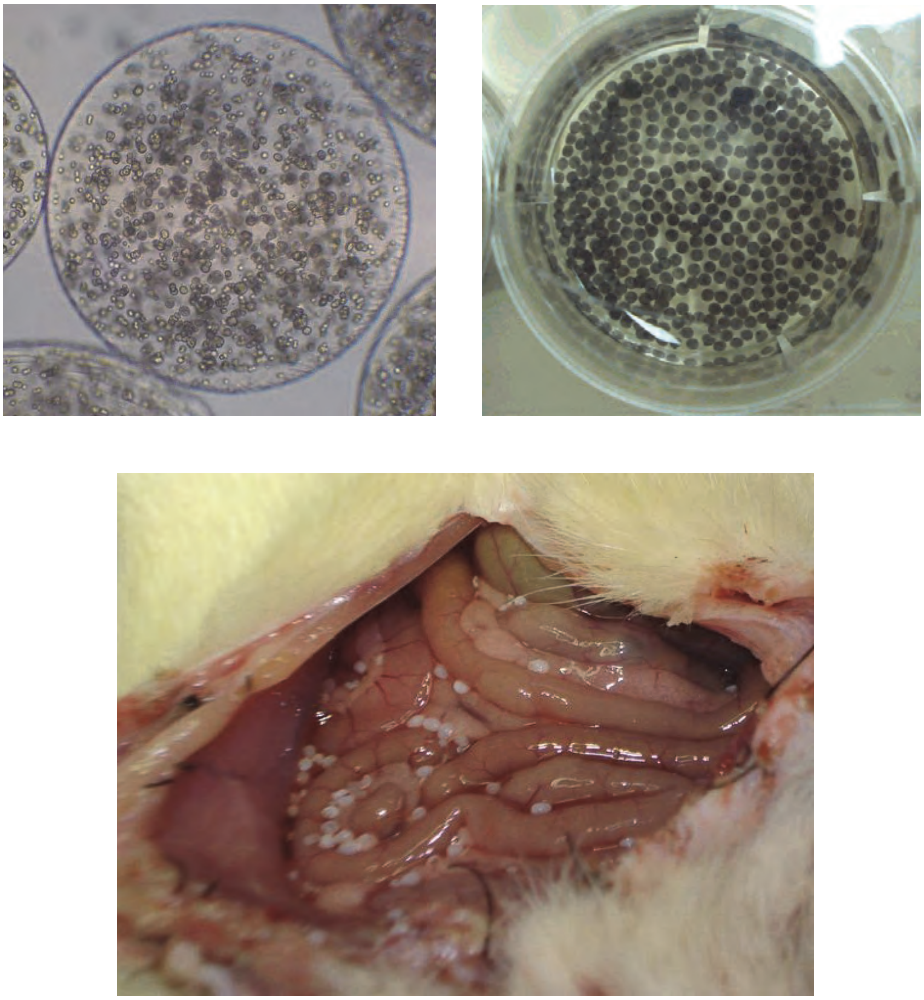

Fig. 6. Microcapsules used for the treatment of MPS I mice. Left upper panel: photomicrography of alginate beads containing recombinant BHK that overexpress IDUA (small round dots). Right upper panel: Macroscopic aspect of the microcapsules (black dots) in a 96-well plate. Capsules were ink stained to help visualization. Lower panel: Aspect of the capsules in the peritoneum ten days after implantation. Note that some capsules are attached to the intestine.

3.4 Transposon-based systems

For human gene therapy we can enumerate some important aspects of transposon systems (special emphasis in this chapter will be given to the *sleeping beauty* transposon) that make them appealing as a vector: (1) the integrated gene has stable expression, providing long-lasting expression of a therapeutic gene, which, as already mentioned, is essential for

lysosomal storage diseases; (2) the transposase directs the integration of single copies of a DNA sequence into chromatin and (3) the system is binary (the transposon is not autonomous or able to transpose on its own) (Hacket et al, 2005).

The most studied transposon system, which has been used in pre-clinical studies for treatment of lysosomal disorders, is the *Sleeping beauty (SB)* system. Sleeping beauty transposon is a type of mobile element that belongs to the *Tc1/Mariner* class and that is able to transpose via movement of a DNA element in a simple cut-and-paste manner. For that, a precise piece of DNA is excised from one DNA molecule and moved to another site in the same or in a different DNA molecule (Plasterk, 1993). This reaction is catalyzed by the protein transposase, which can be supplied *in trans* by another plasmid for gene therapy purposes.

The SB transposon system consists of two components: (i) a transposon, made up of the gene of interest flanked by inverted repeats (IRs), and (ii) a source of transposase (figure 7). For Sleeping Beauty-mediated transposition, the transposase can recognize the ends of the IRs, excises the gene of interest from the delivered plasmid DNA, and then inserts it into another DNA site. Based on studies in about 2,000 integration events in either mouse or human genomes, transposons seem to integrate into random sites, including exons, introns and intergenic sequences (Carlson et al, 2003; Horie et al, 2003; Hacket et al, 2005). This is a potential problem, since it may lead to an event of insertional mutagenesis. A complete list of insertion positions of the SB tranposon can be found at the Mouse Transposon Insertion database at http://mouse.ccgb.umn.edu/transposon/ (Roberg-Perez et al, 2003).

The use of SB transposons as gene therapy approach in LSD is still recent. The first published work was conducted by Aronovich et al (2007) who studied the effects of intravenous hydrodynamic injection of the SB transposon into mice with Mucopolysaccharidosis types I or VII. Without immunomodulation, initial enzyme activities in plasma reached levels higher than 100-fold that of wild-type (WT). However, both GUSB (MPS VII) and IDUA (MPS I) levels fell to background within 4 weeks post-injection.

A second group of animals was performed with immunomodulation only in MPS I mice. Plasma IDUA persisted for over 3 months at up to 100-fold WT activity in one-third of the mice, which was sufficient to reverse lysosomal pathology in the liver and, partially, in distant organs. Histological and immunohistochemical examination of liver sections in IDUA transposon-treated WT mice revealed inflammation 10 days post-injection consisting predominantly of mononuclear cells, which can be seen as a potential side-effect.

A posterior study by the same group (Aronovich et al, 2009) was performed in another MPS I strain, which is immunodeficient (NOD/SCID mice). Using the same approach from the previous experiment, they were able to show a persistent elevation (100-fold normal) in the plasma IDUA levels for 18 weeks. Also, IDUA activity was present in all organs analyzed, including the brain. The SB transposon system proved efficacious in correcting several clinical manifestations of MPS I mice, including bone abnormalities, hepatomegaly, and accumulation of foamy macrophages in bone marrow and synovium. In 2008 the first human clinical trial using the SB transposon was approved in the USA for treatment of cancer (Williams, 2008), however although promising no clinical trials have been conducted in LSDs so far.

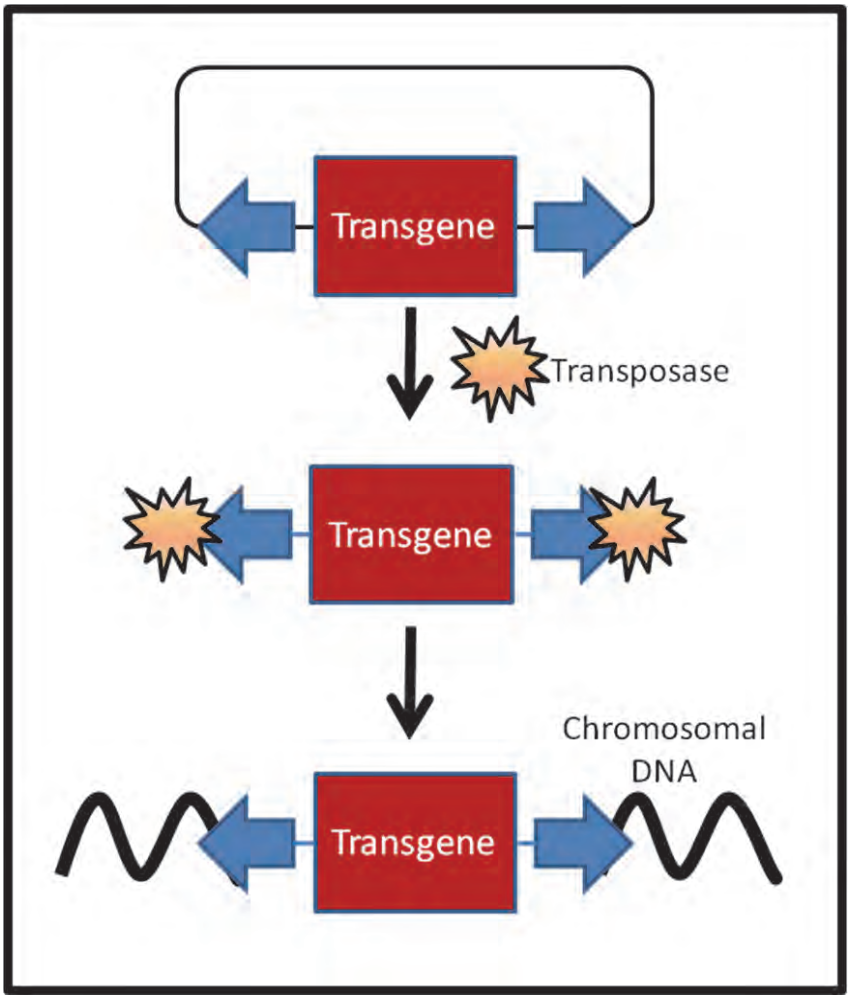

Fig. 7. SB transposon system. This simplified version of the SB transposon system shows the cut-and-paste system used by the SB transposase to insert the DNA into the host genome. The gene of interest is flanked by two inverted repeats regions (IRs, arrows) which will be recognized by the transposase (usually given in *trans* in a second plasmid) and allow the transgene to be inserted into the host genome. This way only the transgene will have prolonged expression, as transposase gene expression is transient. The SB transposon is a non-viral method of gene delivery that allows integration of the transgene in the host cell.

3.5 Minicircle gene therapy

Sustained *in vivo* transgene expression from plasmids can be difficult to achieve due to gene silencing. The mechanism by which this process occurs was postulated to be due to the deposition of repressive heterochromatin on the noncoding bacterial backbone sequences required for plasmid bacterial preparation and propagation (Chen et al, 2008; Riu et al, 2005).

Based on those findings, a new technology has emerged, known as the minicircle (MC) gene therapy. This system uses a phiC31 integrase recombination event to remove the bacterial backbone elements of the plasmid resulting in a DNA circle (the MC), encoding the mammalian expression cassette of choice and a small attR footprint (Chen et al, 2003). This has proven to be resistant to gene silencing *in vivo*, is maintained as an extrachromosomal episome, and therefore represents an interesting platform for gene replacement strategies for lysosomal storage disorders (figure 8).
This technology was recently used for treatment of MPS I mice in a proof-of-concept study (Osborn et al, 2011). In this study, the researchers performed a hydrodynamic injection of a minicircle plasmid containing the IDUA gene combined with immunomodulation, achieving stable expression of the transgene, increased IDUA tissue levels and reduction in GAG storage. As a recent technology, this is the only study performed on LSDs so far, but results are encouraging and should be tested on other diseases soon.

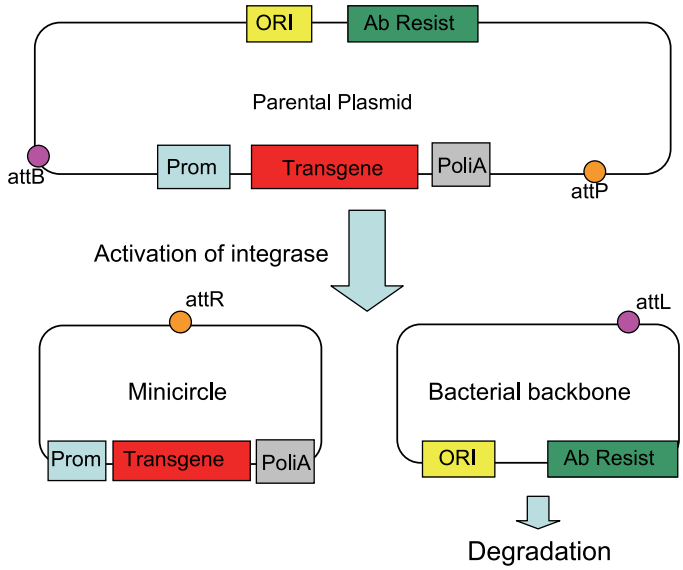

Fig. 8. Production of a minicircle plasmid. This simplified version of the process shows the parental plasmid containing both the gene of interest and the bacterial components, including origin of replication (ORI), genes that confer resistance to antibiotic (Ab resist) and sites that allow attachment of the integrase (att B and P). After activation of the integrase, a cis-recombination event occurs, separating the gene of interest and its regulatory elements from the bacterial backbone, which then is degraded.

4. Conclusions

Still nowadays most lysosomal storage disorders do not have an effective treatment. Moreover, treatments currently available are not able to correct all the manifestations of these multisystemic diseases. Despite the small number of protocols (if compared to other areas, like oncology), gene therapy approaches have shown their potential to be helpful in many of these diseases. Not only proof of concept experiments have been performed, but clinically relevant results were obtained in some cases.

The limitations of non-viral gene transfer, i.e., transient expression of the transgene and low transfection efficiency, are being slowly overcome in the last decade using improved vector design and techniques, such as nanotechnology, transposons, and minicircle approaches (to name a few) as demonstrated throughout this chapter. Novel mechanisms to help the DNA to escape endosomal degradation and pass through the nuclear envelope are also under development but were not in the scope of this chapter. Nevertheless, these improvements help non-viral gene therapy to move towards clinical trials in LSDs, which are expected to happen in the years to come. Non-viral vectors are safer than viral particles, which make them an appealing alternative for treatment of lysosomal storage disorders and even other monogenic diseases. Yet, there is a long way to clinical application but the road is paved and the scientific community advances steadily.

5. Acknowledgements

The authors are thankful to Conselho Nacional de Desenvolvimento Cientifico- CNPq and Fundacao de Amparo a Pesquisa do Rio Grande do Sul- FAPERGS.
We also would like to thank our colleagues Fabiana Quoos Mayer, Carlos Oscar Kieling, Valeska Lizzi Lagranha and Raquel Balestrin for contributing with data to this paper.

6. References

Al-Dosari, M.S., Gao X. (2009). Nonviral gene delivery: principle, limitations, and recent progress. *AAPS J*, Vol 11, No 4, pp 671-681.

Anson, D.S., Bielicki, J., Hopwood, J.J. (1992). Correction of mucopolysaccharidosis type I fibroblasts by retroviral-mediated transfer of the human alpha-L-iduronidase gene. *Hum Gene Ther*, Vol 3, No 4, pp 371-379.

Aronovich, E.L., Bell, J.B., Belur, L.R., Gunther, R., Koniar, B., Erickson, D.C., Schachern, P.A., Matise, I., McIvor, R.S., Whitley, C.B., Hackett, P.B. (2007) Prolonged expression of a lysosomal enzyme in mouse liver after Sleeping Beauty transposon-mediated gene delivery: implications for non-viral gene therapy of mucopolysaccharidoses. *J Gene Med*, Vol 9, No 5, pp 403-415.

Aronovich EL, Bell JB, Khan SA, Belur LR, Gunther R, Koniar B, Schachern PA, Parker JB, Carlson CS, Whitley CB, McIvor RS, Gupta P, Hackett PB. (2009) Systemic correction of storage disease in MPS I NOD/SCID mice using the sleeping beauty transposon system. *Mol Ther*.Vol 17, No 7, pp 1136-1144.

Baiotto, C., Sperb, F., Matte ,U., Silva, C.D., Sano, R., Coelho, J.C., Giugliani, R. (2011) Population analysis of the GLB1 gene in south Brazil. *Gen Mol Biol*, Vol 34, No 1, pp 45-48.

Baldo, G., Quoos Mayer, F., Burin, M., Carrillo-Farga, J., Matte, U., Giugliani, R. (2011) Recombinant Encapsulated Cells Overexpressing Alpha-L-Iduronidase Correct Enzyme Deficiency in Human Mucopolysaccharidosis Type I Cells. *Cells Tissues Organs*, epub.

Balestrin, R.C., Baldo, G., Vieira, M.B., Sano, R., Coelho, J.C., Giugliani, R., Matte, U. (2008) Transient high-level expression of beta-galactosidase after transfection of fibroblasts from GM1 gangliosidosis patients with plasmid DNA. *Braz J Med Biol Res,* Vol 41, No 4, PP 283-288.

Barsoum, S.C., Milgram, W., Mackay, W., Coblentz, C., Delaney, K.H., Kwiecien, J.M., Kruth, S.A., Chang P.L. (2003) Delivery of recombinant gene product to canine brain with the use of microencapsulation. *J Lab Clin Med,* Vol 142, No 6, pp 399-413.

Bellettato, C.M., Scarpa, M. (2010) Pathophysiology of neuropathic lysosomal storage disorders. *J Inherit Metab Dis,* Vol 33, No4, PP 347-362.

Bloch, J., Bachoud-Lévi, A.C., Déglon, N., Lefaucheur, J.P., Winkel, L., Palfi, S., Nguyen, J.P., Bourdet, C., Gaura, V., Remy, P., Brugières, P., Boisse, M.F., Baudic, S., Cesaro, P., Hantraye, P., Aebischer, P., Peschanski, M. (2004). Neuroprotective gene therapy for Huntington's disease, using polymer-encapsulated cells engineered to secrete human ciliary neurotrophic factor: results of a phase I study. *Hum Gene Ther*, Vol 15, No 10, pp 968-975.

Bressel, T., Paz, A.H., Baldo, G., Lima, E.O.C., Matte, U., Saraiva-Pereira, M. (2008) An effective device for generating alginate microcapsules. *Genet. Mol. Biol*, Vol 31, No 1, pp 136-140.

Brunetti-Pierri, N., Stapleton, G.E., Palmer, D.J., Zuo, Y., Mane, V.P., Finegold, M.J., Beaudet, A.L., Leland, M.M., Mullins, C.E., Ng, P. (2007) Pseudo-hydrodynamic delivery of helper-dependent adenoviral vectors into non-human primates for liver-directed gene therapy. *Mol Ther*, Vol 15, No4, pp 732- 740.

Camassola, M., Braga, L.M., Delgado-Cañedo, A., Dalberto, T.P., Matte, U., Burin, M., Giugliani, R., Nardi, N.B. (2005) Nonviral in vivo gene transfer in the mucopolysaccharidosis I murine model. *J Inherit Metab Dis*, Vol 28, No 6, pp 1035-1043.

Carlson, C.M., Dupuy, A.J., Fritz, S., Roberg-Perez, K.J., Fletcher, C.F., Largaespada, D.A. (2003) Transposon mutagenesis of the mouse germline. *Genetics* Vol 165, No 1 pp 243–256.

Chen, Z.Y., He, C.Y., Ehrhardt, A. and Kay, M.A. (2003) Minicircle DNA vectors devoid of bacterial DNA result in persistent and high-level transgene expression in vivo. *Mol Ther,* Vol 8, No 3, pp 495–500.

Chen, Z.Y., Riu, E., He, C.Y., Xu, H. and Kay, M.A. (2008) Silencing of episomal transgene expression in liver by plasmid bacterial backbone DNA is independent of CpG methylation. *Mol Ther,* Vol 16, No 3, pp 548–556.

Consiglio, A., Martino, S., Dolcetta, D. (2007) Metabolic correction in oligodendrocytes derived from metachromatic leukodystrophy mouse model by using encapsulated recombinant myoblasts. *J Neurol Sci*, Vol 255, No 1-2, pp 7-16.

Dass, C.R.(2004) Lipoplex-mediated delivery of nucleic acids: factors affecting in vivo transfection. *J Mol Med*, Vol 82, No 9, pp 579–591.

de Duve, C. (1964) From cytases to lysosomes. *Fed Proc*, Vol 23, pp 1045–1049.

Dunbar, C.E., Kohn, D.B., Schiffmann, R., Barton, N.W., Nolta, J.A., Esplin, J.A., Pensiero, M., Long, Z., Lockey, C., Emmons, R.V., Csik, S., Leitman, S., Krebs, C.B., Carter, C., Brady, R.O., Karlsson, S. (1998) Retroviral transfer of the glucocerebrosidase gene into CD34+ cells from patients with Gaucher disease: in vivo detection of transduced cells without myeloablation. *Hum Gene Ther*, Vol 9, No 17, pp 2629-2640.

Ellinwood, N.M., Vite, C.H., Haskins, M.E. (2004) Gene therapy for lysosomal storage diseases: the lessons and promise of animal models. *J Gene Med*. Vol 6, No 5, pp 481-506.

Estruch, E.J., Hart, S.L., Kinnon, C., Winchester, B.G. (2001) Non-viral, integrin-mediated gene transfer into fibroblasts from patients with lysosomal storage diseases. *J Gene Med*, Vol 3, No 5, pp 488-497.

Fischer, H.D., Gonzalez-Noriega, A., Sly, W.S., Morre, D.J. (1980) Phosphomannosyl-enzyme receptors in rat liver. Subcellular distribution and role in intracellular transport of lysosomal enzymes. J Biol Chem. Vol 255, No 20, pp 9608 – 15.

Fraga, M., Laux, M., Zandoná, B., Santos, G.R., Giuberti, C.S., Oliveira, M.C., Matte, U., Teixeira, H.F. (2008) Optimization of stearylamine-based nanoemulsions obtained by spontaneous emulsification process as nucleic acids delivery systems. *J Drug Del Sci Tech* Vol 18, No 6, pp 398-403.

Fraga, M., Bruxel, F., Lagranha, V., Teixeira, H.F., Matte, U. Influence of phospholipid composition on DNA/cationic emulsions complexes: Physicochemical properties, cytotoxicity and transfection on Hep G2 cells. *International Journal of Nanomedicine*, *in press*.

Fratantoni, J.C., Hall, C.W., Neufeld, E.F. (1968) Hurler and Hunter syndromes: mutual correction of the defect in cultured fibroblasts. *Science*, Vol 162, No 853, pp 570–572.

Friso, A., Tomanin, R., Alba, S. (2005) Reduction of GAG storage in MPS II mouse model following implantation of encapsulated recombinant myoblasts. *J Gene Med*, Vol 7, No 11, pp 1482-1491.

Fuller, M., Meikle, P.J., Hopwood, J.J. (2006) Epidemiology of lysosomal storage diseases: an overview. In *Fabry Disease: Perspectives from 5 Years of FOS.* Mehta A, Beck M, Sunder-Plassmann G, editors. Oxford: Oxford PharmaGenesis.

Glover D, Lipps H, Jans D (2005) Towards safe, non-viral therapeutic gene expression in humans. *Nature Reviews Genetics,* Vol 6, No 4, 299-310.

Hacein-Bey-Abina, S., Garrigue, A., Wang, G.P., Soulier, J., Lim, A., Morillon, E., Clappier, E., Caccavelli, L., Delabesse, E., Beldjord, K., Asnafi, V., MacIntyre, E., Dal Cortivo, L., Radford, I., Brousse, N., Sigaux, F., Moshous, D., Hauer, J., Borkhardt, A., Belohradsky, B.H., Wintergerst, U., Velez, M.C., Leiva, L., Sorensen, R., Wulffraat, N., Blanche, S., Bushman, F.D., Fischer, A., Cavazzana-Calvo, M. (2008) Insertional oncogenesis in 4 patients after retrovirus-mediated gene therapy of SCID-X1. *J Clin Invest*, Vol 118, No 9, pp 3132-3142.

Hackett, P.B., Ekker, S.C., Largaespada, D.A., McIvor, R.S. (2005) Sleeping beauty transposon-mediated gene therapy for prolonged expression. *Adv Genet*, Vol 54, pp 189-232.

Horie, K., Yusa, K., Yae, K., Odajima, J., Fischer, S. E., Keng, V. W., Hayakawa, T., Mizuno, S., Kondoh, G., Ijiri, T., Matsuda, Y., Plasterk, R. H., and Takeda, J. (2003) Characterization of Sleeping Beauty transposition and its application to genetic screening in mice. *Mol. Cell. Biol*, Vol 23, No 24, pp 9189–9207.

Hunter, C. (2006) Molecular hurdles in polyfectin design and mechanistic background to polycation induced cytotoxicity. *Advanced Drug Delivery Reviews,* Vol 58, pp 1523–1531.

Kamimura, K., Zhang, G., Liu, D. (2009) Image-guided, intravascular hydrodynamic gene delivery to skeletal muscle in pigs. *Mol Ther*, Vol 18, No 1, pp 93-100.

Kuijlen, J.M., de Haan, B.J., Helfrich, W., de Boer, J.F., Samplonius, D., Mooij, J.J., de Vos, P. (2006) The efficacy of alginate encapsulated CHO-K1 single chain-TRAIL producer cells in the treatment of brain tumors. *J Neurooncol* Vol 78, No 1, pp 31-39.

Lagranha, V.L., Baldo, G., de Carvalho, T.G. Burin M, Saraiva-Pereira, M.L., Matte, U., Giugliani, R. (2008) In vitro correction of ARSA deficiency in human skin fibroblasts from metachromatic leukodystrophy patients after treatment with microencapsulated recombinant cells. *Metab Brain Dis* Vol 23, No 4, pp 469-84.

Liu, F., Song, Y., Liu, D. (1999) Hydrodynamics-based transfection in animals by systemic administration of plasmid DNA. *Gene Ther*, Vol 6, No 7, pp 1258-1266.

Malatack, J.J., Consolini, D.M., Bayever, E. (2003) The status of hematopoietic stem cell transplantation in lysosomal storage disease. *Pediatr Neurol*, Vol 29, No 5, pp 391-403.

Matte U, de Carvalho T, Mayer F, Lagranha V, Giugliani R. (2011) Cell Microencapsulation: a Potential Tool for the Treatment of Neuronopathic Lysosomal Storage Diseases. *Journal of Inherited Metabolic Diseases,* epub.

Mayer, F.Q., Baldo, G., de Carvalho, T.G., Lagranha, V.L., Giugliani, R., Matte, U. (2010) Effects of cryopreservation and hypothermic storage on cell viability and enzyme activity in

recombinant encapsulated cells overexpressing alpha-L-iduronidase. *Artif Organs*, Vol 34, No 5, pp 434-439.

Meikle, P.J., Fietz, M.J., Hopwood, J.J. (2004) Diagnosis of lysosomal storage disorders: current techniques and future directions. *Expert Rev Mol Diagn.* Vol 4, No 5, pp 677–691.

Moreira, J., Gaspar, R., Allen T. (2001) Targeting Stealth liposomes in a murine model of human small cell lung cancer. *Biochimica et Biophysica Acta,* Vol 1515, pp 167-176.

Morille, M., Passirani, C., Vonarbourg, A., Clavreul, A., Benoit, J.P. (2008) Progress in developing cationic vectors for non-viral systemic gene therapy against cancer. *Biomaterials,* Vol, 29, No 24-25, pp 3477-3496.

Muñoz-Rojas, M.V., Horovitz, D.D., Jardim, L.B., Raymundo, M., Llerena, J.C. Jr, de Magalhães, T.S., Vieira, T.A., Costa, R., Kakkis, E., Giugliani, R. (2010) Intrathecal administration of recombinant human N-acetylgalactosamine 4-sulfatase to a MPS VI patient with pachymeningitis cervicalis. *Mol Genet Metab,* Vol 99, No 4, pp 346-350.

Munoz-Rojas, M.V., Vieira, T., Costa, R., Fagondes, S., John, A., Jardim, L.B., Vedolin, L.M., Raymundo, M., Dickson, P.I., Kakkis, E., Giugliani, R. (2008) Intrathecal enzyme replacement therapy in a patient with mucopolysaccharidosis type I and symptomatic spinal cord compression. *Am J Med Genet A*, Vol 146A, Vol 19, pp 2538-2544.

Muro, S. (2010) New biotechnological and nanomedicine strategies for treatment of lysosomal storage disorders. *Wiley Interdiscip Rev Nanomed Nanobiotechnol*, Vol 2, No 2, pp 189-204.

Naganawa, Y., Ohsugi, K., Kase, R., Date, I., Sakuraba, H., Sakuragawa, N. (2002) In vitro study of encapsulation therapy for Fabry disease using genetically engineered CHO cell line. *Cell Transplant*, Vol 11, No 4, pp 325-329.

Nakama, H, Ohsugi, K, Otsuki, T., Date, I., Kosuga, M., Okuyama, T., Sakuragawa, N. (2006) Encapsulation cell therapy for mucopolysaccharidosis type VII using genetically engineered immortalized human amniotic epithelial cells. *Tohoku J Exp Med*, Vol 209, No 1, pp 23-32.

Nam, H.Y., Park, J.H., Kim, K., Kwon, I.C., Jeong, S.Y. (2009) Lipid-based emulsion system as non-viral gene carriers. *Arch Pharm Res* Vol 32, No 5, pp 639-646.

Niidome, T. and Huang, L. (2002) Gene Therapy Progress and Prospects: Nonviral vectors. *Gene Therapy* Vol 9, No 24, pp 1647–1652.

Orive, G., Ponce, S., Hernandez, R.M., Gascon, A.R., Igartua, M., Pedraz, J.L. (2002) Biocompatibility of microcapsules for cell imobilization alaborated with different type of alginates. *Biomaterials* Vol 23, No 18, pp 3825-3831.

Orive, G., Gascon, R.A., Hernandez, R.M., Igartua, M., Pedraz, J.L. (2003) Cell microencapsulation technology for biomedical purposes: novel insights and challenges. *Trends in Pharmacological Sciences*, Vol 24, No 5, pp 207-210.

Osborn, M.J., McElmurry, R.T., Peacock, B., Tolar, J., Blazar, B.R. (2008) Targeting of the CNS in MPS-IH using a nonviral transferrin-alpha-L-iduronidase fusion gene product. *Mol Ther*, Vol 16, No 8, pp 1459-1466.

Osborn, M.J., McElmurry, R.T., Lees, C.J., Defeo, A.P., Chen, Z.Y., Kay, M.A., Naldini, L., Freeman, G., Tolar, J., Blazar, B.R. (2011) Minicircle DNA-based Gene Therapy Coupled With Immune Modulation Permits Long-term Expression of α-L-Iduronidase in Mice With Mucopolysaccharidosis Type I. *Mol Ther*, 2011 Vol 19, No 3, pp 450-460.

Pardridge, W.M. (2007) Blood-brain barrier delivery of protein and non-viral gene therapeutics with molecular Trojan horses. *J Control Release*, Vol 122, No 3, pp 345-348.

Parkinson-Lawrence, E.J., Shandala, T., Prodoehl, M., Plew, R., Borlace, G.N., Brooks, D.A. (2010) Lysosomal storage disease: revealing lysosomal function and physiology. *Physiology (Bethesda),* Vol 25, No 2, pp 102-115.

Plasterk, R.H. (1993) Molecular mechanisms of transposition and its control. *Cell*, Vol 74, No 5, pp 781–786.

Ragnaill, M.N., Brown, M., Ye, D., Bramini, M., Callanan, S., Lynch, I., Dawson, K.A. (2011) Internal benchmarking of a human blood-brain barrier cell model for screening of nanoparticle uptake and transcytosis. *Eur J Pharm Biopharm*. Vol 77, No 3, pp 360-367.

Resina, S., Prevot, P., Thierry, A.R. (2009) Physico-chemical characteristics of lipoplexes influence cell uptake mechanisms and transfection efficacy. *PLoS One* Vol 4, No 6, e6058.

Richard, M., Arfi, A., Seguin, J., Gandolphe, C., Scherman, D. (2009) Widespread biochemical correction of murine mucopolysaccharidosis type VII pathology by liver hydrodynamic plasmid delivery. *Gene Ther*, Vol 16, No 6, pp 746-756.

Riu, E., Grimm, D., Huang, Z. and Kay, M.A. (2005). Increased maintenance and persistence of transgenes by excision of expression cassettes from plasmid sequences in vivo. *Hum Gene Ther* Vol 16, No 5, pp 558–570.

Roberg-Perez, K., Carlson, C.M., Largaespada, D.A. (2003) MTID: a database of Sleeping Beauty transposon insertions in mice. *Nucleic Acids Res*, Vol 31, No 1, pp 78-81.

Ross, C.J., Bastedo, L., Maier, S.A., Sands, M.S., Chang, P.L. (2000a) Treatment of a lysosomal storage disease, mucopolysaccharidosis VII, with microencapsulated recombinant cells. *Hum Gene Ther,* Vol 11, No 15, pp 2117-2127.

Ross, C.J., Ralph, M., Chang, P.L. (2000b) Somatic gene therapy for a neurodegenerative disease using microencapsulated recombinant cells. *Exp Neurol*, Vol 166, No 2, pp 276-286.

Sifuentes, M., Doroshow, R., Hoft, R., Mason, G., Walot, I., Diament, M., Okazaki, S., Huff, K., Cox, G.F., Swiedler, S.J., Kakkis, E.D. (2007) A follow-up study of MPS I patients treated with laronidase enzyme replacement therapy for 6 years. *Mol Genet Metab*, Vol 90, No 2, pp 171-180.

Skarlatos, S., Yoshikawa, T., Pardridge, W.M. (1995) Transport of [125I]transferrin through the rat blood-brain barrier. *Brain Res*, Vol 683, No 2, pp 164-171.

Sly, W.S., Fischer, H.D., Gonzalez-Noriega, A., Grubb, J.H., Natowicz, M. (1981) Role of the 6-phosphomannosyl-enzyme receptor in intracellular transport and adsorptive pinocytosis of lysosomal enzymes. *Methods Cell Biol,* Vol 23, pp 191-214.

Spuch. C., Antequera, D., Portero, A., Orive, G., Hernández, R.M., Molina, J.A., Bermejo-Pareja, F., Pedraz, J.L., Carro, E. (2010) The effect of encapsulated VEGF-secreting cells on brain amyloid load and behavioral impairment in a mouse model of Alzheimer's disease. *Biomaterials*, Vol 31, No21, pp 5608-5618.

Takakusaki, Y., Hisayasu, S., Hirai, Y., Shimada, T. (2005) Coexpression of formylglycine-generating enzyme is essential for synthesis and secretion of functional arylsulfatase A in a mouse model of metachromatic leukodystrophy. *Hum Gene Ther*, Vol 16, No 8, pp 929-936.

Tomanin, R., Friso, A., Alba, S., Piller Puicher, E., Mennuni, C., La Monica, N., Hortelano, G., Zacchello, F., Scarpa M. (2002) Non-viral transfer approaches for the gene therapy of mucopolysaccharidosis type II (Hunter syndrome). *Acta Paediatr Suppl*, Vol 91, No 439, pp 100-104.

Uludag, H., Vos, P., Tresco, P. (2000) Technology of mammalian cell encapsulation. *Adv Drug Delivery Reviews*, Vol 42, No 1-2, pp 29-64.

Vitner, E.B., Platt, F.M., Futerman, A.H. (2010) Common and uncommon pathogenic cascades in lysosomal storage diseases. *J Biol Chem*, Vol 285, No 27, pp 20423-20427.

Walkley, S.U. (2009) Pathogenic cascades in lysosomal disease-Why so complex? *J Inherit Metab Dis*, Vol 32, No 2, pp 181-189.

Wasungu, L., Hoekstra, D. (2006) Cationic lipids, lipoplexes and intracellular delivery of genes. *Journal of Controlled Release*, Vol. 116, No 2, pp 255-264.

Williams, D.A. (2008). Sleeping beauty vector system moves toward human trials in the United States. *Mol Ther*, Vol 16, No 9, pp 1515-1516.

Wilson JM. (2009) Lessons learned from the gene therapy trial for ornithine transcarbamylase deficiency. *Mol Genet Metab,*Vol 96, No 4, pp 151-157.

Worgall, S., Sondhi, D., Hackett, N.R., Kosofsky, B., Kekatpure, M.V., Neyzi, N., Dyke, J.P., Ballon, D., Heier, L., Greenwald, B.M., Christos, P., Mazumdar, M., Souweidane, M.M., Kaplitt, M.G., Crystal, R.G. (2008) Treatment of late infantile neuronal ceroid lipofuscinosis by CNS administration of a serotype 2 adeno-associated virus expressing CLN2 cDNA. *Hum Gene Ther*, Vol 19, No 5, pp 463-474.

Zhang, Y., Wang, Y., Boado, R.J., Pardridge, W.M. (2007) Lysosomal enzyme replacement of the brain with intravenous non-viral gene transfer. *Pharm Res,* Vol 25, No 2, pp 400-406.